The scattering of charged particles from helium and alkali atoms

Issa, Mohammad R.

THE SCATTERING OF CHARGED PARTICLES FROM HELIUM AND ALKALI ATOMS.

A THESIS SUBMITTED FOR THE DEGREE OF DOCTOR OF PHILOSOPHY IN THE UNIVERSITY OF DURHAM

BY

MOHAMMAD R. ISSA

Department of Theoretical Physics,
University of Durham.

September, 1977

Abstract

The second order potentials method of Bransden and Coleman (1972) has been applied to electron impact excitation of lithium, sodium and helium atoms and to proton impact excitation of helium atoms. The calculations for the e-alkalis are presented in the impact parameter approximation in the energy range 10 - 200 ev., and in the partial wave approximation in the energy range 10 - 50 ev. On comparing between the two results, it is concluded that the impact parameter approximation is reliable for energies larger than 50 ev. The results for the electron and proton scattering from the helium atoms are presented in the energy range 100 - 1000 ev (kev for proton scattering).

Acknowledgements

A special debt of gratitude is owed to Professor B. H. Bransden and Dr. J. P. Coleman, whose advice, guidance and patience in their capacity as supervisors, shaped the course of this work.

The generosity of K. H. Winters, K. A. Berrington, M. R. C. McDowell, H. R. J. Walters, M. R. Flannery, A. D. Stauffer and S. Trajmar, in communicating their results is much appreciated.

My thanks are extended to those who assisted in compiling and preparing the typescript of this thesis.

Finally, my deep gratitude to my brother, whose financial support is greatly valued.

TABLE OF CONTENTS

page

Appendices

Introduction

The electron-atom scattering problem can not be solved exactly; even the simplest is a complicated three-body problem. One must develop techniques that provide a close approximation to the exact solution of the problem. The total cross section, the differential cross section, the polarization of the impact radiation and the scattering amplitude are all different quantities that can be compared with the experimental measurements; which provide a valuable test for the reliability of a particular model of scattering.

The technique that can be used to calculate an excitation cross section depends on the energy at which the cross section is required. The close coupling approximation is very well established in the low energy regime, while the Born approximation and the semi-classical approximations are accurate in the high energy regime. It is the intermediate energy region (higher than the threshold and up to the Born regime) that neither of the two techniques is adequate. Previous results in this energy region have been obtained for the most part by extending the range of application of the low and high energy approximations.

The work presented here is concerned with the theoretical calculations of the scattering of electrons from lithium, sodium and helium atoms and of protons from helium atoms; in the intermediate energy regime using the second order potentials method of Bransden and Coleman (1972).

The general theory of scattering and some relevant scattering models are reviewed in chapters one and two. A comparison between the optical potential and the second order potential is made in chapter three and the reduction of the second order potentials in the impact parameter and partial wave formulations is displayed in chapters four and five. The calculated total cross sections, the differential cross sections, the polarization fractions and the Fano and Macek parameters are presented in chapters six and seven and compared with other theoretical calculations and with the experimental data. Finally, atomic units will be used throughout but cross sections will be expressed in units of πa_o^2.

CHAPTER 1.

GENERAL THEORY OF ATOMIC COLLISIONS.

1.1 Formal Solution of Schrodinger Equation.

There are two basic approaches to the study of collision problems, in quantum theory. The first is the approach that considers the incident beam as being switched on in the distant past, and the whole system being stationary; one then tries to obtain solutions of the Schrodinger equation subject to appropriate boundary conditions. The other approach is the time-dependent scheme which considers the interactions as perturbations that cause transitions from the specified initial state to the permissible final state.

Our interest will be in reactions of the form;

$$a + b \longrightarrow a + b \qquad (1.1.a)$$

$$a + b \longrightarrow c + d \qquad (1.1.b)$$

which represent, specifically, charged particle - atom (direct or rearrangement) scattering.

Since our target-atoms will be light ones and the interactions are coulombic and time independent, we shall pursue the stationary state approach in the centre of mass system.

The Schrodinger equation is

$$(H - E)\Psi = o \qquad (1.2)$$

where H is the total Hamiltonian of the system and has the form

$$H = H_\gamma + V_\gamma \qquad (1.3)$$

where H_γ is the Hamiltonian of the arrangement γ of equation (1.1) when there is no interaction between the aggregates, and it is assumed to have a discrete part besides its continuum spectrum.

Their eigenvalues and eigenvectors are such that

$$(H_\gamma - E)\Phi_{\gamma\alpha} = 0 \qquad (1.4)$$

We assume further, that to each state $\Phi_{\gamma\alpha}$ in the continuous part of H_γ (which has an energy E), there belongs a corresponding state $\Psi_{\gamma\alpha}$ of H with the same energy E, and that $\Phi_{\gamma\alpha}$, $\Psi_{\gamma\alpha}$ are both normalizable, at least in the delta-function sense.

Let us introduce, after Lippmann (Lippmann 1956), the Green's functions which are Hermitian and correspond to outgoing waves;

$$G_\gamma(\lambda) = (\lambda - H_\gamma)^{-1} \qquad (1.5)$$

$$G(\lambda) = (\lambda - H)^{-1}$$

where

$\lambda = E + i\epsilon$; ϵ is a small positive real number to make $G(\lambda)$, $G_\gamma(\lambda)$ well defined.

Operating on $\Phi_{\gamma\alpha}$ by $G_\gamma(\lambda)$ yields

$$G_\gamma(\lambda)\Phi_{\gamma\alpha} = (E - E_\alpha + i\epsilon)^{-1}\Phi_{\gamma\alpha} \qquad (1.6)$$

By adopting the eigenfunction expansion method (Mathews and Walker 1965) and introducing the bras and kets notation we obtain

$$G_\gamma(\lambda) = \sum_\alpha |\Phi_{\gamma\alpha}\rangle(E - E_\alpha + i\epsilon)^{-1}\langle\Phi_{\gamma\alpha}| \qquad (1.7)$$

where the sum over α includes an integration over the continuum.

If $|\mu\rangle$ denotes an arbitrary complete state specification, we can write equation (1.7) as

$$\langle\mu'|G_\gamma(\lambda)|\mu\rangle = \sum_\alpha \langle\mu'|\Phi_{\gamma\alpha}\rangle(E - E_\alpha + i\epsilon)^{-1}\langle\Phi_{\gamma\alpha}|\mu\rangle \qquad (1.8.a)$$

where $\langle \mu | \Phi_{\gamma a} \rangle$ is a representation of $\Phi_{\gamma a}$

in μ-representation, or more specifically

$$\langle R, \underline{X} | \Phi_{\gamma a} \rangle = \psi_{\gamma a} \equiv \exp(i k_b R) U_{\gamma a}(\underline{X}) \qquad (1.8.b)$$

which is the schrodinger wave function in co-ordinate space and $\underline{R}$, $\underline{X}$ are the vector of the incident particle referred to the centre of mass and the internal variables of the atom respectively, and U(X) is the wave function of the target atom.

Making use of the identities

$$A^{-1} - B^{-1} = A^{-1} (B-A) B^{-1} \qquad (1.9.a)$$

$$(a + b)^{-1} = a^{-1} (1 - b (a \mp b)^{-1}) \qquad (1.9.b)$$

it is easy to show that the following equalities hold

$$G(\lambda) = G_\gamma(\lambda) (1 + V_\gamma G(\lambda)) = (1 + G(\lambda) V_\gamma) G_\gamma(\lambda) \qquad (1.10.a)$$

$$G_\gamma(\lambda) = G(\lambda) (1 - V_\gamma G_\gamma(\lambda)) = (1 - G_\gamma(\lambda) V_\gamma) G(\lambda) \qquad (1.10.b)$$

$$(1 - G_\gamma(\lambda) V_\gamma) (1 + G(\lambda) V_\gamma) = 1 \qquad (1.10.c)$$

From equations (1.3), (1.4) and (1.10.a) the solution of (1.2) is

$$\Psi^+_{\gamma a} = \Phi_{\gamma a} + G_\gamma(\lambda) V_\gamma \Psi^+_{\gamma a} \qquad (1.11.a)$$

or by equation (1.10.c)

$$\Psi^+_{\gamma a} = (1 + G(\lambda) V_\gamma) \Phi_{\gamma a} \qquad (1.11.b)$$

The superscript positive sign on $\Psi_{\gamma a}$ refers to an outgoing state from the definition of the Green's functions. Equivalent equations for the incoming states are implied and will be denoted by a negative sign superscript when appropriate.

In the following discussion, i and f will replace γ to mean, respectively, initial and final channels. Then the schrodinger solution for the direct collision is

$$\Psi^{+}_{i\alpha} = \Phi_{i\alpha} + G_i(\lambda) V_i \Psi^{+}_{i\alpha} \qquad (1.11'.a)$$

$$\Psi^{+}_{i\alpha} = (1 + G(\lambda) V_i) \Phi_{i\alpha} \qquad (1.11'.b)$$

To get a solution for the reaction (1.1.b), remembering that

$$H = H_i + V_i = H_f + V_f \qquad (1.12)$$

and using the identity (Wu and Ohmura, 1962)

$$(1 - G_f(\lambda) V_f)(1 + G(\lambda) V_i) = 1 + G_f(\lambda)(V_i - V_f) \qquad (1.13)$$

and operating on (1.11'.b) by $(1-G_f(\lambda) V_f)$ and recognising that

$$(1 + G_f(\lambda)(V_i - V_f)) \Phi_{i\alpha} = i\epsilon\, G_f(\lambda) \Phi_{i\alpha} \qquad (1.14)$$

we obtain

$$\Psi^{+}_{i\alpha} = G_f(\lambda)(i\epsilon \Phi_{i\alpha} + V_f \Psi^{+}_{i\alpha}) \qquad (1.15)$$

Here we emphasise that equation (1.15) which represents a solution of Schrodinger equation in the rearrangement channel is obtained from equation (1.11'.b) by transformation. Therefore, we infer that while $\Psi^{+}_{i\alpha}$ explicitly gives the direct scattering, it also includes implicitly the description of the rearrangement scattering.

1.2 The wave equation in configuration space.

Equation (1.8.a) in configuration space becomes

$$\langle \underline{R}, \underline{X} | G_\gamma(\lambda) | \underline{R}', \underline{X}' \rangle = \sum_\alpha \psi_{\gamma\alpha}(\underline{R}, \underline{X}) (E - E_\alpha + i\epsilon)^{-1} \psi^*_{\gamma\alpha}(\underline{R}', \underline{X}') \tag{1.16}$$

The conservation of energy requires that

$$E = \frac{1}{2\mu_\gamma} k_\gamma^2 + W_\gamma \tag{1.17}$$

where μ_γ , k_γ and W_γ are the reduced mass, wave vector and binding energy of the channel γ respectively.

By taking the sum over α in equation (1.16) including the continuum and using equations (1.8.b) and (1.17), equation (1.16) becomes

$$\langle \underline{R}, \underline{X} | G_\gamma(\lambda) | \underline{R}', \underline{X}' \rangle = \sum_\alpha U_{\gamma\alpha}(\underline{X}) U^*_{\gamma\alpha}(\underline{X}') G_o^+(k_{\gamma\alpha}, \underline{R}, \underline{R}') \tag{1.18}$$

where $G_o^+(k, \underline{R}, \underline{R}')$ (see Messiah, 1970) is

$$G_o^+(k, \underline{R}, \underline{R}') = - \frac{\mu_\gamma}{2\pi} \frac{\exp[ik|\underline{R}-\underline{R}'|]}{|\underline{R}-\underline{R}'|} \tag{1.19}$$

From equations (1.8.b) and (1.18) the integral equation for the complete wave function when the incident state is i_α becomes;

$$\Psi^+_{i\alpha}(\underline{R}\underline{X}) = \psi_{i\alpha}(\underline{R}\underline{X}) \delta_{i\gamma} + \int d\underline{X}' \int d\underline{R}' G^+_\gamma(\underline{R}, \underline{X}; \underline{R}', \underline{X}') V_\gamma(\underline{R}', \underline{X}') \Psi^+_{i\alpha}(\underline{R}', \underline{X}') \tag{1.20}$$

where we have used

$$\langle \underline{R}', \underline{X}' | V_\gamma(\underline{R}, \underline{X}) | \underline{R}'', \underline{X}'' \rangle = V_\gamma(\underline{R}', \underline{X}') \delta(\underline{R}' - \underline{R}'') \delta(\underline{X}' - \underline{X}'') \tag{1.21}$$

and

$$G_\gamma^+(\underline{R},\underline{X};\underline{\acute{R}},\underline{\acute{X}}) = \langle \underline{R},\underline{X}|\, G_\gamma(\lambda)\,|\underline{\acute{R}},\underline{\acute{X}}\rangle \qquad (1.22)$$

Now we are in a position to discuss the asymptotic form of the wave function, which from equations (1.22), (1.18) and (1.20) is

$$\Psi^+_{i\alpha} \underset{R\to\infty}{\sim} \psi_{i\alpha}(\underline{R},\underline{X})\,\delta_{i\gamma} + \sum_b U_{\gamma b}(\underline{X})\ \mathrm{EXP}(ik_{\gamma b}R)\,F_{i\alpha,\gamma b}\,R^{-1} \qquad (1.23)$$

where

$$F_{i\alpha,\gamma b} = \frac{-\mu_\gamma}{2\pi}\int d\underline{X}\int d\underline{\acute{R}}\ U^*_{\gamma b}(\underline{X})\,\mathrm{EXP}(ik_{\gamma b}\cdot\underline{\acute{R}})\,V_\gamma(\underline{\acute{R}},\underline{\acute{X}})\ \Psi^+_{i\alpha}(\underline{\acute{R}},\underline{\acute{X}}) \qquad (1.24)$$

Equation (1.23) is interpreted as representing an incoming wave in the incident channel and outgoing waves in all channels, with a scattering amplitude given by equation (1.24).

By the same method, the rearrangement solution from equation (1.15) is

$$\Psi^+_{i\alpha} \underset{r\to\infty}{\sim} \lim_{\epsilon\to 0}\int d\underline{Y}\int d\underline{\acute{r}}\ G^+_f(\underline{r},\underline{Y};\underline{\acute{r}},\underline{\acute{Y}})\,\psi_{i\alpha}(\underline{\acute{r}},\underline{\acute{Y}}) + \sum_b U_f(\underline{Y})\,\mathrm{EXP}(ik_{fb}r)\,\mathcal{G}_{i\alpha,fb}\,r^{-1} \qquad (1.25)$$

The first term in equation (1.25) will vanish since G_f^+ does not propagate in the channel i, and

$$\mathcal{G}_{i\alpha,fb} = \frac{-\mu_f}{2\pi}\int d\underline{\acute{Y}}\int d\underline{\acute{r}}\ U^*_{fb}(\underline{\acute{Y}})\ \mathrm{EXP}(-i\underline{k}_{fb}\cdot\underline{\acute{r}})\,V_f(\underline{\acute{r}},\underline{\acute{Y}})\ \Psi^+_{i\alpha}(\underline{\acute{r}},\underline{\acute{Y}}) \qquad (1.26)$$

where we have used new sets of co-ordinates to be appropriate with the arrangement of equation (1.1.b) and $\mathcal{G}_{i\alpha,fb}$ is the scattering amplitude in the rearrangement channel.

1.3 The Reaction Rates and Cross Section.

The scattering cross section can be related to the asymptotic form of the wave function in a similar manner to potential scattering. Gerjuoy (1958.b) has formulated an approach to describe the rearrangement collision based on this idea. We will follow his approach considering reactions in equation (1.1), (elaborate algebraic formulations can be consulted from his work).

Assuming that $\underline{r}_i$ is the displacement of particle i referred to particle 1 and $\underline{r}$ is the vector of the set of $\underline{r}i$; i = 2,n and n is the number of constituents of the system.

Equation (1.3) can be re-written as

$$H = T + V \qquad (1.3')$$

where

$$T = -\sum_{i=2}^{n} \frac{1}{2\mu_i} \nabla_i^2 + \frac{1}{2M_1} \sum_{i \neq k} \nabla_i \cdot \nabla_k$$

and

μi, is the reduced mass of particle i relative to particle 1 and M_1 is the mass of particle 1. If Ψ_1 and Ψ_2 are solutions of equation (1.2) at the same energy, then the generalised Green's theorem gives

$$\int dr \left(\Psi_1 T \Psi_2 - \Psi_2 T \Psi_1 \right) = \int dS_{\underline{\nu}} \cdot W(\Psi_2; \Psi_1) = 0 \qquad (1.27)$$

or

$$\int dS\, J(\Psi_2; \Psi_1) = 0$$

where J is the current density vector and

where W is the probability current in the space of (n-1) particles with i^{th} component

$$W_i = \frac{1}{2\mu_i}\left(\Psi_2 \nabla_i \Psi_1 - \Psi_1 \nabla_i \Psi_2\right) + \frac{1}{2M_i}\sum_{j\neq i}\left(\Psi_2 \nabla_j \Psi_1 - \Psi_1 \nabla_j \Psi_2\right) \quad (1.28)$$

and

$\underline{\nu}$ is the outward vector drawn normal to the surface element ds; and the integration is to be taken over an infinite sphere in the space $\underline{r}$.

If Ψ_i^+ is a solution of equation (1.2), so is Ψ_i^{+*} due to the Hermicity of H . Putting $\Psi_1 = \Psi_i^+$ and $\Psi_2 = \Psi_i^{+*}$ in equation (1.27) and noting that the same equation holds for Φ_i and Φ_i^* we obtain

$$\int ds\, j(\Pi_i^*; \Pi_i) = -2\mathrm{Im}\left\{\int d\underline{S}\cdot W(\Phi_i^*; \Pi_i)\right\} \quad (1.29)$$

and

$$\Pi_i = G(\lambda) V_i \Phi_i \quad (1.30)$$

Because of the presence of the bound state in Φ_i^*; the only non-vanishing terms in the right hand side of equation (1.29) come from surface elements along the direction of the formation of the arrangement i. In analogy to the optical theorem, we conclude that

$$F = \int ds\, j(\Pi_i^*; \Pi_i) \quad (1.31)$$

represents the total scattered current summed over all reaction channels.

It is convenient to transform equation (1.31) from the co-ordinates $\underline{r}_i$ into a set of co-ordinates $\underline{r}_{cd}$, $\underline{X}_{cd}$, $\underline{r}_{cd}$ is the vector joining the centre of mass of the aggregates c and d in the rearrangement (c,d) of equation (1.1), $\underline{X}_{cd}$ refers to the internal variables of the bound system of the same arrangement.

Assuming that Π_i behaves asymptotically like the Green's function $G(\lambda)$ (after integrating over the internal variables $\underline{X}_{cd}$), equation (1.31) in the new co-ordinates is;

$$F_{cd} = \sum \int ds_{cd} \underline{\nu}_{cd} \cdot \underline{J}_{cd} \qquad (1.32)$$

where

$\underline{\nu}_{cd}$ is the outward vector, normal to the surface ds_{cd};

$\underline{J}_{cd}$ is a vector current along the vector $\underline{r}_{cd}$ and is

$$\underline{J}_{cd} = \frac{1}{2i\mu_{cd}} \left| Z^*_{cd} \nabla_{cd} Z_{cd} - Z_{cd} \nabla_{cd} Z^*_{cd} \right| \qquad (1.33)$$

and μ_{cd} is the reduced mass of the pair of aggregates c and d, and Z_{cd} is

$$Z_{cd} = \int d\underline{X}_{cd} \; U^*_{cd}(X_{cd}) \; \Pi_i \quad = (U_{cd}, \Pi_i) \qquad (1.34)$$

Without any loss of generality, we will assume that a and c are particles, while b and d are neutral atoms, so Φ_i is given by equation (1.8.b). However, there must be a factor of $\mathrm{EXP}(i\underline{p}.\underline{R})$ missing from equation (1.8.b); where $\underline{p}$ is the total momentum and $\underline{R}$ is the vector of the centre of mass of the system referred to particle 1.

This factor contributes a delta function which expresses the requirement of conservation of momentum between the initial and final channels. We will drop this factor throughout.

From equation (1.30), equation (1.34) becomes

$$Z = | U_i G(\lambda) V_i \Phi_i | \tag{1.35}$$

It should be noted that $G(\lambda) V_i \Phi_i$ implies an integration over the suppressed argument, and care must be made when manipulating formulas such as (1.10.a) according to the boundary conditions (Gerjuoy 1958.a). From equations (1.10.a) and (1.18), we have

$$Z = -\frac{\mu_{cd}}{2\pi} \left| U^*(\underline{\hat{X}}) \frac{\exp(i k|\underline{r}-\underline{\hat{r}}|)}{|\underline{r}-\underline{\hat{r}}|} + U^*(\underline{\hat{X}}) \frac{\exp(i k|\underline{r}-\underline{\hat{r}}|)}{|\underline{r}-\underline{\hat{r}}|} V_f G V_i \Phi_i \right| \tag{1.36}$$

where

$$k^2 = 2 \mu_{cd} E_{cd} \tag{1.37}$$

Because of the presence of $G(\lambda)$ in equation (1.35), the surface integral in equation (1.32) is equivalent to integrating over all space and evaluating the surface integral at infinity only (see Gerjuoy 1958.a). We need the limit of Z when $r \to \infty$;

$$\lim_{r\to\infty} Z = - q(r) \left\{ \Psi_f^- V_i \Phi_i \right\} \tag{1.38}$$

where use of equations (1.10.a) and (1.8.b) has been made, and the braces imply an integration, and

$$q(r) = \frac{\mu_{cd}}{2\pi} \frac{\exp(i k r)}{r} \tag{1.39}$$

Substituting equation (1.38) into equation (1.32) yields

$$F = \frac{\mu_{cd}}{4\pi^2} \int d\Omega_{cd}\, k_{cd} \left| \langle \Psi_f^-, V_i \Phi_i \rangle \right|^2 \qquad (1.40)$$

which is the rate at which the particles c and d are scattered into a solid angle $d\Omega$ along a direction Ω_{cd} and with a wave vector k_{cd} .

The cross section for scattering of particles from the arrangement a into the arrangement b is defined by

$$\sigma_{ab} = \frac{\mu_a F_b}{k_a} \qquad (1.41)$$

or from (1.40)

$$\sigma_{ab} = \frac{\mu_a \mu_b}{4\pi^2} \frac{k_b}{k_a} \int d\Omega_b \left| T_{ab} \right|^2 \qquad (1.42)$$

where

$$T_{ab} = \langle \Psi_f^-, V_i \Phi_i \rangle \qquad (1.43)$$

It is useful to write equation (1.42) in the form

$$\sigma_{ab} = \frac{V_b}{V_a} \int d\Omega_b \left| f_{ab}(\theta) \right|^2 \qquad (1.44)$$

where

V_a , V_b are the relative velocities in the channels a and b , and

$$f_{ab}(\theta) = -\frac{\mu_b}{2\pi} T_{ab} \qquad (1.45)$$

The sign is adopted to agree with equation (1.24).

Equation (1.42) is equivalent to equation (4.26) of Bransden (1970) which is calculated from the transition probability.

CHAPTER 2.

THEORETICAL MODELS OF SCATTERING.

2.1 Born Series.

The formal expansion of Ψ_i^+ from equation (1.11.a) is

$$\Psi_i^+ = \sum_{n=0}^{\infty} \left(G_i^+ V_i \right)^n \Phi_i \qquad (2.1)$$

So that the scattering amplitude from equation (1.45) becomes

$$f_{if}(\theta) = \sum_{n=1}^{\infty} \bar{f}_{if}^{n}(\theta) \qquad (2.2)$$

where

$$\bar{f}_{if}^{n}(\theta) = - \frac{\mu}{2\pi} \langle \Phi_f | V_i (G_i^+ V_i)^{n-1} | \Phi_i \rangle \qquad (2.3)$$

The n^{th} Born approximation to the scattering amplitude is defined by

$$f_{if}^{n}(\theta) = \sum_{j=1}^{n} \bar{f}_{if}^{j}(\theta) \qquad (2.4)$$

The first Born approximation (FBA) is obtained when $n = 1$ in the equations (2.3) and (2.4).

This approximation depends on the assumption that the incident particle interacts weakly with the target atom so that its wave function may be closely approximated by a plane wave, which would be the correct wave function in the absence of all interactions. It has long been accepted that the FBA gives an accurate account of the total cross section for particular inelastic processes (Bell and Kingston 1974) at high energy, though it remains unclear how high this energy must be for the FBA results to be reliable within a certain tolerance. It is equally clear, both on experimental and/

and theoretical grounds that the FBA can never describe inelastic differential cross sections at large angles, but, again, there is no way of predicting in advance the angular range over which one can expect FBA results to be accurate.

An obvious improvement over the FBA is to retain the first two terms in equation (2.2) which gives the second Born approximation.

$$f^{2}_{if}(\theta) = -\frac{\mu}{2\pi}\left[\langle \Phi_f | V_i | \Phi_i \rangle + \langle \Phi_f | V_i G_i^{+} V_i | \Phi_i \rangle\right] \qquad (2.5)$$

The second term in equation (2.5) cannot be computed exactly even in the simplest case. Further subsidiary approximations must be employed. These normally involve taking explicit account of the lowest N states and adopting a mean excitation energy, together with closure, to complete the sum arising from Green's function. Different authors, (Holt and Moiseiwitsch 1968a, Woollings and McDowell (1972, 1973)) make different choices of this mean excitation energy.

Results for inelastic transitions show a marked improvement on the FBA differential cross section at large angles (Woollings and McDowell (1972,1973), Buckley and Watters 1975). This is attributed to the inclusion of the initial state as an intermediate state, elastic scattering being the dominant intermediate process.

The elastic transition in the second Born approximation makes a substantial contribution to the total cross section. The peak in the forward direction of the differential cross section varies with the mean excitation energy (Birman and Rosendorff 1969).

Byron and Joachain (1973 b) argue that in order to include the leading term k_i^{-2} corrections to the FBA cross section, one needs to include real$(\bar{f}_{if}^{3}(\theta))$ (together with exchange) in addition to the second Born amplitude, because the real$(\bar{f}_{if}^{3}(\theta))$ is of order k_i^{-2} and will give contribution of this order to the differential cross section.

The difficulties arising from including extra terms in the Born series and the uncertainties in the methods of choosing the mean excitation energy make the chances of improving this model doubtful.

2.2 The Glauber Approximation.

Glauber (1959) has derived a formula for the direct scattering amplitude, but the fact that the formula for composite collisions involves seemingly intractable integrals has meant that the application to problems in atomic physics was delayed until Franco (1968) was able to reduce the five dimensional integral for the elastic scattering amplitude in electron-Hydrogen scattering to a one dimensional form.

We start from the exact integral equation for the wave-function of equation (1.20).

$$\Psi_i^+(\underline{R},\underline{X}) = \psi_i(\underline{R},\underline{X}) - \sum_b U_b(\underline{X}) \int d\underline{\bar{X}} \int d\underline{\bar{R}}\, U_b^*(\underline{\bar{X}})\, G_o^+(k_b, \underline{R}, \underline{\bar{R}})\, V_i(\underline{\bar{R}},\underline{\bar{X}})\, \Psi_i^+(\underline{\bar{R}},\underline{\bar{X}}) \tag{2.6}$$

Assuming the energy of the incident particle is high enough to justify the substitution of $k_b = k_i$, equation (2.6) with the aid of closure relation reduces to

$$\Psi_i^+(\underline{R},\underline{X}) = \psi_i(\underline{R},\underline{X}) - \frac{2\mu}{(2\pi)^3} \lim_{\epsilon \to 0} \int d\underline{\bar{R}} \int d\underline{P}\, \frac{\exp[i\underline{P}\cdot(\underline{R}-\underline{\bar{R}})]}{P^2 - k_i^2 - i\epsilon}\, V_i(\underline{\bar{R}},\underline{X})\, \Psi_i^+(\underline{\bar{R}},\underline{X}) \tag{2.7}$$

where we have used the Fourier integral representation of $G_o(k_i, R, R)$ from equation (1.18).

The approximate integral equation of Ψ_i^+ in equation (2.7) involves the internal co-ordinates $\underline{X}$ of the composites in the initial channel in parametric form only, hence following Glauber (1959) we write

$$\Psi_i^+(\underline{R},\underline{X}) = \exp[i\underline{k}_i\cdot\underline{R})\, F(\underline{R},\underline{X})\, U_i(\underline{X}) \tag{2.8}$$

Inserting equation (2.8) in equation (2.7), we have

$$F(\underline{R},\underline{X}) = 1 - \frac{2\mu}{(2\pi)^3} \lim_{\epsilon \to 0} \int d\bar{\underline{R}} \int d\underline{P}\ \mathrm{EXP}[-i\underline{k}_i\cdot(\underline{R}-\bar{\underline{R}})] \frac{\mathrm{EXP}[i\underline{P}\cdot(\underline{R}-\bar{\underline{R}})]}{P^2 - k_i^2 - i\epsilon} V_i(\bar{\underline{R}},\underline{X})\, F(\bar{\underline{R}},\underline{X}) \tag{2.9}$$

Introducing $\underline{t} = \underline{P} - \underline{k}_i$ equation (2.9) becomes

$$F(\underline{R},\underline{X}) = 1 - \frac{2\mu}{(2\pi)^3} \lim_{\epsilon \to 0} \int d\bar{\underline{R}} \int dt\ \frac{\mathrm{EXP}[i\underline{t}\cdot(\underline{R}-\bar{\underline{R}})]}{t^2 + 2\underline{k}_i\cdot\underline{t} - i\epsilon} V_i(\bar{\underline{R}},\underline{X}) F(\bar{\underline{R}},\underline{X}) \tag{2.10}$$

By taking the Z-component of $\underline{t}$ along $\underline{k}_i$, the t-intergration in equation (2.10) can be calculated, to order of V/E, using the integral formula

$$\int_{-\infty}^{\infty} \frac{\mathrm{EXP}[i\,q\,x]}{q - i\epsilon}\, dq = 2i\pi\,\Theta(x)$$

and equation (2.10) reduces to

$$F(\underline{R},\underline{X}) = 1 - \frac{i\mu}{k_i} \int d\bar{\underline{R}}\, \delta(\underline{\rho} - \bar{\underline{\rho}})\, \Theta(z - \bar{z})\, V_i(\bar{\underline{R}},\underline{X})\, F(\bar{\underline{R}},\underline{X}) \tag{2.11}$$

where

$\Theta(x)$ is the step function, such that $\Theta(x) = 1$ for $x > 0$ and zero otherwise, $\underline{\rho}$ and $\bar{\underline{\rho}}$ are the projections of $\underline{R}$ and $\bar{\underline{R}}$ onto a plane normal to $\underline{k}_i$ and Z is along $\underline{k}_i$.

After integrating over the delta-function, equation (2.11) is solved by

$$F(\underline{R},\underline{X}) = \mathrm{EXP}\left[-\frac{i\mu}{k_i} \int_{-\infty}^{z} d\bar{z}\ V_i(\underline{X},\underline{\rho},\bar{z})\right] \tag{2.12}$$

Now inserting Ψ_i^+ into equation (1.24) for the direct scattering amplitude and recalling equations (2.8) and (2.12), we have

$$f_{if}(\theta) = -\frac{\mu}{2\pi}\int d\underline{X}' \int d\underline{R}\; U_f^*(\underline{X}')\,\mathrm{EXP}(i\underline{q}\cdot\underline{R})\,V_i(\underline{R},\underline{X}')\,U_i(\underline{X}')\,\mathrm{EXP}\left[-\frac{i\mu}{k_i}\int_{-\infty}^{Z} dZ'\,V_i(\underline{X}',\underline{\rho},Z')\right] \tag{2.13}$$

where

$$\underline{q} = \underline{k}_i - \underline{k}_f \tag{2.14}$$

To make equation (2.13) more amenable for calculations, we choose the path of integration of Z' along the bisector of the scattering angle, which implies that $\underline{q}$ is normal to Z' and therefore, in cylindrical co-ordinates, we have

$$f_{if}(\theta) = \frac{-ik_i}{2\pi}\int d\underline{X}' \int d^2\underline{\rho}\;\mathrm{EXP}(i\underline{q}\cdot\underline{\rho})\,U_f^*(\underline{X}')\,\Gamma(\underline{\rho},\underline{X}')\,U_i(\underline{X}') \tag{2.15}$$

and

$$\Gamma(\underline{\rho},\underline{X}') = \sum_{n=1}^{\infty} \frac{(i\chi)^n}{n!} \tag{2.16}$$

where

$$\chi = \frac{-\mu}{k_i}\int_{-\infty}^{\infty} dZ'\,V_i(\underline{X}',\underline{\rho},Z') \tag{2.17}$$

we recognise that equation (2.15) is the Glauber formula, which for hydrogenic-type eigenfunctions can be put into a closed form (Thomas and Gerjuoy 1971). Despite the simplicity/

simplicity and resultant ease of calculations, Glauber's formula suffers from serious deficiencies. Firstly, no account is taken of rearrangement processes, because the potential in the incident channel differs from the potential in the final channel. Secondly, the approximation $k_b = k_i$ makes the derivation only valid for small angle scattering and leads to a forward direction divergence of the scattering amplitude. Thirdly, the choice of the integration path that makes $\underline{q}$ normal to Z' causes the scattering amplitude to vanish if $l + l' + |m| + |m'|$ is odd, where (l, m) and (l', m') are the quantum numbers in the initial and final channels. Fourthly, the Glauber formula predicts no difference between the cross sections for electron scattering and positron scattering. Fifthly, it is obvious from equation (2.16) that the terms of the Glauber multiple scattering series are alternately purely real and purely imaginary. This is in contrast to the Born series of equation (2.2) where the second order term contains both real and imaginary parts.

Attempts have been made to remedy these deficiencies. Firstly, by choosing different paths of integration (see Gerjuoy and Thomas 1974) and secondly, though this is laborious, by solving equation (2.13).

Byron (1971) derives equation (2.13) in an eikonalized close coupling treatment in which he demonstrates that the Glauber formula and close coupling approximation are complementary. Byron and Joachain (1973a) propose that in electron-atom collision, the direct amplitude $f_{if}(\theta)$ be computed from the following formula

$$f_{if}(\theta) = f_{if}^{2}(\theta) + f_{if}^{G3}(\theta) \qquad (2.18)$$

where $f_{if}^{2}(\theta)$ is the amplitude in the second order Born approximation defined in equation (2.5) and $f_{if}^{G3}(\theta)$ is the Glauber formula arising from the third term in the series of equation (2.16), substituted in equation (2.15). Byron and Joachain, partly on the basis of results obtained for potential scattering (Byron and Joachain 1973b), argue that equation (2.18) yields the amplitude correctly to order k_i^{-2} (when exchange effects are included also). Their method appears to be superior to the Glauber formula because it predicts different cross sections for the electron and positron scattering, and it shows better agreement with experiment (Byron and Joachain 1973c).

2.3 The multichannel eikonal approximation.

From the discussion of the preceding section, it is evident that the total wave function Ψ_i^+ can be approximated by an eikonal method which assumes the projections of Ψ_i^+ on the complete set $U_i(X)$ are small during the entire collision, except for the projection on the initially occupied bound state.

We write the total wave function as a truncated sum over target eigenstate

$$\Psi_i^+ = \sum_{n=1}^{N} A_n(\underline{\rho},Z)\,\mathrm{EXP}[i S_n(\underline{\rho},Z)]\,U_n(\underline{X}) \qquad (2.19)$$

then $A_n(\underline{\rho},Z)\,\mathrm{EXP}[i S_n(\underline{\rho},Z)]$ satisfies

$$[\nabla^2 + k_n^2 - 2\mu V_{nn}]\,A_n(\underline{\rho},Z)\,\mathrm{EXP}[i S_n(\underline{\rho},Z)] = 0 \qquad (2.20)$$

where

$$V_{nm}(\underline{R}) = \int U_n^*(\underline{X})\,V(\underline{R},\underline{X})\,U_m(\underline{X})\,d\underline{X} \qquad (2.21)$$

are the interaction matrix elements, and $\underline{R} = (R,\theta,\phi) = (\underline{\rho},\phi,Z)$ is the vector of the incident particle in spherical and cylindrical co-ordinates frames respectively. In the eikonal method (Bransden 1970, p.79) equation (2.20) gives $S_n(\underline{\rho},Z)$ as

$$S_n(\underline{\rho},Z) = k_n Z + \int_{-\infty}^{Z} dZ' Y_n(\underline{\rho},Z') \qquad (2.22)$$

and

$$Y_n(\underline{R}) = Q_n(\underline{R}) - k_n \qquad (2.23)$$

where

$$Q_n(\underline{R}) = [k_n^2 - 2\mu V_{nn}(\underline{R})]^{1/2} \tag{2.24}$$

Provided $V_{nn}(\underline{R})$ is slowly varying with channel wave length (Flannery and McCann 1974a) the eikonal coefficients $A_n(\underline{\rho},Z)$ satisfy

$$\frac{iQ_f}{\mu}\frac{\partial A_f(\underline{\rho},Z)}{\partial Z} = \sum_{\substack{n=1 \\ \neq f}}^{N} A_n(\underline{\rho},Z)\, V_{fn}(\underline{R})\, \mathrm{EXP}[i(S_n - S_f)] \qquad f=1,2,\ldots N \tag{2.25}$$

Taking the azimuthal dependent factor out of the potentials, and making the phase substitution

$$C_f(\underline{\rho},Z) = A_f(\underline{\rho},Z)\, \mathrm{EXP}[-i\Delta\phi + i\int_{-\infty}^{Z} dZ'\, Y_f(\underline{\rho},Z')] \tag{2.26}$$

where $\Delta = m_i - m_f$ is the difference of the azimuthal quantum number of the channel i and f, reduces equation (2.25) to

$$\frac{iQ_f}{\mu}\frac{\partial C_f(\underline{\rho},Z)}{\partial Z} + [\frac{Q_f}{\mu} Y_f + V_{ff}]C_f(\underline{\rho},Z) = \sum_{n=1}^{N} C_n(\underline{\rho},Z)\, V_{fn}(\underline{\rho},Z)\, \mathrm{EXP}[i(k_n - k_f)Z] \tag{2.27}$$

Substituting Ψ_i^+ from equation (2.19) into equation (1.24), we obtain the direct scattering amplitude with the aid of equation (2.27)

$$f_{if}(\theta) = -\frac{i}{2\pi}\int d^2\underline{\rho}\, [I_1 - iI_2]\, \mathrm{EXP}[i\underline{q}\cdot\underline{\rho} + i\Delta\phi] \tag{2.28}$$

and

$$I_1(\rho,\theta) = \int_{-\infty}^{\infty} dZ\, Q_f \frac{\partial C_f(\rho,Z)}{\partial Z} \exp(i\alpha Z) \qquad (2.29)$$

and

$$I_2(\rho,\theta) = \int_{-\infty}^{\infty} dZ\, [Q_f Y_f(\rho,Z) + \mu V_{ff}] C_f(\rho,Z) \exp(i\alpha Z) \qquad (2.30)$$

where

q' is the component of $\underline{q}$ in the XY - plane, where $\underline{q}$ is defined in equation (2.14), and

$$\alpha = q_z - q_m = k_f(1-\cos(\theta)) \qquad (2.31)$$

where q_z and q_m are the Z-component and the minimum value of the momentum change $\underline{q}$.

On completion of the ϕ-integration using the integral representation for the Bessel function of the first kind:-

$$J_n(X) = \frac{(-i)^n}{2\pi} \int_0^{2\pi} \exp[i X \cos(\phi) + in\phi]\, d\phi \qquad (2.32)$$

we obtain from equation (2.28)

$$f_{if}(\theta) = (-i)^{1+\Delta} \int_0^{\infty} \rho\, d\rho\, J_\Delta(q'\rho)[I_1 - iI_2] \qquad (2.33)$$

The coupled equations (2.27), subject to the boundary conditions $C_n(\rho, -\infty) = \delta_{in}$ and equation (2.33), are the basic formulae needed to solve the scattering problem in this method.

Now consider the following approximations:-

1) $V_{ff} << \frac{k^2}{2\mu}$ or $V_{ff} << E$ (2.34)

2) $k_i \approx k_f$ (2.35)

3) $k_i - k_f \approx \epsilon_{fi} / v_i$ (2.36)

where v_i is the incident velocity of the projectile, ϵ_{fi} is the energy difference. The first approximation is an explicit high energy requirement to ensure that the wavelength of the projectile is small compared with the atomic dimensions. The last two approximations imply that the scattering is confined to small angles only. Furthermore, the small angle scattering is demonstrated explicitly when $a = 0$. Assuming the above approximations in equations (2.27) and (2.33) we have

$$\frac{\partial C_f(\rho, Z)}{\partial Z} = \frac{-i}{v_i} \sum_{n=1}^{N} C_n(\rho, Z)\, V_{fn}(\rho, Z)\, \exp[i \epsilon_{fn} Z / v_i] \qquad (2.37)$$

and

$$f_{if}(\theta) = (-i)^{1+\Delta} k_i \int_0^{\infty} \rho \, d\rho \, J_{\Delta}(\rho q')[C_f(\rho, \infty) - \delta_{if}] \qquad (2.38)$$

and

$$q' = q(1 - \epsilon_{fi}^2 \, q^{-2} v_i^{-2})^{1/2} \qquad (2.39)$$

We recall that equation (2.37) is the standard impact parameter approximation, which can be derived directly from the time-dependent Schrodinger equation when the wave function is expanded in terms of the target eigenstate (see McDowell and Coleman, 1970), Byron (1971) has derived equation (2.37) in an eikonalized close coupling approximation. His analyses lead to equation (2.38) with $q' = 2k_f \sin(\theta/2)$ instead of equation (2.39). We also note that equation (2.38) is in agreement with the formula of Baye and Heenen (1974a), who choose a trajectory which makes the quantum first Born approximation and the eikonal form of the impact parameter Born approximation equivalent. With the further approximation that $\epsilon_{fi}/v_i \longrightarrow 0$ equation (2.37) yields the Glauber formula when $N \longrightarrow \infty$.

From the above approximations we can see that the multi-channel eikonal method is an improvement over the impact parameter method and the Glauber approximation. This has been confirmed by the work of Flannery and McCann (1974, a, b, 1975c),a) on electron-hydrogen and (b), (c) on electron-Helium scattering. However, the adoption of a straight line trajectory in their treatment and the neglect of polarization distortion and electron exchange makes this model less accurate in the lower energy region.

2.4 The Diagonalization Method.

A method which is connected to Born approximation and the close coupling impact parameter method has been suggested by Baye et al (1970), who describe the collision problem in terms of time-dependent interaction picture in which a time displacement operator $\Omega(t, t_0)$ transforms a state vector $|a; t_0>$ into $|a, t>$ such that

$$i \frac{\partial}{\partial t} |a, t> = V(t) |a, t> \tag{2.40}$$

and

$$|a, t> = \Omega(t, t_0) |a, t_0> \tag{2.41}$$

where

$$V(t) = \mathrm{EXP}[-iH_0 t] \; V \; \mathrm{EXP}[iH_0 t] \tag{2.42}$$

where H_0 and V are defined in equation (1.3) for the initial channel.

It is clear that

$$\Omega(t_0, t_0) = 1 \tag{2.43}$$

and $\Omega(t, t_0)$ satisfies the differential equation

$$i \frac{\partial}{\partial t} \Omega(t, t_0) = V(t) \, \Omega(t, t_0) \tag{2.44}$$

or in an integral form, with the aid of equation (2.43)

$$\Omega(t, t_0) = 1 - i \int_{t_0}^{t} V(t') \, \Omega(t', t_0) \, dt' \tag{2.45}$$

Baye et al (1970) show that equation (2.45) can be put (to a second order) into the form

$$\Omega(t,t_o) = \mathrm{EXP}\left[-i\int_{t_o}^{t} dt_1\, V(t_1) - \frac{1}{2}\int_{t_o}^{t} dt_1 \int_{t_o}^{t_1} dt_2 [\,V(t_1), V(t_2)]\right] \tag{2.46}$$

If t_o is taken to the limit, $t_o \longrightarrow -\infty$, we expand $|a,t>$ in terms of the eigenfunction of H_o, $|a,t_o>$ being included in the expansion,

$$|a,t> = \sum_p C_{pm}(t)\, U_p \tag{2.47}$$

the coefficients C_{pm} are the transition amplitudes and depend on the impact parameter ρ at a time t and are given by

$$C_{pm}(\rho,t) = < p | \Omega | m > \tag{2.48}$$

The scattering amplitude is then calculated from equation (2.38) using equation (2.48).

Use of the first term in the right-hand side of equation (2.46) reduces equation (2.48) to the first order diagonalization approximation which can be derived from equation (2.37) (Callaway and Bauer 1965), only if

$$Z = v_i\, t \tag{2.49}$$

and

$$[\,T(t), Q(t)\,] = 0 \tag{2.50}$$

where

$$Q_{mn}(t) = V_{mn}(t)\, \mathrm{EXP}[\,i\epsilon_{mn} t\,] \tag{2.51}$$

and

$$T(t) = \int_{-\infty}^{t} Q(t')\, dt' \qquad (2.52)$$

The works of Callaway and Dugan (1966) and of Baye et al (1970) on proton-Hydrogen and Baye (1970) on proton-Helium show that the first order diagonalization approximation gives results no better than the first Born approximation. Including the second term in the right-hand side of equation (2.46) yields the second order diagonalization approximation.

The importance of the second order term is demonstrated in the following:-

Firstly, if we expand the exponent in equation (2.46) then the first two terms in the series will account for the semi-classical second order Born approximation (Holt and Moiseiwitsch 1968b). Secondly, the matrix elements connecting some degenerate states which vanish in the first order approximation, contribute to second order and hence increase the strong coupling between these degenerate states. Thirdly, the matrix elements of the operator Λ are different in the electron collision from those in the proton or positron case. This is so because the second order term is charge invariant while the first order term is dependent on the charge of the projectile. This effect is reflected in the results of Baye and Heenen (1973, a, b, c , 1974) on the proton and electron scattering from Hydrogen and Helium atoms respectively. The second order diagonalization method has shown (Baye and Heenen (1973, a, b, c ,1974) a general improvement over the first order method and Born approximation. The basic aim of this method is to allow for

an/

an important extension of the basis set and to determine the excitation for the states of higher levels, where the results of this method lead to cross sections quite different from those of Born approximation. However, the straight line assumption limits the reliability of this model to the energy region where the straight line and constant velocity approximations are valid.

2.5 The Close Coupling Approximation.

The electron-atom collision problem can be discussed in terms of a representation in which the total wave function for the system of the incident electron and the target atom is expanded in a complete set of target atom eigenstates, such that

$$\Psi(\underline{R},\underline{X}) = \sum_n U_n(\underline{X})F_n(\underline{R}) + \int d\underline{K}\, U_K(\underline{X})F_K(\underline{R}) \qquad (2.53)$$

From the physical point of view, the completeness of the set means that the expansion must describe all possible distinct physical events as we noticed in Chapter One. In other words, the wave function in equation (2.53) must satisfy both of the boundary conditions in equations (1.23) and (1.25). In practical numerical calculations, only a finite number of eigenstates may be included, and therefore the expansion is no longer complete and the boundary conditions in equations (1.23) and (1.25) cannot be simultaneously satisfied.

Castillejo et al (1960) show that the continuum part of equation (2.53) is singular, and by appropriate choice of the path of integration, the boundary conditions are satisfied. They suggest that the total wave function of the system may be defined uniquely either by specifying the asymptotic form that satisfies the boundary conditions in equation (1.23) and (1.25) or by specifying the asymptotic form that satisfies the boundary conditions in equation (1.23) and by choosing the path of integration for the integral in equation (2.53). The first choice can be shown to/

to be equivalent to a symmetrized wave function (Peterkop and Veldre 1966) of the form:

$$\Psi(\underline{R},\underline{X}) = \sum_{n}^{Nt} A[\, u_n(\underline{X}) F_n(\underline{R})] \qquad (2.54)$$

where A is an exchange operator, changing the order of the electron co-ordinates, and Nt is the number of channels included in the expansion.

In previous sections, the close coupling approximation has been used where the symmetrization of the wave function has been ignored. The problem was then solved in a configuration space and further approximations were employed. For systems of light atoms it is a good approximation to neglect the spin-orbit interaction in the Hamiltonian. In this case both L, the total angular momentum, and S, the total spin, and their Z-components M and M_s respectively, are conserved during the collision.

For electron-alkalis systems, containing one electron outside the closed shell, the equations of the close coupling method are simplified considerably when it is assumed that the same core functions are used for all states of the valency electron (frozen core approximation). Since the atomic wave function of the N-electron system is anti-symmetric with respect to interchange of any two atomic electrons, we can write the anti-symmetric wave function of (N+1) electrons as

$$\Psi(r_j, \underline{X}) = \sum_{k=1}^{N+1} \frac{(-1)^{N+1-k}}{(N+1)^{1/2}} \sum_{r_i} \Phi(r_i, \bar{X}^k \hat{R}_k \sigma_k)\, R_k^{-1} F_{ij}(R_k) \qquad (2.55)$$

where the notations

$$\gamma_i \equiv (a_i l_1 m_1 s_1 m_1^s \; k_i l_2 m_2 \; m_2^s) \quad , \quad (a_i l_1 m_1 \; s_1 m_1^s)$$

are the angular momentum quantum numbers of the atomic electrons, and $(k_i l_2 m_2 \; m_2^s)$ are the wave vector and angular momentum of the colliding electron.

$$\nu \equiv (a_i \; l_1 \; l_2)$$

$$\Gamma_i \equiv (a_i l_1 s_1 l_2 L \; S \; M \; M_S)$$

$$\underline{X} = \underline{X}_1, \underline{X}_2, \cdots \underline{X}_{N+1}$$

$$\overline{X}^k = \underline{X}_1 \cdots \underline{X}_{k-1}, \; \underline{X}_{k+1} \cdots \underline{X}_{N+1}$$

$\underline{X}_k = (\underline{R}_k, \sigma_k)$ space and spin variables of the k^{th} electron.

The function $\Phi(\Gamma_i, \overline{X}^k \hat{R}_k \sigma_k)$ is

$$\Phi(\Gamma_i, \overline{X}^k \hat{R}_k \sigma_k) = \sum_{\gamma} (\gamma | \Gamma) \Phi(a_i l_1 m_1 s_1 m_1^s, \overline{X}^k) Y_{l_2 m_2}(\hat{R}_k) \delta(m_2^s, \sigma_k) \tag{2.56}$$

where

$$(\gamma | \Gamma') = \delta(\nu, \nu') \langle l_1 l_2 ; m_1 m_2 | LM \rangle \langle \tfrac{1}{2} \tfrac{1}{2} ; m_1^s m_2^s | SM_S \rangle \tag{2.57}$$

and $\langle l_1 l_2 ; m_1 m_2 | LM \rangle$ is the Clebsch-Gordan coefficient (Rose 1957), $\delta(\nu, \nu') = \delta_{\nu,\nu'}$

The quantum numbers denoted by Γ_j in equation (2.55) define the incident channel. These will be retained only when necessary. The sum over Γ_i is truncated to a small number of terms.

The Hamiltonian of the (N+1) electrons is

$$H = H_a + H_{N+1} + V \tag{2.58}$$

where

$$H_{N+1} = -\frac{1}{2}\nabla^2_{N+1} - Z/R_{N+1} \tag{2.59}$$

$$V = \sum_{i=1}^{N} (1/R_{i,N+1}) \tag{2.60}$$

H_a is the atomic Hamiltonian, Z is the nuclear charge and $(R_{i,N+1})^{-1} = |X_i - R_{N+1}|^{-1}$.

By substituting equation (2.55) into the Hartree-Fock equation:-

$$\int \Phi^*(\Gamma_i, \bar{X}^{N+1}, \hat{R}_{N+1}\sigma_{N+1})(H-E)\Psi(\Gamma_j, X) R_{N+1} d\bar{X}^{N+1} d\hat{R}_{N+1} d\sigma_{N+1} \tag{2.61}$$

we obtain the coupled integro-differential equation for the function $F_i(R_{N+1})$ in the notation of Percival and Seaton (1957)

$$(L_\nu - 2V_c^{l_2}) F_\nu(R) = 2\sum_{\nu'} (V^L_{\nu\nu'} - W^{LS}_{\nu\nu'}) F_{\nu'}(R) \tag{2.62}$$

where

$$L_\nu = \left(\frac{d^2}{dR^2} - \frac{l_2(l_2+1)}{R^2} + k_\nu^2\right)$$

and V_c^{l2} is the core potential (Salmona and Seaton 1961) and is given by

$$V_c^{l2} F_\nu(R) = \sum_{nl}(\text{closed shells})(2l+1)\Big[2Y_0(P_{nl}^2|R)\,F_\nu(R) - \frac{1}{2}\sum_\lambda C_{l l_2 \lambda} Y_\lambda(P_{nl} F_\nu|R)\,P_{nl}\Big] \tag{2.63}$$

$$V^L_{\nu\nu'}(R) = -\frac{Z}{R}\delta_{\nu\nu'} + \sum_\lambda f_\lambda(l_1 l_2, l_1' l_2'; L)\, Y_\lambda(P_{nl_1} P_{n'l_1'}|R) \tag{2.64}$$

$$W^{LS}_{\nu\nu'}(R,R')F_{\nu'}(R') = (-1)^{1-S}\sum_\lambda g_\lambda(l_1 l_2, l_1' l_2'; L)\Big[(\epsilon_{nl_1} - \frac{k_\nu^2}{2})\delta_{\lambda 0} \times \Delta(P_{nl_1} F_{\nu'}|R') + Y_\lambda(P_{nl_1} F_{\nu'}|R')\Big] P_{n'l_1'}(R) \tag{2.65}$$

$k_\nu^2 = 2(E - E_{nl_1})$. ϵ_{nl_1} are the target energy in the state $(n\,l_1)$ and the energy of the valency electron in the state $(n\,l_1)$ respectively, and E is the total energy.

In general, f_λ, g_λ, Y_λ, Δ and $C_{l_1 l_2 \lambda}$ are defined as

$$f_\lambda(l_1 l_2, l_1' l_2'; L) = (l_1 l_2 L|P_\lambda(w)|l_1' l_2' L) \tag{2.66}$$

$$= (-1)^{L-l_1-l_2}\, g_\lambda(l_1 l_2, l_2' l_1'; L)$$

$$Y_\lambda(AB|R) = \frac{1}{R^{\lambda+1}}\int_0^R A^*(t)B(t)\,t^\lambda\,dt + R^\lambda\int_R^\infty A^*(t)B(t)\,t^{-\lambda-1}\,dt \tag{2.67}$$

$$\Delta(AB|R) = \int_0^\infty A^*(R)B(R)\,dR \tag{2.68}$$

$$C_{l_1 l_2 \lambda} = \int_{-1}^{1} P_{l_1}(w) P_{l_2}(w) P_\lambda(w)\,dw \tag{2.69}$$

$P_{nl}(R)$, $P_l(w)$ are the radial part of the electron orbitals and the Legendre polynomials respectively.

We notice that equation (2.62) is identical to that of Percival and Seaton (1957) for the electron-Hydrogen atom when V_c^{12} is set equal to zero.

The errors in the scattering S-matrix elements calculated from the asymptotic form of $F_\nu(R)$ will be of quadratic order in the error from the wave functions (Percival and Seaton 1957).

Burke and Schey (1962) assume the form of the scattering wave as

$$F_\nu^{LS}(\nu_0, R) \sim k_\nu^{-1/2}\left[\sin(\theta_L)\,\delta_{\nu\nu_0} + T_{\nu\nu_0}^{LS}\,\mathrm{EXP}(i\theta_L)\right] \qquad (2.70)$$

where we have retained the notation $F_\nu(\nu_0, R)$ instead of $F_\nu(R)$ to refer to the incident channel, and

$$\theta_L = k_\nu R - \frac{l_2\pi}{2} \qquad (2.71)$$

$T_{\nu\nu_0}^{LS}$ is the partial wave amplitude.

If we set

$$q_{aa_0}^{\pm} = F_{aa_0} \pm G_{aa_0} \qquad (2.72)$$

where F_{aa_0}, G_{aa_0} are defined in equations (1.24) and (1.26), then equation (1.23) reduces to the form

$$\Psi_a^+ \sim U_n(\chi)\,\mathrm{EXP}(i k_{a_0}\cdot R)\,\delta_{aa_0} + \sum_a q_{aa_0}^{\pm}\,\mathrm{EXP}(i k_a R)\,U_a(\chi)R^{-1} \qquad (2.73)$$

From equation (2.55), the scattering amplitude is

$$F_a(R) \sim \mathrm{EXP}(i\underline{k}_{a_0}\cdot\underline{R})\,\delta_{aa_0} + \sum_a q^{\pm}_{aa_0}\,\mathrm{EXP}(ik_a R) \qquad (2.74)$$

When $F_a(R)$ is expanded in partial waves, equation (2.74) reduces to that of equation (2.70) and $q^{\pm}_{aa_0}$ (the scattering amplitude) is related to $T^{LS}_{\nu\nu_0}$. We follow the method of Bransden (Bransden 1970) to relate $q^{\pm}_{aa_0}$ to $T^{LS}_{\nu\nu_0}$ by projecting the scattering amplitude on basis sets that are diagonal in the total momentum.

The scattering amplitude at an energy E is

$$T_{aa_0}(E) = \langle \Phi_a(k_a)\| V_a \| \Psi^{+}_{a_0} \rangle \qquad (2.75)$$

which can be put in the form

$$T_{aa_0}(E) = \langle \Phi_a(k_a)\| T \| \Phi_{a_0}(k_{a_0}) \rangle \qquad (2.76)$$

where $\langle \Phi_a(k_a)\|$ is defined in equation (1.8b) and has the normalisation on the energy shell:

$$\langle \Phi_a(k_a)\| \Phi_b(k_a) \rangle = (2\pi)^3\,\delta_{ab}\,\delta(\Omega_b - \Omega_a)(\mu_a k_a)^{-1} \qquad (2.77)$$

We define the basis sets that are diagonal in the total orbital angular momentum such that

$$|\Gamma_a\rangle = \sum_{m_1 m_2} i^{l_2}(2\pi)^{-3/2}\sqrt{\mu_a k_a}\int d\Omega_a\, Y_{l_2 m_2}(\Omega_a) \times$$

$$\ll l_1 l_2 m_1 m_2 | LM \gg | \Phi_{a l_1 m_1}(k_a) \rangle \qquad (2.78)$$

where the phase factor i^{l_2} is introduced to match the phase of the asymptotic form in equation (2.70). The spin appears only parametically. The normalisation and the completeness relation of the basis sets are

$$\langle \Gamma_a | \Gamma_{a'} \rangle = \delta(a\, l_1 l_2 L M ; a' l_1' l_2' L' M') \tag{2.79}$$

and

$$\sum_{\Gamma_a} | \Gamma_a \rangle \langle \Gamma_a | = 1 \tag{2.80}$$

Now the scattering amplitude is expanded in the form

$$T_{ba} = \sum_{\Gamma_\xi \Gamma_{\xi'}} \langle \Phi_b(k_b) | \Gamma_\xi \rangle \langle \Gamma_\xi | T | \Gamma_{\xi'} \rangle \langle \Gamma_{\xi'} | \Phi_a(k_a) \rangle \tag{2.81}$$

We introduce

$$\langle \Gamma_\xi | T | \Gamma_{\xi'} \rangle = -\frac{1}{\pi} T_{\Gamma\Gamma'} \tag{2.82}$$

so that the diagonal elements will assume the form of those of potential scattering. When $\underline{k}_a$ (the wave vector in the incident channel) is assumed to be along the Z-axis and M=0, then equation (2.81) with the help of equation (2.78) reduces to

$$T_{ba} = -\sum_{\substack{\Gamma\Gamma' \\ m_1 m_1' \\ m_2 m_2'}} 8\pi^2\, i^{l_2 - l_2'} \sqrt{\frac{2l_2+1}{4\pi \mu_a \mu_b k_a k_b}}\; T^{LS}_{\Gamma\Gamma'}\, Y_{l_2 m_2'}(\Omega_b) \times$$

$$\langle l_1 l_2, 00 | L\, 0 \rangle \langle l_1' l_2', m_1' m_2' | L\, 0 \rangle \tag{2.83}$$

or/

or

$$f_{ba}(\theta) \simeq \sum_{\substack{\Gamma\Gamma' \\ m_1 m_1' \\ m_2 m_2'}} 4\pi i^{l_2 - l_2'} \sqrt{\frac{2l_2+1}{4\pi \mu_a \mu_b k_a k_b}} \; T^{LS}_{\Gamma\Gamma'} \; Y_{l_2' m_2'}(\hat{r}_b) \; \cdot$$

$$\langle l_1 l_2 0 0 | L 0 \rangle \langle l_1' l_2' m_1' m_2' | L \; 0 \rangle \qquad (2.84)$$

Detailed applications of the close coupling approximation (see Moiseiwitsch and Smith 1968) indicate that the method is of good value when all open channels and some of the closed channels are included in the expansion. The method, however, suffers from the drawback that it is only slowly convergent, for systems of low polarizability such as Hydrogen, as the number of states is enlarged (Ormond and Smith 1964). A related difficulty lies in the great increase in computing time required as further states are added to the basis. These drawbacks may be attributed to the insufficient representations of different physical features such as the distortion of the wave function of the target atom (polarization) or correlation effect. The work of Moores and Norcross (1972) (using the close-coupling 3S- 3P states of sodium, which is known to have 99% of the polarizability coming from 3S- 3P states) agrees with the experiment at lower energies thus lending support to the above argument.

A systematic improvement over the close coupling method is to account for these physical features in an expansion that has more favourable convergence properties. Burke and Taylor (1966 ; Taylor and Burke 1967), use the close coupling expansion with additional variationally determined correlation functions. However, on comparing their results with the calculations of Burke et al (1967), wherein the $n=3$ states of electron-hydrogen were explicitly included, it was found that the resonances which arise from the $n=3$ states, due to the long range dipole effects, are not well represented by the correlation terms. Above the $n=3$ threshold, the method shows spurious resonances. It thus appears that the correlation method is of value only if all open channels are included in the truncated expansion and the energy is below that at which resonances which arise from the first set of closed channels begin.

At energies beyond the ionization threshold, different methods are introduced to modify the close coupling expansion. Burke et al (1969) incorporated the close coupling pseudo-states method in which the total wave function (for a two-electron system) is expanded in the form

$$\Psi(\underset{1}{R},\underset{2}{R}) = (1 \pm A_{12}) \sum_{\nu} \frac{P_{nl}(R_1)}{R_1} \frac{F_{\nu}(R_2)}{R_2} \underset{l_1 l_2}{\mathcal{Y}}^{LM}(\hat{R}_1,\hat{R}_2) \qquad (2.85)$$

where now $P_{nl}(R)$ are not necessarily the eigenfunctions of the bound atom. The first few terms of the expansion represent the eigenstates of the bound system, while the higher/

higher bound and continuum states are represented by pseudo-states, chosen to be orthogonal to each other and to the included eigenstates, but otherwise arbitrary. The choice of pseudo-states can be made in a number of ways. At lower energies, the pseudo-states should be chosen to give the right polarizability, while at intermediate energies they could be chosen to represent the correlation effect in the final state (Burke and Webb 1970). Burke and Webb found good agreement between their results for the cross sections for the excitation of H(1S-2S) by electron impact and experiment. It can be argued in this case that at higher energies it is less important to obtain the exact polarizability, but the addition of pseudo-states is still beneficial since they partially account for loss of flux to channels, including continuum, which has not been explicitly included in the calculation. The computed cross sections for e-H (Burke and Webb 1970, Burke and Mitchell 1973) show non-physical resonances close to each of the pseudo-states threshold. Convergence was tested by Burke and Mitchell, and they found it satisfactory for the states with $l = 0$.

A further test on the convergence of the method was made by Callaway et al (1975) who used a combination of pseudo-states method (including eleven states) and the polarized orbital method. To avoid the problem of a large number of coupled channels, the variational methods of Nesbet (1969) and Nesbet and Oberoi (1972) were employed. The non-physical resonances were avoided by varying the pseudo-states parameters set so as to move the artificial threshold away from the energies at which calculations are desired.

The computed cross sections for the e-H are in good agreement with those of Burke and Webb (1970), which shows the stability of the approximation as further pseudo-states are added. An alternative method is to modify the close coupling expansion by including effective potential terms (optical potentials) to represent the influence of the omitted terms in the truncated expansion, and this will be discussed in the following chapter.

2.6 The Polarized Orbital Close Coupling Method.

In this method the reaction of the scattered electron upon the atomic system is to be accounted for. Long range polarization effects, induced by this reaction, are important as has been cited in the previous section.

The total wave function of an (N+1) electron system is the same as that defined in equation (2.55), but now $\Phi(r_i, \bar{x}^k \hat{R}_k \sigma_k)$ is a set of perturbed atomic wave functions which are energy dependent.

Feautrier et al (1971) use the polarized orbital form for $\Phi(r_i, \bar{x}^k \bar{R}_k \sigma_k)$ which was originally introduced by Temkin (1957) and is of the form

$$\Phi(r_i, \bar{x}^k \bar{R}_k) = \bar{\Phi}(r_i, \bar{x}^k) + \Phi^{pol}(r_i, \bar{x}^k \bar{R}_k) \qquad (2.86)$$

where $\bar{\Phi}(r_i, \bar{x}^k)$ represents the unperturbed atomic wave functions, $\Phi^{pol}(r_i, \bar{x}^k \bar{R}_k)$ is the distortion of the atomic wave function and $\bar{R}_k$ is the coordinate R_k when used as a parameter. Other notations are as defined in section (2.5).

The introduction of the distorted part $\Phi^{pol}(r_i, \bar{x}^k \bar{R}_k)$ in the wave function does not alter the Kohn variational principle, since $\Phi^{pol}(r_i, \bar{x}^k \bar{R}_k)$ falls off more rapidly than R_k^{-1} as $R_k \longrightarrow \infty$.

Feautrier et al (1971) show that $F_i(R_{N+1})$ and $\Phi^{pol}(r_i, \bar{x}^{N+1} \bar{R}_{N+1})$ satisfy the following coupled integro-differential equations.

$$(H_a - E_a - \frac{1}{2}\nabla^2_{N+1} + V)(\Phi^{pol}_{\Gamma_j} F_{\Gamma_j} R^{-1}_{N+1}) + V \Phi_{\Gamma_j} F_{\Gamma_j} R^{-1}_{N+1}$$

$$- \nabla_{N+1} \Phi^{pol}_{\Gamma_j} \cdot \nabla_{N+1} (F_{\Gamma_j} R^{-1}_{N+1})$$

$$- N(H - E)(\Phi(\Gamma_j, \bar{R}^N) + \Phi^{pol}(\Gamma_j \bar{R}^N \bar{R}_N))(F_{\Gamma_j}(R_N) R^{-1}_N) = 0 \qquad (2.87)$$

and

$$\sum_{\Gamma_j} \left[(H_{N+1} - \frac{1}{2} k^2_{\Gamma_j}) \delta_{\Gamma_i \Gamma_j} + V_{\Gamma_i \Gamma_j} + V^{pol}_{\Gamma_i \Gamma_j} \right] F_{\Gamma_i} R^{-1}_{N+1} - \qquad (2.88)$$

$$- N \sum_{\Gamma_j} \left[S_{\Gamma_i \Gamma_j} + T_{\Gamma_i \Gamma_j} + W_{\Gamma_i \Gamma_j} + W^{pol}_{\Gamma_i \Gamma_j} \right] = 0$$

where

$$V_{\Gamma_i \Gamma_j} = \int \Phi^*(\Gamma_i, \bar{R}^{N+1}) V \Phi(\Gamma_j, \bar{R}^{N+1}) \, d\bar{\tau}^{N+1} \qquad (2.89)$$

$$V^{pol}_{\Gamma_i \Gamma_j} = \int \Phi^*(\Gamma_i, \bar{R}^{N+1}) V \Phi^{pol}_{\Gamma_j} \, d\bar{\tau}^{N+1} \qquad (2.90)$$

$$S_{\Gamma_i \Gamma_j} = \int \Phi^*(\Gamma_i, \bar{R}^{N+1})(H_{N+1} - \frac{1}{2} k^2_{\Gamma_j}) \left[\frac{\Phi(\Gamma_j, \bar{R}^N) F_{\Gamma_j}(R_N)}{R_N} \right] d\bar{\tau}^{N+1} \qquad (2.91)$$

$$T_{\Gamma_i \Gamma_j} = \int \Phi^*(\Gamma_i, \bar{R}^{N+1})(H_{N+1} - \frac{1}{2} k^2_{\Gamma_j}) \left[\frac{\Phi^{pol}(\Gamma_j, \bar{R}^N \bar{R}_N) F_{\Gamma_j}(R_N)}{R_N} \right] d\bar{\tau}^{N+1} \qquad (2.92)$$

$$W_{\Gamma_i \Gamma_j} = \int \Phi^*(\Gamma_i, \bar{R}^{N+1}) V \Phi(\Gamma_j, \bar{R}^N) R^{-1}_N F_{\Gamma_j}(R_N) \, d\bar{\tau}^{N+1} \qquad (2.93)$$

$$W^{pol}_{\Gamma_i \Gamma_j} = \int \Phi^*(\Gamma_i, \bar{R}^{N+1}) V \Phi^{pol}(\Gamma_j, \bar{R}^N \bar{R}_N) R^{-1}_N F_{\Gamma_j}(R_N) \, d\bar{\tau}^{N+1} \qquad (2.94)$$

where we set $F_{\Gamma_i}(R_{N+1}) = F_{\Gamma_i}$, $\Phi^{pol}(\Gamma_i, \bar{R}^{N+1} R_{N+1}) = \Phi^{pol}_{\Gamma_i}$

In addition to the direct potentials $V_{\Gamma_i\Gamma_j}$ and exchange potentials $W_{\Gamma_i\Gamma_j}$, we have the direct polarization potentials $V^{pol}_{\Gamma_i\Gamma_j}$ and the exchange polarization potentials $W^{pol}_{\Gamma_i\Gamma_j}$ appear in the scattering equation (2.88).

The system of the coupled integro-differential equations (equations (2.87), (2.88)) is an intractable problem. Feautrier et al (1971) make further approximations to decouple the equations of the perturbed atomic wave function Φ^{pol} and the free electron wave function F_i. The reduced equation for Φ^{pol} is that of the first order perturbation theory. Feautrier (1970) applied this method for the calculation of the scattering of electrons from lithium atoms. The results for the polarization of the resonant line $2P-2S$ (including two states $2S-2P$) show a marked improvement over those calculated in the two-state close coupling method of Burke and Taylor (1969). Better agreement with the experiment is achieved in the energy region above threshold up to $5\,ev$. The two calculations seem to converge at $5\,ev$, which leads one to believe that the importance of the method is in the vicinity of the excitation threshold.

If only one state is included in equation (2.88) (elastic), then the method reduces to that of the polarised orbital method of Temkin (1957) which was generalized by Vo Ky Lan (1971). The polarized orbital method, while it gives good agreement with the close coupling method below the threshold with less labour, fails to give satisfactory results/

results above threshold. The exchange polarization term which seems to be important below threshold for e-Li scattering, plays no important role above threshold (Vo ky lan, 1971).

McDowell et al (1973) use the polarized orbital method in an alternative form. They set the scattering amplitude as defined in equation (1.43)

$$f_{if}(\theta) = -\frac{1}{2\pi} < \phi_f | V_f | \Psi_i^+ > \qquad (2.95)$$

where now Ψ_i^+ is calculated using the polarized orbital method discussed by Vo ky lan (1971). Application of the method to systems of Hydrogen and Helium atoms was very successful in agreeing with the experiment in the intermediate energy range (McDowell et al 1974, Scott and McDowell 1975). Further application on electron -alkalis has been reported and its comparison is left for later chapters.

CHAPTER 3.

The Optical Potential Method.

In chapter two we showed that the close coupling approximation would provide a satisfactory method for the study of the scattering problem in the lower energy region. Another approximation scheme for the total wave function Ψ of the system is derived from the close coupling optical potential method.

In this method one seeks to obtain equations for the scattered wave function $F_n(R)$ with a complicated but exact potential. In practice, one has to make an approximation for this potential.

If P is a projection operator, that projects onto the first N states in the infinite expansion of equation (2.53), and is defined as

$$P = \sum_{n=1}^{N} P_n \tag{3.1}$$

then our truncated wave function is

$$\Psi_t = P \Psi \tag{3.2}$$

But Ψ from the discussion of chapter one, has a formal solution as

$$\Psi^+ = \Phi + G_0 W \Psi^+ \tag{3.3}$$

where W represents the direct and exchange potentials, and other notations are as defined in chapter one.

From equations (3.2 and 3.3) we have

$$\Psi_t^+ = \Phi + G_o P W \Psi^+ \qquad (3.4)$$

where the fact that $\left[G_o, P\right] = 0$ has been used (Mittleman and Pu 1962).

Subtracting equation (3.4) from (3.3) we obtain

$$\Psi^+ = \Psi_t^+ + G_o (1 - P) W \Psi^+ \qquad (3.5)$$

or

$$\Psi^+ = (P + G_o (1 - P) W) \Psi^+$$

If we set Ψ^+ as

$$\Psi^+ = D^+ \Psi_t^+$$

where

$$D^+ = P + G_o (1 - P) W D^+ \qquad (3.6)$$

then our truncated wave function Ψ_t^+ becomes

$$\Psi_t^+ = \Phi + G_o U_{op} \Psi_t^+ \qquad (3.7)$$

where

$$U_{op} = P W D^+ \qquad (3.8)$$

Equations (3.7) and (3.8) are the basic equations for the truncated wave function and the effective potential, which were introduced firstly by Mittleman and Pu (1962).

The optical potential can be calculated by iterating the values of D^+ from equation (3.6). The first iteration will/

will give potentials of second order. These potentials are the second order potentials in the method of Bransden and Coleman (1972). The explicit form of U_{op} in this approximation is

$$U_{op} = \sum_{m=0}^{N} \left[W_{nm} + \sum_{j>N}^{\infty} W_{nj} G_o W_{jm} \right] \qquad (3.9)$$

The scattering wave function from equation (3.7) and (3.9) using the properties of Green's function such that

$$(\nabla^2 + k_n^2) G_o(k_n; R, R') = 2 \delta(R - R') \qquad (3.10)$$

is

$$(\nabla^2 + k_n^2) F_n(R) = 2 \sum_{m=0}^{N} \left[W_{nm} F_m + \int K_{nm}(R, R') F_m(R') dR' \right] \qquad (3.11)$$

where

$$K_{nm}(R, R') = \sum_{j>N}^{\infty} W_{nj} G_o(k_j; R, R') W_{jm} \qquad (3.12)$$

From the definition of W_{nm}, K_{nm} consists of three different terms, namely:

(1) polarization terms

(2) exchange exchange terms

(3) exchange polarization terms.

Since $G_o(k_n; R, R')$ is complex for open channels, K_{nm} is complex and its imaginary part represents absorption from channels $0 \leq n \leq N$ to those channels with $n > N+1$.

CHAPTER 4.

Application of the Second Order Potentials Method to Electron-Alkalis in the Impact Parameter Approximation.

4.1 The semi-classical formulation.

From section (2.5) we note that the equations for electron scattering by alkalis system have the same form as the equations for hydrogenic system, with an additional potential caused by the core electrons. Therefore, one can find one-electron descriptions of alkalis in terms of pseudo-potentials, in which the combined effect of the nucleus plus the inner electrons is replaced by a single net effective potential for the valency electron.

Rapp and Chang (1972, 1973) calculated the one-electron wave functions of the valency electron for Li and Na atoms by using pseudo-potentials of the form

$$V^c(X) = -(M-1)\left(1+\frac{X}{2a}\right)\exp(-a^{-1}X)\,X^{-1} - X^{-1} \qquad (4.1)$$

where M is the atomic number, and a is an undetermined parameter. $V^c(X) \longrightarrow \frac{-M}{X}$ as $X \longrightarrow 0$, whereas $\frac{-1}{X}$ as $X \longrightarrow \infty$

We will use these wave functions in our calculations and their forms are given in Appendix A.

Starting from equation (3.11), neglecting exchange, we set

$$F_n(\underline{R}) = C_n(\underline{f}, Z)\exp(i q_n Z) \qquad (4.2)$$

where

$$R = \rho + \hat{k}_o Z \tag{4.3}$$

$$q_n = k_o + \epsilon_{on} k_o^{-1} \tag{4.4}$$

Assuming the high velocity conditions such that

$$\epsilon_{on} k_o^{-1} \approx 0 \quad \text{and} \quad \nabla^2 C_n(\rho, Z) \ll \nabla C_n(\rho, Z)$$

and the rectilinear propagation so that

$$k_o \cdot \nabla = k_o \frac{\partial}{\partial Z}$$

where k_o is the incident wave vector, and $\epsilon_{mn} = \epsilon_m - \epsilon_n$, is the energy difference between states m and n, we have

$$ik_o \frac{\partial C_n(\rho, Z)}{\partial Z} = \sum_{m=0}^{N} \Big[V_{nm}(\rho, Z) C_m(\rho, Z) \exp(i \epsilon_{nm} Z k_o^{-1}) + \int_0^{\infty} d^2\rho' \int_{-\infty}^{\infty} dZ' K_{nm}(\rho', Z'; \rho, Z) C_m(\rho', Z') \exp(i q_m Z' - i q_n Z) \Big] \tag{4.5}$$

The potentials K_{nm} are too complicated to evaluate exactly, the further approximation in which, for $n > N$ the energy ϵ_n of the target in state n is replaced by an effective average energy $\bar{\epsilon}$ and correspondingly k_n^2 is replaced by $\bar{k}^2$. Using closure, we can write K_{nm} as

$$K_{nm}(\rho', Z'; \rho, Z) = G_o(\bar{k}; R, R') \Big[\mu_{nm}(R, R') - \sum_{j=0}^{N} \bar{V}_{nj}(R) \bar{V}_{jm}(R') \Big] \tag{4.6}$$

where

$$\mu_{nm}(R, R') = \int d\chi\, U_n^*(\chi) |R - \chi|^{-1} |R' - \chi|^{-1} U_m(\chi) \tag{4.7}$$

and the bar in $\bar{V}_{nj}(\underline{R})$ is to indicate that the core potential is dropped due to the orthogonality (since $\bar{V}_{nj}$ occurs only when $n \neq j$).

The semi-classical Green's function must be employed in the kernels K_{nm}, which is

$$G_o(\bar{k}, \underline{R}, \underline{R}') = \frac{-i}{k_o} \delta^2(\underline{\rho} - \underline{\rho}') \Theta(Z-Z') \exp[i(Z-Z')\bar{q}] \quad (4.8)$$

where

$$\bar{q} = k_o + \bar{\epsilon}_o k_o^{-1} \quad (4.9)$$

$$\bar{\epsilon}_o = \epsilon_o - \bar{\epsilon}$$

From equation (4.6) and (4.8), equation (4.5) reduces to

$$i k_o \frac{\partial C_n(\underline{\rho}, Z)}{\partial Z} = \sum_{m=0}^{N} \Big[V_{nm}(\underline{\rho}, Z)\, C_m(\underline{\rho}, Z) \exp(i \epsilon_{nm} Z k_o^{-1}) + \frac{1}{i k_o} \exp(i \bar{\epsilon}_n Z k_o^{-1}) \int_{-\infty}^{Z k_o^{-1}} dZ'\, K_{nm}(\underline{\rho}, Z, Z')\, C_m(\underline{\rho}, Z') \Big] \quad (4.10)$$

and

$$K_{nm}(\underline{\rho}, Z, Z') = \exp[-i \bar{\epsilon}_m Z' k_o^{-1}] \Big[\mu_{nm} - \sum_{j=0}^{N} \bar{V}_{nj}(\underline{R})\, \bar{V}_{jm}(\underline{R}') \Big] \quad (4.11)$$

On studying the second order diagonalization approximation, discussed in section 2.4, we note that it is an intermediate in character between the solution of equation (4.10) and the semi-classical second Born approximation.

This can be seen from the series expansion for the matrix elements of $\Omega(\rho,\infty)$ as

$$\langle n|\Omega(\rho,\infty)|m\rangle = \sum_{\lambda} \Omega^{\lambda}_{nm} \qquad (4.12)$$

where

$$\Omega^{0}_{nm} = \delta_{nm}$$

$$\Omega^{1}_{nm} = \frac{1}{ik_0}\int_{-\infty}^{\infty} dZ\, V_{nm}(\rho,Z)\exp[i\epsilon_{nm}Z k_0^{-1}]$$

$$\Omega^{2}_{nm} = \left(\frac{1}{ik_0}\right)^2 \int_{-\infty}^{\infty} dZ_1 \int_{-\infty}^{\infty} \Theta(Z_1 - Z_2)\, dZ_2 \sum_{j=0}^{\infty}\Big[\bar{V}_{nj}(\rho,Z_1)\times$$

$$\bar{V}_{jm}(\rho,Z_2)\exp[i(\epsilon_{nj}Z_1+\epsilon_{jm}Z_2)k_0^{-1}] - \qquad (4.13)$$

$$-\bar{V}_{nj}(\rho,Z_2)\,\bar{V}_{jm}(\rho,Z_1)\exp[i(\epsilon_{nj}Z_2+\epsilon_{jm}Z_1)k_0^{-1}]\Big]$$

If closure were used to calculate Ω_{nm}, we would have an approximation similar to the second order potential method retaining contribution from all intermediate states, including the continuum.

4.2 Many Channel Approximation.

Equation (4.10) can be simplified further by extracting the azimuthal dependence using the transformation

$$C_n(\underline{\rho}, z) = C_n(\rho, z)\,\mathrm{EXP}(-i s_n \phi) \tag{4.14}$$

and the explicit form of $\bar{V}_{nm}$, K_{nm} is given by

$$\begin{aligned} \bar{V}_{nm}(\underline{\rho}, z) &= \bar{V}_{nm}(\rho, z)\,\mathrm{EXP}(i\phi(s_m - s_n)) \\ K_{nm}(\underline{\rho}, z, z') &= K_{nm}(\rho, z, z')\,\mathrm{EXP}(i\phi(s_m - s_n)) \end{aligned} \tag{4.15}$$

where s_n is the magnetic quantum number of the n^{th} state, and ϕ is the azimuthal angle.

We have

$$\begin{aligned} ik_0 \frac{\partial C_n(\rho, z)}{\partial z} = \sum_{m=0}^{N} \Big[& V_{nm}(\rho, z)\, C_m(\rho, z)\,\mathrm{EXP}(i\epsilon_{nm} z k_0^{-1}) \\ & + \frac{1}{ik_0}\mathrm{EXP}(i\bar{\epsilon}_n z k_0^{-1}) \int_{-\infty}^{zk_0^{-1}} dz'\, K_{nm}(\rho, z, z')\, C_m(\rho, z') \Big] \end{aligned} \tag{4.16}$$

The number of coupled channels in equation (4.16) depends on the number of states included and also on the value of l of each state, where we have $(2l+1)$ equations, from each value of l . From the symmetry of equation (4.16) and the properties of the kernels, we can reduce the number of the equations from $(2l+1)$ to $(l+1)$ for each l. To do so, we write down the symmetry properties of $\bar{V}_{nm}$ and μ_{nm} as

$$\begin{aligned} \bar{V}_{mn} \equiv \bar{V}_{nn'}(lm, lm') &= (-1)^{m+m'}\, \bar{V}_{nn'}(l-m, l-m) \\ \mu_{mn} \equiv \mu_{nn'}(lm, lm') &= (-1)^{m+m'}\, \mu_{nn'}(l-m, l-m') \end{aligned} \tag{4.17}$$

Then equation (4.16) for magnetic quantum number (m) and (-m) becomes

$$i k_o \frac{\partial C_{nlm}}{\partial Z} = \sum_{n'l'm'} \Big[V_{nn'}(lm,l'm')\, C_{n'l'm'}\, EXP[\, i \epsilon_{nln'l'} Z k_o^{-1}\,] + \frac{1}{i k_o} EXP[\, i \bar{\epsilon}_{nl} Z k_o^{-1}\,] \int_{-\infty}^{Z k_o^{-1}} dZ'\, K_{nn'}(lm,l'm')\, C_{n'l'm'} \Big] \quad (4.18)$$

and

$$i k_o \frac{\partial C_{nl-m}}{\partial Z} = \sum_{n'l'm'} \Big[V_{nn'}(l-m,l'-m')\, C_{n'l'-m'} EXP[\, i \epsilon_{nln'l'} Z k_o^{-1}\,] + \frac{1}{i k_o} EXP[\, i \bar{\epsilon}_{nl} Z k_o^{-1}\,] \int_{-\infty}^{Z k_o^{-1}} dZ'\, K_{nn'}(l-m,l'-m')\, C_{n'l'-m'} \Big] \quad (4.19)$$

on comparing equations (4.18) and (4.19) with the help of equations (4.17) we have

$$C_{nlm} = (-1)^{m} C_{nl-m} \quad (4.20)$$

Therefore we can write equations (4.18) and (4.19) only for $m \geq 0$ as

$$i k_o \frac{\partial C_{nlm}}{\partial Z} = \sum_{\substack{n'l' \\ m' \geq 0}} \Big[\Big\{ V_{nn'}(lm,l'm') + (-1)^{m'} (1-\delta_{m'0}) V_{nn'}(l\, m,l'-m') \Big\} C_{n'l'm'} \times EXP[\, i \epsilon_{nln'l'} Z k_o^{-1}\,] + \frac{1}{i k_o} EXP[\, i \bar{\epsilon}_{nl} Z k_o^{-1}\,] \int_{-\infty}^{Z k_o^{-1}} dZ' \Big\{ K_{nn'}(lm,l'm') + (1-\delta_{m'0})(-1)^{m'} \times K_{nn'}(lm,l'-m') \Big\} C_{n'l'm'} \Big] \quad (4.21)$$

When the included states are of the form (ns, nP), the equations (4.21) for the states with quantum numbers (nl0) are all equivalent regardless of the value of l, while/

while the states with (n|1) assume different form.
We write down the explicit form of these cases after making the transformation

$$B_{n|m} = \left(\sqrt{2} + \left(1 - \sqrt{2} \right) \delta_{m0} \right) C_{n|m}$$

and

$$^{n}S \equiv 1 \ , \quad ^{n}P_0 \equiv 2 \ , \quad ^{n}P_1 \equiv 3 \quad \text{and} \quad ^{n}B_1 \equiv 4$$

as

$$ik_0 \frac{\delta B_1}{\delta Z} = V_{11} B_1 + \left[V_{12} B_2 + \sqrt{2}\, V_{13} B_3 \right] \mathrm{EXP}\left(i \epsilon_{12} Z k_0^{-1} \right)$$

$$+ \frac{1}{ik_0} \mathrm{EXP}\left(i \epsilon_1 Z k_0^{-1} \right) \int_{-\infty}^{Zk_0^{-1}} dZ' \left[K_{11} B_1 + K_{12} B_2 + \sqrt{2} K_{13} B_3 \right] \qquad (4.22)$$

and similarly for $\frac{\delta B_2}{\delta Z}$ by interchanging 1 by 2.

$$ik_0 \frac{\delta B_3}{\delta Z} = \sqrt{2} V_{31} B_1 \mathrm{EXP}\left(i \epsilon_{31} Z k_0^{-1} \right) + \sqrt{2} V_{32} B_2 + \left(V_{33} - V_{34} \right) B_3$$

$$+ \frac{1}{ik_0} \mathrm{EXP}\left(i \epsilon_3 Z k_0^{-1} \right) \int_{-\infty}^{Zk_0^{-1}} dZ' \left[\sqrt{2} K_{31} B_1 + \sqrt{2} K_{32} B_2 + \left(K_{33} - K_{34} \right) B_3 \right] \qquad (4.23)$$

The kernels

$$K_{n|0,n|0} \ , \quad K_{n|0,n|1} \ , \quad \left(K_{n|1,n|1} - K_{n|1\, n|-1} \right)$$

are defined as

$$K_{11} = \mathrm{EXP}\left(-i \bar{\epsilon}_1 Z k_0^{-1} \right) \left[\mu_{11} - \bar{V}_{11} \bar{V}_{11} - \bar{V}_{12} \bar{V}_{21} - 2 \bar{V}_{13} \bar{V}_{31} - \sum_j V_{1j} \bar{V}_{j1} \right]$$

$$K_{13} = \mathrm{EXP}\left(-i \bar{\epsilon}_3 Z k_0^{-1} \right) \left[\mu_{13} - \bar{V}_{11} \bar{V}_{13} - \bar{V}_{12} \bar{V}_{23} - \bar{V}_{13} \left(\bar{V}_{33} - \bar{V}_{34} \right) - \sum_j \bar{V}_{1j} \bar{V}_{j3} \right]$$

$$\left(K_{33} - K_{34} \right) = \mathrm{EXP}\left(-i \bar{\epsilon}_3 Z k_0^{-1} \right) \left[\mu_{33} - \mu_{34} - 2 \left[\bar{V}_{31} \bar{V}_{13} + \bar{V}_{32} \bar{V}_{23} + \sum_j \bar{V}_{3j} \bar{V}_{j3} \right] - \left(\bar{V}_{33} - \bar{V}_{34} \right)^2 \right] \qquad (4.24)$$

where the sum over j is to account for the spurious core states of Li and Na .

The coupled integro-differential equations (4.22) and (4.23) can now be solved with the kernels K_{nm} given by equations (4.24). The transition amplitude for the excitation of an atom from its ground state to the n-state can be calculated subject to the boundary conditions

$$B_n(\rho, -\infty) = \delta_{n0} \tag{4.25}$$

and the scattering amplitude $f_{0n}(\theta)$ can now be calculated using equation (2.38) and the total cross section is

$$Q_{0n} = 2 \frac{k_n}{k_0} \int_0^\infty \rho \, d\rho \, \left| B_n - \delta_{0n} \right|^2 \qquad (\pi a_0^2) \tag{4.26}$$

Application of the impact parameter approximation to the scattering of electrons from Li and Na atoms is expected to be accurate for higher energies and small angles as is shown in section 2.3. Being aware of this, we apply the method down to lower energies, till 10 ev. The reason for this is to make a quantitative assessment on the reliability and the range of applicability of the method compared with the partial wave method, where no further approximations on the equation (3.11) are made.

We also apply the impact parameter approximation to the scattering of electrons, positrons and protons for the states of $n = 3$ of He atom, using a distorted wave in the initial state. We postpone this discussion to Chapter Seven.

4.3 The Choice of the Average Energy $\bar{\epsilon}$.

The closure approximation inherent in the second order potential method, requires the introduction of an average effective energy for the states not explicitly included in the expansion. Bransden and Coleman (1972) choose the effective energy so that the effective potential in the incident channel had the asymptotic form of the adiabatic polarization potential. For alkali atoms (Li, Na), however, the inclusion of n_0P state in the two-state close coupling expansion will account for 98% of the polarizability of the target atom (Salmona and Seaton 1961). We therefore take the average effective energy to be the energy of the lowest state not explicitly included.

4.4 Numerical Methods.

The system of equations (4.22, 4.23) has a general form

$$\frac{d\,Y_N(Z)}{d\,Z} = F(Z, Y_N(Z)) \qquad (4.27)$$

Subject to the boundary conditions of equation (4.25) and the limits of the integration are $-\infty < Z < \infty$.

To an order of R^{-3}, the value of the transition amplitude at a distance say $Z = -Z_o$ is

$$a_n(\rho, -Z_o) = -\frac{V_{n0}(R)}{\epsilon_{n0}} \exp(i\epsilon_{n0} Z_o k_o^{-1}) (\sqrt{2} + (1-\sqrt{2})\delta_{m0})\, a_0(\rho, -Z_o) \qquad (4.28)$$

Z_o was chosen to make the error of order 10^{-4}.

The determination of the upper limit $Z \longrightarrow \infty$ is different, because the second order potential will introduce an error of order R^{-2} when stopping at a positive large distance and therefore Z should be made large. The value of $Z = 100$ a.u is large enough to make the error of order $\approx 10^{-4}$.

With the new boundary conditions, a Hamming modified predictor corrector method (Ralston and Wilf 1962), was used to solve the system of equation (4.27).

In this method one needs to

1) predict a value of $\bar{Y}_N(Z_{i+1})$
2) modify the predicted value by adding the truncation error which gives $\bar{\bar{Y}}_N(Z_{i+1})$
3) find $Y_N'(Z_{i+1}\cdot)$ from the differential equation and $\bar{Y}_N(Z_{i+1})$
4) find a new value of $Y_N(Z_{i+1})$
5) correct the new value by adding the truncation error.

One very desirable feature of this method is that we can estimate the truncation error in a very simple fashion. This is an invaluable aid in deciding when to change the value of the step length. If the step error indicates that the calculations are more accurate than we require, then the step length is doubled. Conversly the step length is halved if the step error is too large a value. Another advantage of this method is that we need to calculate $F(Z, Y_N(Z))$ only twice at each step. The method is not self starting, and the forward difference Newton's interpolation formula is used to start the calculations.

The integration of the non-local terms appearing in $F(Z,\gamma_N)$ was calculated using a Simpson quadrature.

The kernels V_{nm} in equations (4.22) are elementary (Appendix A), while the kernels μ_{nm} are calculated numerically using the method of Coleman (1972). These kernels have a general form as (Appendix B),

$$\mu_{mn} = \int_0^1 A(Z,Z',\rho,\underline{R},\underline{R}',s)\,ds$$

and were calculated using Gaussian quadrature integration (Abramowitz and Stegun 1965).

The integrand A varies rapidly near the lower limit and therefore the interval was divided into unequal sub-intervals such that

$$0 \leq s \leq 0.1, 0.1 \leq s \leq 0.2, 0.2 \leq s \leq 0.6, 0.6 \leq s \leq 1$$

A test on the accuracy of the numerical integration is provided by the unitarity conditions (Sullivan 1972) such that

$$\sum_{n=0}^{N} B_n(\rho,\infty) \leq 1$$

To calculate the differential cross section and the total cross section, the maximum value of ρ was 35 a.u. which gives a convergence to 2%. The integration for the scattering amplitude, equation (2.38), was evaluated by expressing it as a sum of an infinite series of definite integrals whose limits of integration are successive zeroes of the Bessel function.

CHAPTER 5.

Application of the Second Order Potential Method to Electron-Alkalis using Partial Waves.

5.1 Partial Wave Formulation.

We start from equation (3.11) where K_{nm} is defined in equation (3.12) and W_{nm} is

$$W_{nm} = V_{nm}(R) - W_{nm}(R,R') \tag{5.1}$$

where

$$W_{nm}(R,R') = (-1)^{1-S} \; U_n^*(R') \left[|R - R'|^{-1} + E_n - \frac{1}{2}k_m^2 \right] U_m(R) \tag{5.2}$$

for one-electron systems (Drukareve 1964), S is the total spin and other quantities are as defined in chapter one or section 2.5.

Expanding $F(\underline{R})$ and $G_o(k_n^2,\underline{R},\underline{R}')$ in partial waves,

$$F_{\substack{n l_1 m_1}}(\underline{R}) = \sum_{l_2 m_2} \sqrt{4\pi(2l_2+1)}\; i^{l_2} f_{\substack{n l_1 m_1}}^{l_2 m_2}(R)\, Y_{l_2 m_2}(\hat{R})\, R^{-1} \tag{5.3}$$

$$G_o(k_n^2,\underline{R},\underline{R}') = 2 \sum_{lm} g_l(k_n^2,R,R')\, Y_{lm}^*(\hat{R})\, Y_{lm}(\hat{R}')\, R^{-1} R'^{-1} \tag{5.4}$$

the method of Appendix (C) in the notation of section 2.5 yields

$$L_\nu f_\nu(R) = 2 \sum_{\nu'} \left[\left(V_{\nu\nu'} - W_{\nu\nu'} \right) f_{\nu'}(R) + 2 \int_0^\infty dR'\, H_{\nu\nu'}(R,R')\, f_{\nu'}(R') \right] \tag{5.5}$$

where

$$H_{\nu\nu'}(R,R') = \sum_{\nu>N} \bar{V}_{\nu\nu''}(R)\,\bar{V}_{\nu''\nu'}(R')\,g_{l_2''}(k^2_{\nu''},R,R') \qquad (5.6)$$

and g_l has the explicit form (Bransden 1970) as

$$g_l(k,R,R') = -ikRR'\,j_l(kR_<)\,h_l^1(kR_>) \qquad (5.7)$$

with $R_< = \min(R,R')$, $R_> = \max(R,R')$ and $j_l(kR)$ and $h_l^1(kR)$ are the spherical Bessel function of the first and third kind respectively (Abramowitz and Stegun 1965). We have introduced the bar in $\bar{V}_{\nu\nu'}$ using the same argument as in chapter four.

An alternative method for deriving equation (5.5) is to start from equation (2.62) using the method of Bransden and Coleman (1972) (see Winters 1974).

As in the previous chapter, k_ν^2 is set to $\bar{k}^2$ and using closure, $H_{\nu\nu'}$ simplifies to

$$H_{\nu\nu'}(R,R') = \sum_{\substack{\lambda\lambda' \\ l_1'',l_2''}} g_{l_2''}(\bar{k},R,R') * f_\lambda(l_1 l_2, l_1'' l_2'' L) f_{\lambda'}(l_1'' l_2'', l_1' l_2' L) *$$

$$\left[Z_{\lambda\lambda'}(P_{nl_1}P_{n'l_1'}|RR') - \sum_{\nu''}^{N} Y_\lambda(P_{nl_1}P_{n''l_1''}|R)\,Y_{\lambda'}(P_{n''l_1''}P_{n'l_1'}|R')\right] \qquad (5.8)$$

where

$$Z_{\lambda\lambda'}(AB|RR') = \int_0^\infty A(t)\,B(t)\,\frac{\min^\lambda(R,t)}{\max^{\lambda+1}(R,t)}\,\frac{\min^{\lambda'}(R',t)}{\max^{\lambda'+1}(R',t)}\,dt \qquad (5.9)$$

In obtaining equation (5.5) we dropped terms of second order in the exchange potentials. This is justified on account of

(i) The complexity of these terms and the large amount of computer time needed.

(ii) The work of Vo ky lan (1971) shows that the contribution of the exchange polarization term is negligible above threshold.

5.2 Three Channel Approximation.

Our calculations in the impact parameter method show that the main contribution to the second order potential comes from the term in the elastic channel. For this reason and the practical difficulties in the numerical work, we solve the equation (5.5) for the coupling of the states $(n_o S , n_o P)$, (n_o is the ground state of the target atom), when the second order potential term is in the elastic channel only. In this approximation, a three channel problem results, where for a total angular momentum L the three channels are

ν	l_1	l_2
1	0	L
2	1	L-1
3	1	L+1

The case for L=0 is exceptional since we have two channels only, and the channel with $l_1=1$, $l_2=L$ is excluded by the parity conservation. We can write equation (5.5) as

$$\left(\frac{d^2}{dR^2} - l_2^{\nu}(l_2^{\nu}+1)R^{-2} + k_{\nu}^2 \right) f_{\nu} = 2 \sum_{\nu'} \left(V_{\nu\nu'} - W_{\nu\nu'} \right) f_{\nu'} + 4 \int_0^{\infty} dR' \, H(n_o 0 l_2, n_o 0 l_2) f_{n_o 0} \qquad (5.10)$$

when the explicit form and the symmetry properties of $f_\lambda(l_1 l_2, l_1' l_2'; L)$ (Appendix C) together with equation (5.7) are used, $H(n_o 0 l_2, n_o 0 l_2)$ reduces to

$$H(n_o 0\, l_2, n_o 0\, l_2) = -i\bar{k} RR' \sum_{l_2''=0}^{\infty} (2l_2''+1)\, j_{l_2''}(\bar{k} R_<)\, h^1_{l_2''}(\bar{k} R_>) \times$$

$$\sum_{\lambda=0}^{\infty} \frac{\langle l_2'' \lambda, 00 | L 0\rangle^2}{(2L+1)} \frac{1}{(2\lambda+1)} \Big[Z_{\lambda\lambda}(P_{n_o S}^2 | RR') - \sum_{n'' l_1''}^{N} Y_\lambda(P_{n_o S} P_{n'' l_1''} | R) \times Y_\lambda(P_{n'' l_1''} P_{n_o S} | R') \delta_{\lambda l_1''} \Big] \tag{5.11}$$

The sum over $(n'' l_1'')$ includes the spurious states of the core electrons in the same manner as in chapter four and the presence of the Clebsch-Gordan coefficients restricts the values of λ for each value of l_2'' and L such that

$$|l_2'' - L| \leq \lambda \leq l_2'' + L$$

and therefore we are left with one infinite sum only.

5.3 Numerical Methods.

5.3.1 The iterative method.

Because of the integral terms in equation (5.10), an iterative procedure was used to solve the integro-differential equations. This method was originally presented by Sasakawa (1963) and implemented by Austern (1969) for nuclear physics applications and by Winters (1974) for the scattering of electrons from hydrogen and helium atoms. Let equation (5.10) be written, in matrix form, as

$$L_{,} F = U F \tag{5.12}$$

where U is a two-dimensional matrix and F is a column matrix. The functions $S_L(X)$ and $C_L(X)$ are the usual regular and irregular functions governed by the homogeneous part of equation (5.12), they are (X) and (-X) multiplied by the familiar spherical Bessel ($J_L(X)$) and Neumann functions. Furthermore the function

$$e_L^+ = C_L + iS_L \tag{5.13}$$

is the outgoing wave solution, and is (iX) multiplied by the spherical Bessel function of the third kind ($h_1^1(X)$) (Abramowitz and Stegun 1965).

The basic idea of the iterative procedure is that F_L is computed by iteration of a trial wave function that contains the scattering amplitude T_L

$$F_L^n = S_L \delta_{vv_0} + T_L^n E_L^n \tag{5.14}$$

so that self-consistent calculation of T_L^n from

$$T_L^n = -k_v^{-1} \int_0^\infty S_L \, U \, F_L^n \, dR \tag{5.15}$$

controls the accuracy of the asymptotic parts of the trial wave function. The zero order form for E_L^n is

$$E_L^\circ = \left[1 - \mathrm{EXP}\left[-\left(R/a' \right)^{2L+1} \right] \right] e_L^+ \tag{5.16}$$

which satisfies the boundary conditions of the exact scattered wave both asymptotically and at the origin, a' is an increment number and n is the number of iterations.

To begin the first iteration, the scattering amplitudes T_L° are determined when F_L° and E_L° are substituted from equations (5.14) and (5.16) into equation (5.15) leading to a set of linear equations. The sequence of steps followed in the iteration procedure are:-

a) solve for T_L^n in zero order form

b) insert these zero order amplitudes in the right-hand side of equation (5.12), to reduce the right-hand side to a single term explicit function that contains no unknown parameters.

c) Solve the inhomogeneous differential equations (5.12) numerically.

d) Use the solutions so obtained to define an improved set of scattered waves to replace E_L^n in equation (5.14).

e) Repeat steps (a)-(d), using the improved scattered waves.

5.3.2 The numerical solution of the second order differential equation.

The differential equation (5.12) is set in the form

$$\frac{d^2 F(X)}{dX^2} = f(X)\, F(X) + g(X) \qquad (5.17)$$

where

$$f(X) = l_2(l_2+1)\, X^{-2} - k_\nu^2$$

and

$$g(X) = U F$$

which can be solved using Numerov method (Melkanoff et al 1966). In this method, equation (5.17) is replaced by the algorithm

$$\left(1-\frac{h^2}{12} f_{i+1}\right) F_{i+1} = \left(2+\frac{5h^2}{6} f_i\right) F_i - \left(1-\frac{h^2}{12} f_{i-1}\right) F_{i-1} + \frac{h^2}{12}\left(g_{i+1} + 10 g_i + g_{i-1}\right) \qquad (5.18)$$

where $h = x_{i+1} - x_i$ and in general F_{i+1} denotes $F(x_{i+1})$. The value of h was set to equal 0.02 for $X < 0.4\, q_s$ and 0.1 otherwise.

When X is large, a test for the asymptotic solution was performed using Burke and Schey (1962) method. This method is based on the idea that once the potential has reached its asymptotic form, and the exchange terms can be neglected, the solution of (5.12) may be written as

$$E_i^3 \sim \sum_j \left[\sin(k_j R) \sum_{p=0}^{\infty} a_p^{ij} R^{-p} + \cos(k_j R) \sum_{p=0}^{\infty} b_p^{ij} R^{-p} \right] \tag{5.19}$$

where j is the sum over all different values of k_j appearing in the coupled-channel equations. Substituting equation (5.19) into (5.12) when only the asymptotic forms of the potentials are included, the following recursion relations for the coefficients a_p^{ij} and b_p^{ij} are obtained.

$$\begin{aligned}
&(k_i^2 - k_j^2)\, a_p^{ij} + \left[(p-1)(p-2) - l_i(l_i+1) \right] a_{p-2}^{ij} + \\
&\qquad 2k_j(p-1)\, b_{p-1}^{ij} = -\sum_{m=0}^{N} \sum_{\lambda} C_{im}^{\lambda}\, a_{p-\lambda-1}^{mj} \\
&(k_i^2 - k_j^2)\, b_p^{ij} + \left[(p-1)(p-2) - l_i(l_i+1) \right] b_{p-2}^{ij} - \\
&\qquad 2k_j(p-1)\, a_{p-1}^{ij} = \sum_{m=0}^{N} \sum_{\lambda} C_{im}^{\lambda}\, b_{p-\lambda-1}^{mj}
\end{aligned} \tag{5.20}$$

where C_{im}^{λ} are the asymptotic coefficients of the potentials.

The coefficients a_o^{ij} and b_o^{ij} are set to give the leading term in the expansion of e_L^+, they are

$$a_o^{ij} = -(-i)^{l_i+1} \delta_{k_i k_j} \tag{5.21}$$

and

$$b_o^{ij} = (-i)^{l_i} \delta_{k_i k_j}$$

Having determined a_p^{ij} and b_p^{ij} from equations (5.20), the maximum number of terms in the infinite sum over P and the approximate value of the asymptotic distance, say R_a, are calculated to a required accuracy ($1:10^3$) in the expansion for E_i^B .

when $X \geq R_a$, F is set as

$$F_L^n \sim A\, S_L + B\, T_L^{n-1}\, E_L^B \qquad (5.22)$$

and on comparing the values of the left-hand side of equation (5.22) with those values of the right-hand side for two successive values of X, A and B can be obtained. This method provides a valuable criteria for stopping the numerical solution of equation (5.17) when the value of B is equal to 1. The scattered wave function E_L^n is now

$$E_L^n = (F_L^n - A\, S_L) \Big/ T_L^n$$

which is to be iterated again.

5.3.3 Numerical evaluation of the integrals.

To evaluate the scattering amplitude T_L^n from equation (5.15), different integrals arise due to the matrix U they are

a) $\int_0^\infty S_L\, V_{ij}\, F_j \, dX$ from the direct potentials contribution.

b) $\int_0^\infty dX\, S_L \int_0^\infty dX'\, W_{ij}(X,X')\, F_j(X')$ from the exchange potentials contribution.

c) $\int_0^\infty dX\, S_L \int_0^\infty dX'\, H(X,X')\, F_0(X')$ from the second order potential contribution.

Nearly all of the above integrals were performed using the method of Clenshaw and Curtis (1960), because it is one of the most economical of all methods in the sense of accuracy obtained for a given number of points and it allows precise and reliable error estimates for each number of points. The implementation of the method was based on the work of O'Hara and Smith (1968) and Oliver (1972) from which the error estimates were also taken.

The direct potential matrix elements were tabulated for small values of X while their asymptotic forms were used for large X. The long range behaviour of some potentials makes the integral in (a) slowly convergent. For this case, the infinite limit was set to the asymptotic distance (R_a) and the remaining contribution was calculated analytically by expanding S_L as

$$\mathrm{Sin}(X-\tfrac{1}{2}\pi)P_L(X^{-1}) + \mathrm{Cos}(X-\tfrac{1}{2}\pi)Q_L(X^{-1})$$

with the same expression for C_L. The polynomials $P_L(X^{-1})$ and $Q_L(X^{-1})$ are given by Abramowitz and Stegun (1965). This expansion together with the asymptotic expansion of V_{ij} will lead to linear combinations of integrals of the form

$$\int_{R_a}^{\infty} \mathrm{Cos}(aX)X^{-n}\,dX \qquad \text{and} \qquad \int_{R_a}^{\infty} \mathrm{Sin}(aX)X^{-n}\,dX \qquad (5.23)$$

which are calculated using their recursion relations and the auxiliary functions given by Abramowitz and Stegun (1965).

The exchange terms $W_{ij}F_j$ were evaluated using Simpson's rule and the second integral over the exchange terms was calculated by **the Clenshaw-Curtis method. The** presence of the bound state wave functions in the exchange terms makes the integral rapidly convergent.

The symmetry property of the second order potential in X and X' was used in tabulating the kernel $H(X, X')$ only for values of $X' < X$. The method of Winters (1974) was followed in evaluating $H(X, X')$ in which $Z_{\lambda\lambda}(P^2_{n_0 S}|XX')$ of equation (5.9) are linear combinations of the integrals

$$M_\lambda(a|X\ X') = A_\lambda(a|X\ X') + B_\lambda(a|X\ X') + C_\lambda(a|X\ X')$$

where

$$A_\lambda(a|X\ X') = (X_< X_>)^{-\lambda-1}\int_0^{X_<} dt\ t^{2\lambda+2}\,\mathrm{EXP}[-at]$$

$$B_\lambda(a|X\ X') = \left(\frac{X_<}{X_>}\right)^{\lambda}\frac{1}{X_>}\int_{X_<}^{X_>} t\,dt\,\mathrm{EXP}[-at]$$

$$C_\lambda(a|X\ X') = (X_< X_<)^{\lambda}\int_{X_>}^{\infty} dt\ t^{-2\lambda}\,\mathrm{EXP}[-at] \qquad (5.24)$$

Evaluation of the integrals A_λ, B_λ and C_λ follows from the recursion relations that govern them and their initial values; there derivation is given in Appendix (D). As pointed out by Winters (1974), the recursion relation for $A_\lambda(a|X_< X_>)$ becomes unstable in the forward direction when $\lambda > aX_<$. For this case the backward recursion relation was used starting with a large value of λ. The behaviour of $H(X,X')$ in the limit of $X' \longrightarrow \infty$ is worth examining.

Consider

$$Z_{\lambda\lambda}(P^2_{n_0 S}|X X') - \sum_{n''_1}^{N} Y_\lambda(P_{n_0 S} P_{n'_1}|X)\, Y_\lambda(P_{n''_1} P_{n_0 S}|X')\, \delta_{\lambda l''_1} \tag{5.25}$$

which, from the properties of A_λ, B_λ and C_λ, has an $X_>^{-\lambda-1}$ behaviour and the leading term in the asymptotic region comes from $\lambda = 1$. The asymptotic form of $H(X,X')$ in the leading term becomes

$$H_L(X,X') \sim \frac{-i\bar{k} X X'}{3(2L+1)}\Big[L\, j_{L-1}(\bar{k}X_<)\, h^1_{L-1}(\bar{k}X_>)(1-\delta_{L0}) + \nu\, j_\nu(\bar{k}X_<)\, h^1_\nu(\bar{k}X_>)\Big]\frac{f(X_<)}{X_>^2} \tag{5.26}$$

where the function $f(X_<)$ is calculated from equation (5.25), $\nu = 1$ when $L = 0$ and $\nu = L+1$ otherwise.

Interpolation of $H(X, X')$ was avoided when X and X' are small, because in this case the kernel $H(X, X')$ changes rapidly. The asymptotic behaviour of $H(X, X')$ was used to calculate the contribution of the integral for large values of X. This was done by setting $H(X, X')$ as

$$H_L \sim A_1 h^1_{L-1}(\bar{k}X_>)(1-\delta_{L0}) + A_2 h^1_\nu(\bar{k}X_>) \tag{5.27}$$

which when substituted for two successive values of $X_>$ will lead to a set of linear equations for A_1 and A_2.

Using the expansion of h_L^1 and F_L^n, linear combinations of the integrals of equation (5.23) were obtained and calculated in the same method as mentioned before. The method of Corbato and Uretsky (1959) was implemented for generating the spherical Bessel function $J_L(X)$.

5.3.4 Corrections for higher partial waves.

The integro-differential equations were solved for values of L up to 15 partial waves. The contribution from the exchange terms was negligible for values of L higher than 10. The scattering amplitudes for higher partial waves (> 15) were calculated in the unitarized Born approximation (Seaton 1961). The scattering amplitude in this approximation is defined as

$$T_L^{II} = (-2iR)(1-iR)^{-1} \tag{5.28}$$

where

$$R_{ij} = -(k_i k_j)^{1/2} \int_0^\infty S_{L_i}(k_i X)\, V_{ij}\, S_{L_j}(k_j X)\, dX \tag{5.29}$$

The differential cross section was calculated using equation (2.84). The total cross section for the excitation of the state nP_m with magnetic quantum number m is from equations (2.84) and (1.44)

$$Q(nS - nP_m) = \frac{1}{k_{nS}^2} \sum_S (2S+1) \sum_{\substack{l_2 l_2' \\ L L'}} i^{L-L'} [(2L+1)(2L'+1)]^{1/2} \times$$

$$T^{LS} T^{*L'S} \langle l_2, -m\, m | L 0 \rangle \langle l_2', -m\, m | L' 0 \rangle\, \delta_{l_2' l_2} \tag{5.30}$$

where S is the total spin.

Finally the total cross section for a transition from an ns level to $n'l'_1$ is

$$Q(ns, n'l'_1) = \sum_{S,L,l_2} \frac{(2S+1)(2L+1)}{k_{ns}^2} \left| T^{LS}_{l_2} \right|^2 \qquad (5.31)$$

There are two sources of inaccuracy in the calculations of the iterative method. The first due to stopping the integration of the differential equation (5.12) in the asymptotic region is of the order 3%. The second, due to stopping the iteration process was of order 2.5%. Some difficulty was found in obtaining results for the partial wave L=0 with sufficient accuracy. We found it very helpful to use the final solution at higher energy as a zero order solution for a lower energy.

CHAPTER 6.

Present Calculations on the Scattering of Electrons by Alkali Atoms.

6.1 Introduction.

In this chapter, two different sets of calculations are presented. The first set are the results in the impact parameter method (IP). The calculations in this method are of three types, where they differ to the extent to which the second order potentials were included. They are:

a) IP.1, the impact parameter close coupling method where equation (4.10) was solved with the inclusion of n_oS and n_oP states but omitting the second order potentials in all channels.

b) Method IP.2, is as method IP.1 but with the inclusion of the second order potential in the elastic channel.

c) Method IP.3, uses the three-channel coupling, where the second order potentials were included in all channels.

The second set of calculations are in partial wave form, again three different types of results are presented:

1) Method PW.1, is the two-state (n_oS, n_oP) partial wave close coupling approximation where equation (5.10) was solved when the exchange terms and the second order potentials were omitted.

2) Method PW.2, is as method PW.1 but the exchange terms were included.

3) Method PW.3, is the two-state partial wave close coupling approximation where equation (5.10) was solved.

The calculations in the impact parameter method are presented for the electron energies at 10, 25, 50, 100, 200 ev. The partial wave results are presented for the electron energies at 10, 15, 20, 25, 50 ev, and both calculations are given in tables (6.1 - 6.7) for e-Li and e-Na scattering.

6.2 Total Cross Section for e-Li Scattering.

There have been several previous theoretical studies of the e-Li scattering. Burke and Taylor (1969) have calculated the elastic and the resonance excitation cross section in the two-state close coupling approximation. Walters (1973) has calculated the elastic and the resonance excitation cross section in the Glauber approximation (GA). The elastic cross section has been calculated in the polarized eikonal approximation (Sarkar et al 1973) and in a model based on a simple adiabatic R^{-4} polarization potential (Inokuti and McDowell 1974). Several other models have been applied to the calculations of the resonance excitation cross section. These are, the distorted wave polarized orbital method (DWPO II) by Kennedy et al (1976), McCavert and Rudge (1970) calculations based on a variational model, and the calculations of Vainshtein et al (1965) and of Felden and Felden (1973) based on a model that makes allowance for the repulsion of the electrons in the wave function.

On the experimental side, there have been some recent measurements for the resonance excitation cross section. Different normalization schemes have been adopted for these various measurements to obtain the absolute cross section. Williams et al (1976) who measured the elastic and the resonance excitation differential and integrated total cross sections, normalized the sum of the elastic plus the inelastic cross section in arbitrary units to the total cross section of Kasdan et al (1971) after subtracting the ionization cross section at each energy. The most recent measurements of Zapesochnyi et al (1975) for the resonance excitation cross section are normalised to the Born approximation cross section at 30x threshold energy. On the other hand, Leep and Gallagher (1974) normalized their values for the resonance excitation cross section to the Born approximation cross section at 1404 ev.

The measurements of Williams et al (1976) for the resonance excitation and those of Zapesochnyi et al (1975) are in agreement to 5% and they are larger than those values of Leep and Gallagher (1974) by about 15% in the energy region 10 - 30 ev.

Mathur et al (1971, 1972) have calculated the elastic and the resonance excitation cross sections in the Glauber approximation where the core effect was ignored. The work of Walters (1973) shows that the core effect makes a significant contribution to the elastic cross section at the higher energies. Their resonance excitation cross sections are in disagreement with the calculations of Walters.

The method PW.2 is similar to the work of Burke and Taylor (1969). Our results in this method for the elastic and the resonance excitation cross sections differ from those of Burke and Taylor by about 5 - 8%. We believe that this difference is due to the use of different target wave functions in the calculations. We have calculated the Born approximation for the elastic and the resonance excitation cross sections which are shown in Figures (6.1 and 6.2), and our values are larger by about 5% than the calculated Born cross sections of some other authors (Walters 1973; Greene and Williamson 1974). We do not show the work of Burke and Taylor and the work of Mathur et al in figures (6.1) and (6.2) in the light of the previous arguments.

6.2.1 The Elastic Cross Section.

Figure (6.1) shows the elastic cross section calculated in the method IP.2, PW.2 and PW.3 together with those of GA results, Born approximation and the measurements of Williams et al (1976).

The agreement between the measurements and the theoretical values is very poor in the lower energy region, where the measured values are twice the values of PW.3 at 10 and 20 ev. The discrepancy between the GA values and the PW.3 results is about 10 - 15% in the energy region 50 - 10 ev, while there is a good agreement between the IP.2 and those of GA results in the energy range 20 - 200 ev. The Born cross sections are larger than the other theoretical values.

The other calculations which are not shown in the figure, are those of Sarkar et al (1973) which predict too large a cross section. It is argued (Inokuti and McDowell 1974) that the polarized eikonal approximation accounts for the polarizability twice. The polarized orbital method (Dai and Stauffer 1971 and private communication) and the Inokuti and McDowell (1974) calculations based on the adiabatic polarization potential, predicted cross sections close to those of Sarkar et al (1973). The work of Walters (1976) showed that the considerable difference between the calculations of Inokuti and McDowell and the other calculations based on the close coupling approximation or the Glauber approximation is due to the use of the adiabatic polarization potential. The results of PW.2 and PW.3 confirm the conclusion that at the higher energies, the long range interaction (which is accounted for through the second order potential) is not dominant, unlike the results of the polarized eikonal method, the polarized orbital method and the work of Inokuti and McDowell would suggest.

6.2.2 The Resonance Excitation

Figure (6.2) displays the results in the PW.3 and IP.2 methods along with the Born approximation, the GA and the DWPO II cross sections and the experimental data of Leep and Gallagher (1974), Zapesochnyi et al (1975) and Williams et al (1976). In the energy region 10 - 30 ev the results of PW.3 and those of DWPO II are in very good agreement with the measurements of Williams et al and those of Zapesochnyi et al. On the other hand, the IP.2 and the GA results show a better agreement/

agreement with the data of Leep and Gallagher in the same energy region. The GA results show a maxima earlier than the other theoretical calculations. In the energy region 30 - 50 ev, the results of PW.3 and the DWPO II cross sections are in better agreement with the data of Leep and Gallagher, while the GA cross sections are about 5% larger than the PW.3 values and the IP.2 cross sections are 10% smaller than the PW.3 values in the same energy region. A good agreement to 10% between the data of Leep and Gallagher and the theoretical predictions is noticed in energy region 50 - 200 ev. Because of the conflicting results from the experimental measurements, no decisive conclusion can be drawn for the agreement between the data and the theoretical predictions. The work of Felden and Felden (1973) (not shown in the figure) in the framework of the modified model of Vainshtein, predicted small cross sections. Their values are smaller than those in the IP.2 by about 50 - 30% in the energy region 10 - 50 ev, and they show an earlier maxima. Other calculations not shown are those of McCavert and Rudge (1970). Their values show an improvement over the Born cross sections, but are still larger than the other theoretical cross sections in the lower energy region (<20 ev) where they produced their results.

6.3 Total Cross Section for e-Na Scattering.

The theoretical models which have been applied to the scattering of electrons from lithium atoms, have been applied as well to the scattering of electrons from sodium atoms. The Glauber approximation (Walters 1973; Tripathi et al 1973a) and the polarized orbital method (Garrett 1965) have been applied to calculate the elastic cross section. The close coupling approximation (Barnes et al 1965; Carse 1972; Korff et al 1973), the Glauber approximation (Walters 1973, Tripathi et al 1973a), the DWPO II (Kennedy et al 1976), the modified model of Vainshtein (Felden and Felden 1973) and the variational calculations of McCavert and Rudge (1970) have been applied to the resonance excitation.

Enemark and Gallagher (1972) have measured the resonance excitation cross section, using the Born approximation cross section at 1000 ev for the normalization of their values. The experimental data of Zapesochnyi et al (1975) for the resonance excitation cross sections are larger than those of Enemark and Gallagher by about 30 - 60% in the energy region 40 - 10 ev.

6.3.1 The Elastic Cross Section

We show in Figure (6.3) the present results in the method PW.2, PW.3 and IP.2 compared with the GA calculations (Walters 1973) and the Born approximation cross sections. One can notice that the Born approximation cross sections overestimate the elastic cross sections compared with the other calculations. The cause for this large difference comes from the S -partial wave (l=0) which violates the unitarity bound and contributes 60% of the total cross section.

Walters (1976) has calculated the total cross section (the sum of the contributions from the elastic, inelastic and ionization cross sections) and compared them with the measured values of Kasdan et al (1973). The experimental data are larger than the theoretical cross sections at the intermediate energies. The discrepancy is about 10% at 10 ev, but increases for higher energies, being 60% at 50 ev. The difference between the results in the PW.3 method and the GA calculations will account for the 10% disagreement with the data at 10 ev. But we do not see how the large difference between the data and the theoretical calculations at high energies can be explained, since the difference between the GA calculations and the present results is small at these high energies. In conjunction with the results for the elastic scattering of electrons from lithium atoms, one would speculate some doubts on the total cross sections of Kasdan et al (1971; 1973) for the higher energies.

The calculations of Tripathi et al (1973a) are excluded from the figure because they ignored the core effect, while the results of Garrett (1965) are too large. The large cross sections from the polarized orbital method at intermediate energies are due mainly to the use of the adiabatic approximation which has doubtful validity in this energy region.

6.3.2. The Resonance Excitation

Different authors (Barnes et al 1965; Carse 1972 and Korff et al 1973) have calculated the resonance excitation cross section in the method PW.1. The results of Barnes et al and those of Carse are in agreement to within 5%, they are 10% larger than the results of Korff et al. Korff et al argue that the/

the difference between the two sets of results is due to the use of different target wave functions. The present results in the method PW.1 are closer to those of Barnes et al and Carse.

Seaton (1962) has calculated the resonance excitation cross section in the method IP.1. His cross sections are larger than the present IP.1 results. The difference between the two results is due to the distortion potentials which were ignored in Seaton's work in addition to the replacement of the interaction potentials by their asymtotic forms.

Figure (6.4) shows the results in the PW.3 and IP.2 methods compared with the Born approximation, GA of Walters (1973), DWPO II (Kennedy et al 1976) and the experimental data of Enemark and Gallagher and Zapesochnyi et al. The calculations of Korff et al (1973) in the seven-state close coupling approximation (not shown) are in very good agreement with the data of Enemark and Gallagher. The measurements of Gould (1970, quoted by Enemark and Gallagher 1972) are 10% larger than those of Enemark and Gallagher. Enemark and Gallagher suggested that the different cascade corrections and normalizations could have caused the 10% difference between the two measurements.

In the energy region 10 - 30 ev, the results in the PW.3 and DWPO II methods are in agreement to 5% and are larger than the data of Enemark and Gallagher by about 20 - 6%. On the other hand, the data of Zapesochnyi et al are larger than the two calculations by about 20 - 12% in the same energy region. The results in the IP.2 method are in better agreement with the data of Enemark and Gallagher. We feel that the agreement achieved by the IP.2 and the GA calculations with the data of Enemark/

Enemark and Gallagher below 20 ev is fortuitous. This can be seen from the GA results where they show an earlier maxima and therefore the agreement is an accidental one. On the other hand the results in the IP.1 method are smaller than the results in the PW.1 method in the same energy region, and since they are the results of the calculations of the same equation we can not expect the IP method to yield better results if we suppose that the data of Enemark and Gallagher is reliable.

In the region 30 - 50 ev, the PW.3 results are in agreement with the data of Enemark and Gallagher. In this energy region all the theoretical calculations (apart from the Born approximation) are in good accord with the experimental data to 5%. In the energy region 50 - 200 ev, the IP.2 results are smaller than the other calculations, but they start to joint the curves of the other calculations at 200 ev. In this energy region the agreement with the data of Enemark and Gallagher is fairly good.

The other calculations not mentioned so far are the GA calculations of Tripathi et al (which are in disagreement with the calculations of Walters 1973), the calculations of Felden and Felden (1973) and those of McCavert and Rudge (1970) which are respectively smaller and larger than the other theoretical calculations as in the lithium case.

6.4 Discussion.

Comparing the results in the IP.1 method with those of PW.1 results in tables (6.1 - 6.4) for the elastic and the excitation cross sections, shows the differences between the IP and the partial wave approximations. These differences are purely due to the semi-classical approximation, since we are solving the same equation. We can see a substantial difference between the values of the two sets for the elastic as well as for the excitation cross sections. The discrepancy is large at the lower energies and is about 8% and 10% at 50 ev for the elastic and the excitation cross sections respectively.

The second order potential makes a substantial contribution to the elastic cross sections, while the contribution to the resonance transition is less significant. Comparing the results for the resonance transition from the IP.2 and IP.3 methods, shows that the effect of including the higher states is insignificant for the e-Li results. This is in agreement with the conclusion of Burke and Taylor (1969) who studied the effect of 3d-state coupling in the low energy region. This is not the case for the resonance transition of e-Na scattering, where the coupling to the 3d-state makes an important contribution to the cross section (Korff et al 1973). This is also the case for the calculations in the IP.2 and IP.3 methods which leads us to believe that the second order potential in the elastic channel (IP.2 and PW.3 methods) does not account fully for the effect of the coupling to the 3d-state. The three channels must be included to obtain the right contribution from the higher states. The extension of the three-channel method to the lower energy region is very desirable, but the numerical computations become time consuming even when the IP method is applied.

6.5 The Differential Cross Section for e-Li Scattering.

6.5.1 The Elastic Differential Cross Section.

The results of the present calculations in the PW.3 and IP.2 methods are displayed in figures 6.5a) - 6.5d) for energies of 10, 20, 25 and 50 eV.

At 10 eV there is a slight difference between the results from PW.3 and PW.2 methods and their agreement with the measurements of Williams et al (1976, they quote an error of $\pm$35%) is poor. They predict the shape of the angular distribution but the data are larger than the present work for angles smaller than 100°. Williams et al have extrapolated their values for angle smaller than 10° and their values in the forward direction are 50% larger than the present calculations. The GA calculations at 11 eV predict cross sections at 1.3° close to the extrapolated values of Williams et al.

The results from IP.2 and GA calculations are in good agreement with the results from the PW.3 method for small angles, up to 60° for the GA and 40° for the IP.2 method. The two calculations decrease rapidly for large angles.

At 50 eV, the IP.2 and GA results are in good agreement with each other and are in agreement with the PW.3 results at angles smaller than 60°. The profile for the other energies is the same.

6.5.2 The Resonance Excitation Differential Cross Section.

We compare in figures 6.6a) - 6.6d) at 10, 20, 25 and 50 eV, the PW.3 and IP.2 results along with the GA calculations at 11 and 54.4 eV, the DWPO II results at 12.1, 20, 27.2 and 54.4 eV and the data of Williams et al.

At 10 ev, the DWPO II and the GA calculations are in better agreement with the data in the forward direction, but the PW.3 results are in better agreement with the data elsewhere. The results from the IP.2 method are in very good accord with the PW.3 results for small angles, but they do not show the deep minimum at large angles.

At the other energies, the same pattern can be noticed, where at 50 ev the DWPO II and the GA calculations are strongly peaked in the forward direction, but they are in good agreement with the present calculations for small angles. The GA calculations become vanishingly small beyond 60^{o}, while the DWPO II are in better agreement with the PW.3 results at large angles.

In general, the differential cross sections for e-Li scattering show a minimum around $90-100^{o}$ and are strongly peaked in the forward direction. The present results fail to show the strong peaking in the forward direction, but their predictions of the shape of the scattering angular distributions are quite satisfactory.

6.6 The Differential Cross Section for e-Na Scattering.

6.6.1 The Elastic Differential Cross Section.

In figures 6.7a) - 6.7e) we compare the present results at 10, 15, 20, 25 and 50 ev with the available data and the GA calculations.

The experimental data of Geneau and Reichert (1972) in arbitrary units were normalised to the PW.3 results at the energies 10, 15 and 20 ev. The agreement between the data and the PW.3 results is fair, where the oscillating structure is predicted satisfactorily but the height and widths of the oscillations/

oscillations are not in very good accord with the measurements. The GA calculations at 11 eV are in good agreement with the present results for angles smaller than 60° but they do not show the oscillatory structure at large angles. The IP.2 results are in good accord with the PW.3 results for angles smaller than 40°. The variations between the PW.3 and PW.2 results are small in all the angular range and they show an oscillatory behaviour at all the energies considered. The agreement between the PW.3 results and the IP.2 and GA calculations at 50 eV is good for angles smaller than 50°.

6.6.2 The Resonance Excitation Differential Cross Section.

Figures 6.8a) - 6.8d) at 10, 20, 25 and 50 eV display the results from the PW.3 and IP.2 methods along with the GA results at 11 and 54.4 eV and the DWPO II calculations at 12.1, 22.1 and 54.4 eV.

At 10 eV, the GA and DWPO II results are close to each other but are larger than the present calculations at the forward peak, and are smaller elsewhere. Here again, the IP.2 results are in good accord with the PW.3 results for small angles. The results from the PW.3 method show an oscillatory structure in the large angle region for all the energies considered, while the DWPO II calculations show a shallow minimum in the same angular range.

At 50 eV, the agreement between the theoretical calculations and the measurements of Shuttleworth et al (1977) is very good at small angles (where they are available). The GA calculations at this energy become very small for angles larger than 40°, while the DWPO II show a very deep minimum at 100° and are close to the PW.3 for large angles.

However, the oscillations at large angles are believed to be non-physical. Perhaps the switch to Born approximation in the calculations caused such oscillations. In conjunction with the results for the resonance excitation of e-Li scattering, we notice that the present calculations predict small cross sections in the forward peak, while the calculations in the DWPO II and GA methods, though large, yield better predictions at this angle. We thought that the neglect of the coupling of the higher levels to the 3^1P level would explain the difference, but the differential cross sections in the IP.3 method at 50 eV (which accounts for the effect of the higher levels) do not make this substantial difference between the two results. The work of Moores and Norcross (1972) in the framework of the four-state close coupling approximation does not show a strong peaking in the forward direction when compared with the DWPO II results at 5 eV (see Kennedy 1976).

6.7 The Polarization Fractions and the Fano and Macek Parameters for Li and Na.

Experimental determinations of the total and differential cross sections produced by electron impact have provided important tests for theoretical models of electron-atom scattering processes. However, obtaining absolute cross sections is a difficult task for the experimentalists to overcome and, as we have seen, a considerable disagreement between the experimental data is mainly due to different normalization procedures.

The polarization of atomic line radiation and λ parameter are measurable quantities, but free from normalization difficulties and therefore they provide a better test for the theory when the excitation to the nP_m level is involved.

The percentage polarization of the resonance line of Li and Na at right angles with the incident beam is (Flower and Seaton 1967)

$$P = 300\ x\ /\ (12\ Q_o + 24\ Q_1 + X) \qquad (6.1)$$

where $X = (9a-2)\ (Q_o - Q_1)$ and Q_o and Q_1 are the excitation cross sections of the level nP_m with magnetic quantum number m=o, ± 1 respectively. The value of a depends on the ratio of the hyperfine structure energy separation to the natural line width and is 0.413 for ^{6}Li and 0.288 for Na.

In figures (6.9) and (6.10) we show the polarization fractions calculated in the PW.3 and IP.2 methods together with the DWPO II calculations and the measurements of Leep and Gallagher for the case of Li and Enemark and Gallagher and Gould (1970, quoted in Enemark and Gallagher) for the case of Na. The calculations of Tripathi et al (1973b) in the Glauber approximation are also shown. However, the disagreement between the total cross sections calculated by Walters (1973) and those of Mathur et al (1972) and Tripathi et al (1973a) for Li and Na respectively, cast doubt on the polarization fractions calculated by Tripathi et al.

The present calculations in the PW.3 method are lower than the experimental data for Li and Na, their agreement with the data is only fair. On the other hand, the DWPO II values are higher than the data in the same energy region considered here. The predictions of the polarization fractions by the IP method are very poor as is noticed from the figures. Recently, Kumar and Srivastava (1976) have calculated the polarization fractions for Li in the Glauber approximation including the core effect. Their values are close to the DWPO II values in the low energy region and they are in agreement with the data

of Leep and Gallagher to 2% above 50 eV.

In table (6.7) the polarization fractions calculated in the PW.3 and PW.2 methods are compared. The small variations between the two calculations suggest that the two-state close coupling approximation is good for predicting the polarization fractions in the intermediate energy region.

Fano and Macek (1973) have developed a comprehensive theory for the connection between the distribution of the emitted radiation and the relevant scattering amplitude. This is expressed in terms of an orientation vector which is proportional to the expectation value of the angular momentum of the target atom and an alignment tensor whose components are proportional to the mean values of expressions quadratic in the components of the target angular momentum. The analysis of the parameters for the np-state of Li and Na atoms is similar to that for H atoms. Following Morgan and McDowell (1975), the wavefunction for this state is

$$|np\rangle = a_o|np,0\rangle + a_1 [|np,1\rangle - |np,-1\rangle] \qquad (6.2)$$

where $a_\nu(\nu=o,\pm1)$ is the amplitude for exciting the state $|np, M_L=\nu\rangle$.

We may define the quantities

$$\langle a_\mu, a_\mu \rangle = \sigma_\mu \qquad \mu = 0, \pm 1 \qquad (6.3)$$

where σ_μ is the differential cross section for the excitation of the $M=\mu$ magnetic sub level and the brakcets imply summation over the spin states.

The general expression in terms of the T-matrix elements for these quantities is

$$\langle a_\mu, a_\nu \rangle = \frac{1}{16\pi^2} \frac{k_f}{k_i} \left[T_{i_f}^{*+}(\mu)\, T_{i_f}^{+}(\nu) + 3T_{i_f}^{*-}(\mu)\, T_{i_f}^{-}(\nu) \right] \quad (6.4)$$

where the superscripts + and - denote singlet and triplet and k_i and k_f are the initial and final wave vectors. The off diagonal term $\langle a_0, a_1 \rangle$ is complex.

If $\sigma = \sigma_0 + 2\sigma_1$ is the total differential cross section for the excitation, the dimensionless parameter, λ, is defined as

$$\lambda = \sigma o / \sigma \quad (6.5)$$

For an s-p transition, the alignment and orientation parameters of Fano and Macek can be written, in the collision plane, as (see Morgan and McDowell, 1975)

$$\begin{aligned} A_0^{col} &= \tfrac{1}{2}(1 - 3\lambda) \\ A_{1+}^{col} &= \sqrt{2}\, X \\ A_{2+}^{col} &= \tfrac{1}{2}(\lambda - 1) \\ O_{1-}^{col} &= -\sqrt{2}\, Y \end{aligned} \quad (6.6)$$

where

$$X = \mathrm{Re}\, \langle a_0, a_1 \rangle / \sigma$$

$$Y = \mathrm{Im}\, \langle a_0, a_1 \rangle / \sigma$$

Note that the parameters X and Y are dimensionless quantities also. The problem is then reduced to evaluating the parameters λ, X and Y.

We show in figures 6.11a) - 6.11c) for Li and 6.12a) - 6.12c) for Na, the parameter $\lambda(\theta)$ calculated from the PW.3 method. These are compared with the DWPO II calculations of Kennedy (1976) at 50, 25 and 10 eV respectively.

For the Li case, the agreement between the two calculations is good only at 50 eV. The common feature between the two results is their predictions for the two minima, but the

positions and the depths of the minima are different in the two results.

The structure of $\lambda(\theta)$ for the Na case is more complicated, where three minima appear at high energies. Again here the agreement between the two calculations is only satisfactory for angles smaller than 40^{o}.

Figures 6.11d) and 6.12d) display the PW.3 results for Li and Na respectively, comparing the variations of $\lambda(\theta)$ at the different energies 10, 15 and 20 eV.

The results from the IP method cannot be compared with the other calculations since the quantization axis adopted for calculating the scattering amplitude is not along the incident momentum.

The parameters X and Y are calculated at several energies. Fig. (6.13) and (6.14) show the X parameter for Li and Na atoms respectively and the results are compared with the calculations of Kennedy (1976). The two calculations are in disaccord. For Li case, the X parameter exhibits two minima and three maxima at the lower energies (10 eV). The first minimum shifts towards the small angle region and becomes a dip at higher energies (50 eV). The behaviour of the X parameter for the Na case is similar to the behaviour of Li at small angles but it has only two maxima.

The Y parameter is displayed in fig. (6.15) and (6.16) for Li and Na atoms respectively along with the calculations of Kennedy. It appears that there is a difference in sign between the present calculations and those of Kennedy, perhaps this is due to a difference in defining the Y parameter. Morgan (private communications) mentioned the wrong sign in all their published papers. The Y parameter for Li case makes

severe oscillations at large angles and higher energies (50 eV). The structure for the Na case is a complicated one.

Finally, we conclude this chapter by the following remarks:

The effect of exchange and the second order potential is very noticeable at the lower energies for the elastic cross section and to a lesser extent for the excitation cross section. The impact parameter method while giving total cross section to 20% accuracy in the low energy region, fails to give the right shape of the differential cross section at large angles. It can be said that the IP method predicts a total cross section to 10% accuracy for energies larger than twenty five times the first threshold energy, and it yields good predictions for the differential cross sections for angles smaller than 40^{o}. Its predictions for the polarization fractions are very poor.

CHAPTER 7.

The Excitation of the n=3 levels of Helium by Electron and Proton Impact.

7.1 The distorted wave approximation.

In this chapter, the numerical calculations for the excitation of the n=3 levels of helium by electron and proton (and some results for the positron scattering) impact, in the distorted wave approximation, are presented. The general theory of the impact parameter approximation was discussed in chapter four, its application is straight forward. The couplings between the n=3 levels of helium and the couplings to the ground state and to the 2^1P states are retained. In the notation of chapter four the coupled channel equation becomes

$$ik_o \frac{\partial C_i(\rho,z)}{\partial z} = \sum_{j=0}^{N} V_{ij}(\rho,z)\, C_j(\rho,z)\, \exp(i\epsilon_{ij} z k_o^{-1}) + \sum_{k} V_{ik}(\rho,z)\, C_k(\rho,z)\, \exp(i\epsilon_{ik} z k_o^{-1}) \qquad (7.1)$$

where $C_k(\rho,z)$, ($k = {}^1S, {}^2P$ states)

are the probability amplitudes for scattering by helium in the ground state and the 2^1P states respectively. These amplitudes are taken from an unpublished supplement to the works of Berrington et al (1973) and Begum et al (1973) in which allowance for distortion and absorption in the elastic channel was made by including the second order potential in the elastic channel. The indices i and j refer to the six n=3 levels of helium; 3^1S, 3^1Po, $3^1P_{\pm1}$, 3^1D_o, $3^1D_{\pm1}$ $3^1D_{\pm2}$.

The actual number of levels for the n=3 states is nine, but they are reduced to six levels only, when equation (4.21) is used. The forms of the coupled differential equations, neglecting the second order potential terms, for the levels (nl0), (nl1) and (nl2) are

$$ik_o \frac{\partial B_{nl0}}{\partial Z} = \sum_k V(nl0,k) B_k \, EXP(i\epsilon_{nl,k} Z k_o^{-1}) + \sqrt{2} \sum_j V(nl0,j) B_j \, EXP(i\epsilon_{nl,j} Z k_o^{-1})$$

$$ik_o \frac{\partial B_{nlm}}{\partial Z} = \sqrt{2} \sum_k V(nlm,k) B_k \, EXP(i\epsilon_{nlk} Z k_o^{-1}) + \sum_{n'l'm'} [V(nlm, n'l'm') + (-1)^{m'} V(nlm, nl'-m')] B_{n'l'm'} \qquad (7.2)$$

where $EXP(i\epsilon_{nl,n'l'} Z k_o^{-1})$

$j = nlm = n'l'm' = nP_1 , nD_1 , nD_2$

$k = nS , nS , nD_o$

The matrix elements in equation (7.2) are evaluated in a general form in Appendix A. The ground state and the 2^1P wave functions of helium were those described by Flannery (1970). For the excited states, the 3^1P and 3^1D wave functions of Goldberg and Clogston (1939) and 3^1S wave function of Cohen and McEachran (1967) were used. The coupled-differential equations (7.2) were solved numerically by a step-by-step iterative procedure using the five points formulas (Milne 1953). The differential cross sections and the total cross sections are calculated in the same manner as in chapter four.

To assess the effect of coupling between the n=3 levels and of coupling via the 2^1P level, the cross sections are obtained in a number of different approximations, for electron, proton and positron excitation, which are shown in tables (7.1), (7.2) and (7.3) together with the Born approximation for comparison. These approximations differ in the number of levels coupled through equation (7.1) as follows:

(1S – k) (two-state, three-state and four-state approximation, when only one element of the set k is included)

(1S – j) (seven-state approximation, all the elements of the set j are included and are coupled to 1S and to each other)

(1S — j + $2P_0$ + $2P_{\pm1}$) (nine-state approximation)

$$j=k = \{ 3^1S , 3^1P_0 , 3^1P_{\pm1} , 3^1D_0 , 3^1D_{\pm1} , 3^1D_{\pm2} \}$$

7.2 Excitation of helium by electron impact.

Recently, a large number of theoretical calculations have become available on the total cross sections for the excitation of helium from its ground state to the n=3 levels. These calculations were performed in a variety of different models. Some fall into the regime of semi-classical approximations, others are in Born approximation or its modified forms. They are, the ten-channel eikonal approximation (E10) of Flannery and McCann (1975), the second-order diagonalization (SOD) of Baye and Heenen (1974), the Glauber approximation (GA) (Chan and Chen (1974) for 3^1P excitation; Chan and Chang (1975) for 3^1D excitation), the distorted wave polarized orbital approximation (DWPO) (Scott and McDowell (1975) for 3^1S excitation), the second Born approximation (SBA) (Woollings and McDowell (1973) for 3^1D excitation) and the Born approximation (BA) of Bell et al (1969). The difference between the results in the semi-classical approximations(E10, SOD, GA and the present results) will be, mainly, due to the different combinations in the coupled channels and partly, due to the use of different wave functions for the helium atom. On the experimental side, different investigators (Moussa et al (1969) for n=3 levels; de Jongh and van Eck (1971), van Raan et al (1971) and Donaldson et al (1972) for 3^1P excitation) have measured the absolute total cross sections for the excitation of helium. Discrepancies exist between the various measured cross sections, particularly as to the position and magnitude of the peak in the cross section.

7.2.1 3^1S State Excitation of Helium.

The total cross sections for 3^1S excitation are shown in table (7.1). The variations in the cross section values due to different couplings are noticable. It is interesting to note that much of the change in the cross section that occurs when transitions via the 3^1P level are taken into account (going from column II to column III of table (7.1)) is cancelled when transitions via the 2^1P level are included (column IV). Figure (7.1) shows the nine-state results and the results of DWPO, E10, SOD, BA and the measurements of Moussa et al.

The agreement between the nine-state results and the measurements is good beyond 500 ev, they are 15% higher than the experimental values at 100 e v. At 400 e v , the measured cross sections show a sudden change which is not noticed in any of the theoretical calculations. The differences between the nine-state values and the E10 and the SOD values are due to the effect of coupling of different channels. The large discrepancy between the nine-state results and the SOD results which include the effect of twenty-two states, reflects the importance of coupling to higher levels. The DWPO (which allows for the effects of distortion in the initial channel, including polarization, and also for the distortion of the target by dipole polarization) results are very close to the nine-state results above 200 e v. This agreement may suggest that the adoption of the impact parameter approach for this transition is very reasonable beyond 200 e v.

7.2.2 3^1P State Excitation of Helium.

From table (7.1) it is seen that the difference between the cross sections calculated in the three approximations is quite small for the strong transition to the 3^1P level. Figure (7.2) shows the nine-state results compared with the BA, GA, E10 and SOD results, and the measurements of Moussa et al, Donaldson et al and those of de Jough and van Eck. The nine-state results are very close to those of BA, E10 and SOD results. In general, the maximum difference between the nine-state values and the lowest theoretical values does not exceed 20% at 100 e.v , while the discrepancy is very small at 1000 e v. The measurements of Moussa et al and those of de Jough and van Eck are 25% and 6% lower than the nine-state values at 100 and 1000 e.v respectively, while the measurements of Donaldson et al are 17% lower and 5% higher than the nine-state values at the same energies.

Within the errors of the experiments the agreement between the theoretical predictions and the measurements is satisfactory. The agreement of the Born approximation cross sections with the other calculations above 200 e.v., strengthens the conclusion that the Born approximation can provide total cross sections for the optically allowed transitions in helium which are accurate to within 10% above 200 e.v.

7.2.3 3^1D State Excitation of Helium.

The work of Woollings and McDowell (1973) in the framework of the second Born approximation, indicates that indirect coupling of the 3^1D level to the ground state via the 2^1P level is only important at small angles of scattering ($\Theta < 5^\circ$ for electrons) and is not expected to be important for the calculation of total excitation cross sections integrated over all solid angles. On the other hand, table (7.1) shows that the cross sections for the excitation of 3^1D level are very sensitive and more dependent on the approximation employed. The inclusion of the effect of 3^1P level caused a substantial increase, but this was cancelled by the effect of the 2^1P level. Similar evidence for the importance of the 2^1P coupling effect has been obtained by Somerville (1963) for the excitation of Hydrogen by electron impact. Figure (7.3) shows the nine-state results together with the SOD, E10, BA and GA results and the measurements of Moussa et al. The SBA results of Woollings and McDowell (1973), (not shown), are lower than those of GA results.

From the figure, it is seen that the $Q \times E$ values remain almost constant for energies higher than 600 e v. Agreement between the measurements and the theoretical values is very poor, they are 30% higher the nine-state results at 1000 e v. This large difference at such high energy can not be attributed to a deficiency in the approximations considered. It can be argued that the coupling from higher levels is not important, since the SOD results are very close to the present results for energies higher than 500 e.v. Moussa et al suggested that some sort of experimental inaccuracy might have caused this large discrepancy. The measurements of St. John et al (1964), (not shown), are still higher than

those/

those of Moussa et al, but they show a strong rise in Q_{*E} values at 200 e v and do not show a straight line behaviour above this energy.

7.3 Excitation of Helium by Proton Impact.

The theoretical calculations that exist, for the n=3 levels of helium are based on either Born approximation and distortion approximation (see Van Den Bos 1969a) or close coupling impact parameter approximation (Van Den Bos 1969b) and the SOD approximation (Baye and Heenen 1973c).

The work of Van Den Bos in the impact parameter approximation is very similar to this work but differs in the number of channels included. His nine-state calculations are similar to the present nine-state calculations except that the 2^1S level in his work is replaced by 3^1S level and our ground state wave function accounts for distortion and absorption in the elastic scattering channel. In general, the results of the two calculations show the same features.

There are few measurements for the excitation of 3^1P level of helium (Hippler and Schartner (1974); Hasselkamp et al (1971); Van Den Bos et al (1968); Thomas and Bent (1967)). The agreement between the measurements of Hasselkamp et al and those of Hippler and Schartner is very good (see Hippler and Schartner (1974)), but those of Van Den Bos et al (for E <150 kev) and those of Thomas and Bent (for E >150 kev, and they quote an error of 35%) are 10% higher than the measurements of Hippler and Schartner. For the 3^1S excitation, only the measurements of Van Den Bos et al (1968 for E<150 kev) and those of Scharmann

and/

and Schartner (1969a)are available. Van Den Bos et al suggested that their 3^1S excitation results are the less accurate cross sections in their measurements. Their values are higher than those of Scharmann and Schartner in the same energy region. Only the measurements of Van Den Bos et al ($E < 150$ kev) exist for the excitation of the 3^1D level.

7.3.1 3^1S State Excitation of Helium.

The situation for the proton excitation is very similar to the electron case. The variations due to different couplings are demonstrated in table (7.2). There is a difference of the order of 10% between the present results and those of the SOD results (see Figure 7.4). The measurements of Scharmann and Schartner (higher than Born approximation) show the same shape of Born approximation. On the other hand, the present results in the nine-state approximation and those of the SOD results have the same shape, which is different from that of Born approximation. The measurements of Van Den Bos et al agree to 10% with the nine-state and SOD results.

7.3.2 3^1P State Excitation of Helium.

Figure (7.5) shows the present nine-state results, SOD and BA results and the measurements of Hippler and Schartner and the measurements of Van Den Bos et al. There is, once more, a very good agreement between the various theoretical calculations and the experimental measurements. The nine-state results of Van Den Bos (not shown), are slightly higher than the present calculations. The discrepancy might be attributed to the effect of 3^1S level coupling and the distortion of the ground state in this work.

7.3.3 3^1D State Excitation of Helium.

Again the contributions of transitions via the 2^1P and 3^1P levels are of opposite sign, but in contrast to the electron case, this cancellation is much less complete and indeed for the 3^1D excitation transitions via the 2^1P level are of major importance. Van Den Bos (1969b) found that replacement in the six-state approximation of 3^1P level by 2^1P level caused an increase in the cross section by three-fold and ten-fold at 1000 and 100 kev respectively. This feature is common in the present results (see table 7.2 column III and IV) and in those of SOD results.

The Born approximation disagrees very badly with those results that include transitions via the 2^1P level (see Figure 7.6). This may suggest that the 3^1D excitation cross section is a typical feature in close coupling calculations. The measurements of Van Den Bos et al are about half the present nine-state results.

7.4 The Differential Cross Sections for Electron-Helium Excitation.

The only available measurements are those of Lassettre et al (1964) for the 3^1P excitation at small angles ($\Theta < 10^\circ$). The nine-state results are compared with the E10 results of Flannery and McCann (private communications). Figures (7.7a, b, c), (7.8a, b, c) and (7.9a, b, c) show the differential cross sections for the 3^1S, 3^1P and 3^1D levels respectively. The agreement with the measurements for the 3^1P excitation at 511 e v is very good. The two results agree well for the 3^1P excitation, but differ for the/

the 3^1S excitation for angles larger than 30° where it is expected that the two approximations will be inaccurate.

The difference between the two results is most noticed in the shape of the 3^1D excitation, where the discrepancy is large for large angles and they show a different peak in the forward direction.

7.5 The Polarization Fractions for Electron-Helium Scattering.

The percentage polarization fractions for the radiation emitted from the n^1P and n^1D states respectively (Percival and Seaton 1958) are

$$P(n^1P) = \frac{Q_0 - Q_1}{Q_0 + Q_1}$$

and

$$P(3^1D) = \frac{3(Q_0 + Q_1 - 2Q_2)}{(5Q_0 + 9Q_1 + 6Q_2)}$$

where Q_i is the total cross section for the excitation of a sublevel i. Figures (7.10) and (7.11) display the polarization of the 3^1P-2^1S and 3^1D-2^1S lines, in which the nine -state results and the E10, SOD, and GA results are compared with those measurements of Moussa et al (1969) and Van Raan et al (1971) (for 3^1P-2^1S line only). The two measurements agree well (to 10%) for the 3^1P-2^1S line, while the nine-state results show very bad agreement with the measurements and with other theoretical values. The SOD results are in very good agreement with the measurements.

On comparing the nine-state values for the 3^1P-2^1S line with the results of Berrington et al (1973) for the 2^1P-2^1S line, one notes that the polarization is approximately independent of the principal quantum number n. These values are:

Polarization Fractions of the Radiation emitted from He(n^1l)

Energy (ev)	2^1P	3^1P
100	+ 0.017	+ 0.019
200	- 0.084	- 0.088
500	- 0.20	- 0.22
1000	- 0.26	- 0.27

For the 3^1D-2^1P line, the nine-state and SOD results are in fair agreement with the measurements. Above 600 ev, the measurements show a straight line shape, while the theoretical values are still decreasing. The GA results underestimate the polarization line, while those of E10 show a very steep rise in the lower energies and they are lower than the measurements.

7.6 Polarization Fractions for Proton-Helium Scattering.

Figures (7.12) and (7.13) show the nine-state results together with the BA, SOD and the nine-state results of Van Den Bos (1969b), the measurements of Scharmann and Schartner (1967 for 3^1P-2^1S line; 1969b for 3^1D-2^1S line) and those of Van Den Bos et al (1968, for $E<150$ kev).

The theoretical predictions for the 3^1P-2^1S line, apart from BA values, are in disagreement with the measurements. It is striking that the BA results are in good agreement with the measurements for energies higher than 600 e v. As in the electron case, the polarization is independent of the principal quantum number n.

The 3^1D-2^1S line is similar to the electron-helium scattering case, where the present results are in fair agreement with the measurements. The nine-state and the SOD results are very close to each other, while the nine-state results of Van Den Bos (1969b) overestimate the polarization values and the BA values underestimate the polarization line.

7.7 Excitation of Helium by Positron Impact.

The cross sections for the excitation of helium by positron impact have been calculated, for comparison with the electron-helium scattering cross sections, since there are no experimental measurements for the positron scattering. Table (7.3) shows the cross sections in the approximations (two-state, three-state and four-state for 3^1S, 3^1P and 3^1D excitation respectively) and the seven-state approximation.

It is noted that the values of column I of table (7.3) are approximately ($< 5\%$) equal to those values of column II of table (7.1) for energies higher than 300 ev. This shows that the sign of the potential has little effect in this approximation. In contrast to that, the effect of the sign in the dipole and quadropole couplings in the seven-state approximation is most noticed in the 3^1S and 3^1D excitation. The seven-state approximation (which includes the effect of the 3^1P level) reduces the cross sections for electron scattering for the 3^1S and 3^1P levels and increases the cross sections for 3^1D level, while the positron scattering cross sections for the 3^1S are increased and those of the 3^1P and 3^1D levels are decreased. The increase or decrease in the cross section for the electron case, are not accounted for by the same amount for the positron case. This feature was noticed in the proton scattering also.

Conclusions.

In this work, the second order potentials method has been applied to the scattering of electrons from lithium and sodium atoms in the impact parameter and partial wave formulations and to the scattering of electrons and protons from helium atoms in the impact parameter formulation.

In application to e-alkalis, the second order potentials make a substantial contribution to the elastic cross section. However, the agreement between the experimental data and the calculated cross sections for the e-Li case is very poor. The measured total cross sections for e-alkalis are 60% larger than the theoretical calculations at energies as high as 20 - 50 ev. This large discrepancy at such high energy warrants further work to verify the disagreement between the data and the theoretical work.

The effect of the second order potential in the elastic channel was less significant in the resonance transition, and the extension of the method to the three-channel to account fully for the contribution from the coupling to higher levels is very much desirable. The diversity between the experimental measurements for the resonance excitation of Li and Na due to different normalization procedures adopted, makes it difficult to draw a firm conclusion on the agreement between the data and the theoretical calculations in the intermediate energy region.

On the credit side, our calculations have predicted the shape of the differential cross section for the elastic and the resonance excitation quite satisfactory and the polarization fractions are in fair agreement with the measurements.

Application of the method in partial waves and in the impact parameter approximation, highlights the range of applicability of the later approximation, where it was found that the impact parameter approximation is reliable for energies larger than 50 ev and for angles smaller than 40^{o}.

The application of the impact parameter approximation was generally adequate for the excitation of the dipole allowed transition states of helium ($3^{1}P$ state) at energies larger than ten times the threshold energy compared with twenty five times the threshold energy for the alkalis case.

The weakest transitions, specially the $3^{1}D$ level, showed an important dependence on the coupling to the intermediate states of the $2^{1}P$ and $3^{1}P$ levels, and their calculated cross sections are larger (smaller) than the measurements for the electron (proton) impact.

APPENDIX A.

a) The radial part of the wave function of a state n is normalized such that

$$\langle R_n | R_{n'} \rangle = \delta_{nn'}$$

b) Wave functions of Li atom

$$R_{1s}(r) = N_1 \left(e^{-\lambda_1 r} + \lambda_2 e^{-2\lambda_1 r}\right)$$

$$R_{2s}(r) = N_2 (r-a_1) \left(e^{-a_2 r} + a_3 e^{-a_4 r}\right)$$

$$R_{2p}(r) = N_3 r \left(e^{-b_1 r} + b_2 e^{-b_3 r}\right)$$

where

$N_1 = 4.74739$ $\quad \lambda_1 = 2.131038$ $\quad \lambda_2 = 1.0001$

$N_2 = 0.6719289$ $\quad a_1 = 0.869875$ $\quad a_2 = 0.713054$

$a_3 = 1.6028$ $\quad a_4 = 2.05067$

$N_3 = 0.219217$ $\quad b_1 = 0.518$ $\quad b_2 = 0.834$

$b_3 = 1.75$

c) Wave functions of Na atom.

$$R_{1s}(r) = N_1 \left(e^{-\lambda_1 r} + \lambda_2 e^{-\lambda_3 r}\right)$$

$$R_{2s}(r) = N_2 (r-s_1) \left(e^{-s_2 r} + s_3 e^{-s_4 r}\right)$$

$$R_{2p}(r) = N_{2p} r \left(e^{-b_1 r} + b_2 r\, e^{-b_3 r}\right)$$

$$R_{3s}(r) = N_3 (r-c_1) \left(e^{-c_2 r} + (c_3 + c_4 r)\, e^{-c_5 r}\right)$$

$$R_{3p}(r) = N_4 r \left(e^{-a_1 r} + a_2 e^{-a_3 r}\right)$$

where

$N_1 = 46.339$ $\lambda_1 = 9.00738$ $\lambda_2 = 0.5458$ $\lambda_3 = 17.99983$

$N_2 = 9.4054$ $S_1 = 0.20475$ $S_2 = 2.82724$ $S_3 = 10.0$

$S_4 = 5.5$

$N_{2p} = 0.59201$ $b_1 = 0.98865$ $b_2 = 75.22339$

$b_3 = 4.6236$

$N_3 = 0.702244$ $C_1 = 0.961$ $C_2 = 0.71$ $C_3 = -4.76$

$C_4 = 14.$ $C_5 = 3.6$

$N_4 = -0.148743$ $a_1 = 0.44$ $a_2 = -25.4$ $a_3 = 3.8$

It should be noted that the wave functions R_{1s} for Li and R_{1s}, R_{2s} and R_{2p} for Na are spurious states that have to be removed from the closure relation.

We calculated these wave functions in the variational method.

We write down the form of the potentials, for a general wave function to avoid repetition of the calculations of He, Li and Na. The interaction potential between the charge particle, of charge Q, and the atom is

$$V = Q\, V^C(R) - \sum_i Q\, |R - X_i|^{-1}$$

where V^C is defined in equation (4.1) for the alkali atoms and is R^{-1} otherwise, $i = 1$ for alkali atoms and 2 for He.

In general the wave function will be of the form

$$\Phi_{nlm}(\underline{x}) = R_{nl}(x)\, Y_{lm}(\hat{x})$$

where

$$R_{nl}(x) = \sum_j a_j x^j e^{-b_j x}$$

and/

and

$$R_{nl}(x)\, R_{n'l'}(x) = \sum_{j=o}^{N} C_j\, x^j\, e^{-a_j x}$$

and

$$\langle R_{nl} \mid R_{n'l'} \rangle = \delta_{nn'}\, \delta_{ll'}$$

$$\langle \Phi_{ns} \mid V \mid \Phi_{ns} \rangle = Q\left[V^C(R) + N_{ns}^2\, E_1 - R^{-1}\right] \qquad A.1$$

$$E_1 = C_o b_o(2,a_o) + C_1\, b_o(3,a_1) + C_2 b_o(4,a_2) + \ldots\ldots$$

$$\langle \Phi_{ns} | V | \Phi_{np_m} \rangle = \langle \Phi_{np_m} | V | \Phi_{ns} \rangle \quad \text{(azimuth } \phi\text{- independent)}$$

$$= \sqrt{4\pi}\; Y_{1m}(\hat{R})\; Q\, N_{ns} N_{np} \left[G_1 - G_2 \right] \qquad A.2$$

$$G_1 = (3R^2)^{-1}\left[\, 3!\left(\frac{C_o}{a_o^4} + 4\left(\frac{C_1}{a_1^5} + 5\left(\frac{C_2}{a_2^6} + \ldots\ldots\right)\right)\right)\right]$$

$$G_2 = C_o\, b_1(2, a_o) + C_1\, b_1(3, a_1) + C_2\, b_1(4, a_2) + \ldots.$$

$$\langle \Phi_{np_{m_1}} | V | \Phi_{np_{m_2}} \rangle = (-1)^{m_1+m_2} \langle \Phi_{np_{m_1}} | V | \Phi_{np_{-m_2}} \rangle \qquad A.3$$

$$= Q\left[\, V^C(R)\, \delta_{m_1 m_2} - h_1 - h_2 \,\right]$$

$$h_1 = R^{-1} - N_{np}^2\, E_1$$

$$h_2 = (-1)^{m_1-m_2}\sqrt{20\pi}\; Y_{2\,m_2-m_1}(\hat{R})\; N_{np}^2 \langle 2,1;m_1-m_2,m_2 | 1,m_1 \rangle \langle 2,1;0,0 | 1,0 \rangle \times$$

$$\left[\frac{1}{5R^3}\left(4!\left(\frac{C_o}{a_o^5} + 5\left(\frac{C_1}{a_1^6} + 6\left(\frac{C_2}{a_2^7} + \ldots\ldots\right)\right)\right)\right)\right.$$

$$\left. -\left(C_o\, b_2(2, a_o) + C_1\, b_2(3, a_1) + C_3\, b_2(4, a_2) + \ldots\right)\right]$$

$$\langle \Phi_{nS} | V | \Phi_{nD_m} \rangle = Q\, 4\pi\, Y^{*}_{2m}(\hat{R})\, N_{nS} N_{nD} \left[\frac{H_1}{5R^3} - H_2 \right] \qquad \text{A.4}$$

$$H_1 = \sum_n C_n \int_0^\infty t^{4+n} e^{-a_n t}\, dt$$

$$H_2 = \sum_n C_n\, b_2(2+n, a_n)$$

$$\langle \Phi_{np_{m_1}} | V | \Phi_{nD_{m_2}} \rangle = N_{np} N_{nD} \left[\sqrt{20\pi} \langle 21; m_2 m_1 | 1 m_1 - m_2 \rangle \langle 21; 0\,0 | 1\,0 \rangle \times \right.$$
$$Y^{*}_{1 m_1 - m_2}(\hat{R}) \left(\frac{H_3}{3R^2} - H_4 \right) + \sqrt{\frac{140\pi}{3}} \langle 21; m_2 m_1 | 3 m_1 - m_2 \rangle \times \qquad \text{A.5}$$
$$\left. \langle 21; 00 | 3\,0 \rangle Y^{*}_{3 m_1 - m_2}(\hat{R}) \left(\frac{H_5}{7R^4} - H_6 \right) \right]$$

$$H_3 = \sum_n C_n \int_0^\infty dt\, t^{3+n} e^{-a_n t}$$

$$H_4 = \sum_n C_n\, b_1(2+n, a_n)$$

$$H_5 = \sum_n C_n \int_0^\infty dt\, t^{5+n} e^{-a_n t}$$

$$H_6 = \sum_n C_n\, b_3(2+n, a_n)$$

$$\langle \Phi_{nD_{m_1}} | V | \Phi_{nD_{m_2}} \rangle = N_{nD}^2 \left[R^{-1} \delta_{m_1 m_2} - H_7 \delta_{m_1 m_2} \right.$$
$$+ \sqrt{20\pi} \langle 22; m_2 m_1 | 2 m_1 - m_2 \rangle \langle 22; 00 | 2\,0 \rangle Y^{*}_{2 m_1 - m_2}(\hat{R}) \times \qquad \text{A.6}$$
$$\left(\frac{H_8}{5R^3} - H_9 \right) + \sqrt{36\pi} \langle 22; m_2 m_1 | 4 m_1 - m_2 \rangle \times$$
$$\left. \langle 22; 00 | 4\,0 \rangle Y^{*}_{4 m_1 - m_2}(\hat{R}) \left(\frac{H_{10}}{9R^5} - H_{11} \right) \right]$$

$$H_7 = \sum_n C_n \; b_0(2+n, a_n)$$

$$H_8 = \sum_n C_n \int_0^\infty dt \; t^{4+n} \; e^{-a_n t}$$

$$H_9 = \sum_n C_n \; b_2(2+n, a_n)$$

$$H_{10} = \sum_n C_n \int_0^\infty dt \; t^{6+n} \; e^{-a_n t}$$

$$H_{11} = \sum_n C_n \; b_4(2+n, a_n)$$

In general

$$b_L(n, a) = \frac{1}{2L+1} \int_R^\infty \left(\frac{t^{L+n}}{R^{L+1}} - \frac{t^n R^L}{t^{L+1}} \right) e^{-at} \, dt$$

and N_{nL} is the normalization constant.

APPENDIX B.

The second order potentials in configuration space.

To evaluate the kernel K_{nm} in equation (4.11), the kernel μ_{nm} needs closer examination, the matrix elements V_{nm} have been evaluated in Appendix A.

The kernel

$$\mu_{nm} \equiv \mu(l_1 m_1; l_2 m_2) = \int \frac{f(X)\, Y^{*}_{l_1 m_1}(\Omega)\, Y_{l_2 m_2}(\Omega)}{|\underline{R}' - \underline{X}|\,|\underline{R} - \underline{X}|}\, d\underline{X} \qquad \text{B.1}$$

where $f(X)$ is the product of the radial part of the wave functions for the states n and m, can be expressed as a linear combination of the integrals I(L,M) such that:

$$\mu(l_1 m_1; l_2 m_2) = \sum_{L} \left[\frac{(2l_1+1)(2l_2+1)}{4\pi(2L+1)}\right]^{1/2} \langle l_1 l_2; m_1 m_2 | L M \rangle \times \langle l_1 l_2 0 0 | L 0 \rangle I(L,M) \qquad \text{B.2}$$

and

$$I(L,M) = \int \frac{f(X)\, Y_{LM}(\Omega)\, d\underline{X}}{|\underline{R}' - \underline{X}|\,|\underline{R} - \underline{X}|} \qquad \text{B.3}$$

when the two-state close coupling ($n_o s$ - $n_o p$) are considered, the special cases arise

$$\mu(00;00) = I(0,0) \qquad \text{B.4}$$

$$\mu(00;10) = I(1,0)$$

$$\mu(00;11) = I(1,1)$$

$$\mu(10;10) = I(0,0)/4\pi + I(2,0)/\sqrt{5\pi}$$

$$\mu(10;11) = \left(\frac{3}{20\pi}\right)^{\frac{1}{2}} I(2,1)$$

$$\mu(1\text{-}1;11) = -\left(\frac{3}{10\pi}\right)^{1/2} I(2,2)$$

$$\mu(11;11) = \frac{I(0,0)}{4\pi} - \frac{I(2,0)}{\sqrt{20\pi}}$$

Because of the properties of the spherical harmonics,

$$\mu(l_1 m_1;\ l_2 m_2) = \mu(l_2 m_2;\ l_1 m_1)$$

and B.5

$$\mu(l_1 -m_1;\ l_2 -m_2) = (-)^{m_1 + m_2}\, \mu(l_1 m_1;\ l_2 m_2)$$

furthermore, $\mu(l_1 m_1;\ l_2 m_2)$ is real for any l_1, m_1, l_2 and m_2.

The spherical harmonics in the integral I(L,M) are defined with respect to a coordinate frame (S) OXYZ with Z axis along the incident velocity $\underline{V}$ and the collision plane as the XZ plane with the polar coordinates as (r,θ,Φ).

To simplify the integral, it is more convenient to use a second frame (W) Oxyz with polar axis along R, R and R′ are coplanar.

The polar coordinates of R′ depend on its position with respect to R. We have

$$\underline{R} = \underline{\rho} + \underline{V}t \qquad \text{B.6}$$

and $\underline{R}' = \underline{\rho} + \underline{V}t'$

Case I

$R < R'$ and $t' < t$

here $t' < 0$ and $t > 0$ and therefore R' lies to the left of R in the xz plane and the polar angles of R' are $(\Theta, 0)$ as in Figure (B.1).

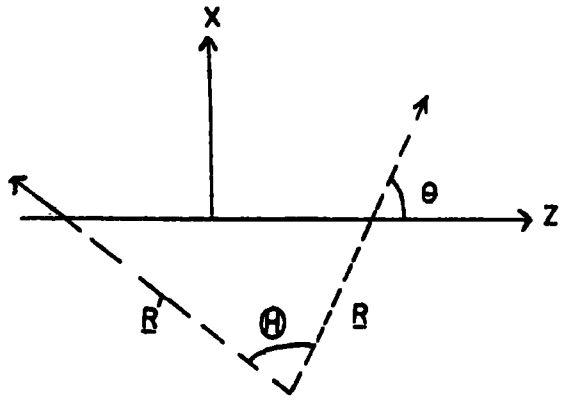

Fig. B.1

To bring the $0xyz$ frame into coincidence with $0XYZ$ frame, the Euler angles are

$$\alpha = \pi, \quad \beta = \theta, \quad \gamma = \pi \qquad \text{B.7}$$

and the transformation matrix that brings the system $0xyz \longrightarrow 0XYZ$ is such that

$$Y_{lm}(\omega) = (-1)^m \sum_{m'=-l}^{l} (-1)^{m'} Y_{lm'}(W)\, r^{l}_{m'm}(\theta) \qquad \text{B.8}$$

and the coefficients $r^{l}_{m'm}(\theta)$ are the elements of the rotation matrix (Messiah 1970).

When the elements $r^{l}_{m'm}(\theta)$ are substituted, the special cases for $n_o s - n_o p$ close coupling are:-

$$\mu(00;10) = \cos(\theta) I(1,0) + \sqrt{2}\sin(\theta) I(1,1)$$

$$\mu(00;11) = -\frac{\sin(\theta)}{\sqrt{2}} I(1,0) + \cos(\theta)\, I(1,1)$$

$$\mu(10;10) = \cos^2(\theta)\left[\frac{I(0,0)}{4\pi} + \frac{I(2,0)}{\sqrt{5\pi}}\right] + 2\sqrt{2}\sin(\theta)\cos(\theta)\left[\sqrt{\frac{3}{20\pi}}\, I(2,1)\right]$$

$$+ \sin^2(\theta)\left[\frac{I(0,0)}{4\pi} - \frac{I(2,0)}{\sqrt{20\pi}} + \sqrt{\frac{3}{10\pi}}\, I(2,2)\right]$$

$$\mu(11;11) - \mu(1-1;11) = \sin^2(\theta)\left[\frac{I(0,0)}{4\pi} + \frac{I(2,0)}{\sqrt{5\pi}}\right] \qquad \text{B.9}$$

$$+ \cos^2(\theta)\left[\frac{I(0,0)}{4\pi} - \frac{I(2,0)}{\sqrt{20\pi}} + \sqrt{\frac{3}{10\pi}}\, I(2,2)\right]$$

$$+ 2\sqrt{2}\,\sin(\theta)\cos(\theta)\left[\sqrt{\frac{3}{20\pi}}\, I(2,1)\right]$$

$$(10,11) = -\frac{\sin(\theta)\cos(\theta)}{\sqrt{2}}\left[\left(\frac{I(0,0)}{4\pi} + \frac{I(2,0)}{\sqrt{5\pi}}\right)\right.$$

$$+ \left(-\sqrt{\frac{3}{10\pi}}\, I(2,2)\right)$$

$$\left. - \left(\frac{I(0,0)}{4\pi} - \frac{I(2,0)}{\sqrt{20\pi}}\right)\right]$$

$$+ \left(\cos^2(\theta) - \sin^2(\theta)\right)\left[\sqrt{\frac{3}{20\pi}}\, I(2,1)\right]$$

Case II

when $t' > t$ and R' lies to the right of R in the xz plane, the polar angles of R' are (Θ, π).

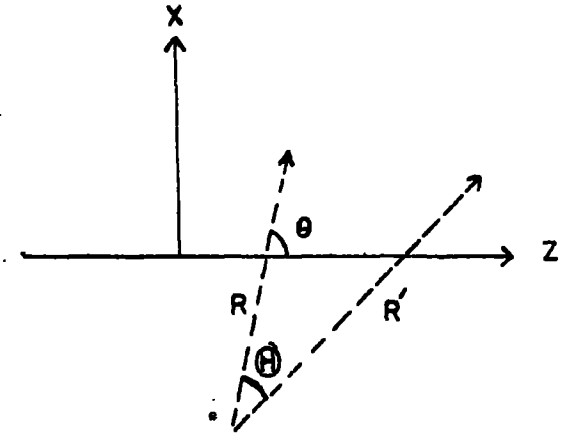

Fig. B.2

The only difference in this case is that I(L,M) of Case I is to be multiplied by $(-1)^M$.

The reduction of the integrals I(L,M) is done following the method of Coleman (1972) and their final forms for l = 0, 1, 2 and M = 0,1,2 are

$$I(0,0) = \frac{4\pi}{R'}\int_0^1 \frac{A(RY, R'/Y)}{D^{1/2}}\, dY$$

where

$$D = (1-2\,XZY^2 + x^2y^4)$$

and

$$A\,(a,b) = \int_a^b dX \quad f(X)\,X \qquad \text{B.10}$$

$$I\,(1,0) = \frac{\sqrt{3\pi}}{2RR'}\left[\int_0^1 \frac{T_1(Y) + 2q_3(1)\,2XY(Z-XY^2)}{D^{1/2}}\,dY - 2q_3(1)\right]$$

where

$$T_1(Y) = (1+XY^2)\left[A_{-1}(0,R'/Y) - (R'/Y)^2\,A_1(R'/Y,\infty)\right]$$

$$+ \frac{(1+Y^2)}{Y^2}\left[(RY)^2 A_1(RY,\infty) - A_{-1}(0,RY)\right]$$

$$2q_3(1) = A_{-1}(0,R') + (R')^2 A_1(R',\infty)$$

$$I(1,1) = \frac{\sqrt{6\pi}}{2(R')^2}\sin(\Theta)\left[\int_0^1 \frac{T_2(Y) - S_2 * sub}{D^{3/2}}\,dY - S_2\right]$$

where

$$S_2 = A_{-1}(0,R') - (R')^2\,A_1(0,R')$$

$$T_2(Y) = (1-Y^2)\,Q_1 + Y^2(1-X^2Y^2)\,Q_2$$

$$Q_1 = A_{-1}(0,RY) - (RY)^2\,A_1(0,RY)$$

$$Q_2 = A_{-1}(0,R'/Y) - (R'/Y)^2\,A_1(0,R'/Y)$$

$$sub = 2XY(Z - XY^2)$$

$$I\,(2,0) = \frac{\sqrt{5\pi}}{32R'}\left[\int_0^1 \frac{(Q_3 + Q_3')\,+\,S_3 * sub}{D^{1/2}}\,dY - S_3\right]$$

where

$$S_3 = \frac{3}{R^2}\Big[(X^2 + 4XZ + 3) A_{-2}(o,R') + (R')^4 A_2(R',\infty)(1 + 4XZ + 3X^2)$$

$$+ 2(R')^2 (1 - X^2) A_o(R',\infty) + 2 R^2 A_o(0,\infty) \Big]$$

$$Q_3 = - \frac{(3 + 2Y^2 + 3Y^4)}{R^2 Y^4}\Big[3 A_{-2}(o,RY) + 2(RY)^2 A_o(o,RY) + 3(RY)^4 A_2(o,RY) \Big]$$

$$Q'_3 = \frac{1}{R^2}\Big[3R^4 (3 + 2Y^2 + 3Y^4) A_2(o,\infty) + (3 + 2X^2Y^2 + 3X^4Y^4)\Big(3 A_{-2}(o,R'/Y)$$

$$- 2 (R'/Y)^2 A_o(R'/Y,\infty) - (R'/Y)^4 A_2(R'/Y,\infty)\Big) + 2R^2 (3Y^2 + 2 + 3X^2Y^2) A_o(o,\infty)\Big]$$

$$I(2,1) = \frac{\sqrt{3\,0\pi}}{16R'} \sin(\Theta)\Big[\int_o^1 \frac{XY^2 (Q_4 + Q'_4) + S_4 \times sub}{D^{3/2}}\, dY + S_4 \Big]$$

where

$$S_4 = \frac{1}{RR'}\Big[(X^2 - 4XZ - 1) A_{-2}(o,R') + (R')^4 A_2(R',\infty)(1 - 4XZ - X^2)$$

$$+ 2(RR')^2 A_2(o,\infty) + 2(R')^2 (1 - X^2) A_o(o,R') \Big]$$

$$Q_4 = \frac{(1 - Y^2)}{R^2 Y^4}\Big[2(RY)^2 (1 - Y^2) A_o(o,RY) + (1 + 3Y^2) A_{-2}(o,RY) - (3 + Y^2)(RY)^4 A_2(o,RY) \Big]$$

$$Q'_4 = \frac{(1 - X^2Y^2)}{R^2}\Big[(3 + X^2Y^2) A_{-2}(o,R'/Y) + (1 + 3X^2Y^2)(R'/Y)^4 A_2(R'/Y,\infty)$$

$$- 2(R'/Y)^2 (1 - X^2Y^2) A_o(o,R'/Y)\Big] - (2 - 3X^2Y^2 + X^2Y^6)(R''/Y)^2 A_2(o,\infty)$$

$$I(2,2) = \frac{3}{8R'}\sqrt{\frac{15\pi}{2}} \sin^2(\Theta)\Big[\int_o^1 \frac{X^2Y^4 (Q_5 + Q'_5) + S_5 \times sub}{D^{5/2}}\, dY + \frac{S_5}{3} \Big]$$

where

$$S_5 = \frac{(1 + 3X^2 - 4XZ)}{(R')^2} A_{-2}(o,R') - (R')^2(3 + X^2 - 4XZ) A_2(o,R')$$

$$+ 2(1 - X^2) A_o(0,R')$$

$$Q_5 = - \frac{(1-Y^2)^2}{Y^2}\left[(RY)^2 A_2(o,RY) - 2A_o(o,RY) + (RY)^{-2} A_{-2}(o,RY) \right]$$

$$Q'_5 = \frac{(1-X^2Y^2)^2}{X^2Y^2}\left[(R'/Y)^2 A_2(o,R'/Y) - 2A_o(o,R'/Y) + (R'/Y)^{-2} A_{-2}(o,R'/Y) \right]$$

In general

$$A_n(a,b) = \int_a^b X^{1-n} f(X)\, dX$$

and $Y = R'/X$ or $Y = X/R$, $Z = \cos(\Theta)$

$$X = \frac{\text{Min}(R,R')}{\text{Max}(R,R')}$$

The integrals in the set of equations B.10 are to be calculated numerically.

APPENDIX C

We will expand the following equation

$$(\nabla^2 + k_a^2) F_a(R) = 2\sum_{a'} \int (W_{aa'}(R,R') + K_{aa'}(R,R')) F_{a'}(R') dR' \quad (C.1)$$

where $W_{aa'}$ and $K_{aa'}$ are defined in equations (5.2) and (3.12) respectively. We have dropped $V_{aa'}$ because the analysis is similar to that of $K_{aa'}$ and will appear only in the final form.

Inserting equations (5.3) and (5.4) in equation (C.1) and multiplying by $(R\, y^*_{l_2 m_2}(\hat{R}))$ and integrating over $d\Omega$ we have

$$\sqrt{2l_2+1}\; i^{l_2} L_\nu f^{l_2 m_2}_{n_1 l_1 m_1}(R) = 2\sum_{a'} \left[\int_0^\infty W^{l_2 m_2, \lambda}_{n_1 l_1 m_1, n' l'_1 m'_1} f^{l'_2 m'_2}_{n' l'_1 m'_1}(R')\, dR' + 2\int_0^\infty K^{l_2 m_2, l'_2 m'_2}_{n_1 l_1 m_1, n' l'_1 m'_1}(\lambda \epsilon)\, f^{l'_2 m'_2}_{n' l'_1 m'_1}(R')\, dR' \right] \quad (C.2)$$

where

$$W^{l m_2, \lambda}_{2\; n_1 l_1 m_1, n' l'_1 m'_1} f^{l' m'_2}_{2\; n' l'_1 m'_1} = \sum_{\lambda} \sum_{l'_2 m'_2} \sqrt{2l'_2+1}\; i^{l'_2} \int y^*_{l_2 m_2}(\hat{R}) y^*_{l_1 m_1}(\hat{R}') P_\lambda(\hat{R}\cdot\hat{R}') \times y_{l'_2 m'_2}(\hat{R}')\, y_{l'_1 m'_1}(\hat{R})\, d\Omega\, d\Omega' \left[\left\{ Y_\lambda(P_{n_1 l_1} f^{l' m'_2}_{2\; n' l'_1 m'_1}(R'), (\epsilon_{n_1 l_1} - \tfrac{1}{2} k^2_{n' l'_1}) \times \Delta(P_{n_1} f^{l' m'_2}_{2\; n' l'_1 m'_1}) \right\} \delta_{\lambda 0} \left\{ n_1 = 1 \right\} \right] \quad (C.3)$$

and

$$K^{l m_2, l' m'_2}_{2\; n_1 m_1, n' l'_1 m'_1}(\lambda\epsilon) = \sum_{\nu' \le N} \sum_{\lambda\epsilon} \sqrt{2l'_2+1}\; i^{l'_2} \quad \bar{V}^{l m_2, \lambda\epsilon}_{2\; n_1 l_1 m_1, n'' l''_1 m''_1}(R)\; \bar{V}^{l' m'_2, \lambda\epsilon}_{2\; n' l'_1 m'_1, n'' l''_1 m''_1}(R') \times \quad (C.4)$$

$$g_\lambda(k_{n'' l''_1}, R, R')$$

and

$$\bar{V}^{l m_2, \lambda\epsilon}_{2\; n_1 l_1 m_1, n'' l''_1 m''_1}(R) = \sum_{\lambda'} Y_{\lambda'}(P_{n_1 l_1} P_{n'' l''_1}(R)) \times$$

$$\int d\Omega\, d\Omega_{\hat{x}}\; y^*_{l m_2}(\hat{R})\, y^*_{l m''_1}(\hat{x})\, P_{\lambda'}(\hat{R}\cdot\hat{x})\, y_{l' m''}(\hat{x})\, y_{\lambda\epsilon}(\hat{R}) \quad (C.5)$$

To transform equation (C.2) from a representation of $(l_1 m_1, l_2 m_2)$ to a representation (l_1, l_2, L) we use

$$\langle l_1 l_2, m_1 m_2 | L M \rangle | l_1 l_2 L M \rangle = \sqrt{2l_2+1}\; i^{l_2} | l_1 l_2 m_1 m_2 \rangle \quad (C.6)$$

and multiplying by $\langle l_1 l_2, m_1 m_2 | L M \rangle$ and summing over m_1, m_2 using the fact that the Clebsch-Gordan coefficients satisfy

$$\sum_{m_1 m_2} \langle l_1 l_2, m_1 m_2 | L M \rangle \langle l_1 l_2, m_1 m_2 | L' M' \rangle = \delta_{LL'} \delta_{MM'} \quad (C.7)$$

and retaining the definition of $\nu = (n l_1 l_2)$ we have

$$L_\nu f_\nu(R) = 2 \sum_{\nu'} \left[\int_0^\infty W_{\nu\nu'}(R, R') f_{\nu'}(R')\, dR' + 2 \int_0^\infty K_{\nu\nu'}(R, R') f_{\nu'}(R')\, dR' \right] \quad (C.8)$$

where

$$W_{\nu\nu'}(R, R') f_{\nu'}(R') = \sum_\lambda g_\lambda(l_1 l_2, l_1' l_2'; L) \left\{ Y_\lambda(P_{n l}) f_{\nu'}(R') + (\epsilon_\nu - \tfrac{1}{2} k_{\nu'}^2) \Delta(P_{n l} f_{\nu'}) \delta_{\lambda 0} \right\} P_{n l}(R) \quad (C.9)$$

and

$$K_{\nu\nu'}(R, R') = \sum_{\nu'' > N} \bar{V}_{\nu\nu''}(R)\, \bar{V}_{\nu''\nu'}(R')\, g_{l_2''}(k_{\nu''}, R, R') \quad (C.10)$$

In obtaining equation(C.10) , we have inserted equation (C.7) when $(l_1 l_2, m_1 m_2)$ are replaced by $(l_1' \lambda, m_1'' \epsilon)$ in equation (C.4) and used the definitions

$$A^{LM}_{l_1 l_2, l_1' l_2'} = \sum_{\substack{m_1 m_1' \\ m_2 m_2'}} \langle l_1 l_2, m_1 m_2 | L M \rangle \langle l_1 l_2', m_1' m_2' | L M \rangle A^{l_1 m_2 \; l_2 m_2'}_{l_1 m_1 \; l_1' m_1'} \quad (C.11)$$

and

$$f_\lambda(l_1 l_2, l_1' l_2'; L) = \sum_{\substack{m_1 m_1' \\ m_2 m_2'}} \langle l_1 l_2, m_1 m_2 | L M \rangle \langle l_1' l_2', m_1' m_2' | L M \rangle \times$$

$$\int d\Omega_{\hat{x}} \, d\Omega_{\hat{R}} \; Y^*_{l_1 m_1}(\hat{x}) \, Y^*_{l_2 m_2}(\hat{R}) \, P_\lambda(\hat{x} \cdot \hat{R}) \, Y_{l_1' m_1'}(\hat{x}) \, Y_{l_2' m_2'}(\hat{R}) \quad (C.12)$$

and for equation (C.9) $g_\lambda(l_1 l_2, l_1' l_2'; L)$ is defined as

$$g_\lambda(l_1 l_2, l_1' l_2'; L) = (-1)^{l_1 + l_2 - L} f_\lambda(l_1 l_2, l_1' l_2'; L) \quad (C.13)$$

From the symmetry properties of the Clebsch-Gordan coefficients it is clear that

$$f_\lambda(l_1 l_2, l_1' l_2'; L) = f_\lambda(l_1' l_2', l_1 l_2; L)$$

For the special case $f_\lambda(0 l_2, l_1' l_2'; L)$, using equations (C.12) and (C.7) with the help of (Rose 1957)

$$\int d\Omega \, Y^*_{l_3 m_3}(\Omega) \, Y_{l_2 m_2}(\Omega) \, Y_{l_1 m_1}(\Omega) = \left[\frac{(2l_1+1)(2l_2+1)}{4\pi(2l_3+1)}\right]^{1/2} \times$$

$$\langle l_1 l_2, m_1 m_2 | l_3 m_3 \rangle \langle l_1 l_2, 0\,0 | l_3 0 \rangle \quad (C.14)$$

we have

$$f_\lambda(0 l_2, l_1' l_2'; L) = \left[\frac{(2l_2'+1)}{(2l_2+1)(2\lambda+1)}\right]^{1/2} \langle l_2' l_1', 0\,0 | L\,0 \rangle \, \delta_{l_2 L} \delta_{\lambda l_1'}$$

(C.15)

APPENDIX D.

The integrals $A_\lambda(a, R,R^1)$, $B_\lambda(a; R,R^1)$ and $C_\lambda(a, R,R^1)$ from equation (5.24) are

$$A_\lambda = (R_< R_>)^{-\lambda-1} \int_0^{R_<} dt\ t^{2\lambda+2}\ \Theta^{-at} \qquad D.1$$

$$B_\lambda = \frac{1}{R_>} \left(\frac{R_<}{R_>}\right)^\lambda \int_{R_<}^{R_>} dt\ t\ \Theta^{-at} \qquad D.2$$

$$C_\lambda = (R_> R_<)^\lambda \int_{R_>}^{\infty} dt\ t^{-2\lambda}\ \Theta^{-at} \qquad D.3$$

now

$$A_0 = \frac{2}{a^3 R_< R_>} - \frac{\Theta^{-aR_<}}{a R_>}\left[R_< + \frac{2}{a} + \frac{2}{a^2 R_<} \right] \qquad D.4$$

Integrating equation D.1 by parts twice we obtain the recurrence relations for $\lambda > 0$

$$A_\lambda = \frac{(2\lambda+1)(2\lambda+2)}{a^2 R_< R_>} A_{\lambda-1} - \frac{\Theta^{-aR_<}}{a}\left(\frac{R_<}{R_>}\right)^{\lambda+1}\left[1 + \frac{2\lambda+2}{a R_<}\right] \qquad D.5$$

which is stable for $\lambda_{max} < aR_<$.

For $\lambda_{max} > aR_<$ we begin with the expansion for large λ_{max}

$$A_\lambda = \frac{\Theta^{-aR_<}}{2\lambda+3}\left(\frac{R_<}{R_>}\right)^{\lambda+1} R_<\left[1 + \frac{aR_<}{2\lambda+4} + \frac{(aR_<)^2}{(2\lambda+4)(2\lambda+5)} + \cdots\right] \qquad D.6$$

to give a reasonable value for $A_{\lambda_{max}}$ and then recur downwards.

In the same method

$$B_0 = \frac{e^{-aR_<}}{a R_>}\left[R_< + \frac{1}{a} \right] - \frac{e^{-aR_>}}{aR_>}\left[R_> + \frac{1}{a} \right] \qquad D.7$$

and its recurrence relation for $\lambda > 0$ is

$$B_\lambda = \frac{R_<}{R_>} \; B_{\lambda-1} \qquad D.8$$

Similarly

$$C_0 = \frac{e^{-aR_>}}{a} \qquad D.9$$

and in writing

$$E_1(R) = \int_R^\infty dt\, t^{-1} e^{-t} \qquad D.10$$

(see Abramowitz and Stegun 1965)

we obtain

$$C_1 = R_< e^{-aR_>} - a R_< R_> E_1(aR_>) \qquad D.11$$

and the recurrence relation for $\lambda > 1$ is

$$C_\lambda = \frac{a^2 R_> R_<}{(2\lambda-1)(2\lambda-2)} C_{\lambda-1} + \frac{e^{-aR_>}}{(2\lambda-1)} R_> \left(\frac{R_<}{R_>}\right)^\lambda \left[1 - \frac{a R_>}{(2\lambda-2)} \right] \qquad D.12$$

References.

Abramowitz, M. and Stegun, I., 1965, Handbook of Mathematical Functions, Dover Publications, Inc., New York.

Austern, N., 1969, Phys.Rev. 188, 1595 - 603.

Barnes, L.L., Lane, N.F. and Lin, C.C., 1965, Phys.Rev., 137A, 388 - 91.

Baye, D., Binon, F. and Demeur, M., 1970, Bull. Acad. r. Belg., C1. Sci.56, 1238 - 73.

Baye, D., 1970, Bull. Acad. r. Belg. C1.Sci. 56, 1274 - 90.

Baye, D., and Heenen, P-H., 1973a J.Phys.B.6, 105 - 13.
1973b J.Phys.B.7, 928 - 37.
1973c J.Phys.B.6,1255 - 64.
1974 J.Phys.B.7, 938 - 48.

Begum, S., Bransden, B.H. and Coleman, J.P. 1973, J.Phys.B.6 837 - 9.

Bell, K.L., Kennedy, D.F. and Kingston, A.E., 1968, J.Phys.B.7 . 1037 - 47. 1969, J.Phys.B.2, 26 - 43.

Bell, K.L. and Kingston, A.E., 1974, Advan. in Atomic and Molec. Phys. 10, 53 - 130.

Berrington, K.A., Bransden, B.H. and Coleman, J.P., 1973, J. Phys. B.6, 436 - 49.

Birman, A. and Rosendorff, S. 1969, IL Nuovo Cimento B63, 89-104.

Bransden, B.H., 1970, "Atomic Collision Theory", W.A.Benjamin Inc., New York.

Bransden, B.H. and Coleman, J.P., 1972, J.Phys.B.5, 537-45.

Buckley, B.D. and Walters, H.R.J. 1975, J.Phys.B.8, 1693-15.

Burke, P.G. and Taylor, A.J., 1966, Proc.Phys.Soc.(Lond), 88, 549-62. 1969, J.Phys. B.2, 869-77.

Burke, P.G. and Schey, H.M., 1962, Phys.Rev. 126, 147-62.

Burke, P.G. Ormonde, S. and Whitaker, W., 1967, Proc.Phys. Soc. (Lond) 92, 319.

Burke, P.G., Gallagher, D.F. and Geltman, S., 1969, J.Phys.B.2, 1142-54.

Burke, P.G. and Webb, T.G. 1970, J.Phys. B.3, L131.

Burke, P.G. and Mitchell, J.F.B., 1973, J.Phys. B.6, 320-8.

Byron, Jr. F.W., 1971, Phys. Rev. A4, 1907-17.

Byron, Jr. F.W., and Joachain, C.J., 1973a, Phys.Rev.A8 1267-81.
1973b, Physica 66, 33-42.
1973c, Phys.Rev.A8, 3266-69.

Callaway, J. and Bauer, E., 1965, Phys.Rev. 140A, 1072.

Callaway, J. and Dugan, A.F., 1966, Phys.Lett.21, 295 - 97.

Callaway, J. and McDowell, M.R.C. and Morgan, L.A., 1975, J. Phys. B.8, 2181 - 89.

Carse, G.D., 1972, J.Phys. B.5, 1928 - 37.

Castillejo, L., Percival, I.C. and Seaton, M.J., 1960, Proc. Roy. Soc. A 254, 259 - 72.

Chan, F.T. and Chen, S.T., 1974, Phys. Rev. A 10, 1151 - 6.

Chan, F.T. and Chang, C.H., 1975, Phys. Rev. A 12, 1383 - 92.

Clenshaw, G.W. and Curtis, A.R. 1960, Num. Math.2, 197 - 05.

Cohen, M. and McEachran, R.P. 1967, Proc. Phys. Soc. 92, 37 - 41.

Coleman, J.P. 1972, J. Phys. B.5, 2155-2167.

Corbato, F.J. and Uretsky, J.L., 1959, J.Assn.Comp.Mach.6,366-75.

Davis, P.J. and Rabinowitz, P., 1967, "Num.Integration", Blaisdell Publishing Co., Waltham, Mass.

de Jongh, J.F. and van Eck, J., 1971,Proc. 7th Int.conf. on Physics of electronic and atomic collision. (Amsterdam:North Holland), pp 701-3.

Dai, B.T. and Stauffer, A.D.,1971, Canad.J.of Phys. 49,1670-79.

Donaldson, F.G.,Hender,M.A. and McConkey,J.W.,1972 , J.Phys. B 5, 1192-210.

Drukarev, G.F. ,1965,"The Theory of Electron-Atom collisions", Academic Press, London.

Enemark, E.A. and Gallagher, A.,1972,Phys.Rev. A 6, 192-05.

Fano, U. and Macek, J.H.,1973, Rev.Mod. Phys. 45, 553-73.

Feautrier,N.,1970, J.Phys. B 3, L152-4.

Feautrier,N.,Regemorter, H.V. ,and Vo Ky Lan 1971 , J.Phys. B 4 ,670-80.

Felden, M.M. and Felden, M.A. ,1973, Canad.J.Phys. 51, 1709.

Flannery, M.R., 1970, J.Phys. B 3 ,306-14.

Flannery, M.R. and McCann,K.J.,1974a , J.Phys. B 7 ,2518-32.
1975c ,J.Phys. B 8 , 1716-33.

Flower, D.R. and Seaton, M.J., 1967 ,Proc.Phys.Soc. 91 ,59.

Franco, V. ,1968, Phys.Rev.Lett. 20 , 709.

Gerjuoy, E. ,1958a, Phys.Rev. 109 , 1806-13.
1958b, Annals. of Phys. 5, 58-93.

Gerjuoy, E. and Thomas, B.K., 1974 , Rep.Prog. in Phys. 37, 1345-1431.

Garrett, W.R. ,1965 , Phys.Rev. 140 A , 705-14.

Gehenn, W. and Reichert, E.,1972 , Z.Physik. 254, 28-34.

Glauber,R.J. ,1959 ,"Lectures in Theor. Phys. " , vol. 1, Ed. W.E.Brittin et al (New York:Interscience), pp 315-414.

Goldberg, L. and Clogston, A.M.,1959 ,Phys.Rev. 56 , 696-9.

Gould, G.N. ,1970 , Thesis, (results quoted in Enemark and Gallagher).

Greene, T.J. and Williamson, W.Jr., 1974, Atomic data and Nuclear data tables, 14, 161-75.

Hasselkamp, D., Hippler, R., Scharmann, A. and Schartner, K-H., 1971, Z. Phys. 248, 254-63.

Hippler, R. and Schartner, K-H., 1974, J.Phys. B.7, 618-25.

Holt, A.R. and Moiseiwitsch, B.L., 1968a, J.Phys.B.1, 36-47.

1968b, Advances in Atom. Molec. Phys.4, 143-72.

Inokuti, M. and McDowell, M.R.C., 1974, J.Phys. B.7, 2382-95.

Kennedy, J.V., Myerscough, V.P. and McDowell, M.R.C., 1976, Private Communication.

Kennedy, J.V., 1976, Ph.D. Thesis, Univ. of London.

Kasdan, A., Miller, T. and Bederson, B., 1971, Proc.3rd Int.Conf. on Atom. Phys. (Boulder:Univ.of Colorado) Abstracts pp 120-2.

1973, Phys. Rev. A.8, 1562-9.

Kumar, S. and Srivastava, M.K., 1976, J.Phys. B.9, 1911 - 14.

Korff, D.F., Chung, S. and Lin, C.C., 1973, Phys. Rev. A.7,545-56.

Lippmann, B.A., 1956, Phys. Rev. 102, 264.

Lassettre, E.N., Krasnow, M.E. and Silverman, S., 1964, J. Chem. Phys. 40, 1242-8.

Leep, D. and Gallagher, A., 1974, Phys. Rev. A.10, 1082-90.

Mathews, J. and Walker, R.L., 1965, "Math. Methods of Phys.", W. A. Benjamin, Inc., New York.

Mathur, K.C., Tripathi, A.N. and Joshi, S.K., 1971, J.Phys. B.4, L39-41. 1972, Phys.Rev. A.5, 746-8.

McDowell, M.R.C. and Coleman, J.P., 1970, "Introduction to the theory of Ion-atom Collision" (North-Holland, Publishing Company Amsterdam-London).

Morgan,L.A. and McDowell,M.R.C.,1975,J.Phys.B8,1073-81

McDowell, M.R.C., Morgan, L.A. and Myerscough, V.P., 1973, J. Phys. B.6, 1435-51.

McDowell, M.R.C., Myerscough, V.P. and Narain, U., 1974, J. Phys. B.7, L 195-7.

McCavert, P. and Rudge, M.R.H., 1970, J. Phys. B.3, 1286-99.

McCann, K.J. and Flannery, M.R., 1974b, Phys. Rev. A.10, 2264-72.

Melkanoff, M.A., Sawada, T. and Raynal, J., 1966, Meth. Comput. Phys.6, 11-45.

Messiah, A., 1970, "Quantum Mechanics", Vol.II, (North-Holland Publishing Co., Amsterdam).

Milne, W.E., 1953, "Num. Solution of Dif.Equations", New York, John Wiley and Sons, Inc. London, Chapman and Hall, Ltd.

Mittleman, M.H. and Pu, R.T., 1962, Phys. Rev. 126, 370-2.

Moiseiwitsch, B.L. and Smith, S.J., 1968, Rev.Mod.Phys. 40, 238-53.

Moores, D. and Norcross, D.W., 1972, J.Phys.B.5, 1482-05.

Moussa, M.H.R., de Heer, F.J. and Schutter, J., 1969, Physica 40, 517-49.

Nesbet, R.K., 1969, Phys. Rev. 179, 60-70.

Nesbet, R.K. and Oberoi, R.S., 1972, Phys. Rev. A.6, 1855-62.

O'Hara, H. and Smith, F.J. 1968, Computer J. 11, 213-9.

Oliver, J. 1972, Computer J. 15, 141-7.

Ormonde, S. and Smith, K., 1964, "Atomic Collision Processes", (M.R.C.McDowell, ed.), p 274, North-Holland Pub.Amsterdam.

Percival, I.C. and Seaton, M.J. 1957, Proc. Cambridge Phil. Soc. 53, 654-62.

1958, Phil. Trans. Roy. Soc. A 251, 113-38.

Peterkop, R. and Veldre, V. 1966, Advan. in Atom. Molec.Phys.2, 263-325.

Rapp, D. and Chang, C.M., 1972, J. Chem. Phys. 57, 4283-86.
1973, J. Chem. Phys. 58, 2657.

Ralston, A. and Wilf, H.S., 1967, "Math. Methods of Digital Computers", Wiley, New York.

Rose, M.E., 1957, "Elementary Theory of Angular Momentum", Wiley, New York.

Sarkar, K., Saha, E.C. and Ghosh, A.S., 1973, Phys. Rev. A.8, 236-3.

Salmona, A. and Seaton, M.J., 1961, Proc. Phys. Soc.(Lond),77, 617-29.

Sasakawa, T., 1963, Prog.Theory. Phys. (Kyoto) Supp.27, 1.

Scharmann, A. and Schartner, K-H., 1967, Phys. Lett. 25A, 51-2.
1969a, Z.Phys. 228, 254-63.
1969b, Z.Phys. 219, 55-69.

Scott, T. and McDowell, M.R.C., 1975, J.Phys.B.8, 1851-65.

Seaton, M.J. 1961, Proc. Phys. Soc.(Lond), 77, 174-83.
1962, Proc. Phys. Soc.(Lond), 79, 1105-17.

Shuttleworth,T.,Newell, W.R. and Smith, A.C.H.,1977 , J.Phys. B 10,1641-51 .

Somerville, W.B., 1963, Proc.Phys. Soc. 82, 446-55.

St. John, R.M.,Miller,F.L. and Lin, C.C , 1964, Phys.Rev. 134A, 888.

Sullivan, J., 1972 , Ph. D. Thesis, Durham University.

Taylor, A.J., and Burke, P.G., 1967, Proc.Phys.Soc. 92,336-44.

Temkin, A. ,1957, Phys.Rev. 107, 1004-12.

Thomas, E.W. and Bent, G.D. ,1967 ,Phys.Rev. 164, 143-50 .

Thomas , B.K. and Gerjuoy, E. ,1971 ,J.Math.Phys. 12 ,1567-76.

Tripathi, A.N., Mathur, K.C. and Joshi, S.K., 1973a,
J. Chem. Phys. 58, 1384.
1973b, J. Phys. B.6, 1431-34.

Vainshtein, L., Opykhtin, V. and Presnyakov, L., 1965,
Sov. Phys. JETP 20, 1542-5.

Van Den Bos, J., Winter, G.J., and De Heer, F.J., 1968,
Physica 40, 357-84.

Van Den Bos, J., 1969a, Physica, 42, 245-59.
1969b, Phys. Rev. 181, 191-7.

Van Raan, A.F.J., De Jongh, J.P., Van Eck, J. and Heideman,H.G.M.,
1971, Physica 53, 45-59.

Vo Ky Lan, 1971, J. Phys. B.4, 658-69.

Walters, H.R.J., 1973, J. Phys. B.6, 1003-19.
1976, J. Phys. B.9, 227-37.

Williams, W., Trajmar, S. and Bozinis, D., 1976, J.Phys.B.9, 1-9.

Winters, K.H., Clark, C.D., Bransden, B.H. and Coleman, J.P.,
1974, J. Phys. B.7, 788-98.

Winters, K.H., 1974, Ph.D. Thesis, Durham University.

Woollings, M.J. and McDowell, M.R.C., 1972, J.Phys. B.5, 1320-31.
1973, J.Phys. B.6, 442-61.

Wu, T-Y., and Ohmura, T., 1962, "Quantum Theory of Scattering",
P 213.

Zapesochnyi, I.P., Postoi, E.N. and Aleksakhin, I.S., 1975,
Sov. Phys. JETP,41, 865-70.

Table 6.1

Total elastic cross sections for e-Li (πa_o^2)

Energy eV	a	b	c	1	2	3
10	15.88	21.30	-	17.73	22.44	26.2
15	-	-	-	13.0	14.85	17.18
20	-	-	-	10.81	11.85	13.27
25	7.43	8.94	-	9.02	9.26	9.87
50	4.45	4.90	4.96	5.06	5.16	5.33
100	2.58	2.72	2.78	-	-	-
200	1.56	1.61	1.62	-	-	-

a) IP.1 b) IP.2 c) IP.3

1) PW.1 2) PW.2 3) PW.3

Table 6.2

Total cross sections (πa_o^2) for the 2^2P excitation of e-Li

Energy eV	a	b	c	1	2	3
10	53.89	49.10	-	63.18	57.66	51.89
15	-	-	-	53.5	50.46	46.11
20	-	-	-	44.75	42.8	40.21
25	34.42	33.01	-	38.72	37.89	36.12
50	20.75	20.0	19.75	22.66	22.27	22.06
100	12.11	12.0	11.99	-	-	-
200	7.50	7.36	7.29	-	-	-

See Table 6.1 for key

Table 6.3

Total elastic cross sections for e-Na (πa_o^2)

Energy eV	a	b	c	1	2	3
10	15.71	22.64	-	19.97	23.16	31.87
15	-	-	-	15.61	17.36	21.99
20	-	-	-	12.19	13.74	15.85
25	7.44	8.91		9.75	9.97	11.57
50	5.30	5.72	5.74	5.67	5.85	6.17
100	3.19	3.31	3.32	-	-	-
200	2.68	2.69	2.69	-	-	-

See Table 6.1 for key

Table 6.4

Total cross sections (πa_o^2) for the 3^2P excitation of e-Na

Energy eV	a	b	c	1	2	3
10	47.16	42.35	-	57.29	52.30	47.54
15	-	-	-	49.06	47.11	42.71
20	-	-	-	41.17	40.00	37.97
25	31.84	30.36	-	34.87	33.87	32.78
50	19.76	18.97	17.96	22.21	22.00	21.77
100	11.87	11.50	10.85	-	-	-
200	7.10	6.90	6.81	-	-	-

See Table 5.1 for key

Table 6.5.a

ANGULAR DISTRIBUTION E-LI EXCITATION CROSS SECTION
PARTIAL WAVE TREATMENT. $(\frac{d\sigma}{d\Omega}/a_0^2)$

ENERGY (ev) / ANGLE	10	15	20	25	50
0	4.97+2	9.76+2	1.04+3	1.56+3	1.73+3
10	5.76+2	4.17+2	2.45+2	3.19+2	5.50+1
20	5.51+1	4.55+1	2.10+1	2.04+1	5.60 0
30	1.22+1	4.53 0	1.76 0	2.73 0	7.62-1
40	5.85 0	1.12 0	9.51-1	9.63-1	3.71-1
50	2.10 0	7.87-1	5.02-1	7.65-1	1.78-1
60	9.35-1	6.53-1	4.90-1	7.08-1	8.28-2
70	5.33-1	5.11-1	4.72-1	4.42-1	3.92-2
80	5.27-1	4.58-1	4.50-1	4.07-1	2.20-2
100	5.53-1	3.33-1	5.22-1	4.40-1	1.65-2
120	6.23-1	4.38-1	6.58-1	7.27-1	1.68-2
140	8.57-1	6.03-1	8.84-1	1.27 0	1.82-2
160	1.59 0	1.42 0	1.35 0	1.45 0	3.01-2
180	2.68 0	1.64 0	3.07 0	1.11+1	7.22-2

ANGULAR DISTRIBUTION E-LI ELASTIC CROSS SECTION
PARTIAL WAVE TREATMENT.

ENERGY (ev) / ANGLE	10	15	20	25	50
0	4.64+2	3.99+2	3.32+2	2.86+2	1.94+2
10	1.89+2	1.09+2	7.65+1	4.91+1	2.68+1
20	3.07+1	1.78+1	1.56+1	1.16+1	7.77 0
30	7.54 0	5.89 0	5.77 0	3.85 0	2.69 0
40	3.15 0	2.78 0	2.58 0	2.08 0	1.44 0
50	1.36 0	1.43 0	1.55 0	1.05 0	8.98-1
60	8.61-1	9.91-1	9.35-1	8.08-1	5.83-1
70	7.23-1	9.80-1	7.90-1	5.31-1	4.18-1
80	7.57-1	8.85-1	7.33-1	4.48-1	3.61-1
100	1.24 0	9.66-1	8.07-1	4.01-1	2.58-1
120	2.26 0	1.32 0	1.01-1	4.25-1	2.82-1
140	2.72 0	1.70 0	1.17 0	5.11-1	2.73-1
160	3.45 0	2.12 0	1.64 0	8.93-1	2.26-1
180	3.90 0	2.27 0	1.85 0	1.78 0	1.96-1

Table 6.5-b

ANGULAR DISTRIBUTION E-LI EXCITATION CROSS SECTION
IMPACT PARAMETER METHOD. $\left(\frac{d\sigma}{d\Omega}\right)a_0^2$

ENERGY(ev) / ANGLE	10	25	50	100	200
0	1.06+3	2.53+3	3.76+3	5.10+3	7.14+3
10	4.60+2	1.67+2	1.16+2	2.82+1	3.27 0
20	4.42+1	1.51+1	2.78 0	7.16 0	9.15-2
30	1.55+1	2.22 0	8.58-1	1.19-1	1.56-2
40	5.45 0	8.96-1	2.34-2	3.89-2	7.33-3
50	1.81 0	4.59-1	1.06-2	1.66-2	3.45-3
60	1.45 0	2.94-1	5.39-2	9.19-3	1.89-3
70	9.71-1	1.77-1	3.05-2	5.14-3	2.53-3
80	8.06-1	1.14-1	1.94-2	4.42-3	2.36-4
90	5.41-1	8.08-2	1.37-2	2.86-3	1.08-3
105	3.47-1	5.31-2	8.42-3	1.83-3	4.44-4
120	2.45-1	3.91-2	5.02-3	1.17-3	3.48-4
135	1.89-1	3.17-2	4.46-3	9.64-4	2.94-4
150	1.59-1	2.74-2	3.66-3	8.56-4	2.62-4
165	1.45-1	2.65-2	3.23-3	7.91-4	2.36-4
180	1.39-1	2.44-2	3.13-3	7.74-4	2.31-4

ANGULAR DISTRIBUTION E-LI ELASTIC CROSS SECTION
IMPACT PARAMETER METHOD.

ENERGY(ev) / ANGLE	10	25	50	100	200
0	5.53+2	4.19+2	2.97+2	2.04+2	1.46+2
10	1.07+2	4.59+1	2.96+1	1.74+1	1.12+1
20	3.90+1	1.00+1	6.20 0	3.68 0	1.89 0
30	6.07 0	2.53 0	2.03 0	1.14 0	5.94-1
40	7.30-1	1.00 0	9.07-1	5.00-1	2.62-1
50	5.86-2	5.52-1	4.96-1	2.59-1	1.38-1
60	2.44-3	3.74-1	3.01-1	1.52-1	8.28-2
70	2.27-3	2.78-1	1.95-1	9.69-2	5.45-2
80	3.49-3	2.17-1	1.31-1	6.71-2	3.93-2
90	7.22-3	1.17-1	9.49-2	4.93-2	3.00-2
105	1.13-2	1.34-1	6.09-2	3.45-2	2.18-2
120	1.47-2	1.08-1	4.22-2	2.71-2	1.74-2
135	1.73-2	9.15-2	3.26-2	2.29-2	1.48-2
150	1.85-2	8.16-2	2.71-2	2.07-2	1.33-2
165	1.94-2	7.63-2	2.42-2	1.93-2	1.25-2
180	1.92-2	7.44-2	2.33-2	1.90-2	1.22-1

Table 6.6.a

ANGULAR DISTRIBUTION E-NA ELASTIC CROSS SECTION
PARTIAL WAVE TREATMENT. $(\frac{d\sigma}{d\Omega}) a_0^2$

ENERGY(ev) / ANGLE	10	15	20	25	50
0	5.43+2	3.55+2	3.27+2	2.61+2	2.05+2
10	2.21+2	9.29+1	6.83+1	4.22+1	2.15+1
20	3.62+1	1.44+1	9.56 0	4.96 0	2.45 0
30	8.11 0	5.18 0	3.92 0	2.00 0	1.46 0
40	2.33 0	1.45 0	1.92 0	2.15 0	1.52 0
50	1.14 0	8.49-1	2.13 0	2.49 0	1.55 0
60	5.14-1	2.91 0	4.20 0	2.33 0	1.38 0
70	7.27-1	4.74 0	3.99 0	2.28 0	1.18 0
80	1.29 0	3.13 0	2.41 0	1.49 0	8.09-1
90	2.32 0	2.56 0	1.66 0	8.90-1	5.81-1
100	2.47 0	1.45 0	8.73-1	5.39-1	3.47-1
110	2.33 0	1.08 0	8.45-1	4.05-1	2.82-1
120	1.25 0	9.76-1	1.24 0	6.45-1	3.45-1
130	9.52-1	1.45 0	1.89 0	1.38 0	5.71-1
140	6.73-1	2.49 0	2.57 0	2.14 0	8.78-1
150	1.31 0	4.09 0	3.18 0	3.38 0	1.45 0
160	5.33 0	5.44 0	3.64 0	4.18 0	1.88 0
180	6.05 0	3.03 0	5.03 0	6.02 0	2.46 0

ANGULAR DISTRIBUTION E-NA EXCITATION CROSS SECTION
PARTIAL WAVE TREATMENT.

ENERGY(ev) / ANGLE	10	15	20	25	50
0	8.43+2	1.24+3	1.41+3	1.59+3	2.61+3
10	4.21+2	3.63+2	3.07+2	2.70+2	8.05+2
20	4.68+1	4.89+1	5.42+1	2.32+1	2.57 0
30	1.70+1	4.92 0	4.38 0	2.27 0	7.88-1
40	6.15 0	3.60 0	2.81 0	3.17-1	3.17-1
50	4.01 0	2.59 0	1.24 0	2.12-1	1.79-1
60	1.67 0	1.26 0	7.39-1	6.73-1	1.34-1
70	1.24 0	4.33-1	3.52-1	9.23-1	3.28-1
80	7.55-1	2.49-1	1.51-1	4.09-1	1.91-1
90	7.23-1	3.12-1	2.08-1	1.01-1	1.42-1
100	5.86-1	3.51-1	3.50-1	4.54-2	1.19-1
110	5.95-1	2.34-1	1.81-1	7.58-2	9.94-2
120	6.50-1	5.28-1	1.45-1	1.30-1	1.53-1
130	1.48 0	5.40-1	4.29-1	2.20-1	3.52-1
140	7.73-1	5.85-1	7.06-1	2.92-1	1.93-1
150	4.65-1	6.41-1	8.57-1	3.11-1	1.60-1
160	6.81-1	6.78-1	1.07 0	3.26-1	2.35-1
180	1.28-1	6.81-1	1.99 0	3.94-1	1.69 0

Table 6.6.b

ANGULAR DISTRIBUTION E-NA ELASTIC CROSS SECTION
IMPACT PARAMETER METHOD. $\left(\frac{d\sigma}{d\Omega}\right) a_o^2$

ENERGY (ev) / ANGLE	10	25	50	100	200
0	5.12+2	4.26+2	3.22+2	2.28+2	1.55+2
10	2.09+2	6.95+1	3.31+1	2.02+1	1.35+1
20	4.31+1	9.88 0	6.57 0	4.44 0	3.51 0
30	7.44 0	2.17 0	2.31 0	1.55 0	1.54 0
40	1.05 0	7.83-1	1.23 0	6.84-1	7.25-1
50	2.22-1	4.26-1	7.58-1	3.32-1	5.03-1
60	5.17-2	2.91-1	4.93-1	1.71-1	3.93-1
70	6.02-2	2.13-1	3.30-1	1.03-1	2.71-1
80	3.85-2	1.59-1	2.24-1	7.56-2	1.86-1
90	6.52-2	1.21-1	1.56-1	6.49-2	1.36-1
105	6.92-2	8.27-2	9.41-2	6.01-2	7.29-2
120	7.59-2	6.21-2	5.96-2	5.93-2	3.89-2
135	8.00-2	5.03-2	4.10-2	5.87-2	2.37-2
150	8.07-2	4.49-2	3.04-2	5.79-2	1.72-2
165	8.10-2	4.12-2	2.56-2	5.79-2	1.26-2
180	8.12-2	4.76-2	2.41-2	5.76-2	1.09-2

ANGULAR DISTRIBUTION E-NA EXCITATION CROSS SECTION
IMPACT PARAMETER METHOD.

ENERGY (ev) / ANGLE	10	25	50	100	200
0	5.45+2	2.10+3	3.40+3	4.78+3	6.47+3
10	4.33+2	1.69+2	1.06+2	1.71+1	2.16 0
20	6.00+1	1.37+1	2.29+1	6.63-1	5.43-1
30	1.89+1	2.08 0	7.30-1	1.06-1	6.98-2
40	3.22 0	9.25-1	2.25-1	8.04-2	1.58-2
50	2.65 0	4.79-1	1.11-1	4.87-2	1.13-2
60	1.67 0	2.46-1	6.22-2	1.12-2	1.20-2
70	9.45-1	1.45-1	3.80-2	6.49-3	4.32-3
80	8.24-1	9.32-2	2.56-2	1.04-2	5.36-3
90	3.46-1	5.28-2	1.80-2	7.65-3	1.12-2
105	3.41-1	4.06-2	1.10-2	2.52-3	8.20-3
120	3.55-1	2.94-2	7.60-3	2.21-3	1.09-3
135	3.67-1	2.33-2	1.55-2	7.28-3	2.05-3
150	3.46-1	2.00-2	4.56-3	2.00-3	5.27-3
165	3.20-1	1.80-2	1.09-2	1.94-3	6.72-3
180	3.09-1	1.78-2	3.87-3	1.92-3	7.09-3

Table 6.7

POLARIZATION FRACTIONS FOR THE RESONANCE EXCITATION OF LI AND Na.

Energy (eV)	Na			LI		
	I	II	III	I	II	III
	1.27	1.24	-2.48	4.69	4.84	-6.27
	-0.07	-0.10		-0.57	-0.635	
	-0.85	-0.92		-1.89	-2.11	
	-1.23	-1.22	-2.07	-3.28	-3.35	-5.07
	-1.75	-2.10	-1.21	-7.54	-7.57	-3.12

PW.3

PW.2

I P.

Table 7.1 e-He Excitation Cross-Section in πa_o^2

	3^1S				3^1P				3^1D			
Energy (eV)	I	II	III	IV	I	II	III	IV	I	II	III	IV
100	5.00(3)	3.56(3)	3.12(3)	3.46(3)	36.60(3)	38.2 (3)	40.20(3)	40.88(3)	10.30(4)	10.10(4)	34.17(4)	14.8(4)
200	2.65(3)	2.15(3)	1.95(3)	2.10(3)	26.43(3)	27.18(3)	26.90(3)	27.82(3)	5.84(4)	5.64(4)	14.17(4)	6.90(4)
300	1.78(3)	1.54(3)	1.42(3)	1.51(3)	20.79(3)	21.13(3)	20.60(3)	21.03(3)	4.05(4)	3.90(4)	8.40(4)	4.56(4)
400	1.36(3)	1.21(3)	1.13(3)	1.18(3)	17.28(3)	17.69(3)	16.96(3)	17.35(3)	3.06(4)	2.99(4)	5.76(4)	3.42(4)
500	1.09(3)	0.985(3)	0.93(3)	0.97(3)	14.87(3)	15.10(3)	14.11(3)	14.65(3)	2.50(4)	2.42(4)	4.26(4)	2.70(4)
1000	0.55(3)	0.52(3)	0.50(3)	0.51(3)	9.10(3)	9.22(3)	8.73(3)	8.97(3)	1.28(4)	1.23(4)	1.80(4)	1.35(4)

I Born approximation, Bell et al (1968, 1969)

II Present work:- 2 state approximation for 3^1S excitation
3 state approximation for 3^1P excitation
4 state approximation for 3^1D excitation

III Present work:- 7 state approximation (not including transitions via the 2^1P levels)

IV Present work:- 9 state approximation (including transitions via the 2^1P level)

The number in round brackets (n) represents the power of ten by which the entry should be divided

Table 7.2 Proton-He excitation cross-section in πa_o^2

	3^1S				3^1P				3^1D			
Energy(keV)	I	II	III	IV	I	II	III	IV	I	II	III	IV
50	14.50(3)	-	10.70(3)	-	5.65(2)	4.47(2)	1.22(2)	-	22.70(4)	20.57(4)	8.85(4)	-
100	8.58(3)	6.25(3)	10.14(3)	11.51(3)	4.99(2)	4.45(2)	2.42(2)	3.66(2)	16.40(4)	15.53(4)	10.53(4)	51.44(4)
200	4.68(3)	3.91(3)	6.40(3)	5.84(3)	3.76(2)	3.56(2)	2.75(2)	3.33(2)	9.90(4)	9.59(4)	8.18(4)	26.94(4)
300	3.21(3)	2.82(3)	4.40(3)	3.73(3)	3.04(2)	2.90(2)	2.53(2)	2.84(2)	7.05(4)	6.86(4)	6.18(4)	15.92(4)
400	2.44(3)	2.20(3)	3.25(3)	2.69(3)	2.57(2)	2.50(2)	2.29(2)	2.47(2)	5.45(4)	5.34(4)	4.88(4)	10.61(4)
500	1.97(3)	1.79(3)	2.55(3)	2.08(3)	2.24(2)	2.16(2)	2.05(2)	2.10(2)	4.45(4)	4.31(4)	4.00(4)	7.80(4)
1000	1.00(3)	0.94(3)	1.18(3)	0.96(3)	1.41(2)	1.39(2)	1.37(2)	1.39(2)	2.30(4)	2.27(4)	2.11(4)	3.07(4)

I Born approximation, Bell et al (1968, 1969)

II Present work:- 2 state approximation for 3^1S excitation
3 state approximation for 3^1P excitation
4 state approximation for 3^1D excitation

III Present work:- 7 state approximation (not including transitions via the 2^1P levels)

IV Present work:- 9 state approximation (including transitions via the 2^1P level)

The number in round brackets (n) represents the power of ten by which the entry should be divided

Table 7.3

Positron-Helium Excitation Cross Sections in

	3^1S		3^1P		3^1D	
Energy(ev)	I	II	I	II	I	II
100	4.21(3)	6.49(3)	36.94(3)	27.55(3)	10.27(4)	8.45(4)
200	2.35(3)	3.4 (3)	26.4 (3)	23.68(3)	5.75(4)	5.19(4)
300	1.64(3)	2.28(3)	20.63(3)	19.58(3)	3.8 (4)	3.67(4)
400	-	1.66(3)	-	16.86(3)	-	2.83(4)
500	1.02(3)	1.3 (3)	14.82(3)	14.62(3)	2.47(4)	2.29(4)
1000	.526(3)	0.61(3)	8.96(3)	9.175(3)	1.26(4)	1.19(4)

I present work: Two-state approximation for 3^1S excitation
Three-state approximation for 3^1P excitation
Four-state approximation for 3^1D excitation

II present work: Seven-state approximation

The number in round brackets (n) represents the power of ten by which the entry should be divided.

FIGURE CAPTIONS

Fig. 6.1 Elastic scattering of electrons by Li atoms.

———— Present work (method PW.3)

— — — — Present work (method Ip.2)

+ + + + + Glauber approximation (Walters 1973)

⊕ ⊕ ⊕ Experiment (Williams et al 1976)

—o—o—o— Born approximation.

Fig 6.2 e-Li 2S-2P excitation

Δ Δ Δ Δ Experiment (Zapesochnyi et al 1975)

⊕ ⊕ ⊕ ⊕ Experiment (Williams et al 1976)

I I I I Experiment (Leep and Gallagher 1974)

● ● ● ● DWPO II (Kennedy et al 1976)

other symbols are as in Fig. 6.1

Fig. 6.3 Elastic scattering of electrons by Na atoms.

AS in Fig. 6.1

Fig. 6.4 e-Na 3s-3p excitation

-------- Experiment (Zapesochnyi et al 1975)

Δ Δ Δ Δ Experiment (Enemark and Gallagher 1972)

● ● ● ● DWPO II (Kennedy et al 1976)

other symbols are as in Fig. 6.1

Fig 6.5 Differential cross sections for the elastic scattering of (a)10 ev, (b) 20 ev, (c) 25 ev (d)50 ev electrons from lithium.

———— Present work (method PW.3)

— — — — Present work (method IP.2)

Δ Δ Δ Δ Experiment (Williams et al 1976)

+ + + + Glauber approximation at 11ev and 54.4 ev (Walters 1973)

The points at 0^{o} in the GA calculations are in fact not at 0^{o} ,since at this angle the Glauber approximation is known to diverge for elastic scattering. They are at 1.3^{o} for the elastic e-Li scattering and 2^{o} and 1.4^{o} at 11 and 54.4 ev respectively, for e-Li excitation. For the elastic e-Na scattering ,they are 2.6^{o} and 1.34^{o} at 11 and 54.4 ev respectively and 2.3^{o} and 0.55^{o} at 11 and 54.4 ev for the e- Na excitation.

Fig. 6.6 Differential cross sections for the $2^{2}P$ excitation of lithium by (a)10 ev, (b)20 ev,(c) 25 ev, (d)50 ev electrons.

● ● ● ● DWPO II at 12 ev, 22 ev and 54.4 ev (Kennedy et al 1976)

other symbols are as in Fig. 6.5

Fig. 6.7 Differential cross sections for the elastic scattering of (a) 10 ev, (b) 15 ev, (c)20 ev, (d)25 ev, (e) 50 ev electrons from Na .

Δ Δ Δ Δ Experiment (Gehenn and Reichert 1972)

other symbols are as in Fig. 6.5

Fig. 6.8 Differential cross sections for the $3^{2}P$ excitation of sodium by (a)10ev, (b)20ev, (c)25ev, (d)50ev electrons.

● ● ● ● DWPO II at 12 ev,22 ev and 54.4 ev (Kennedy et al 1976)

Δ Δ Δ Δ Experiment (shuttleworth et al 1977)

other symbols are as in Fig. 6.5

Fig. 6.9 Percentage polarizations of the resonance line 2p-2s emitted from ^{6}Li by electron impact.

⊕—⊕—⊕ DWPO II (Kennedy et al 1976)

——— Present work (method PW.3)

⊕ ⊕⊕ ⊕ Experiment (Leep and Gallagher 1974)

—·—·— Glauber approximation (Tripathi et al 1973b)

– – – – – Present work (method IP.2)

Fig. 6.10 Percentage polarizations of the resonance line 3p-3s emitted from Na by electron impact.

⊕ ⊕ ⊕ ⊕ Experiment (Enemark and Gallagher 1972)

Δ Δ Δ Δ Experiment (Gould 1970, quoted in Enemark and Gallagher)

other symbols are as in Fig. 6.9

Fig. 6.11 The parameter λ for Li
(a)50 ev, (b) 25 ev , (c) 10 ev

..... Present work (method PW.3)

× × × × DWPO II (Kennedy 1976)

Fig. 6.12 The parameter λ for Na
(a) 50 ev, (b) 25 ev, (c) 10 ev

symbols are as in Fig. 6.11

Fig. 6.13 The parameter $X = \mathrm{Re}\langle a_0 a_1 \rangle / \sigma$ for Li

(a) 10 ev , (b) 25 ev , (c) 50 ev

..... Present work (method PW.3)

× × ×× DWPO II (Kennedy 1976)

Fig. 6.14 The parameter $X = \mathrm{Re}\langle a_0 a_1 \rangle / \sigma$ for Na

(a) 10 ev ,(b) 25 ev , (c) 50 ev

symbols are as in Fig. 6.13

Fig. 6.15 The $Y = \mathrm{Im}\langle a_0 a_1 \rangle / \sigma$ parameter for Li

(a)10 ev

symbols are as in Fig. 6.13

Fig. 6.16 The $y = \mathrm{Im}\langle a_0 a_1 \rangle / \sigma$ parameter for Na

(a) 10 ev , (b) 25 ev , (c) 50 ev

symbols are as in Fig. 6.13

Fig. 7.1 Excitation cross sections of the level 3^1S of helium by electron impact. (QV^2 versus energy), Q is the total cross section in πa_0^2

and V is the velocity in a. u.

———— Present work (9-state method)

—o—o—o— Born approximation (Bell et al 1969)

- - - - - - - ElO (Flannery and McCann 1975)

—·—·—·— DWPO (Scott and McDowell 1975)

o—o—o SOD (Baye and Heenen 1974)

Δ Δ Δ Δ Experiment (Moussa et al 1969)

Fig. 7.2 Excitation cross section of the level 3^1P of helium by electron impact .

⊙ ⊙ ⊙ SOD (Baye and Heenen 1974)

o o o Born approximation (Bell et al 1969)

+ + + experiment (Donaldson et al 1972)

ϕ ϕ ϕ experiment (de Jongh and Van Eck 1971)

—·····— Glauber approximation (Chan and Chen 1974)

other symbols are as in Fig. 7.1

Fig. 7.3 Excitation cross section of the level 3^1D of helium by electron impact .

—·····— Glauber approximation (Chan and Chang 1975)

other symbols are as in Fig. 7.1

Fig. 7.4 Excitation cross section of the 3^1S level of helium by proton impact .

——————— present work (9-state method)

— — — — SOD (Baye and Heenen 1973c)

× × × × Born approximation (Bell et at 1968)

I I I I experiment (Scharmann and Schartner 1969a)

o o o o experiment (Van Den Bos et al 1968)

Fig. 7.5 Excitation cross section of the 3^1P level of helium by proton impact.

Δ Δ Δ experiment (Hippler and Schartner 1974)

other symbols are as in Fig. 7.4

Fig. 7.6 Excitation cross section of the 3^1D level of helium by proton impact

symbols are as in Fig. 7.4

Fig. 7.7 Excitation differential cross section of the 3^1S level of helium by electron impact at (a) 200 ev, (b) 300 ev, (c) 500 ev

——— present work (9-state method)

● ○ ● E10 (Flannery and McCann 1975)

Fig. 7.8 Excitation differential cross section of the 3^1P level of helium by electron impact at (a) 200 ev, (b) 300 ev, (c) 500 ev

× × × experiment (Lassettre et al 1964)

other symbols are as in Fig. 7.7

Fig. 7.9 Excitation differential cross section of the 3^1D level of helium by electron impact at (a) 200 ev, (b) 300 ev, (c) 500 ev

symbols are as in Fig. 7.7

Fig. 7.10 Polarization fractions of the line 3^1P-2^1S emitted from helium by electron impact.

——— present work (9-state method)

———○——— SOD (Baye and Heenen 1974)

———·—·——— Glauber approximation (Chan and Chen 1974)

- - - - - - - E10 (Flannery and McCann 1975)

Δ Δ Δ experiment (Moussa et al 1969)

Φ Φ Φ experiment (Van Raan et al 1971)

Fig. 7.11 Polarization fractions of the line 3^1D-2^1P emitted from helium by electron impact.

—·—·— Glauber approximation (Chan and Chang 1975)

other symbols are as in Fig. 7.10

Fig. 7.12 Polarization fractions of the line 3^1P-2^1S emitted from helium by proton impact.

——— present work (9-state method)

●——●——● SOD (Baye and Heenen 1973c)

—··—··— impact parameter (Van Den Bos 1969b)

— — — — Born approximation (Van Den Bos 1969a)

Δ Δ Δ experiment (Scharmann and Schartner 1967)

o o o experiment (Van Den Bos 1968)

Fig. 7.13 Polarization fractions of the line 3^1D-2^1P emitted from helium by proton impact.

Δ Δ Δ experiment (Scharmann and Schartner 1969b)

other symbols are as in Fig. 7.12

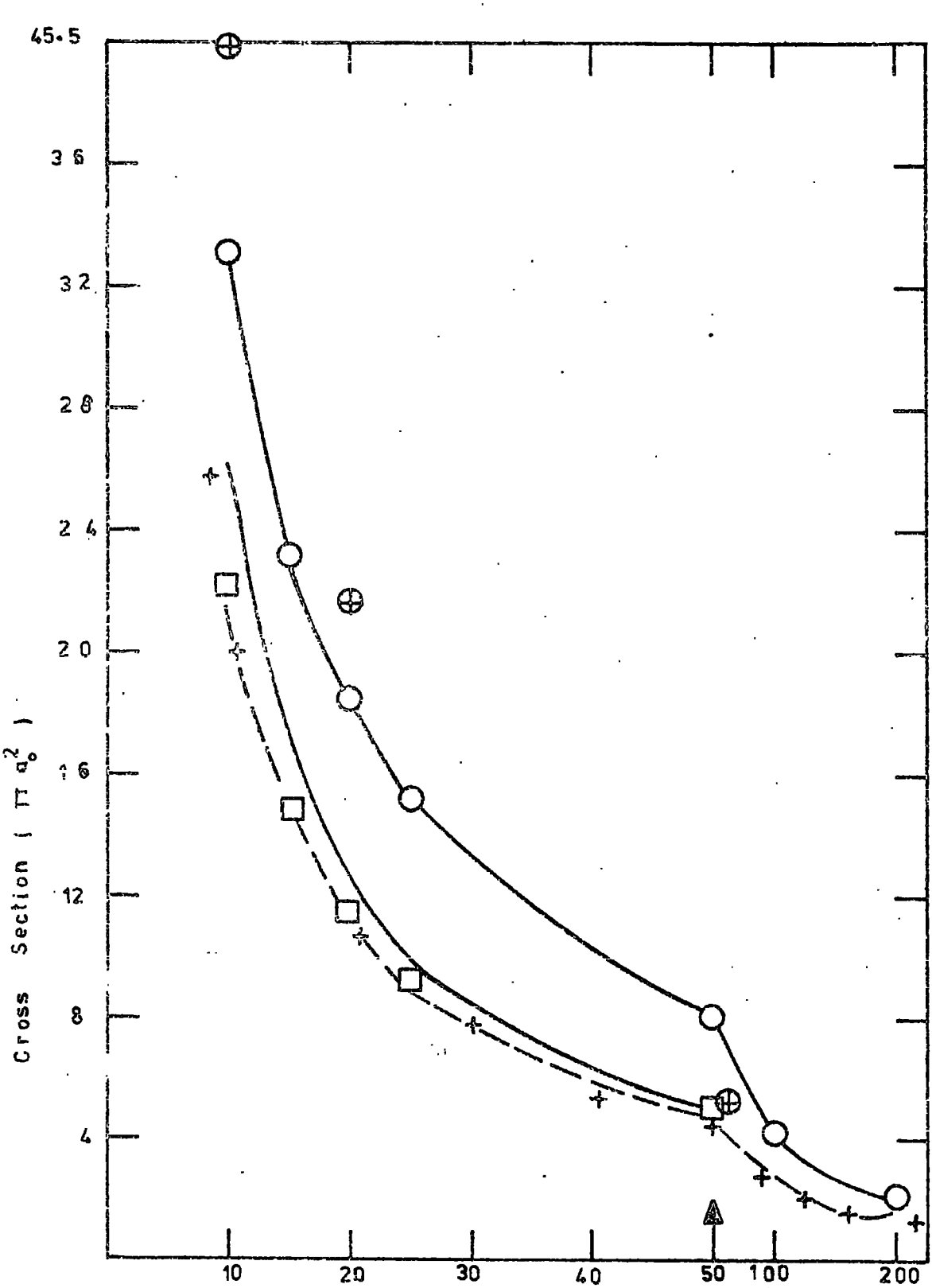
45.5
36
32
28
24
20
16
12
8
4
Cross Section (πa_0^2)
10
20
30
40
50
100
200
Incident Energy (e v)

Fig 6.1

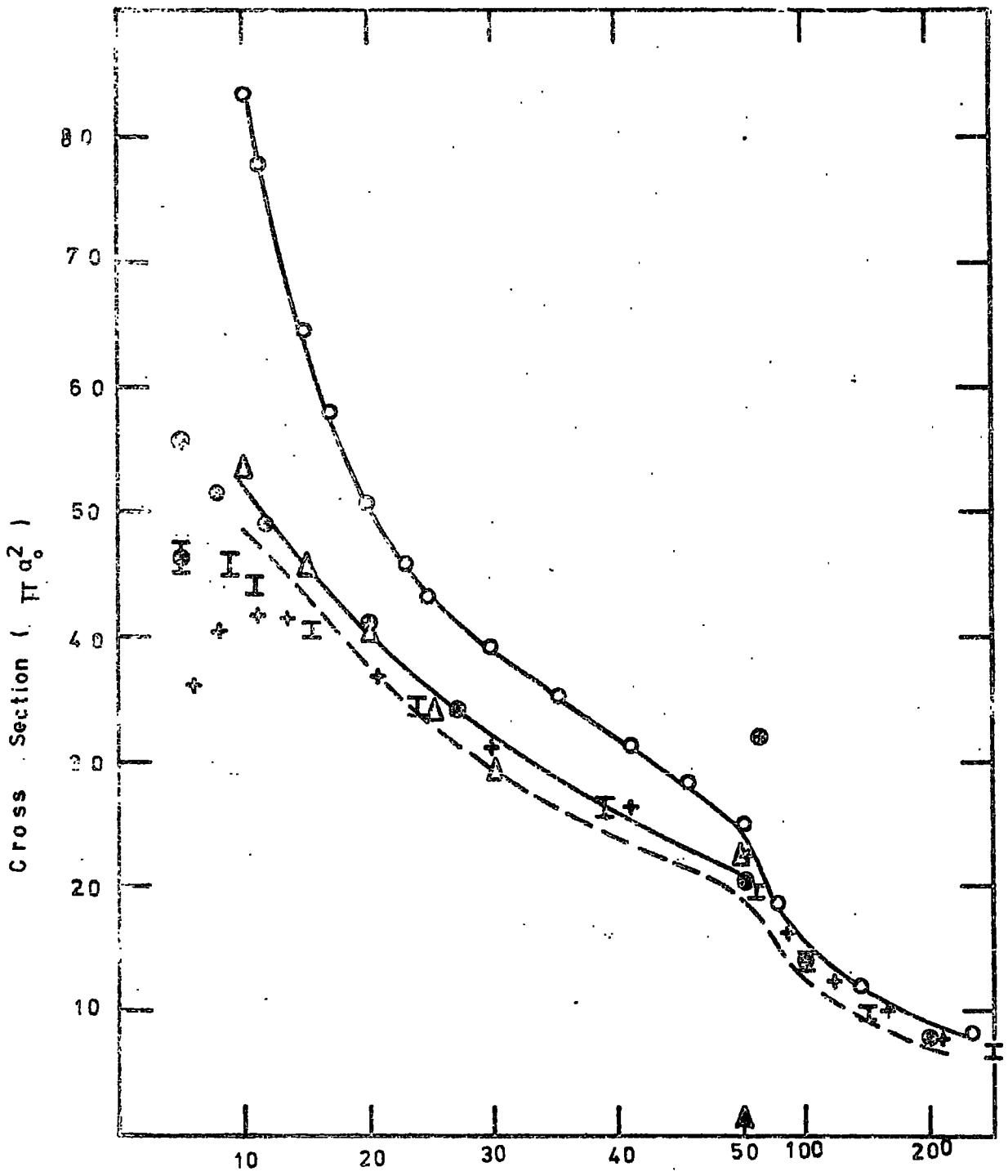
Cross Section (πa_o^2)
80
70
60
50
40
30
20
10
10
20
30
40
50
100
200
Incident Energy (e v)

Fig 6.2

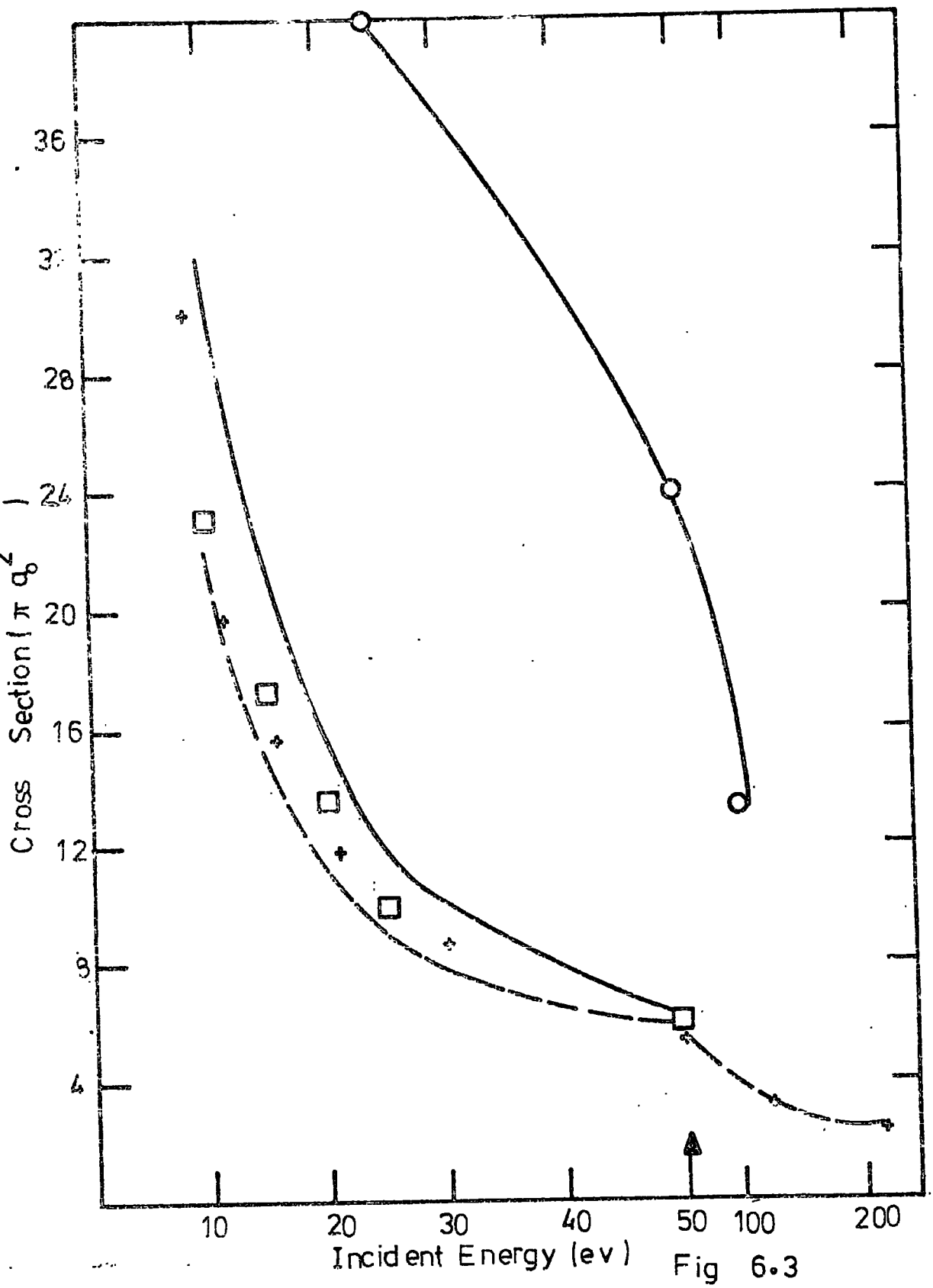
36
32
28
24
20
16
12
8
4
Cross Section (πa_0^2)
10
20
30
40
50
100
200
Incident Energy (ev)

Fig 6.3

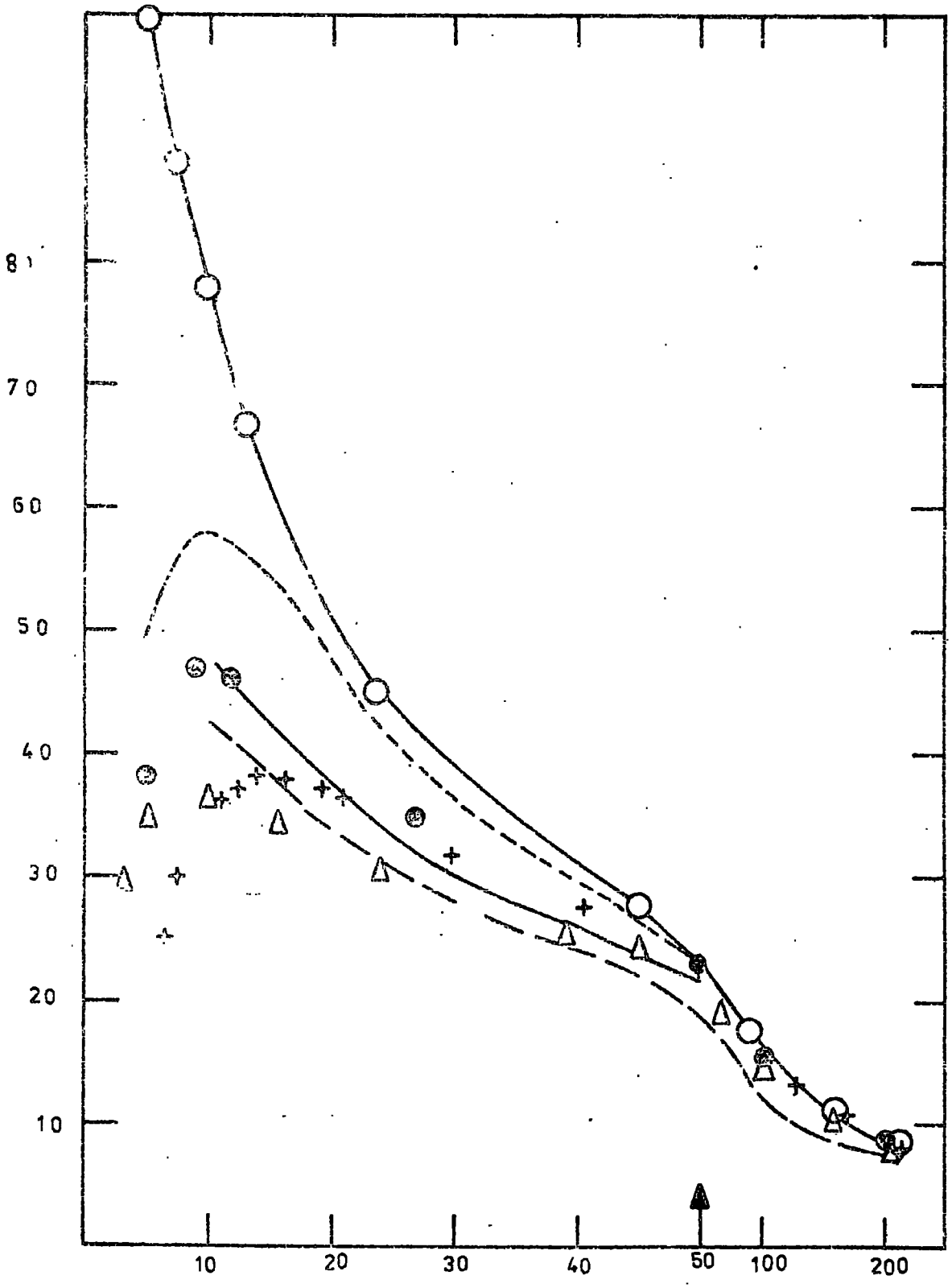
80
70
60
50
40
30
20
10
10
20
30
40
50
100
200
Cross Section (πa_o^2)
Incident Energy in (e.v)

Fig 6.4

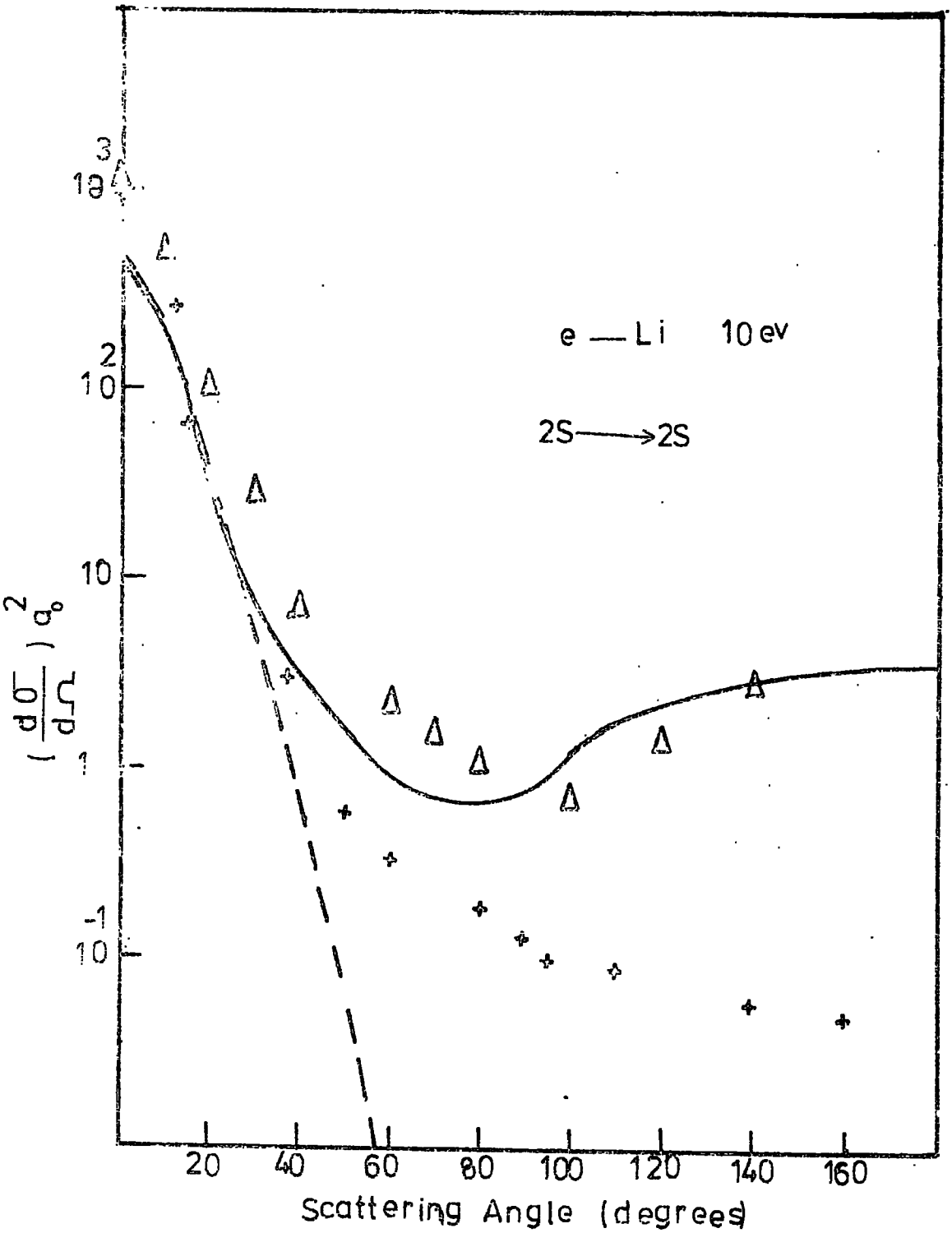
e — Li 10 ev
2S ⟶ 2S
$(\frac{d\sigma}{d\Omega})a_0^2$
10^3
10^2
10
1
10^{-1}
20
40
60
80
100
120
140
160
Scattering Angle (degrees)

Fig 6.5.a

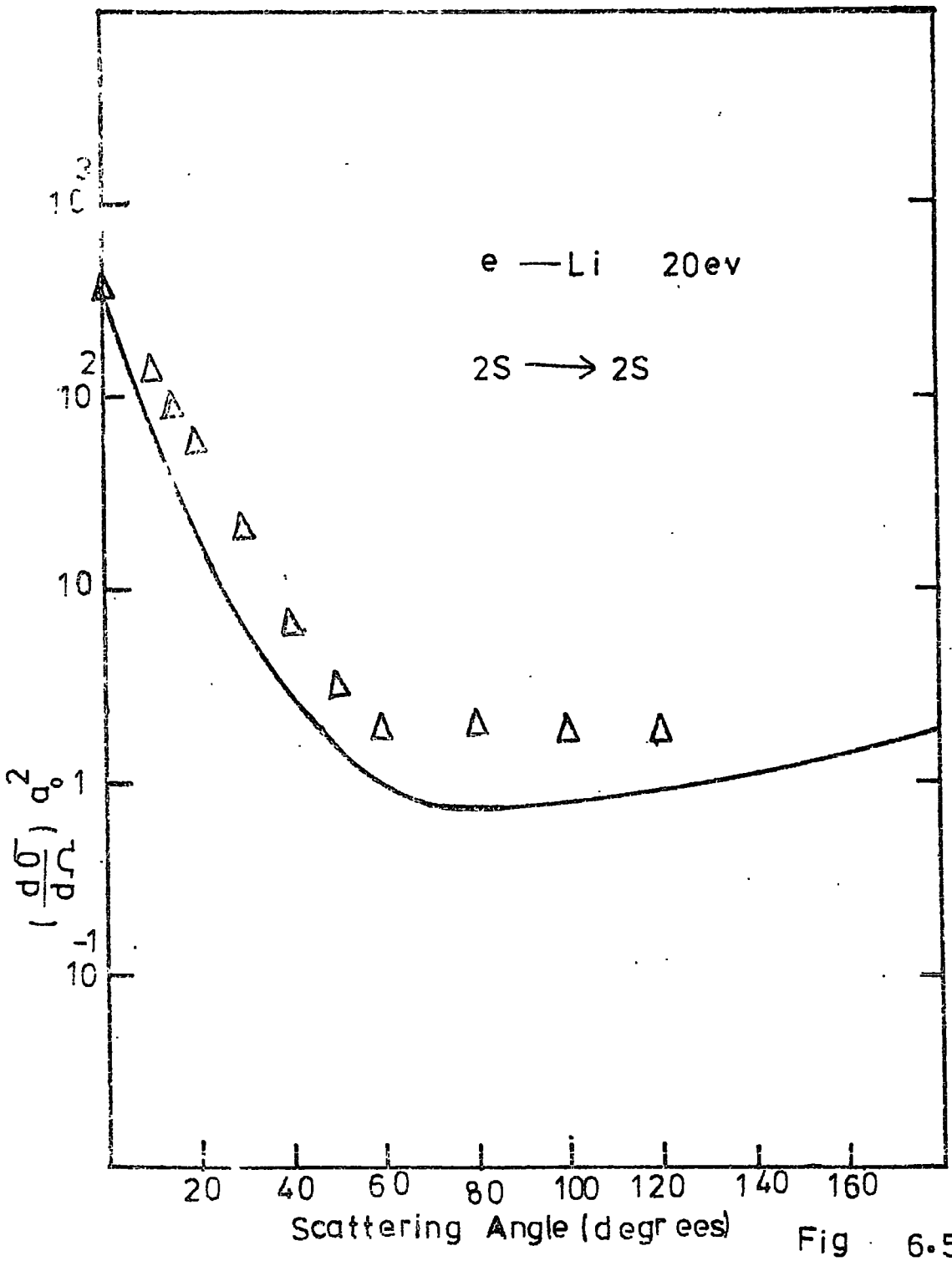
e —Li 20ev
2S ⟶ 2S
10^2
2×10
10
1
10^{-1}
$\left(\frac{dp}{d\Omega}\right) a_0^2$
20
40
60
80
100
120
140
160
Scattering Angle (degrees)

Fig 6.5.b

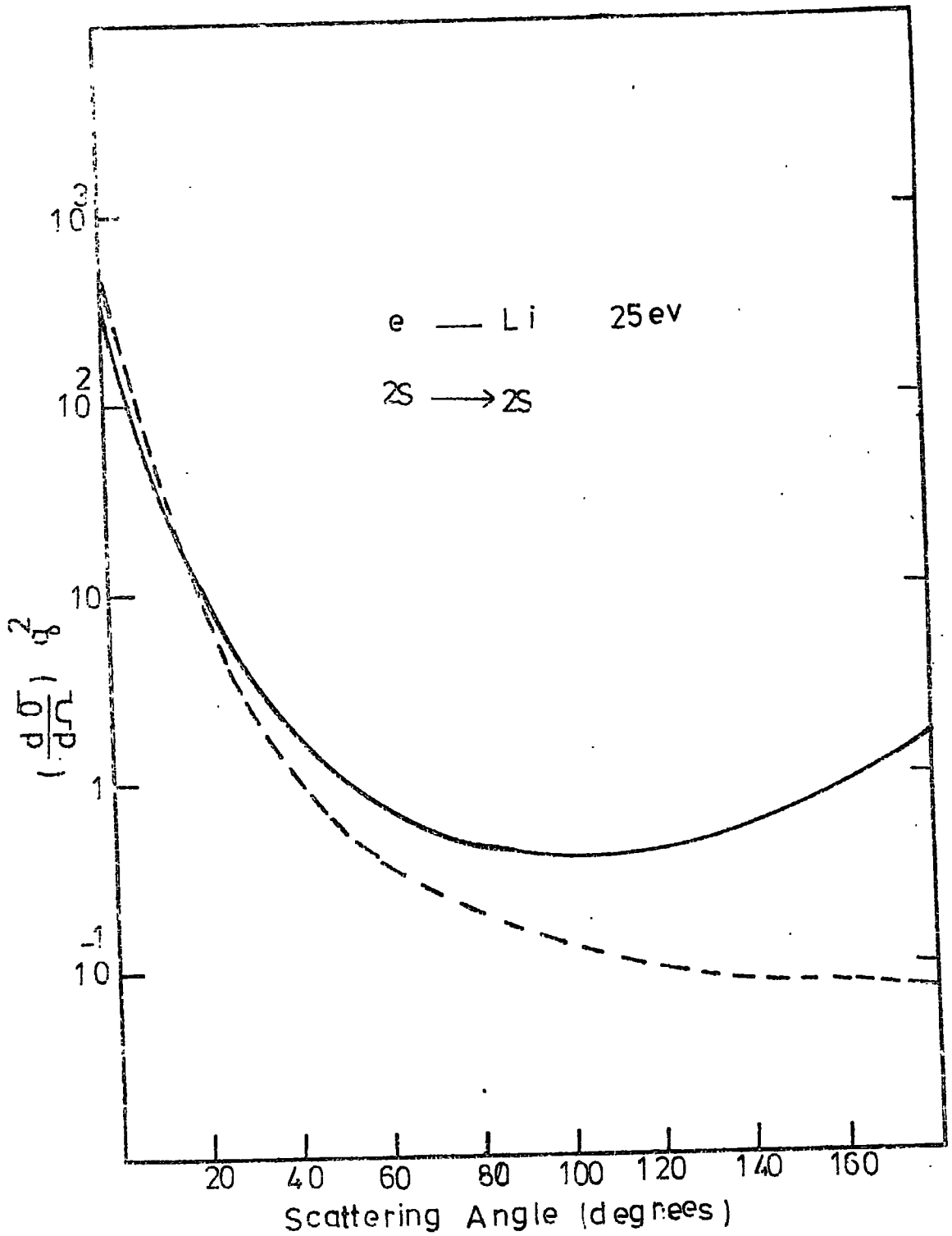
e — Li 25ev
2S ⟶ 2S
10^2
10^2
10
1
10^{-1}
$(\frac{d\sigma}{d\Omega})\ a_0^2$
20
40
60
80
100
120
140
160
Scattering Angle (degrees)

Fig 6.5.C

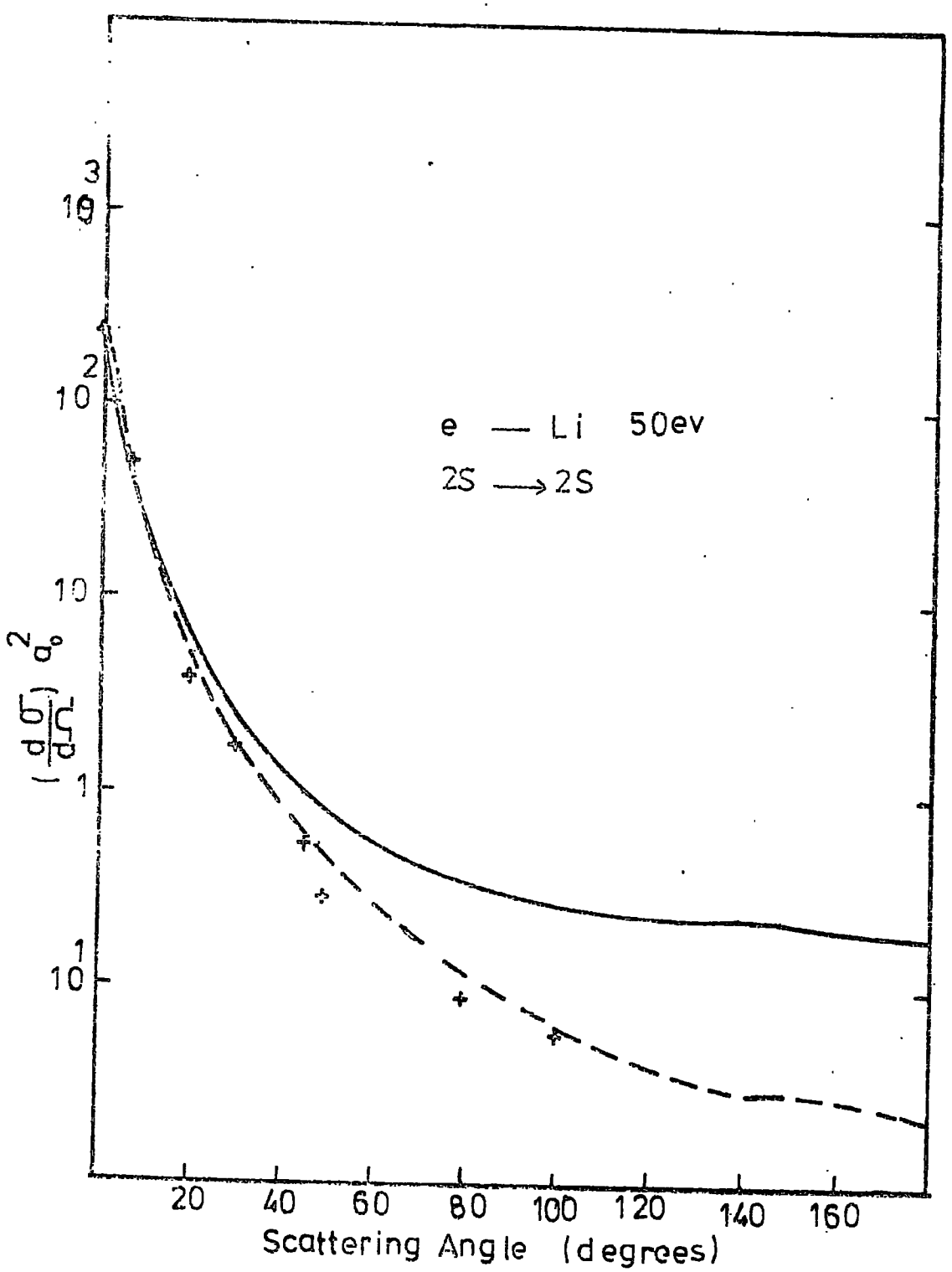
e — Li 50ev
2S ⟶ 2S
$(\frac{d\sigma}{d\Omega}) a_0^2$
10^3
10^2
10
1
10^{-1}
20
40
60
80
100
120
140
160
Scattering Angle (degrees)

Fig 6.5.d

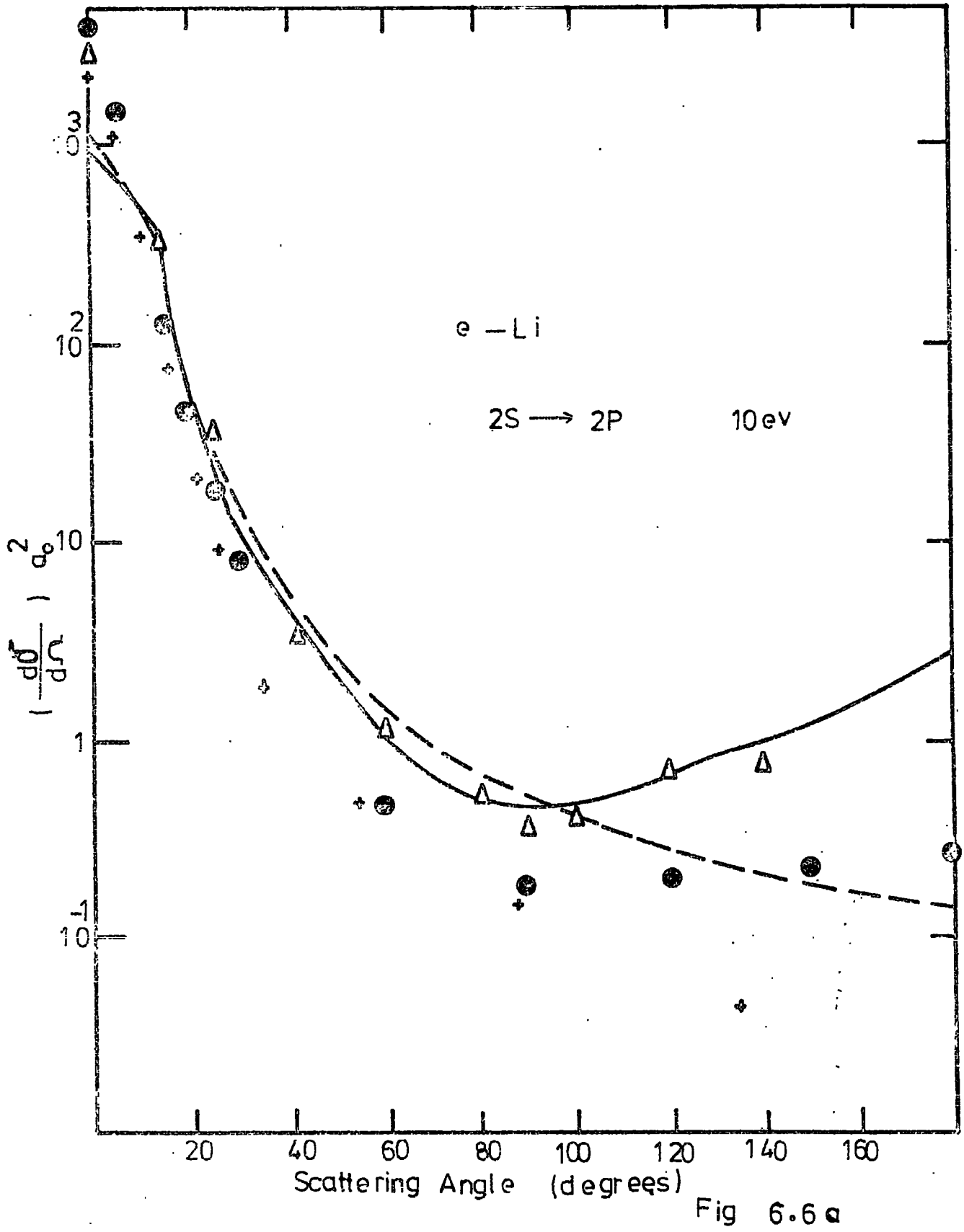
e – Li
2S ⟶ 2P
10 ev
$\left(\frac{d\sigma}{d\Omega}\right) a_0^2$
3
2
10
1
-1
10
20
40
60
80
100
120
140
160
Scattering Angle (degrees)

Fig 6.6a

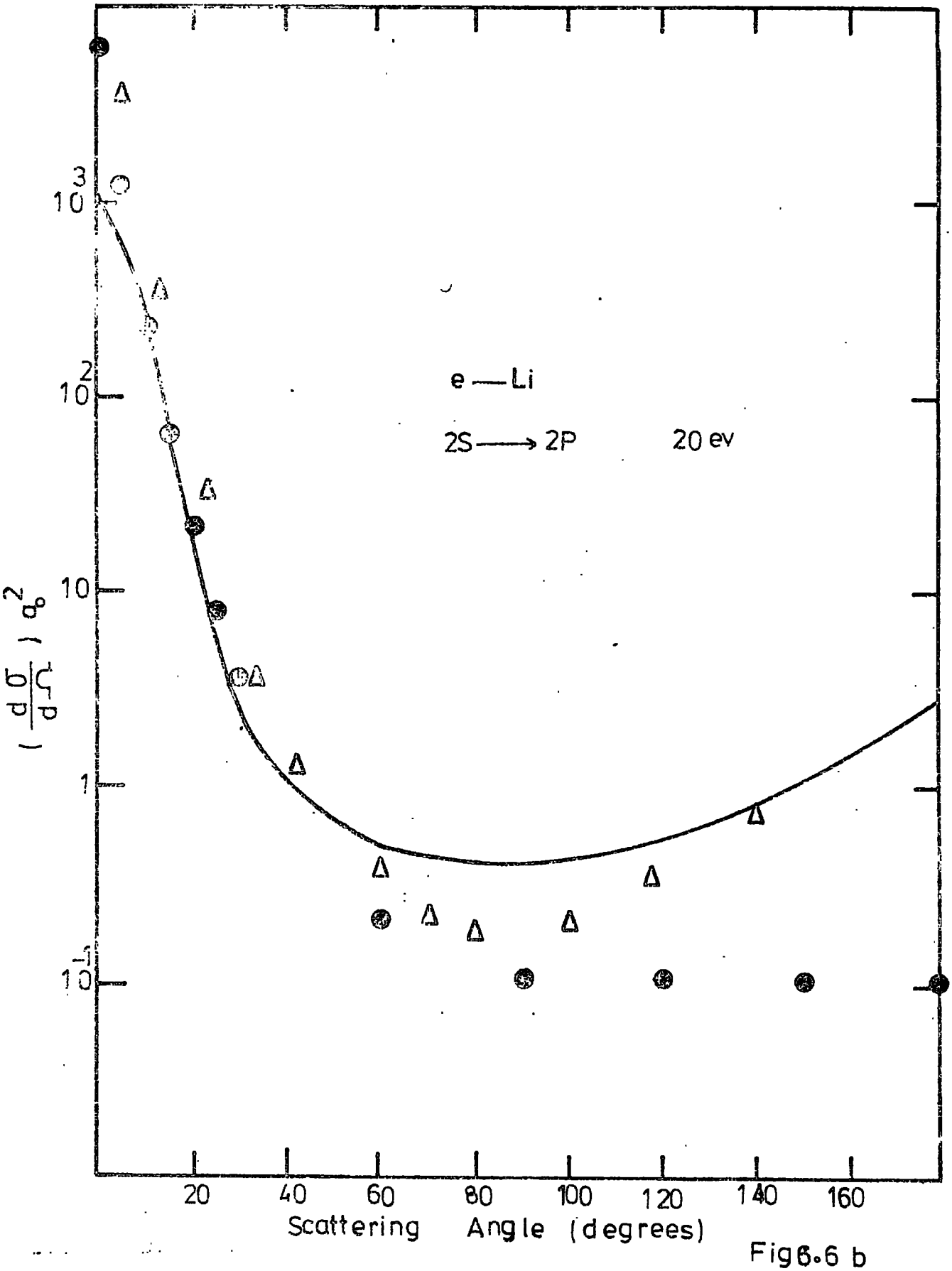
e — Li
2S ⟶ 2P
20 ev
10^3
10^2
10
1
10^{-1}
$\left(\frac{d\sigma}{d\Omega}\right) a_0^2$
20
40
60
80
100
120
140
160
Scattering Angle (degrees)

Fig 6.6 b

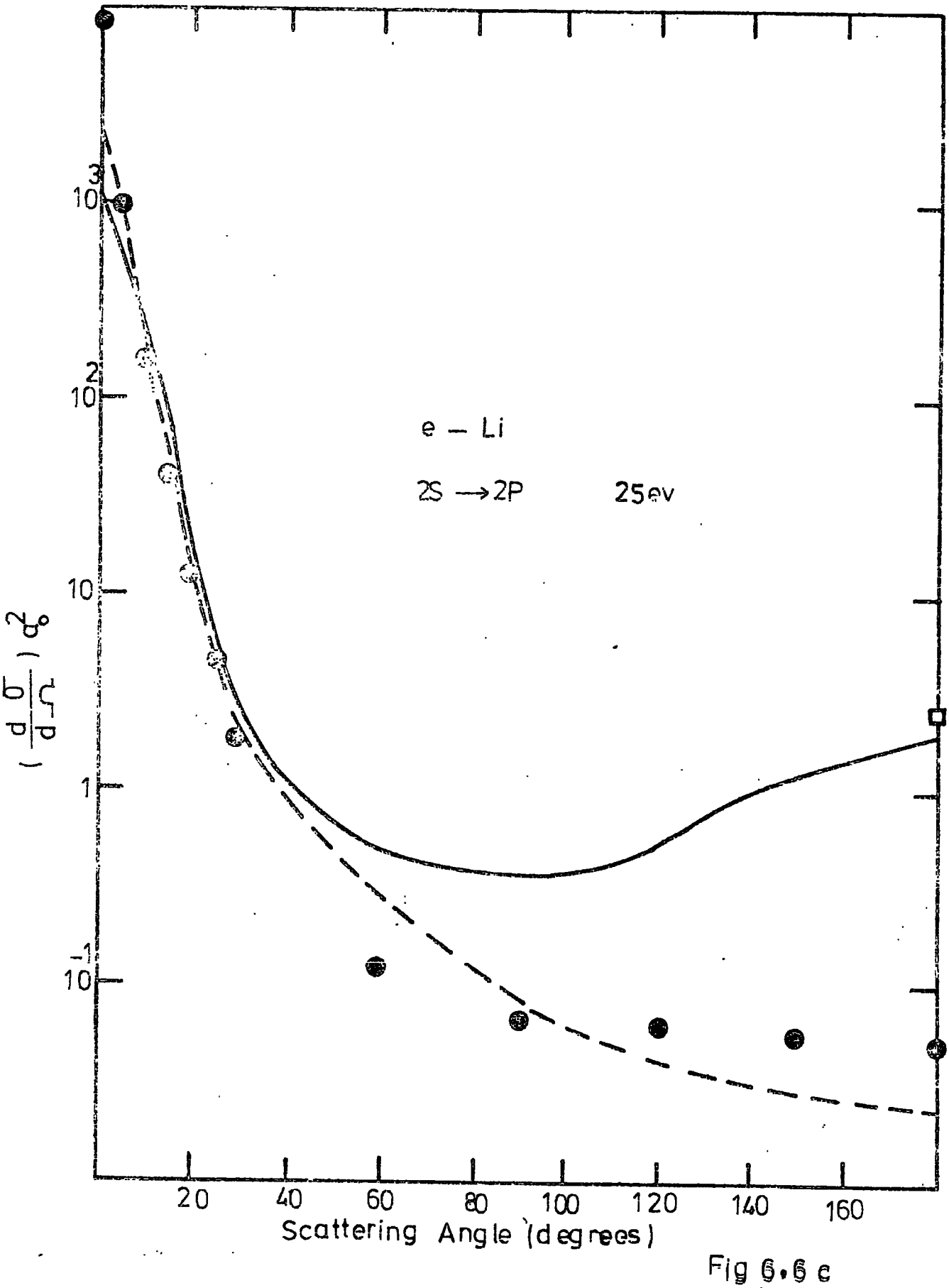
e – Li
2S → 2P 25ev
$(\frac{d\sigma}{d\Omega})a_0^2$
10^3
10^2
10
1
10^{-1}
20
40
60
80
100
120
140
160
Scattering Angle (degrees)

Fig 6.6 c

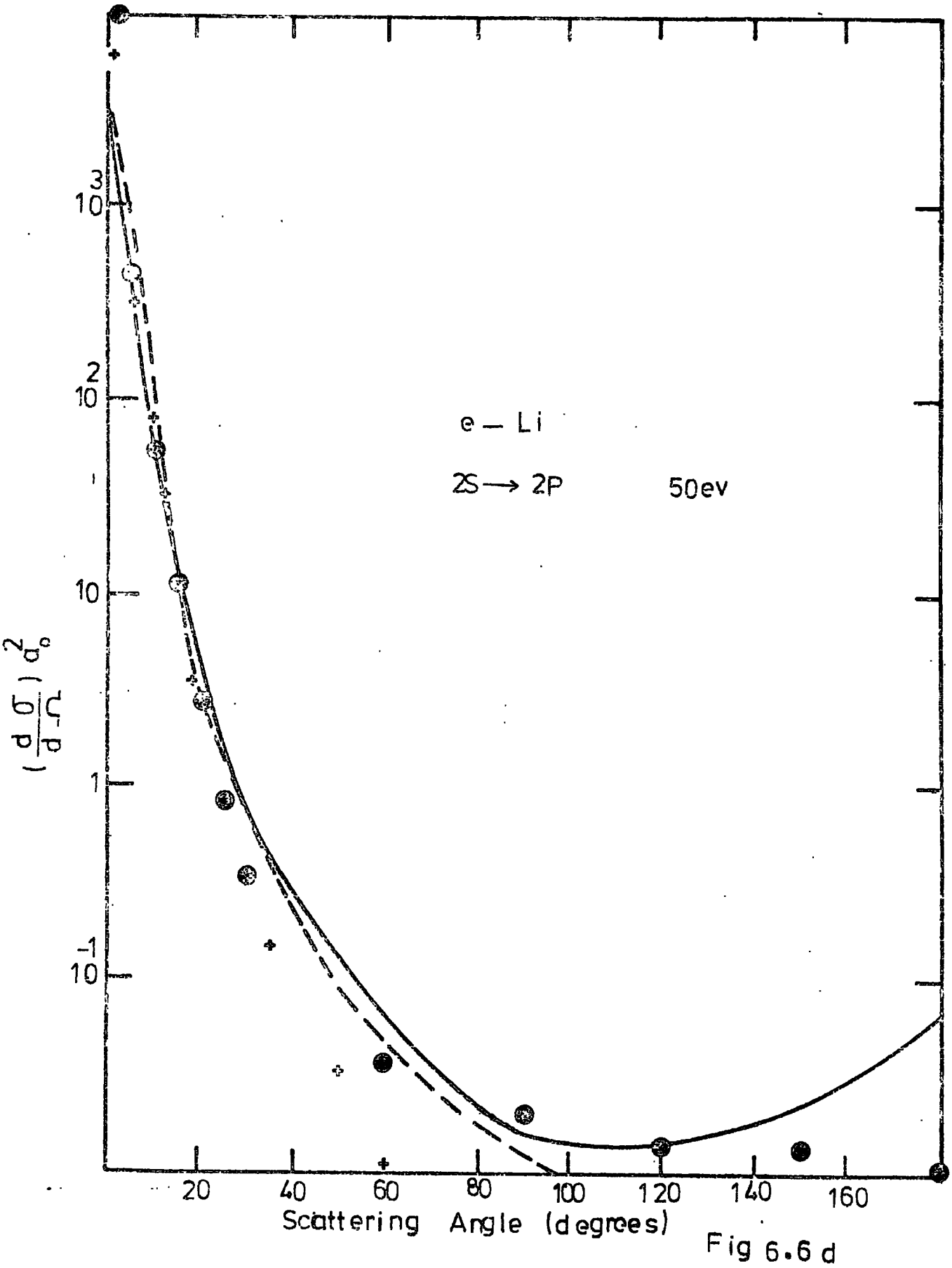
e — Li
2S → 2P
50ev
$(\frac{d\sigma}{d\Omega})a_o^2$
3
10
2
10
10
1
-1
10
20
40
60
80
100
120
140
160
Scattering Angle (degrees)

Fig 6.6 d

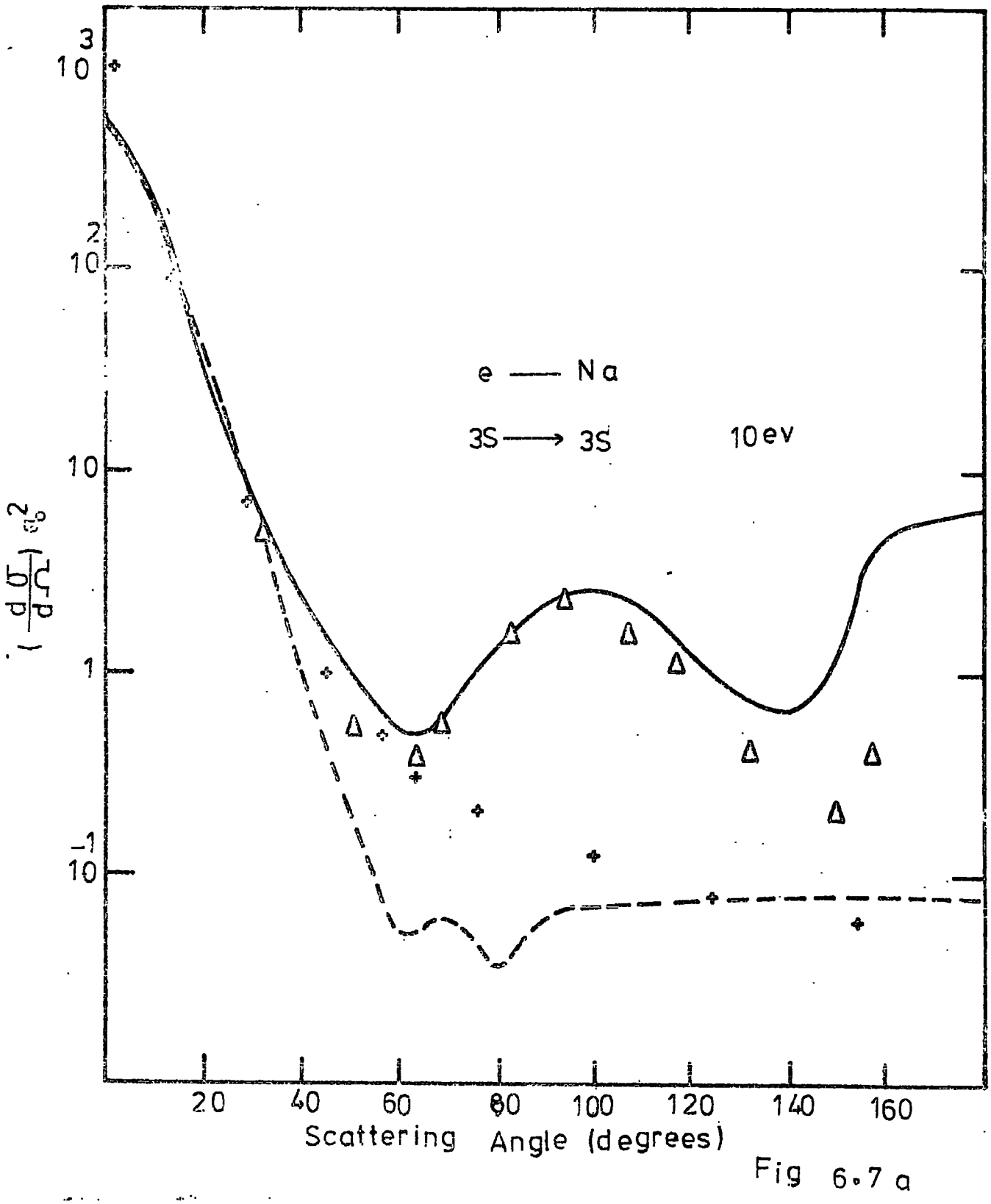
e —— Na
3S ⟶ 3S
10 ev
$(\frac{d\sigma}{d\Omega})\,a_0^2$
3
10
2
10
10
1
10^{-1}
20
40
60
80
100
120
140
160
Scattering Angle (degrees)

Fig 6.7 a

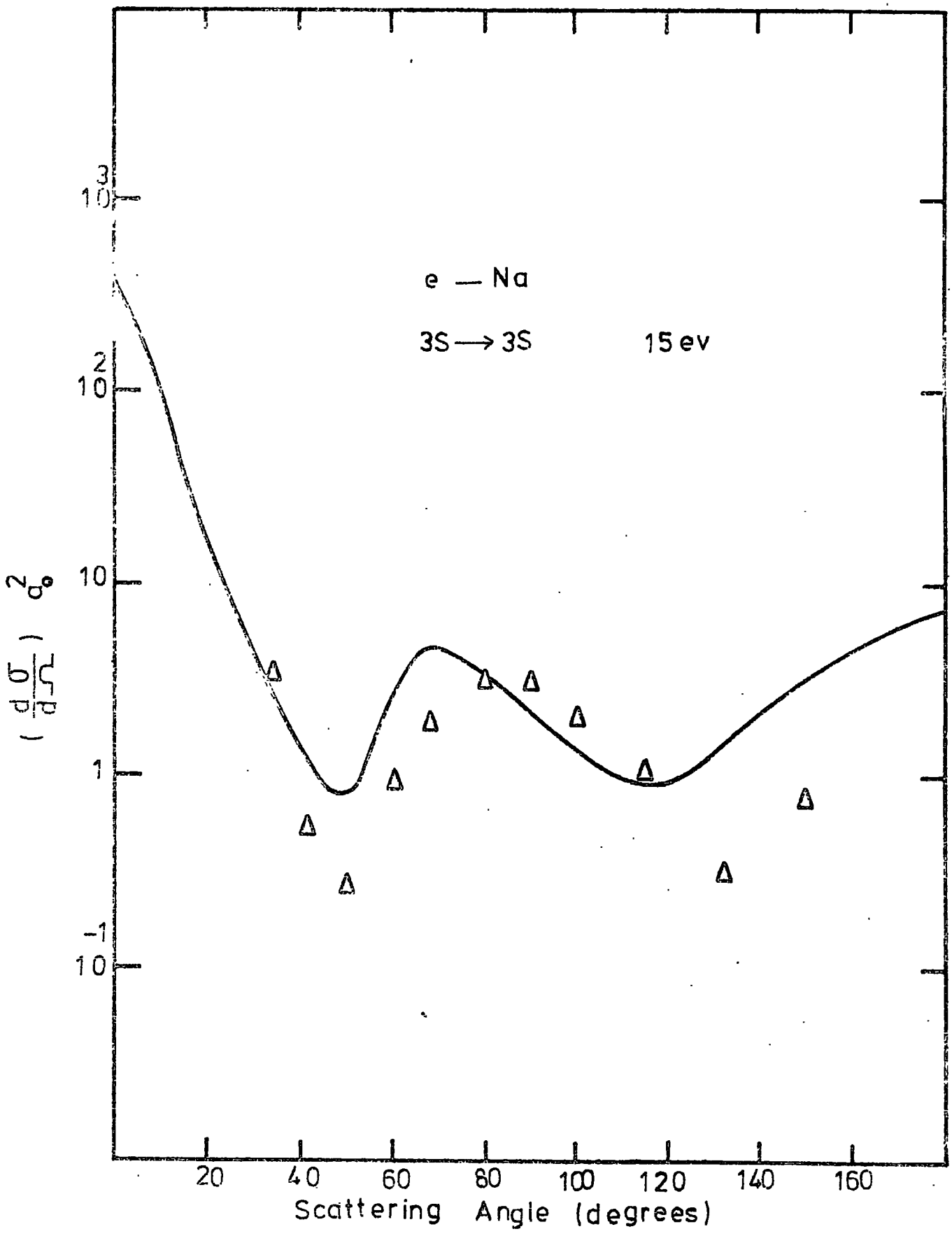
e — Na
3S ⟶ 3S 15 ev
10^3
10^2
10
1
10^{-1}
$\left(\frac{d\sigma}{d\Omega}\right) a_0^2$
20
40
60
80
100
120
140
160
Scattering Angle (degrees)

Fig 6.7 b

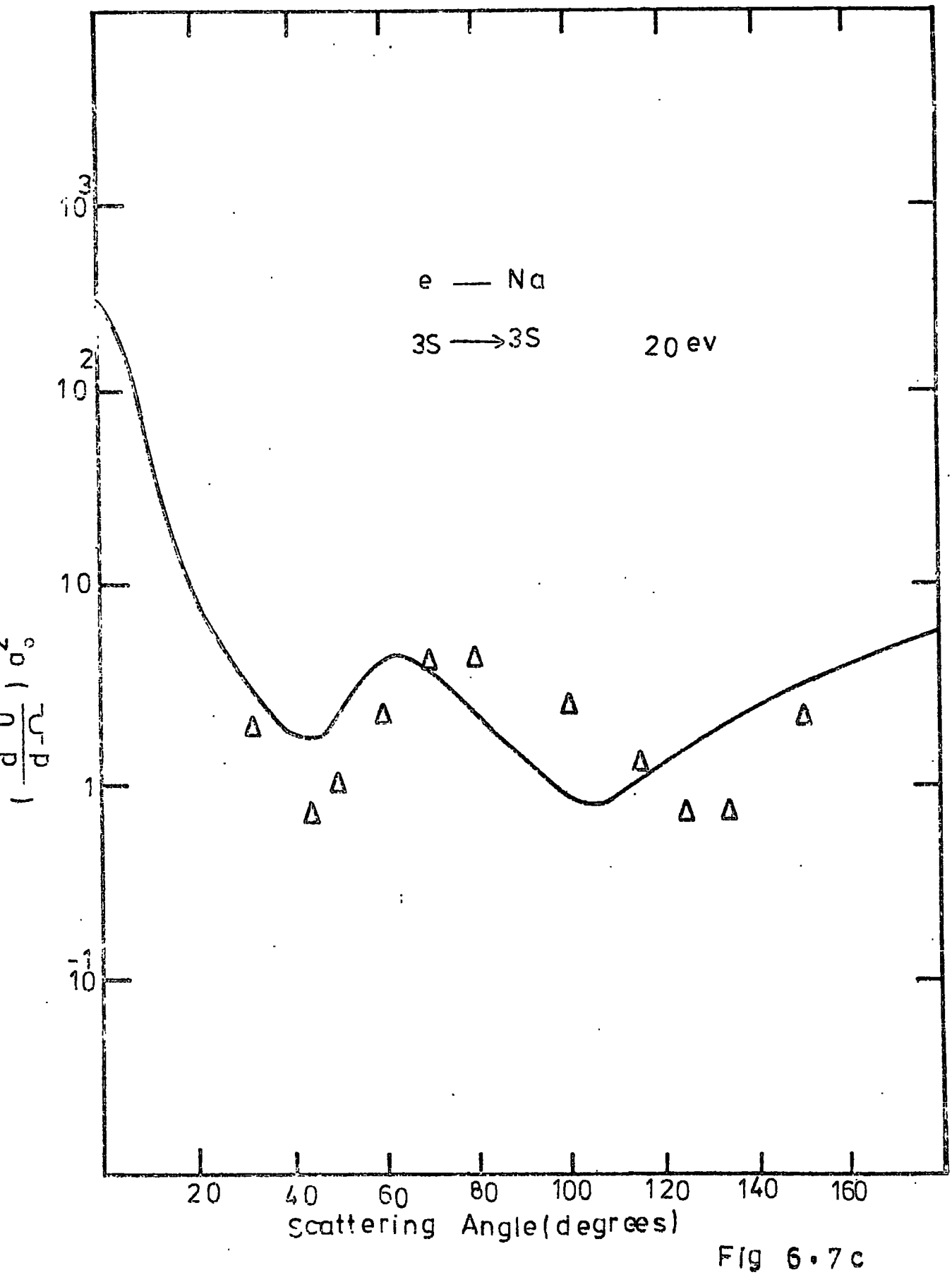
e — Na
3S ⟶ 3S
20 ev
10^3
10^2
10
1
10^{-1}
$(\frac{d\sigma}{d\Omega})a_0^2$
20
40
60
80
100
120
140
160
Scattering Angle (degrees)

Fig 6.7c

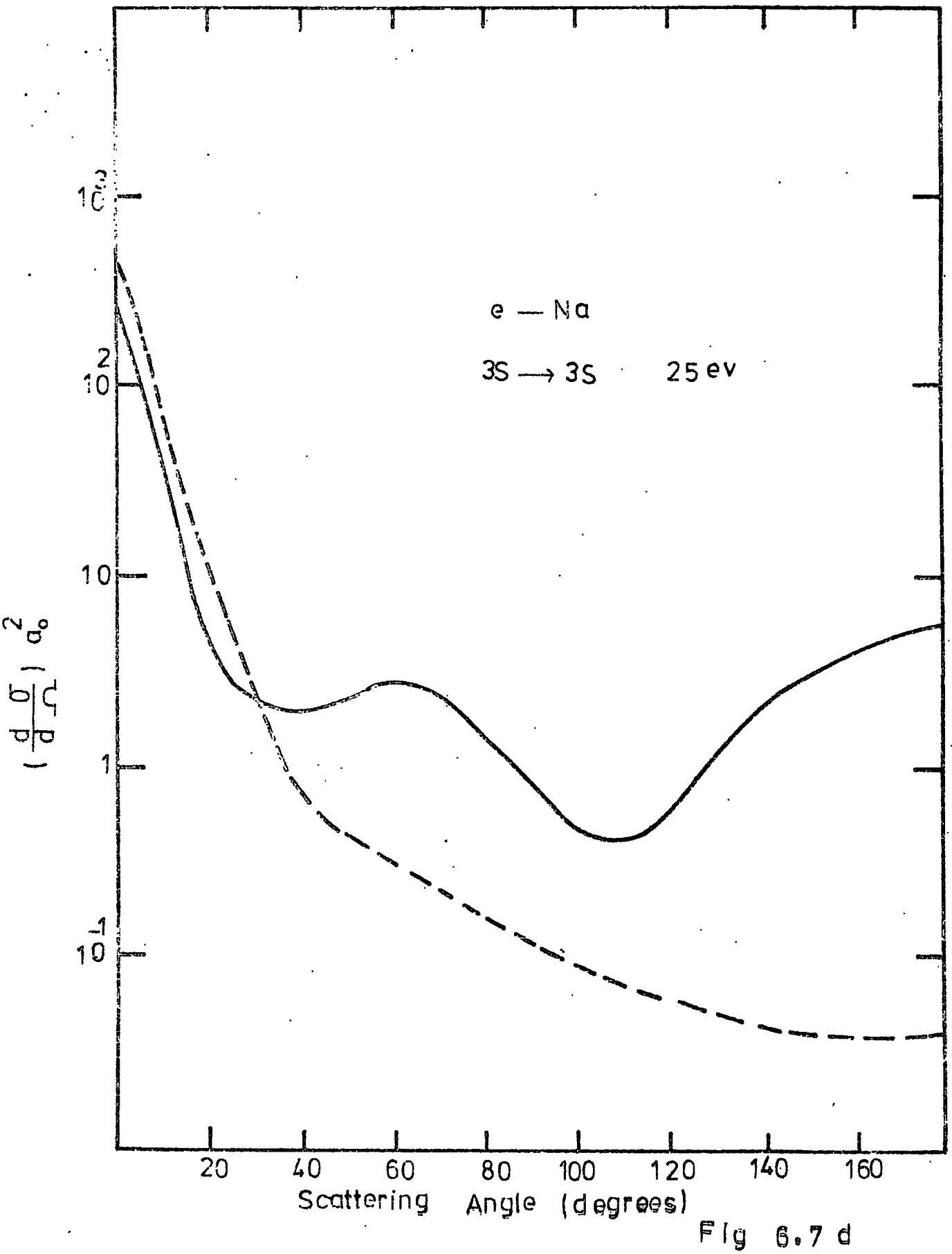
e — Na
3S ⟶ 3S 25 ev
10^2
10^1
1
10^{-1}
$(\frac{d\sigma}{d\Omega})\, a_o^2$
20
40
60
80
100
120
140
160
Scattering Angle (degrees)

Fig 6.7 d

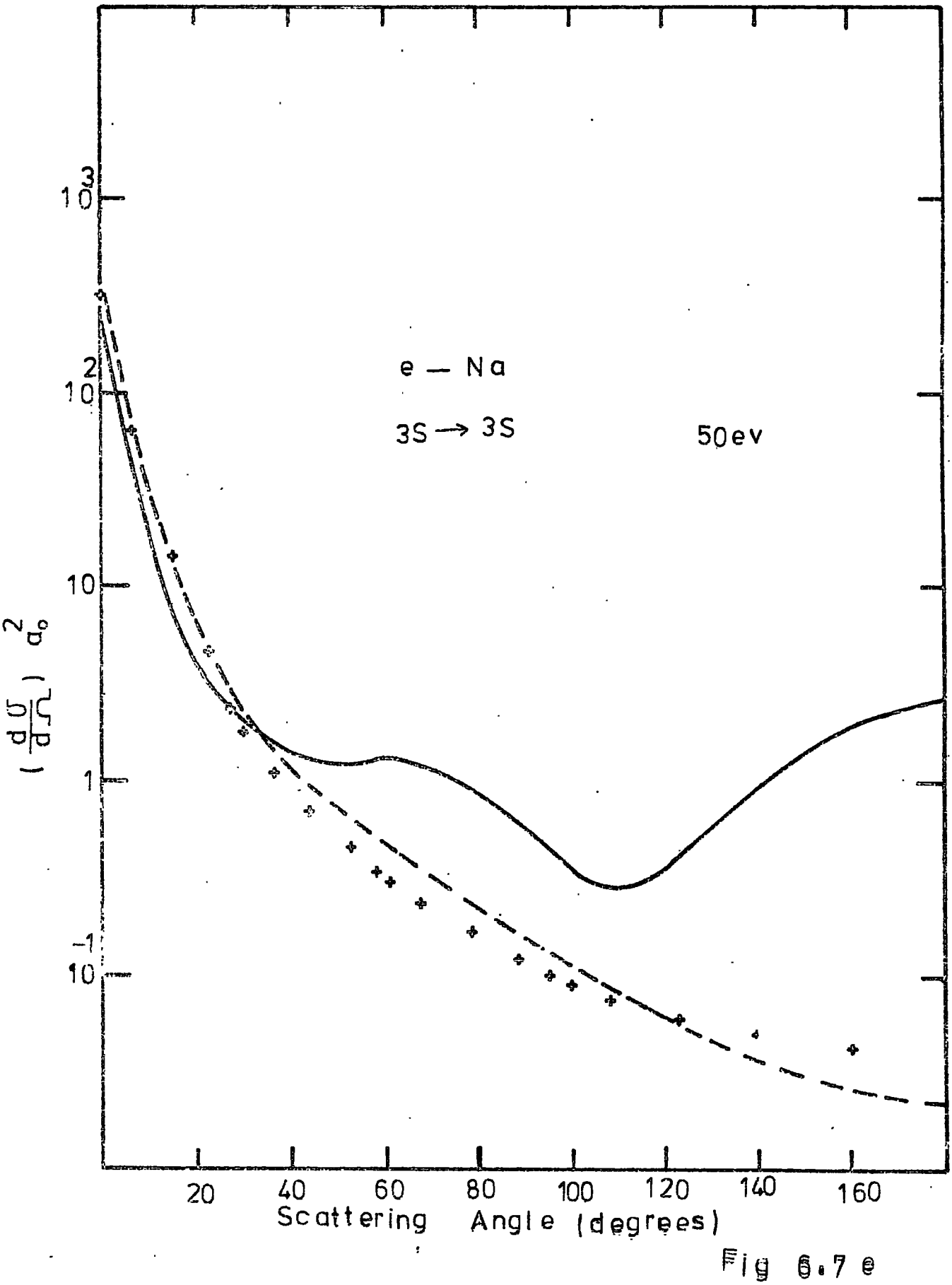
e — Na
3S → 3S
50ev
10^3
10^2
10
1
10^{-1}
$(\frac{d\sigma}{d\Omega})\ a_o^2$
20
40
60
80
100
120
140
160
Scattering Angle (degrees)

Fig 6.7 e

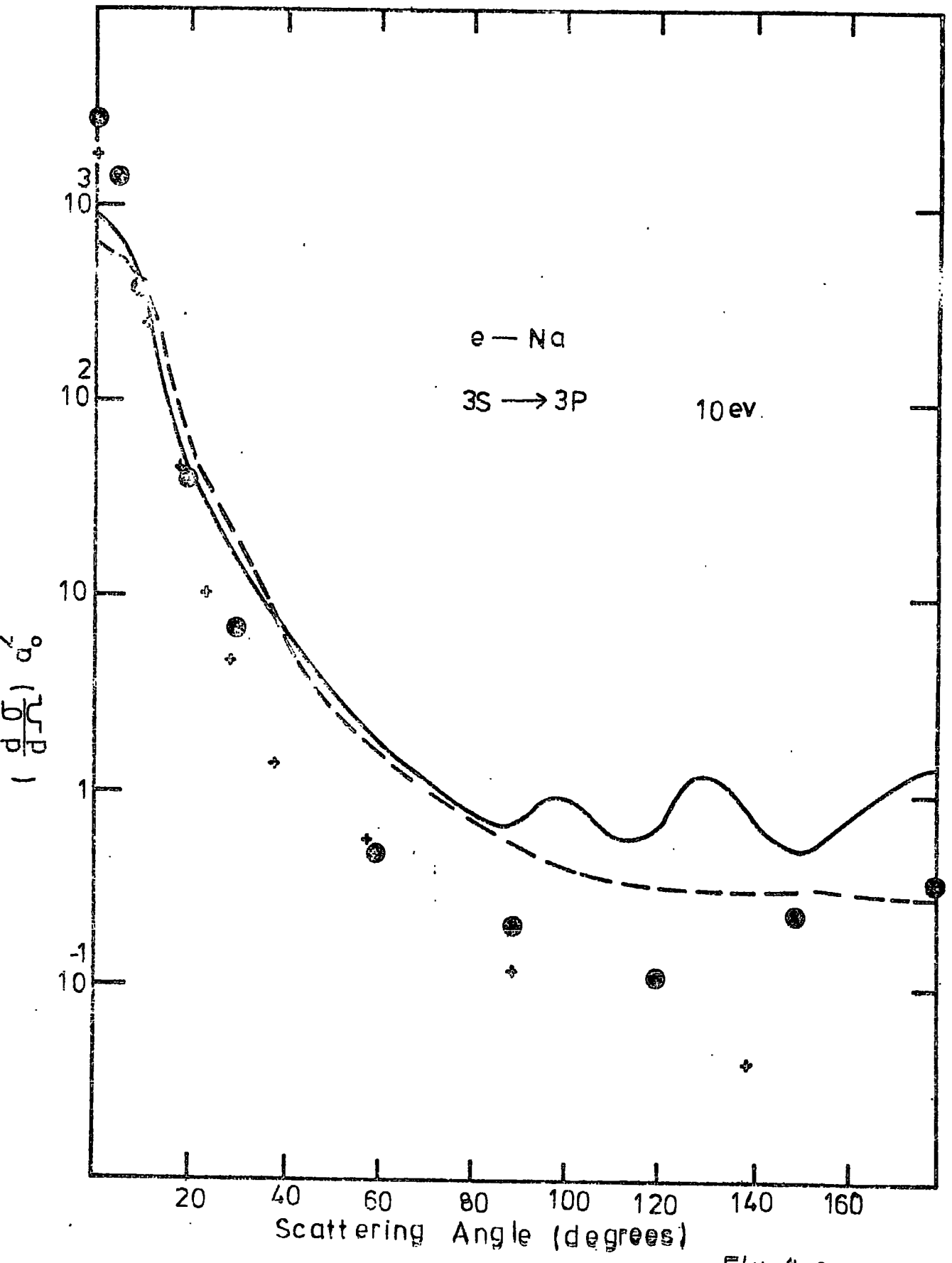
e — Na
3S ⟶ 3P
10 ev.
$(\frac{d\sigma}{d\Omega})\, a_o^2$
10^3
10^2
10
1
10^{-1}
20
40
60
80
100
120
140
160
Scattering Angle (degrees)

Fig 6.8a

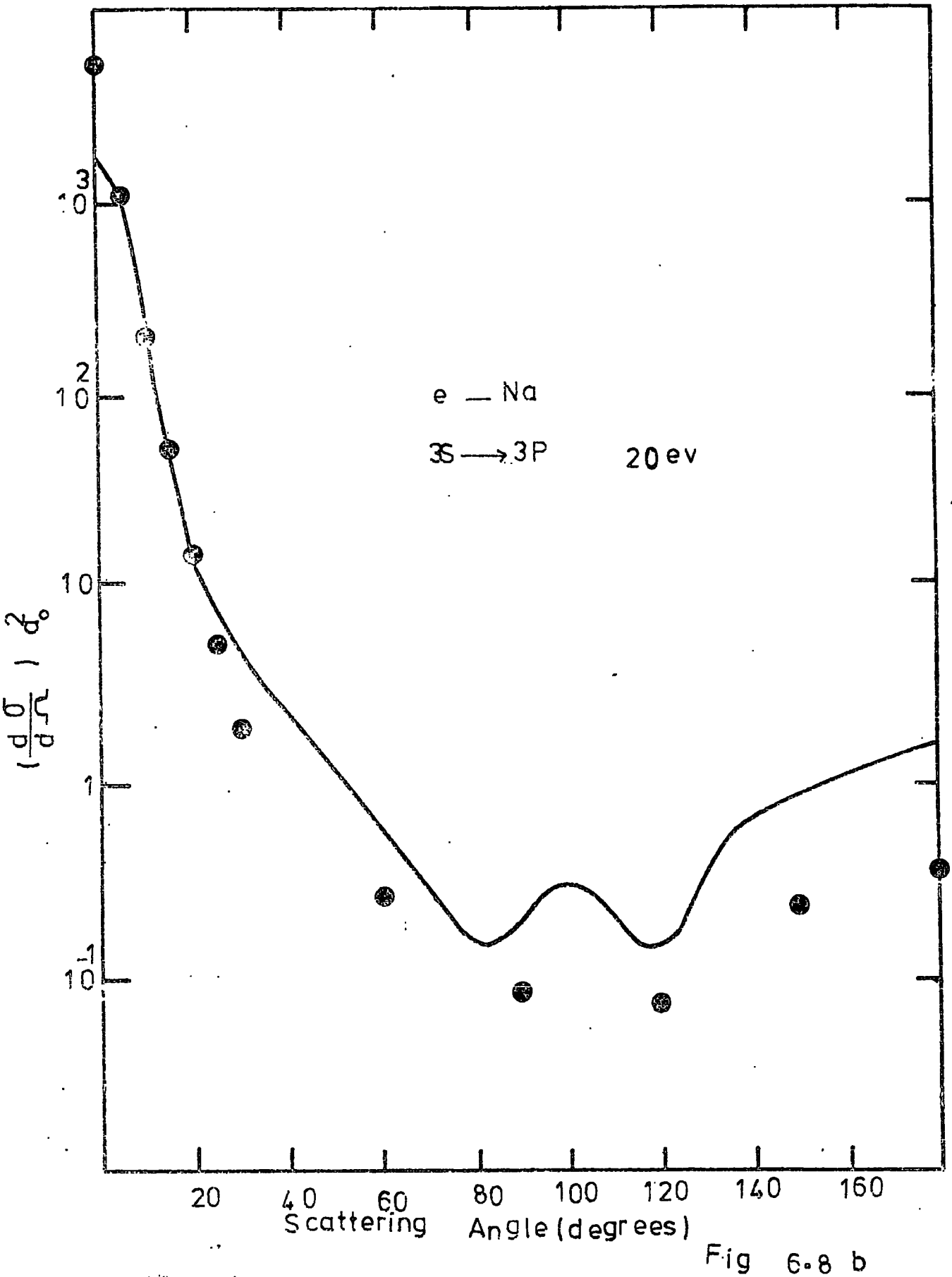
e — Na
3S ⟶ 3P
20 ev
$(\frac{d\sigma}{d\Omega})_P$ / a_0^2
10^3
10^2
10
1
10^{-1}
20
40
60
80
100
120
140
160
Scattering Angle (degrees)

Fig 6.8 b

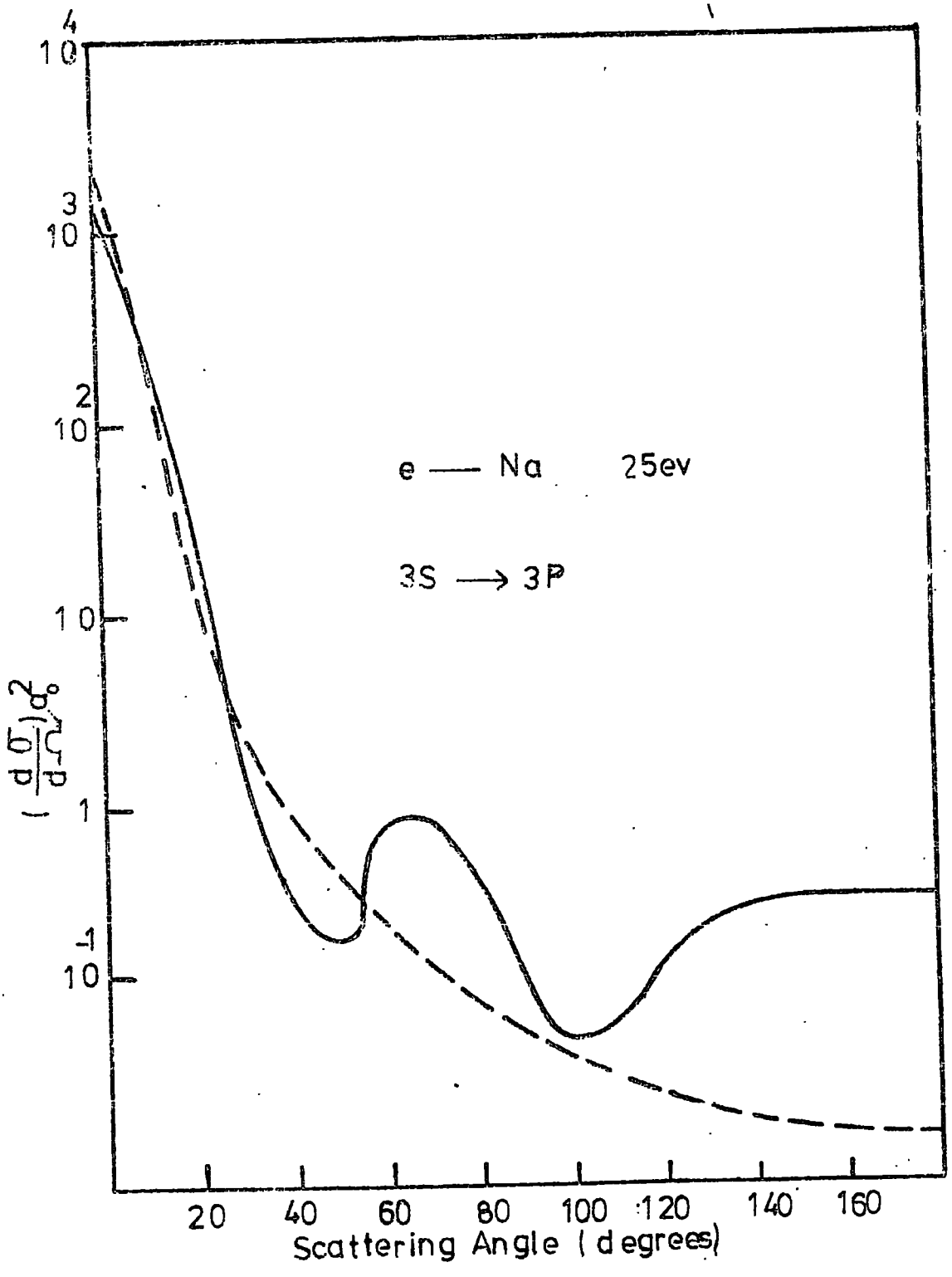
4
10
3
10
2
10
10
1
-1
10
e —— Na 25ev
3S ⟶ 3P
$(\frac{d\sigma}{d\Omega})a_0^2$
20
40
60
80
100
120
140
160
Scattering Angle (degrees)

Fig 6.8.C

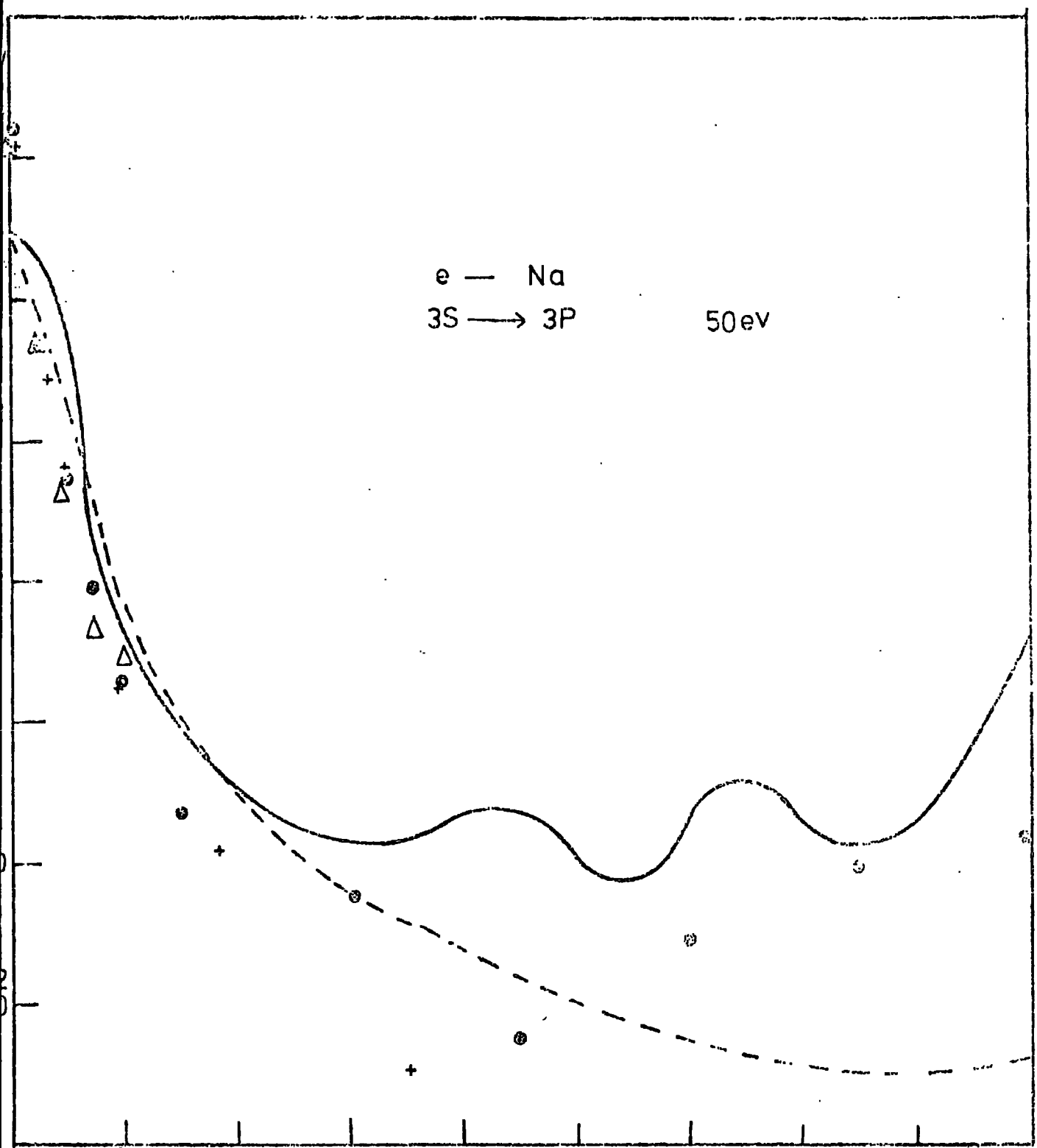
e — Na
3S ⟶ 3P
50eV
20
40
60
80
100
120
140
160
Scattering Angle (degrees)

Fig 6.6 d

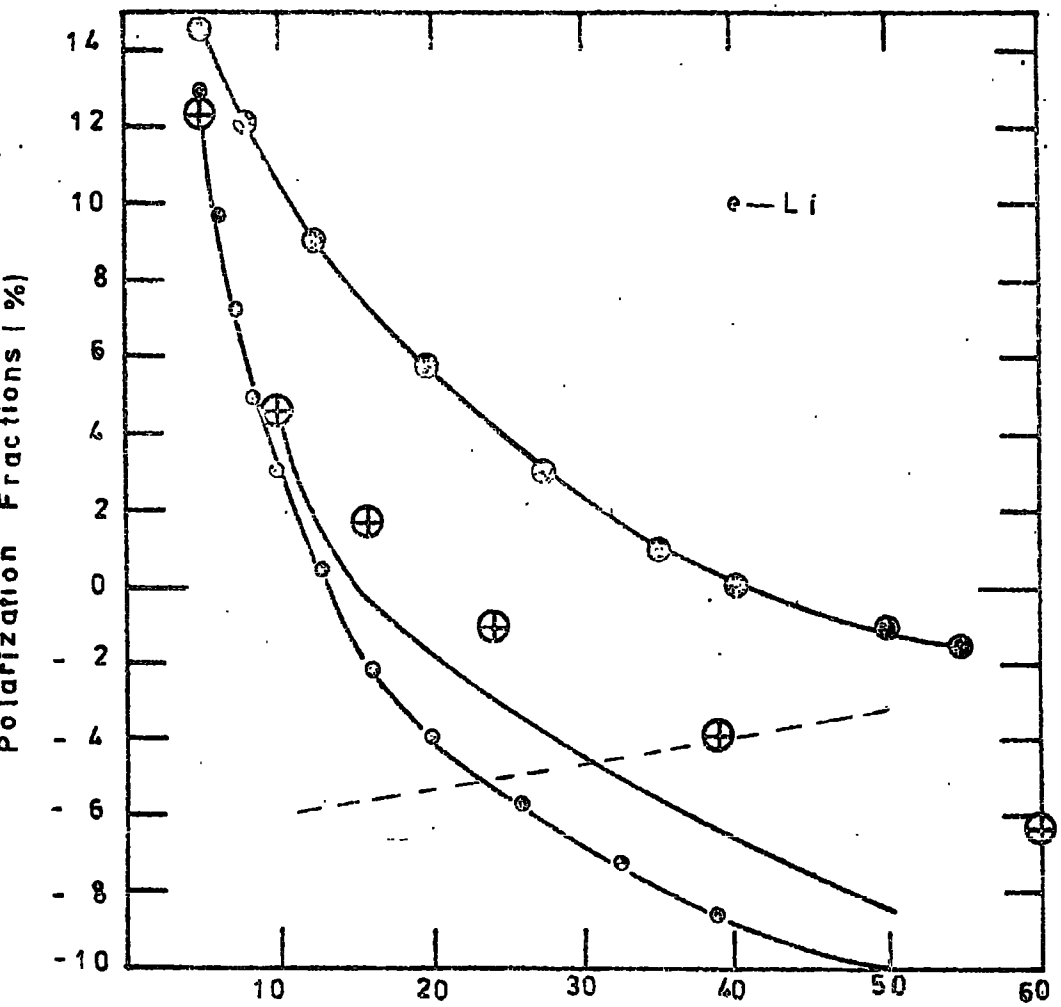
14
12
10
8
6
4
2
0
- 2
- 4
- 6
- 8
-10
10
20
30
40
50
60
e—Li
Polarization Fractions (%)
Incident Energy (ev)

Fig 6.9

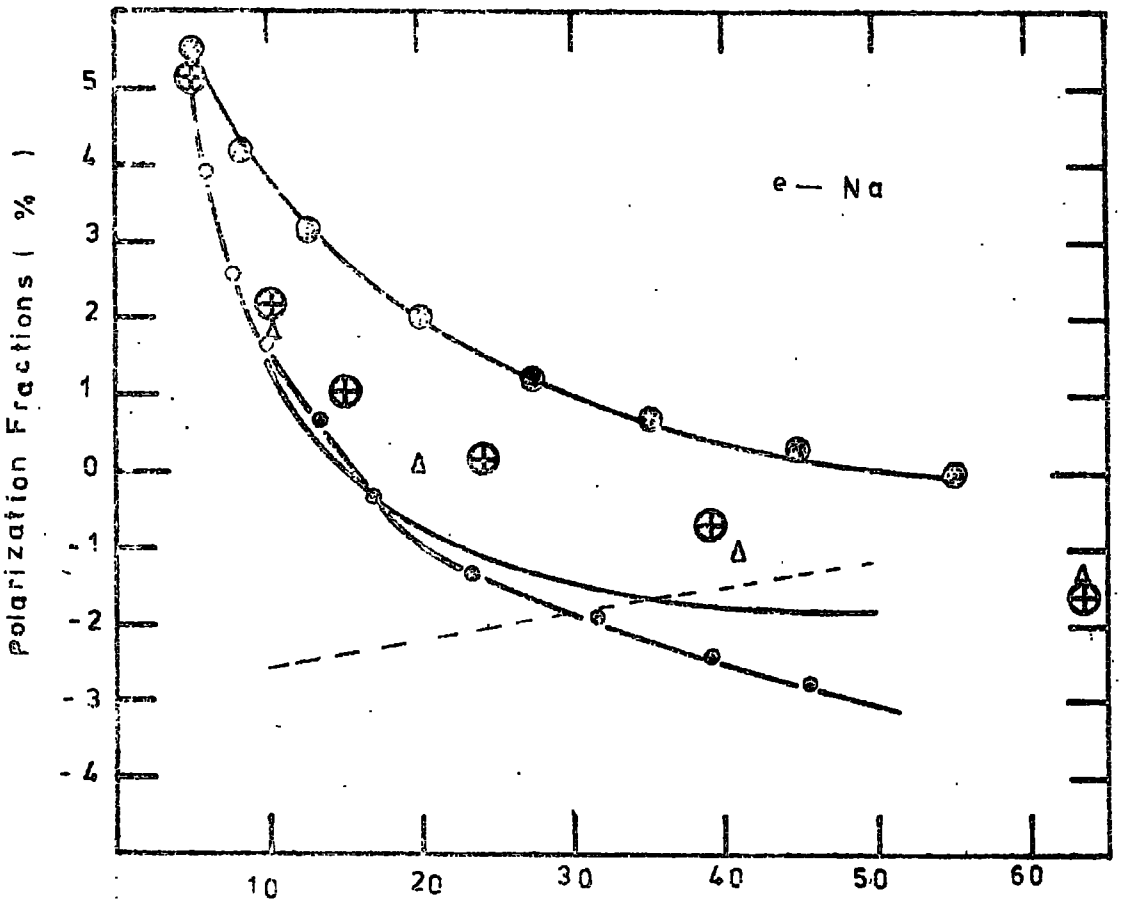
e — Na
Polarization Fractions (%)
5
4
3
2
1
0
-1
-2
-3
-4
10
20
30
40
50
60
Incident Energy (e v)

Fig 6.10

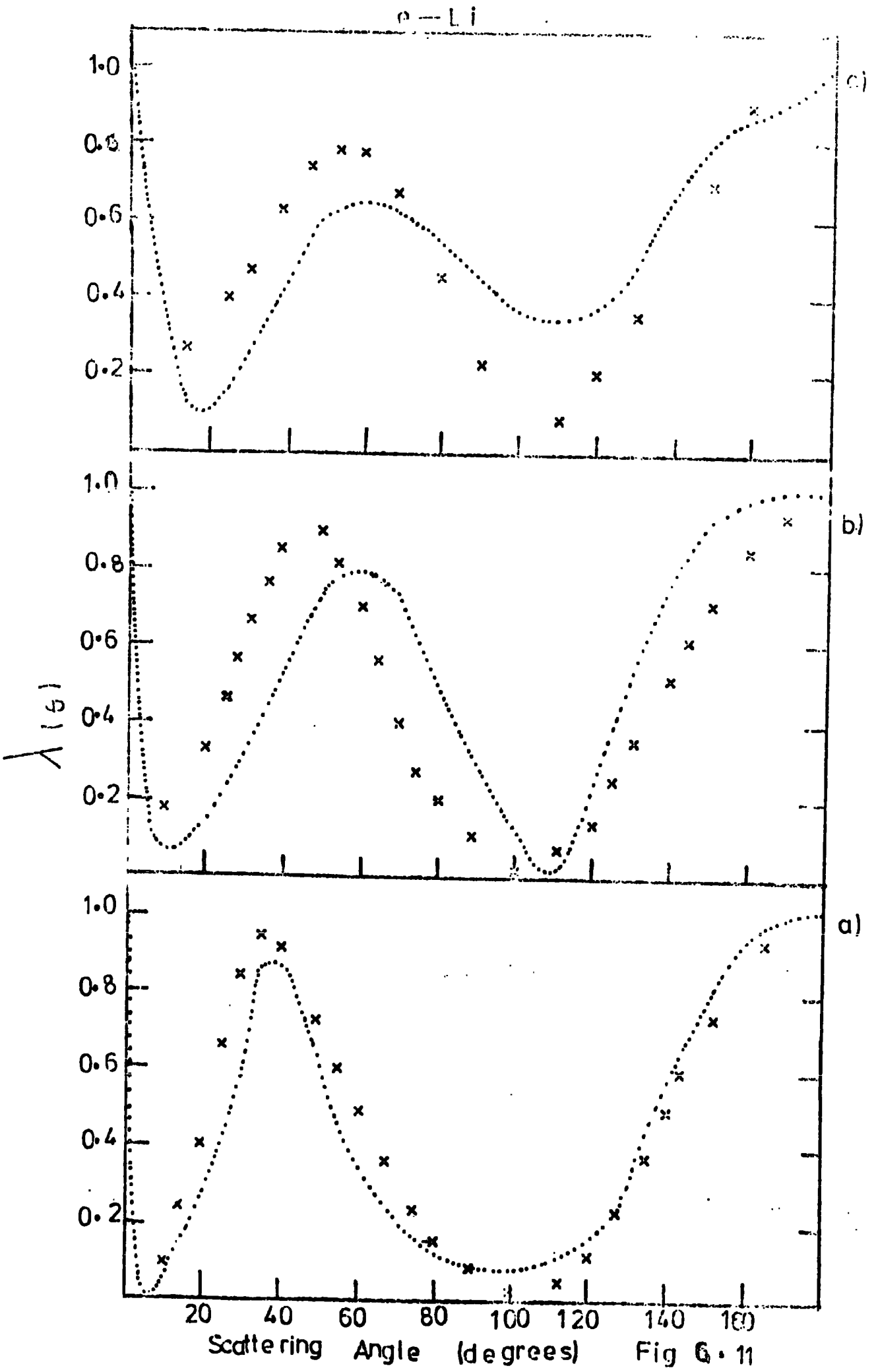
α — Li
1·0
0·8
0·6
0·4
0·2
c)
b)
a)
λ (θ)
20
40
60
80
100
120
140
160
Scattering Angle (degrees)

Fig 6·11

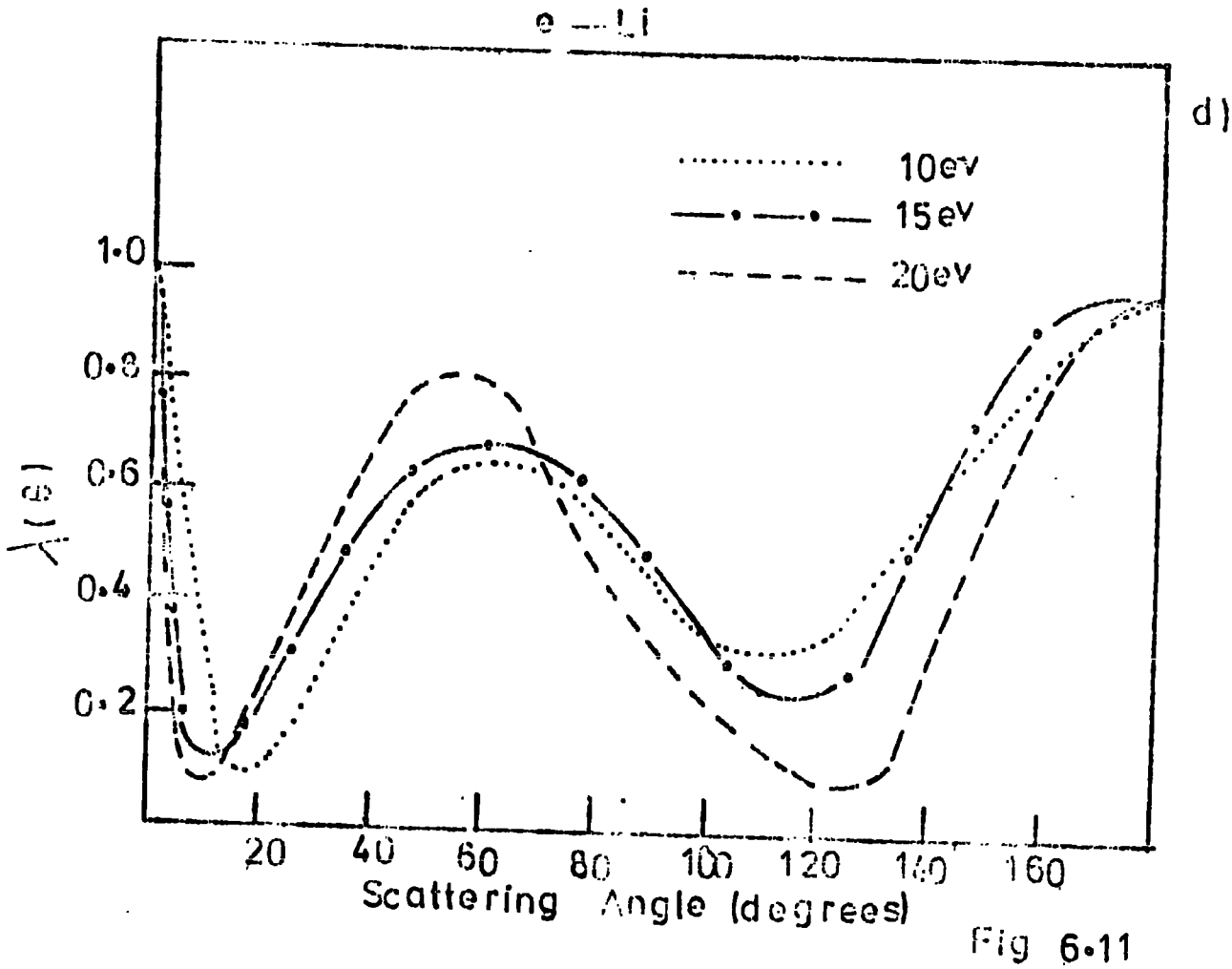
e — Li
d)
10ev
15eV
20ev
1·0
0·8
0·6
0·4
0·2
I (θ)
20
40
60
80
100
120
140
160
Scattering Angle (degrees)

Fig 6·11

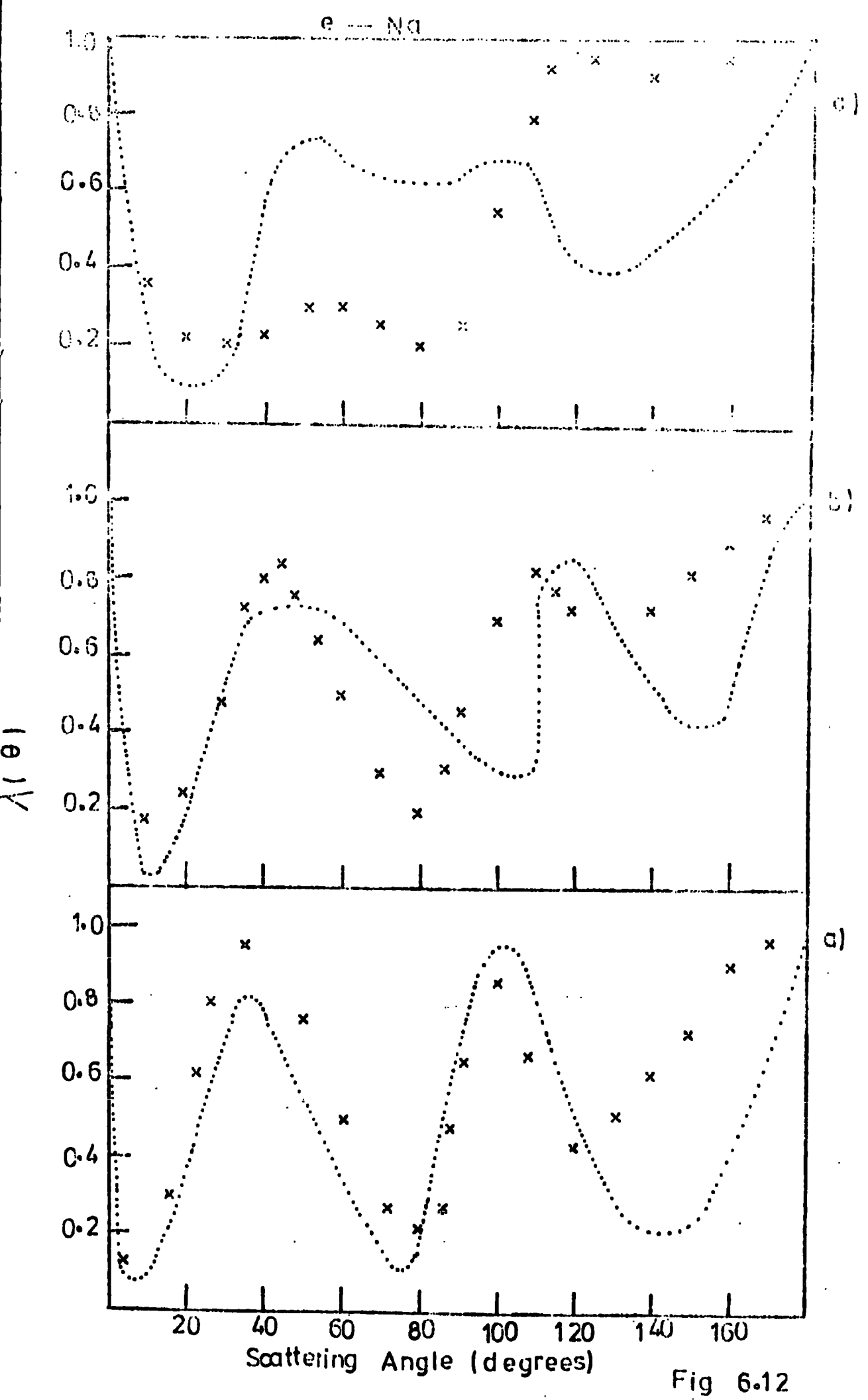
e — Na
1.0
0.8
0.6
0.4
0.2
c)
1.0
0.8
0.6
0.4
0.2
b)
1.0
0.8
0.6
0.4
0.2
a)
A(θ)
20
40
60
80
100
120
140
160
Scattering Angle (degrees)

Fig 6.12

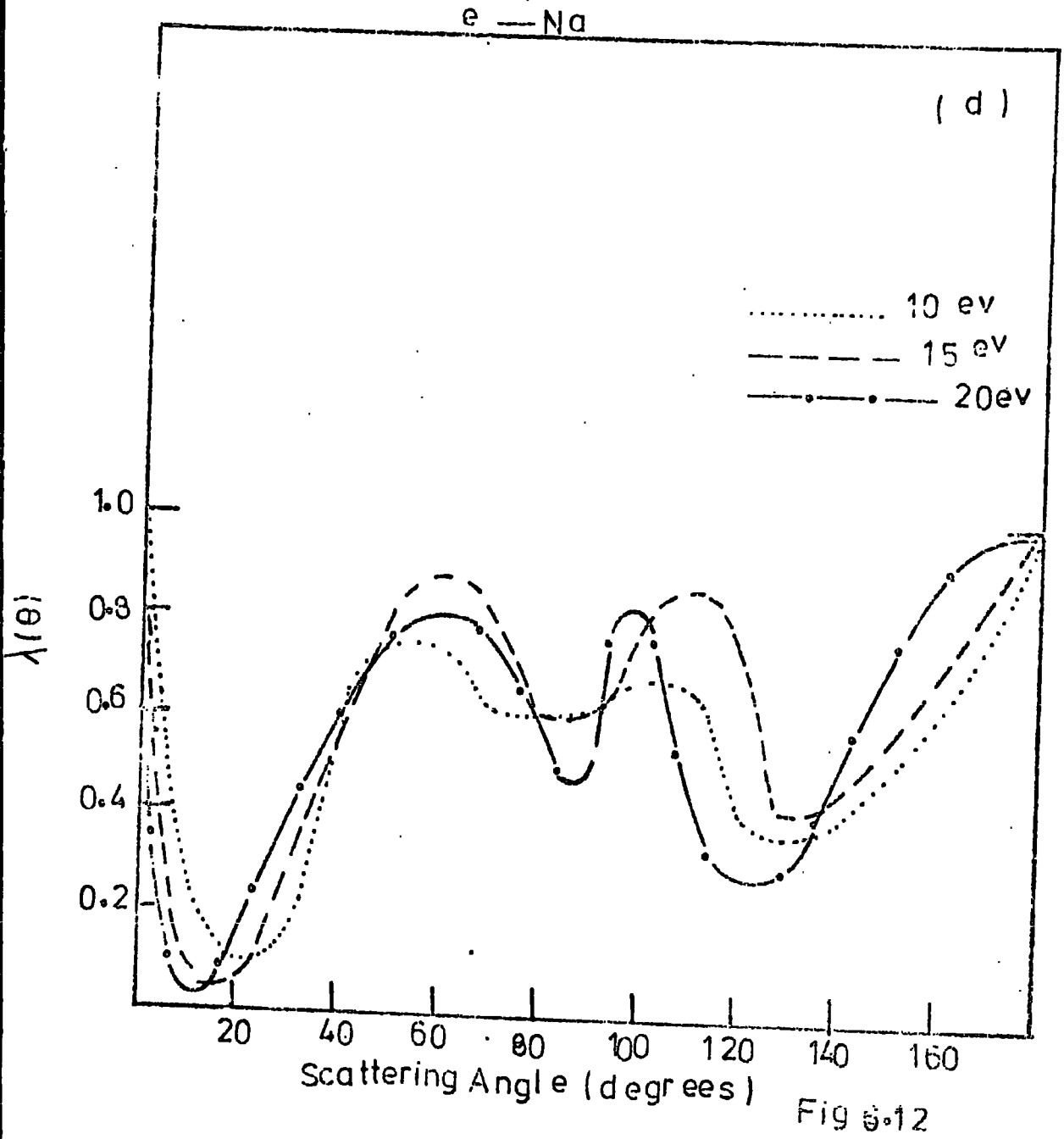
e — Na
(d)
10 ev
15 ev
20ev
1.0
0.8
0.6
0.4
0.2
I(θ)
20
40
60
80
100
120
140
160
Scattering Angle (degrees)

Fig 5.12

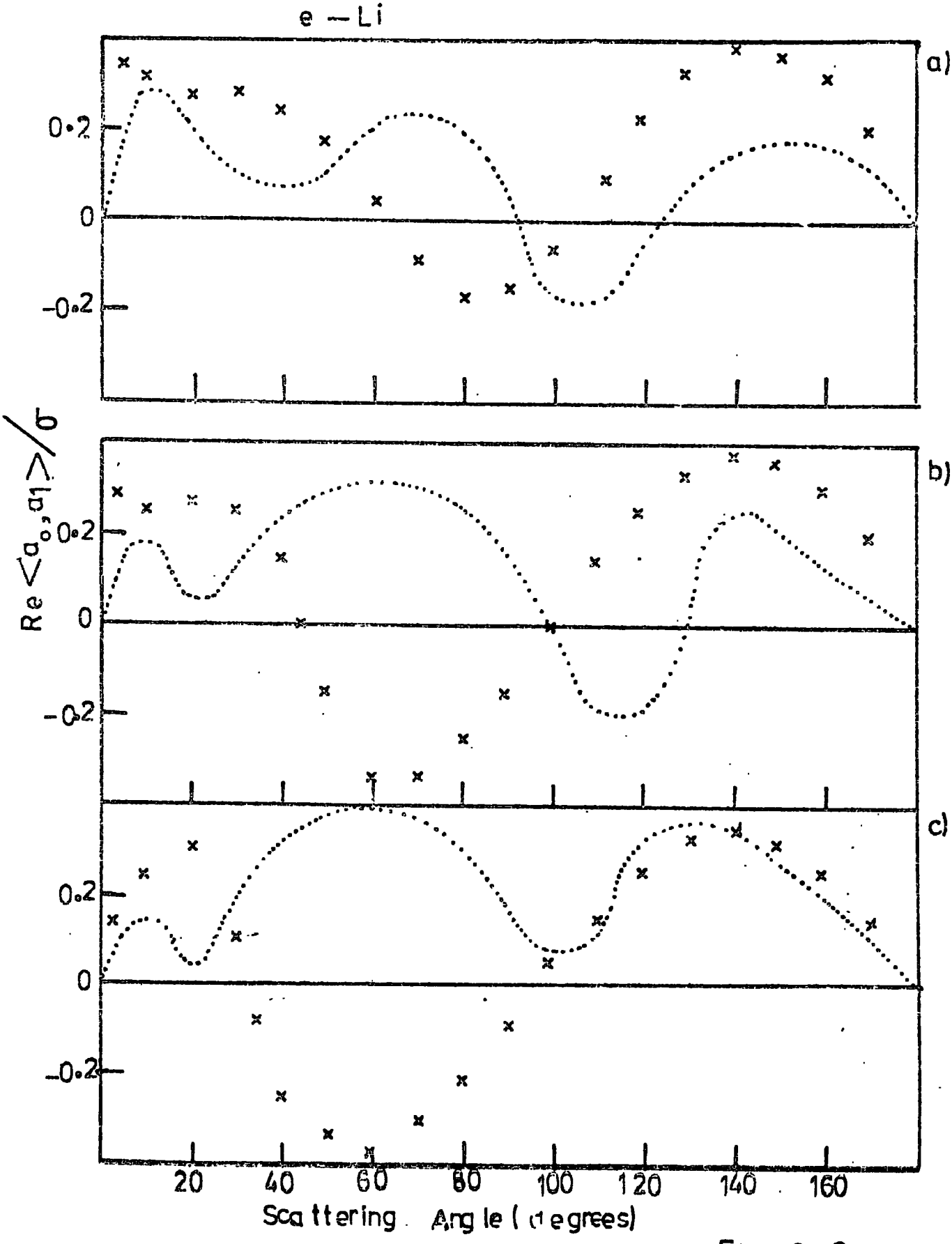
e — Li
a)
b)
c)
0·2
0
-0·2
Re <a0, a1>/σ
20
40
60
80
100
120
140
160
Scattering Angle (degrees)

Fig 6.13

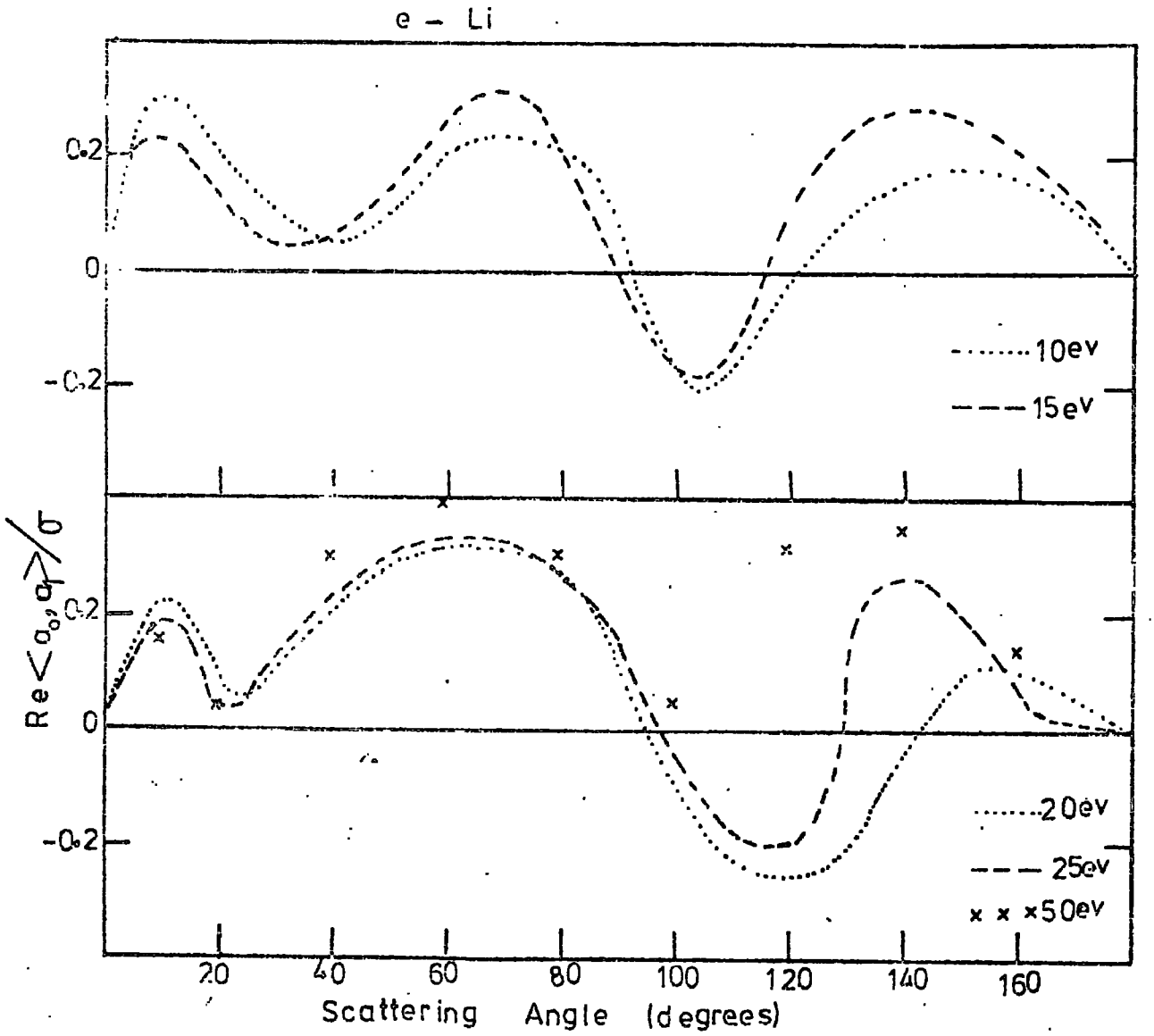
e – Li
0.2
0
-0.2
10ev
15ev
Re<a₀, a_f>/σ
0.2
0
-0.2
20ev
25ev
×50ev
20
40
60
80
100
120
140
160
Scattering Angle (degrees)

Fig 6.13.d

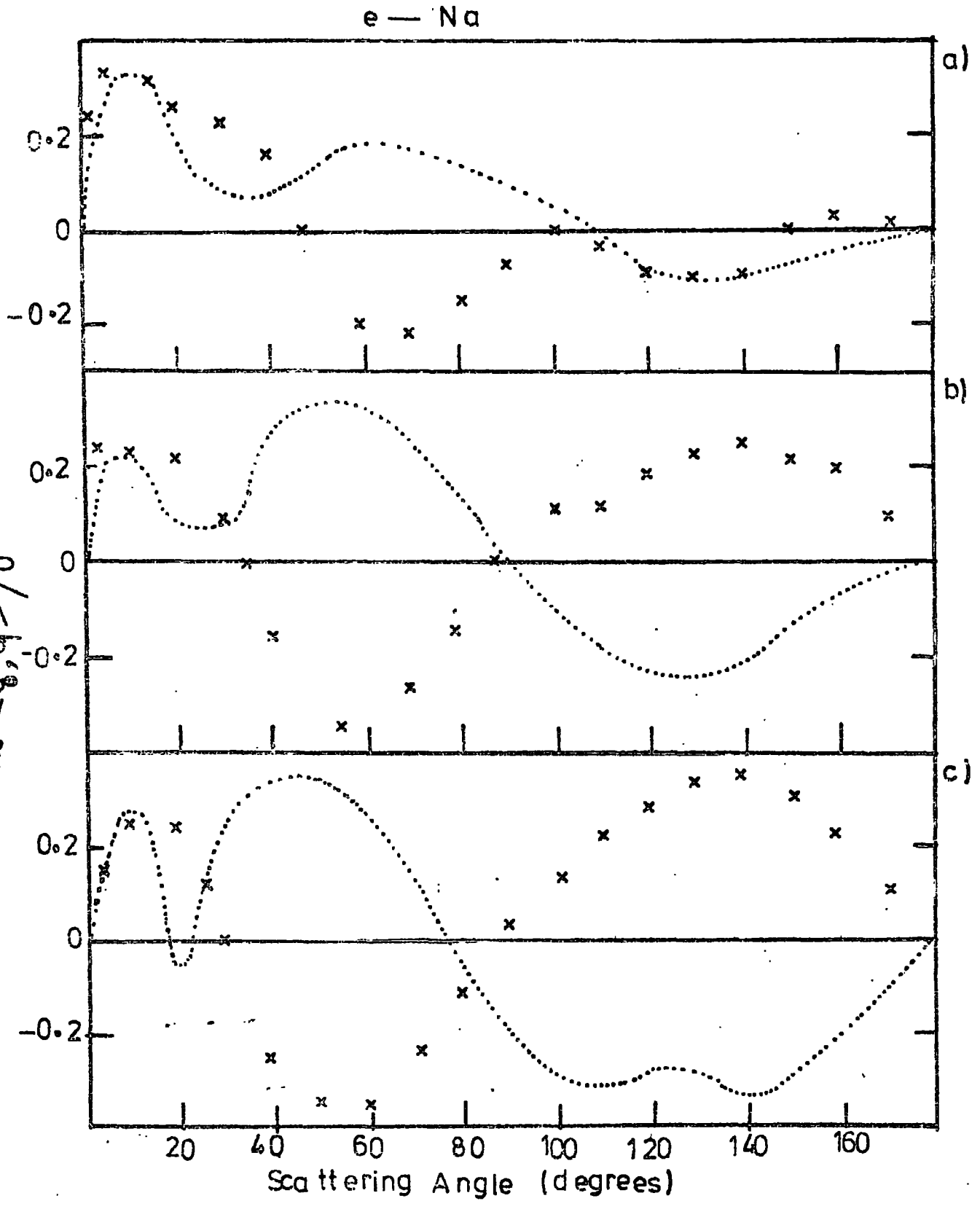
e — Na
a)
b)
c)
0·2
0
-0·2
Re<q, q'>/σ
20
40
60
80
100
120
140
160
Scattering Angle (degrees)

Fig 6.14

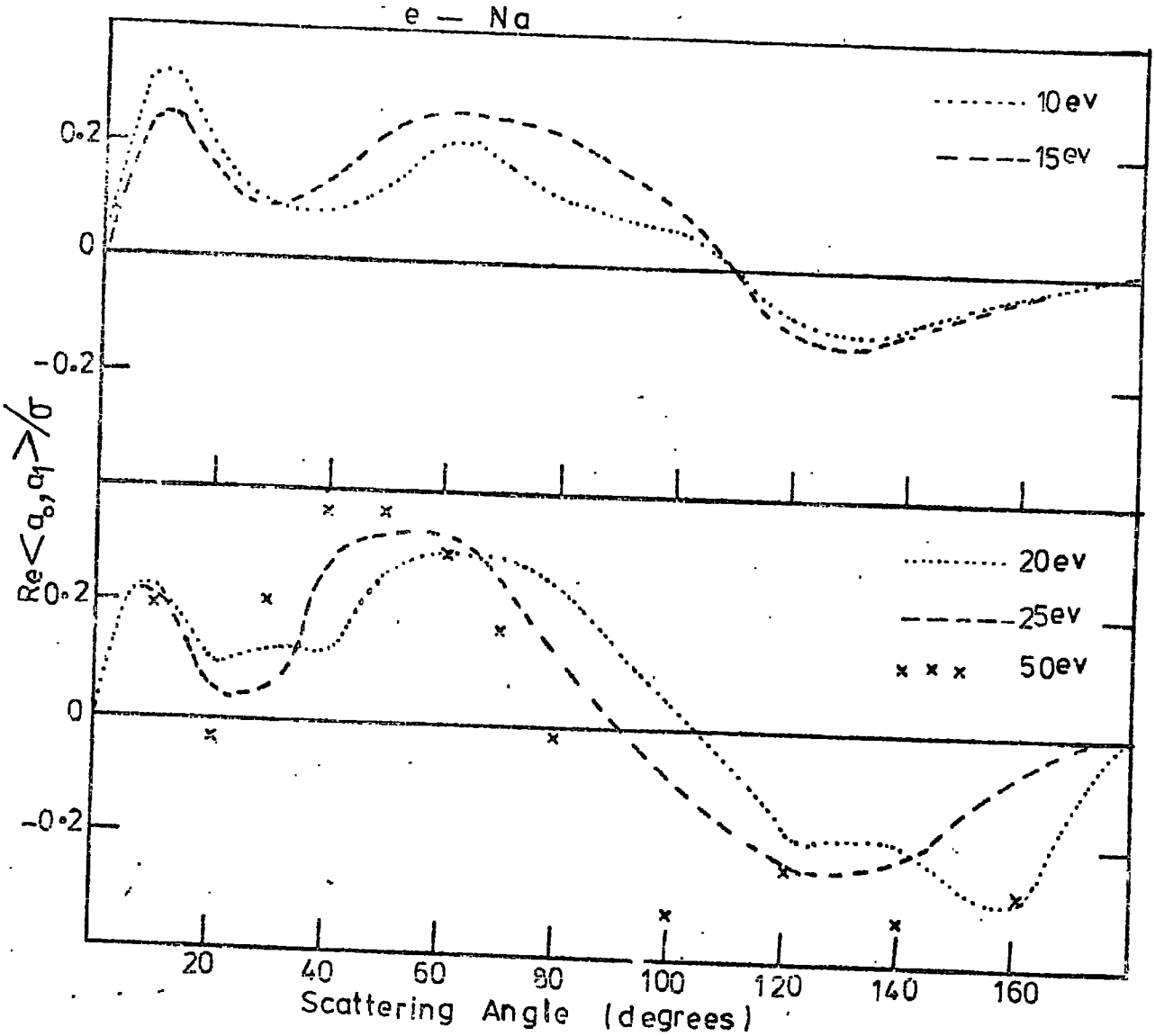
e — Na
10 ev
15 ev
20 ev
25 ev
50 ev
0.2
0
-0.2
Re<a0, aj>/σ
20
40
60
90
100
120
140
160
Scattering Angle (degrees)

Fig 6.14d

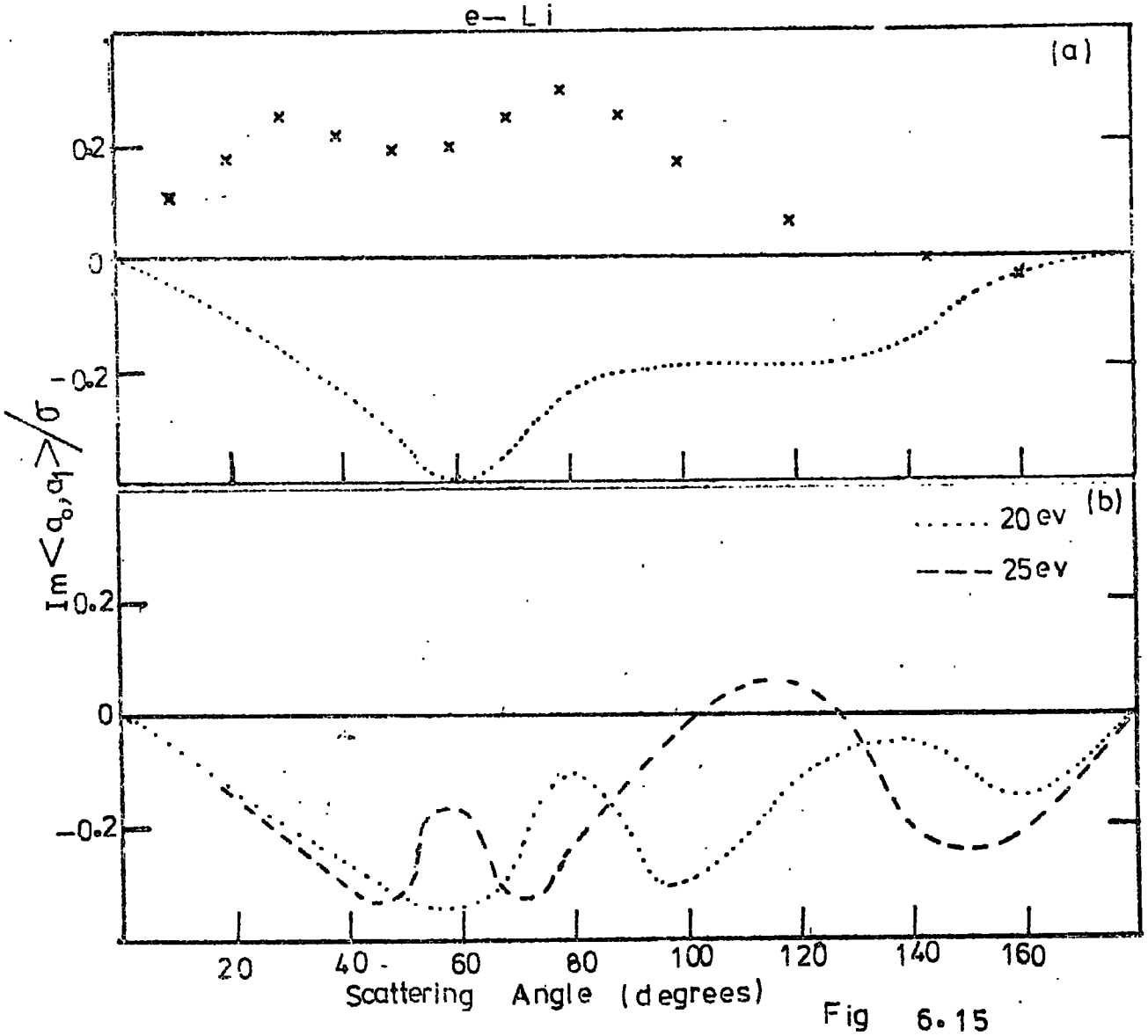
e— Li
(a)
0.2
0
-0.2
(b)
..... 20 ev
——— 25 ev
0.2
0
-0.2
20
40
60
80
100
120
140
160
Scattering Angle (degrees)
Im < a0, a1 > / σ

Fig 6.15

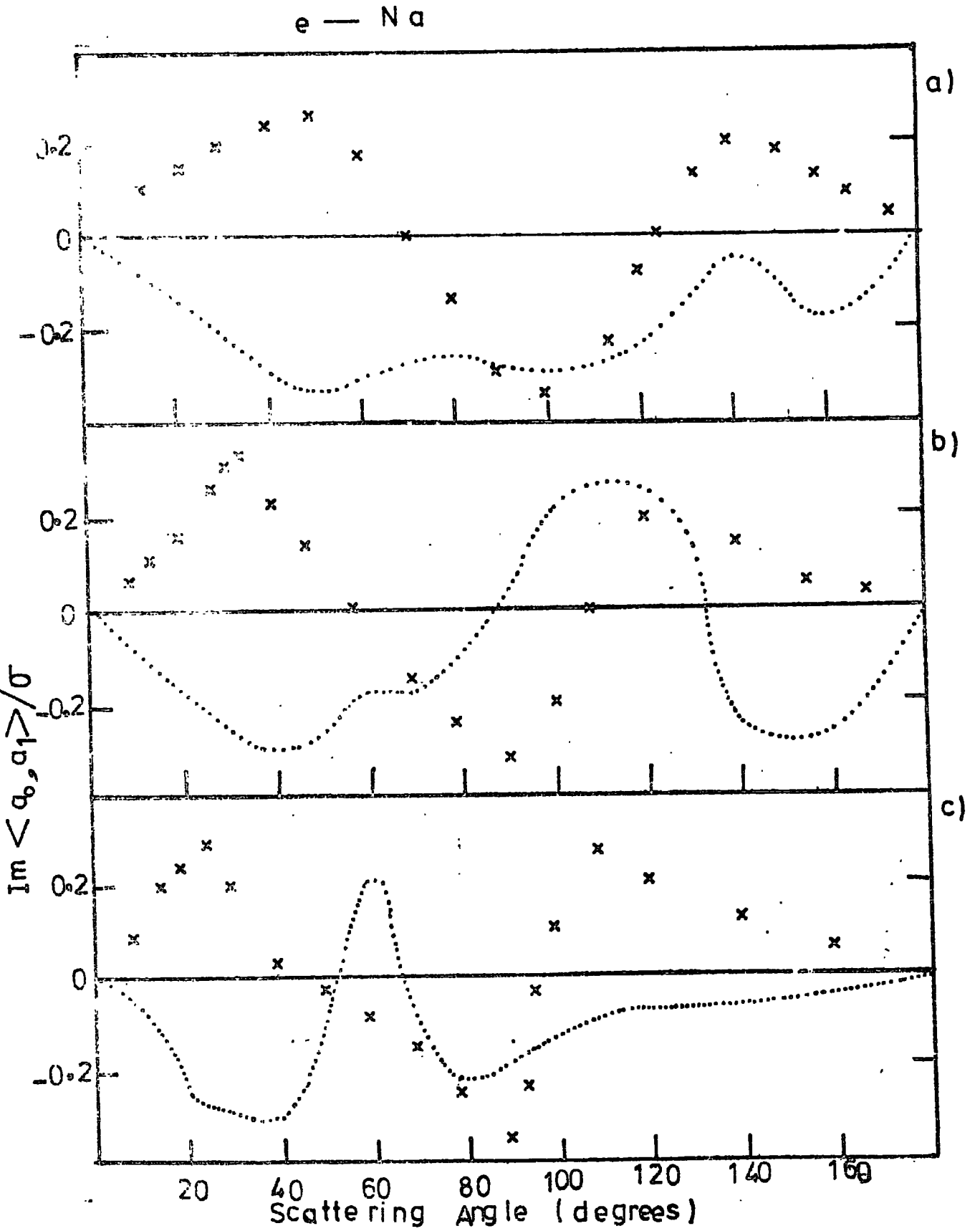
e — Na
a)
b)
c)
0.2
0
-0.2
0.2
0
-0.2
0.2
0
-0.2
Im < a0, a1 > /σ
20
40
60
80
100
120
140
160
Scattering Angle (degrees)

Fig 6.16

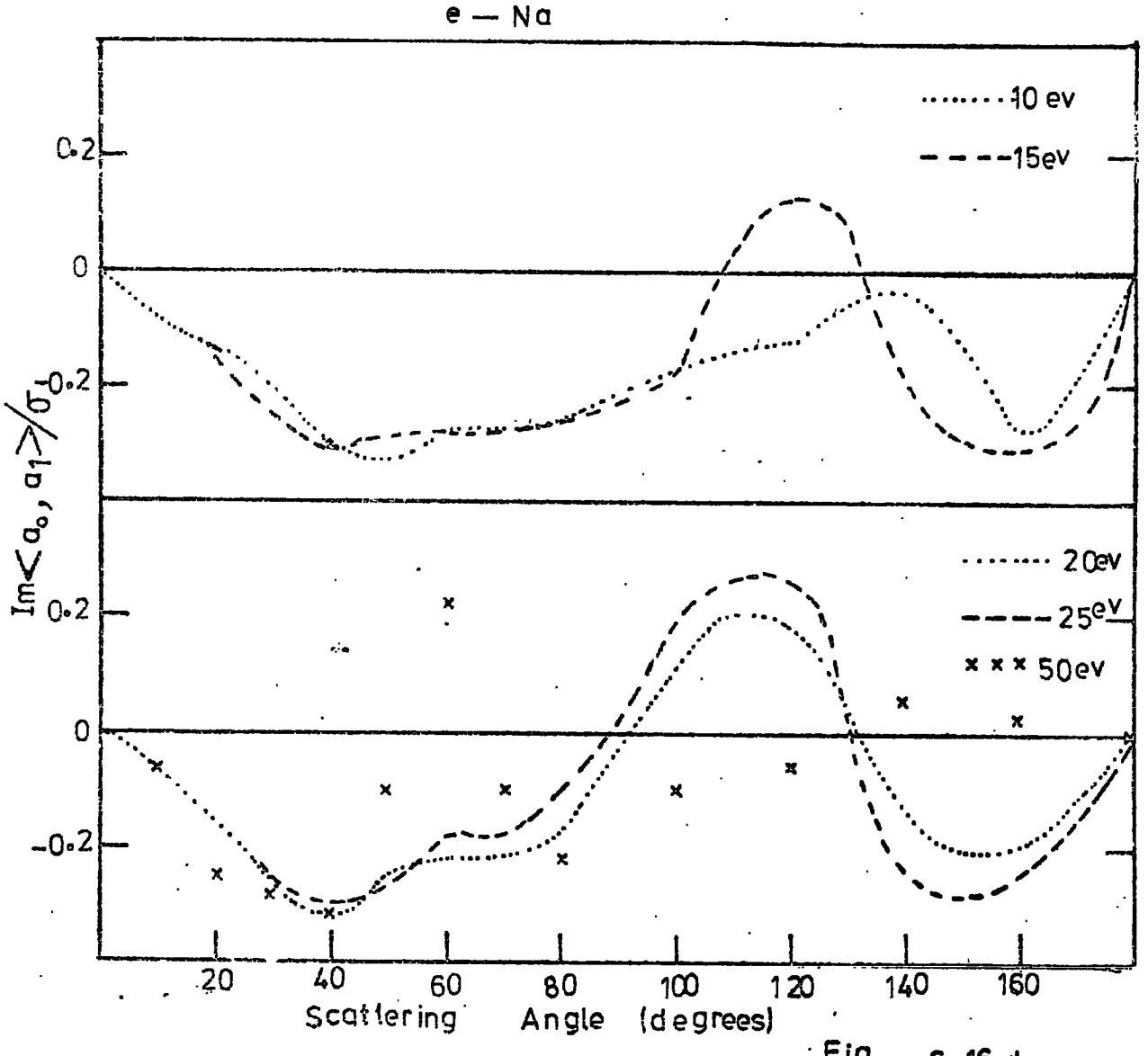
e — Na
10 ev
15ev
20ev
25ev
50ev
0.2
0
-0.2
0.2
0
-0.2
Im<a₀, a₁>/σ_t
20
40
60
80
100
120
140
160
Scattering Angle (degrees)

Fig 6.16.d

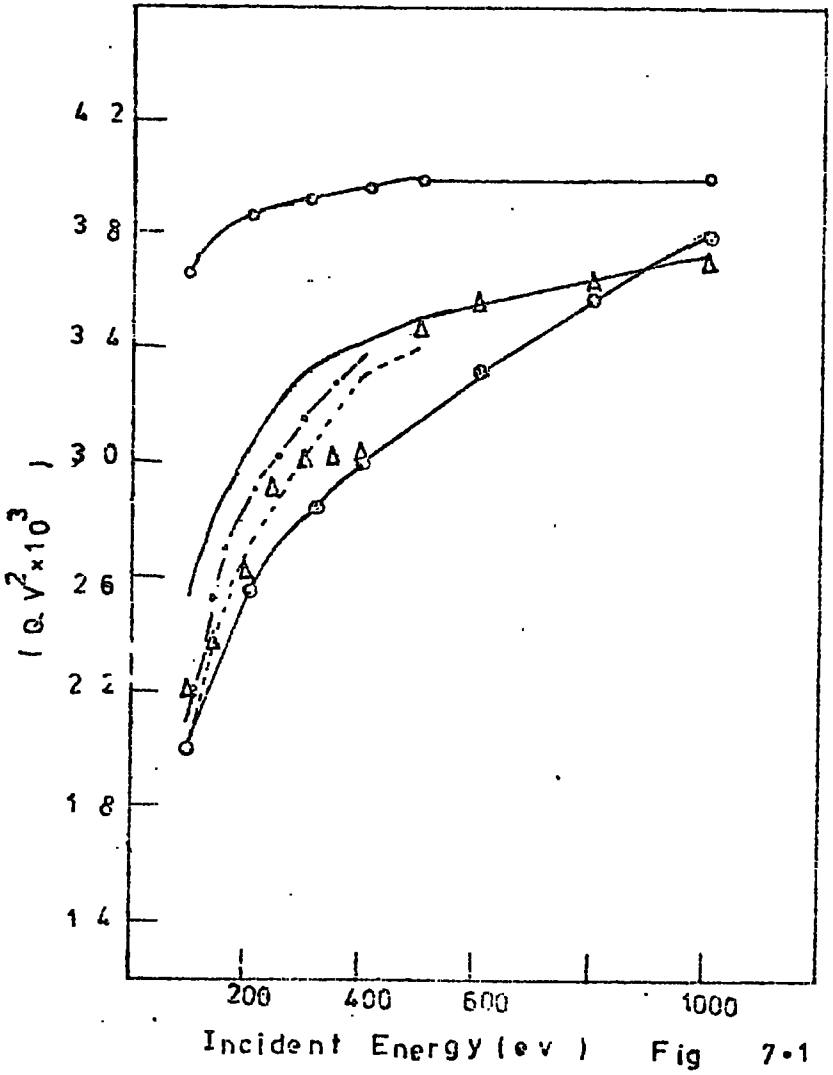
4 2
3 8
3 4
3 0
2 6
2 2
1 8
1 4
(Q V² ×10³)
200
400
600
1000
Incident Energy (ev)

Fig 7·1

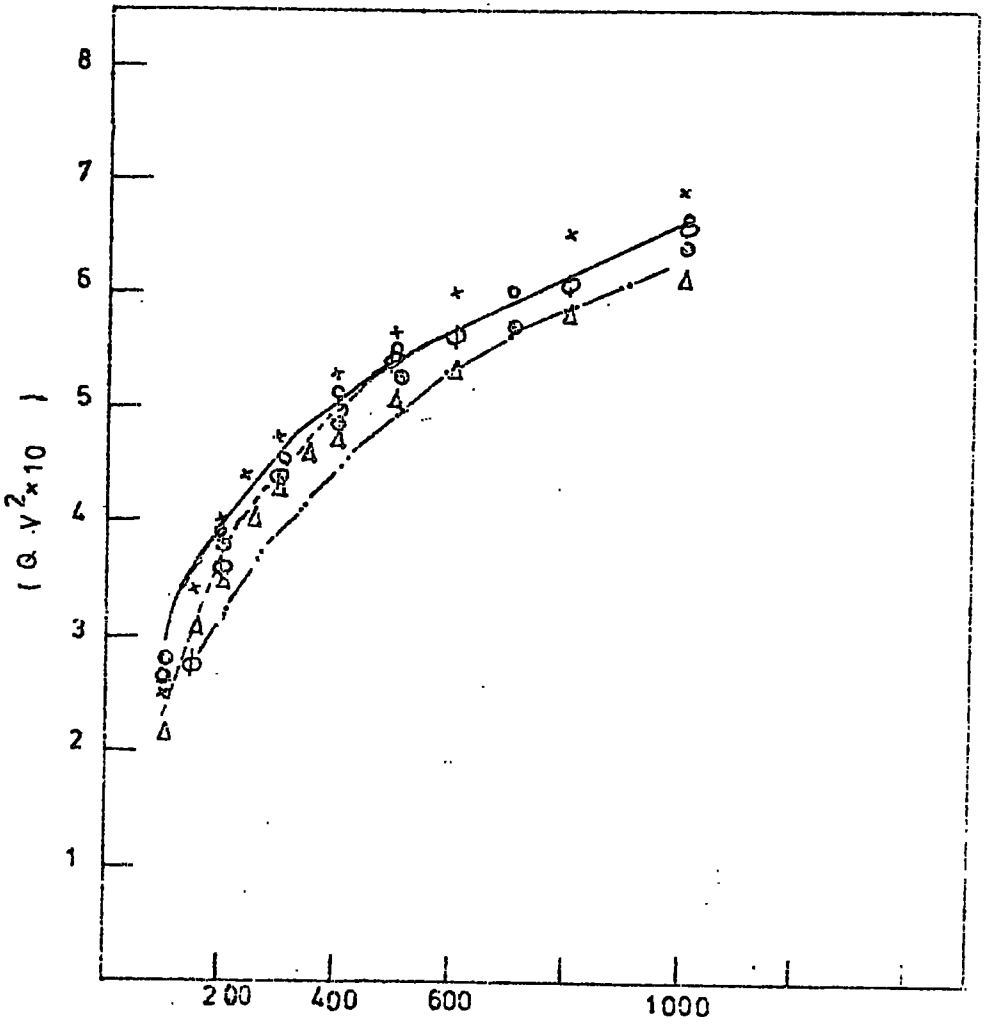
8
7
6
5
4
3
2
1
(Q V² ×10)
200
400
600
1000
Incident Energy (ev)

Fig 7·2

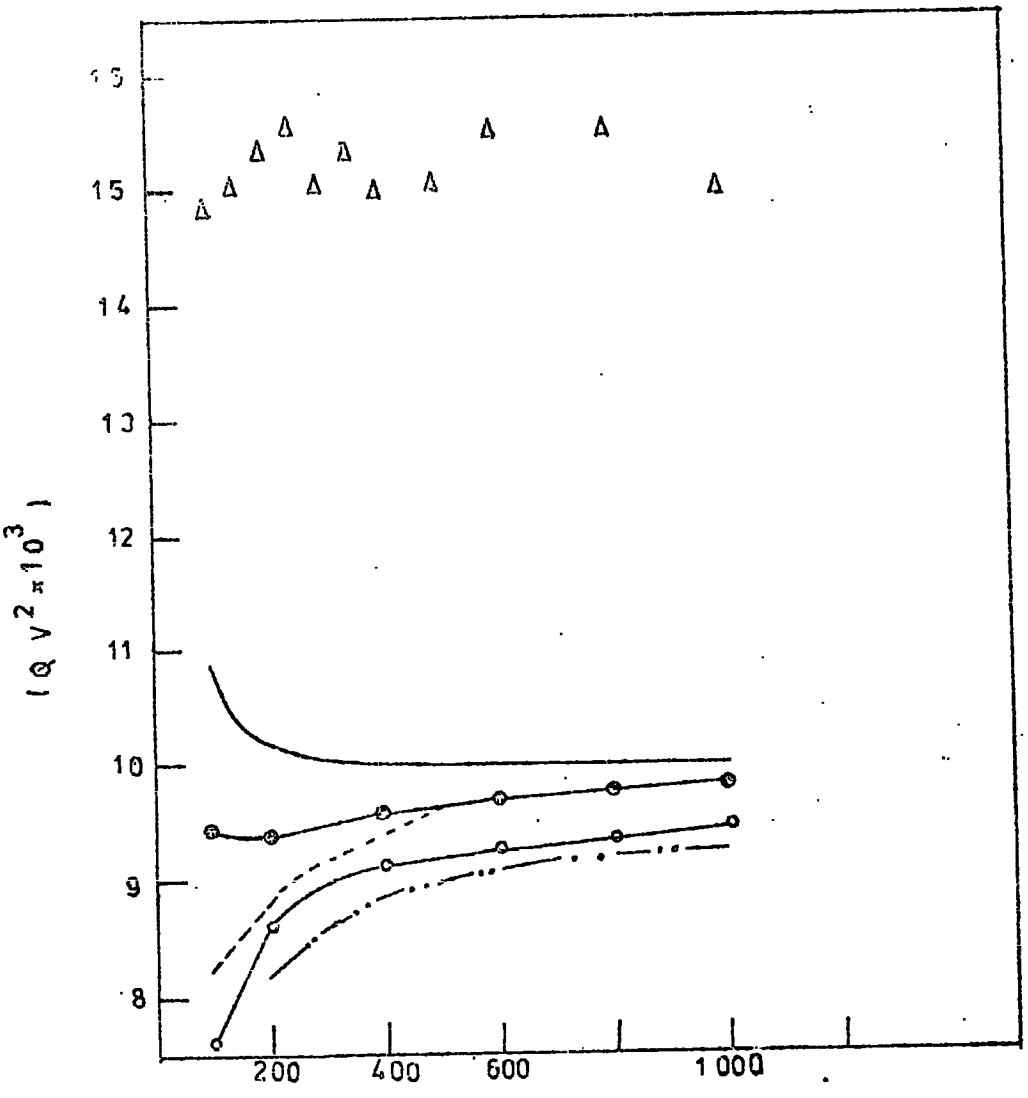
16
15
14
13
12
11
10
9
8
200
400
600
1000
(Q v² × 10³)
Incident Energy (ev)

Fig 7.3

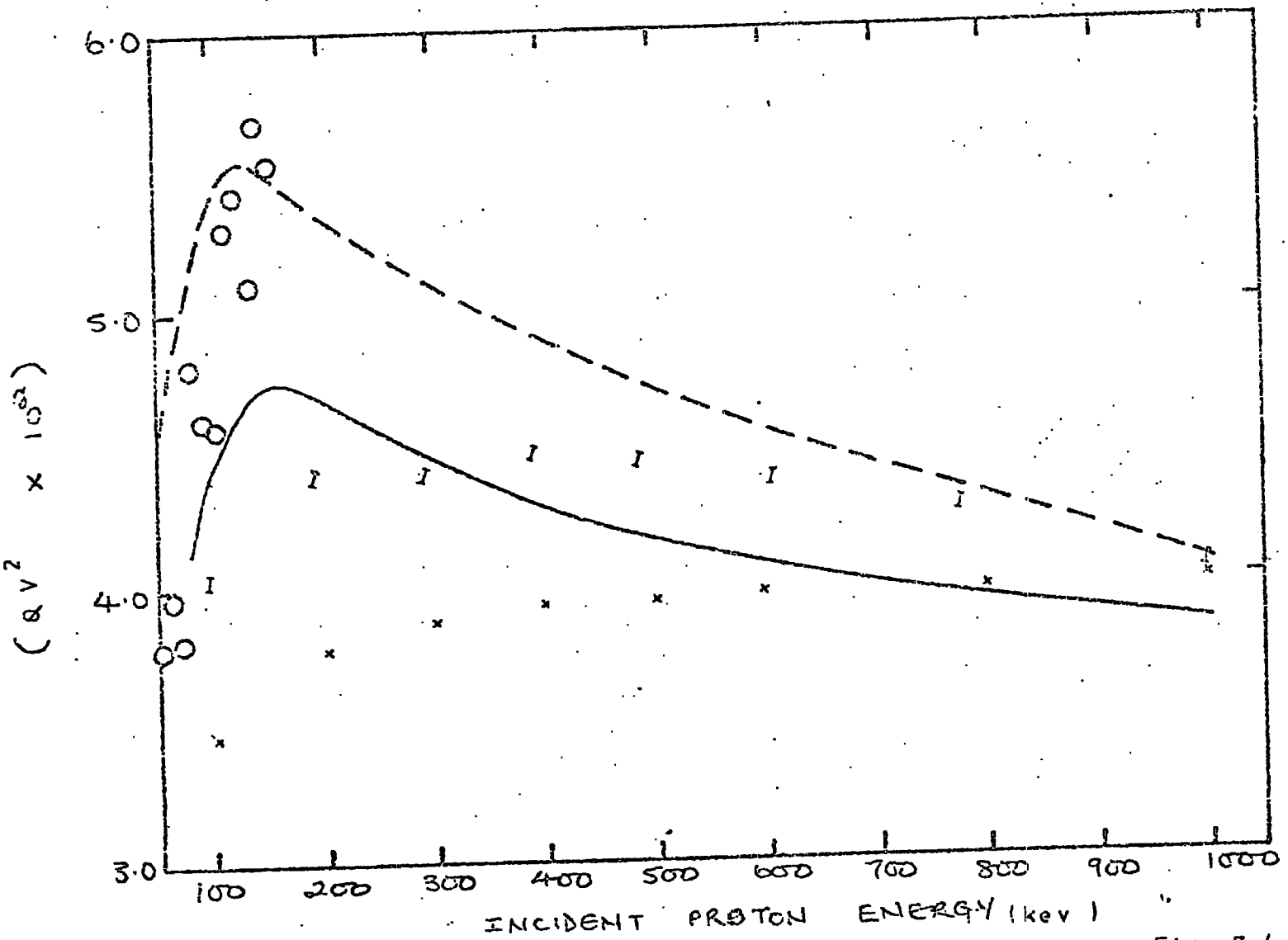
6·0
5·0
4·0
3·0
(σ V² × 10⁵²)
100
200
300
400
500
600
700
800
900
1000
INCIDENT PROTON ENERGY (kev)

Fig 7.4

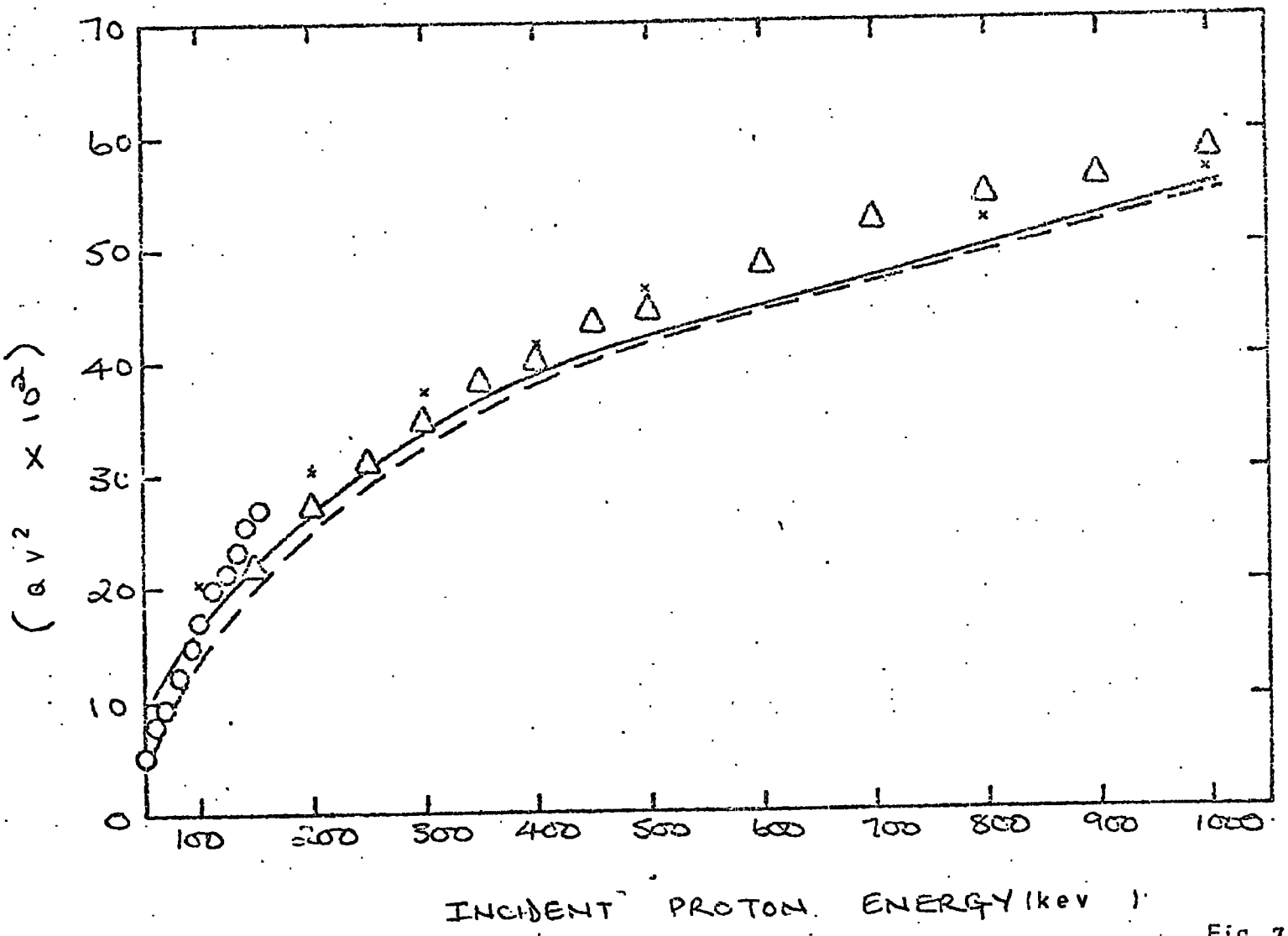
70
60
50
40
30
20
10
0
100
200
300
400
500
600
700
800
900
1000
(σ v² x 10²⁰)
INCIDENT PROTON ENERGY (kev)

Fig 7.5

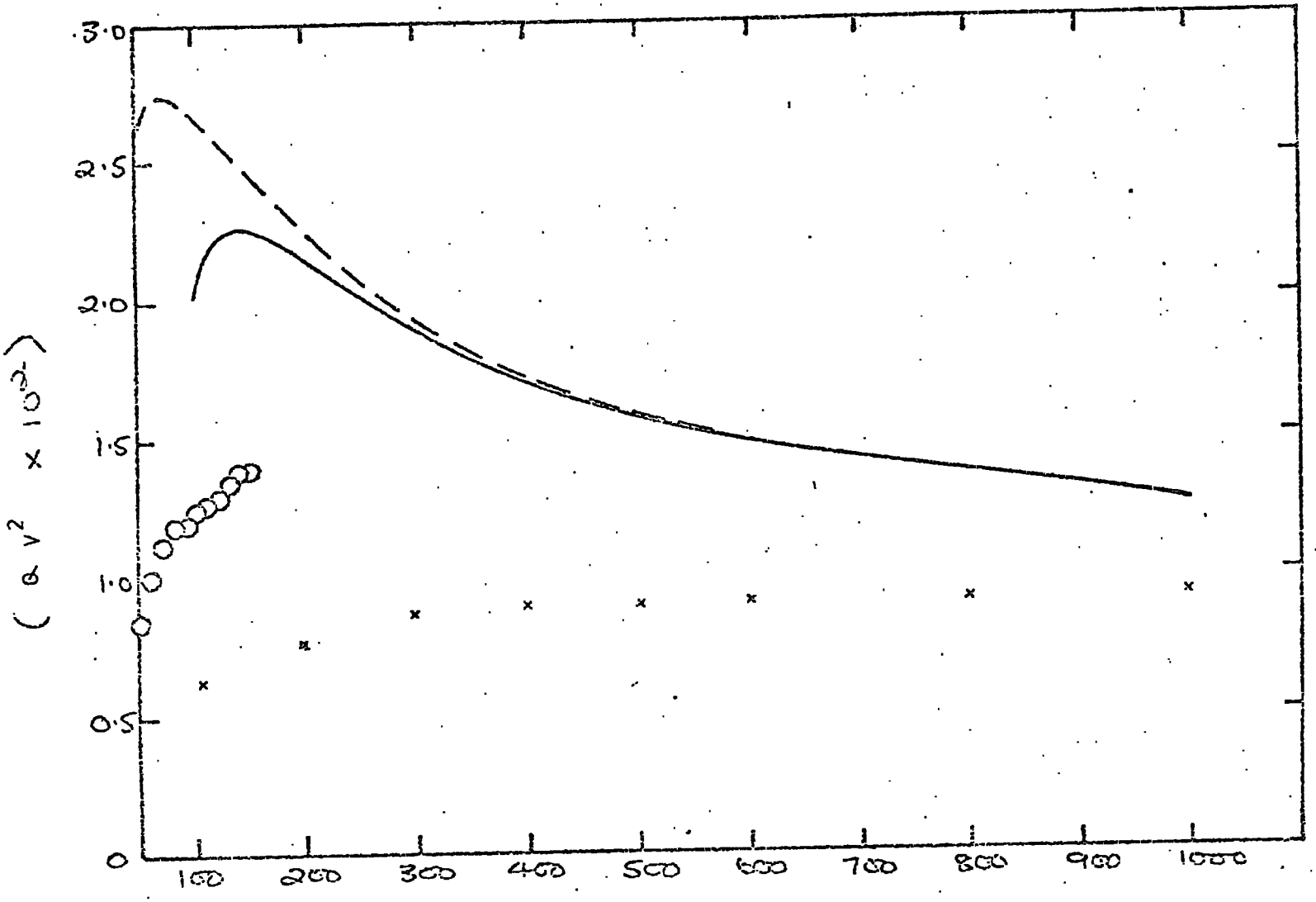
3·0
2·5
2·0
1·5
1·0
0·5
0
(σ v² × 10³²)
100
200
300
400
500
600
700
800
900
1000
Incident Proton Energy (kev)

Fig 7.6

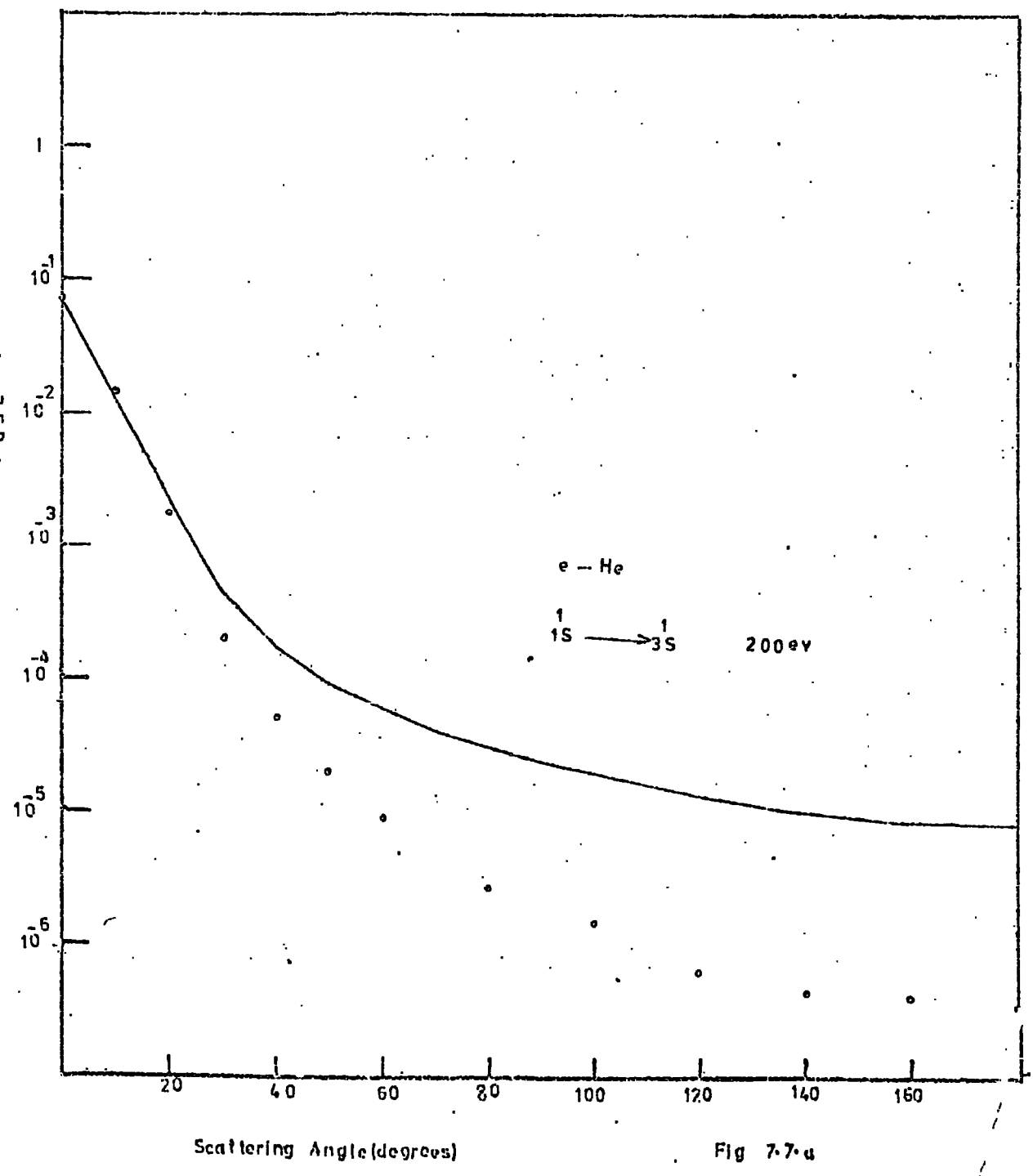
$\left(\frac{d\sigma_P}{d\Omega}\right) a_0^2$
1
10^{-1}
10^{-2}
10^{-3}
10^{-4}
10^{-5}
10^{-6}
e — He
$^1_1S \longrightarrow ^1_3S$
200 ev
20
40
60
80
100
120
140
160
Scattering Angle (degrees)

Fig 7.7.a

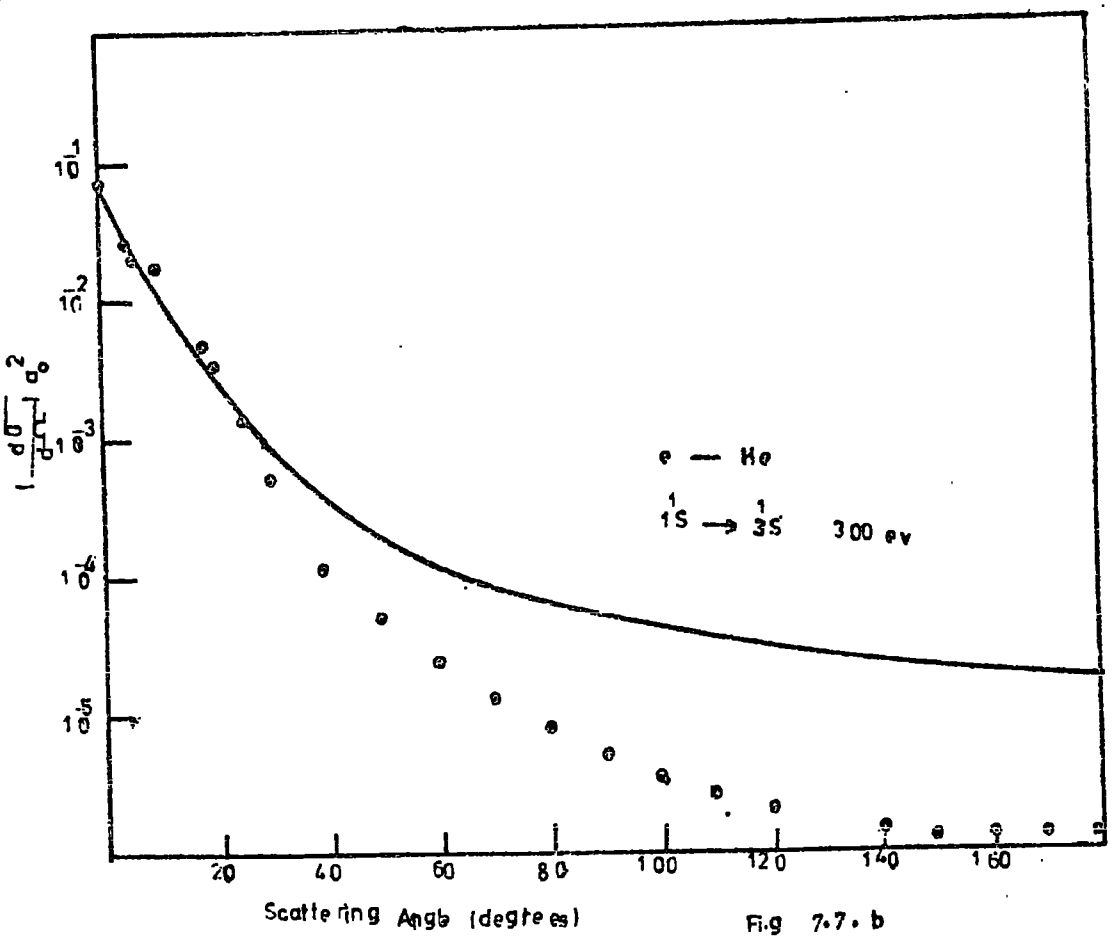
$\frac{1}{I}\frac{dI}{d\Omega}a_0^2$
10^{-1}
10^{-2}
10^{-3}
10^{-4}
10^{-5}
e — He
$1^1S \rightarrow 3^1S$ 300 ev
20
40
60
80
100
120
140
160
Scattering Angle (degrees)

Fig 7.7. b

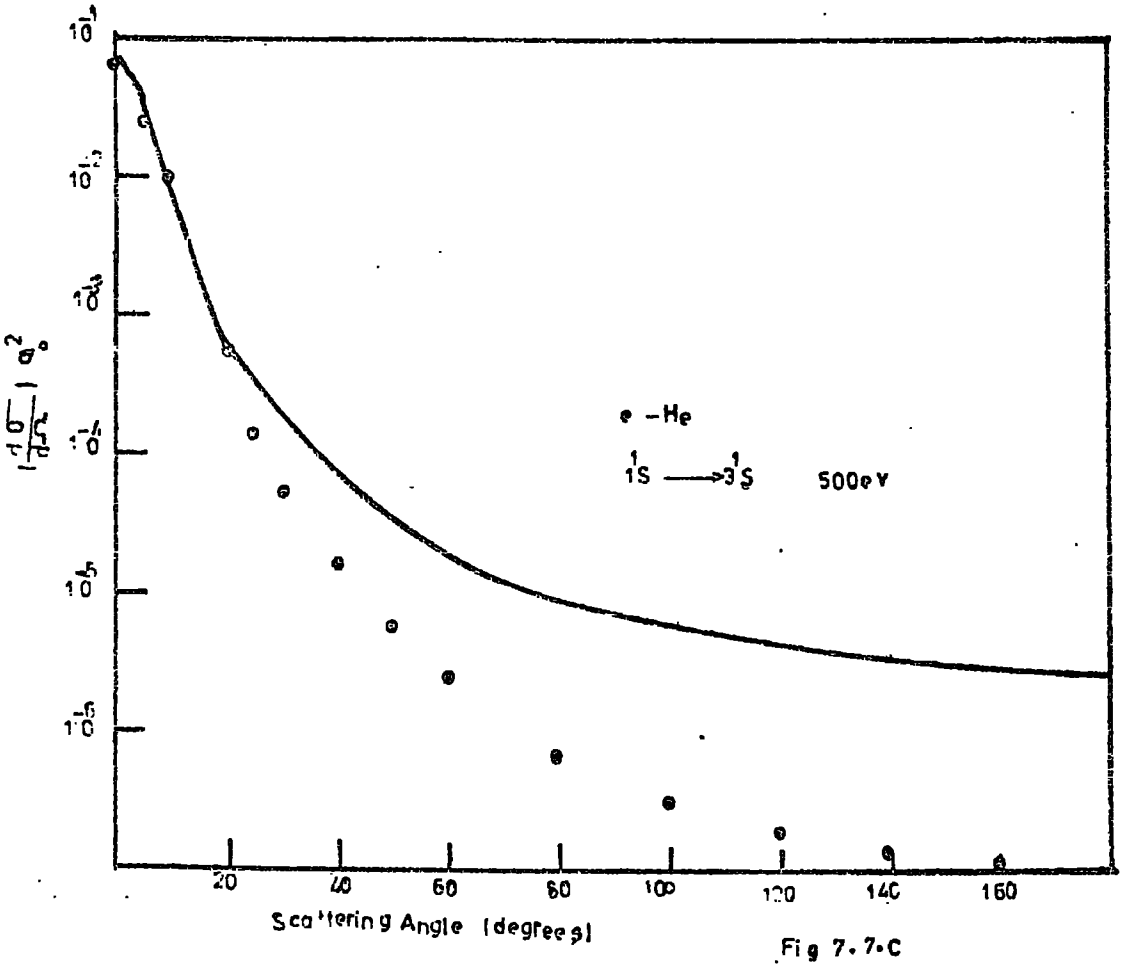
e – He
1S ⟶ 3S
500eV
20
40
60
80
100
120
140
160
Scattering Angle (degrees)

Fig 7.7.C

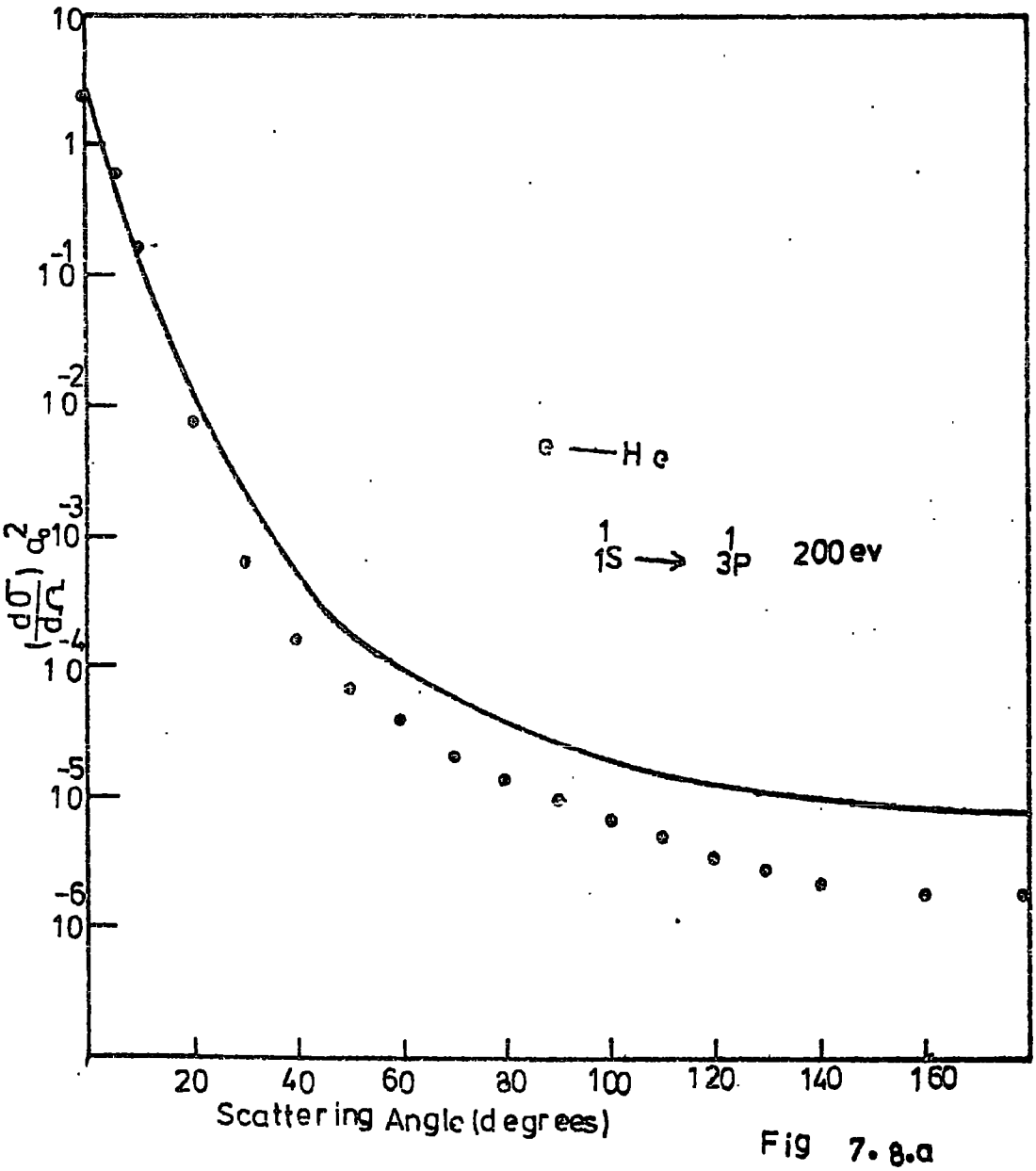
10
1
10^{-1}
10^{-2}
10^{-3}
10^{-4}
10^{-5}
10^{-6}
$(\frac{d\sigma}{d\Omega})^2 a_0$
e — He
$^1_{1S} \rightarrow ^1_{3P}$ 200 ev
20
40
60
80
100
120
140
160
Scattering Angle (degrees)

Fig 7.8.a

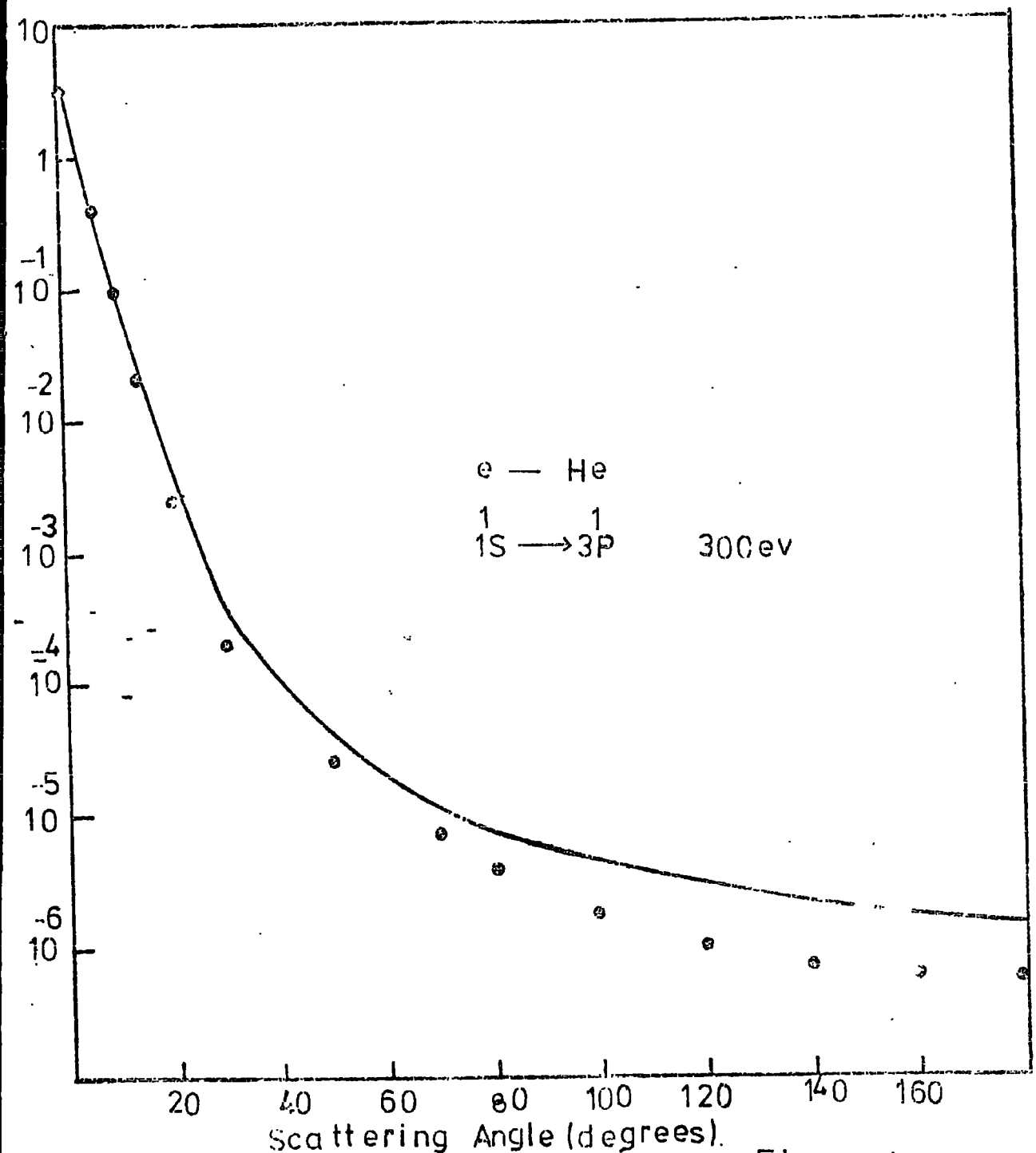
10
1
-1
10
-2
10
-3
10
-4
10
-5
10
-6
10
e — He
1 1
1S ⟶ 3P
300ev
20
40
60
80
100
120
140
160
Scattering Angle (degrees).

Fig 7.8 b

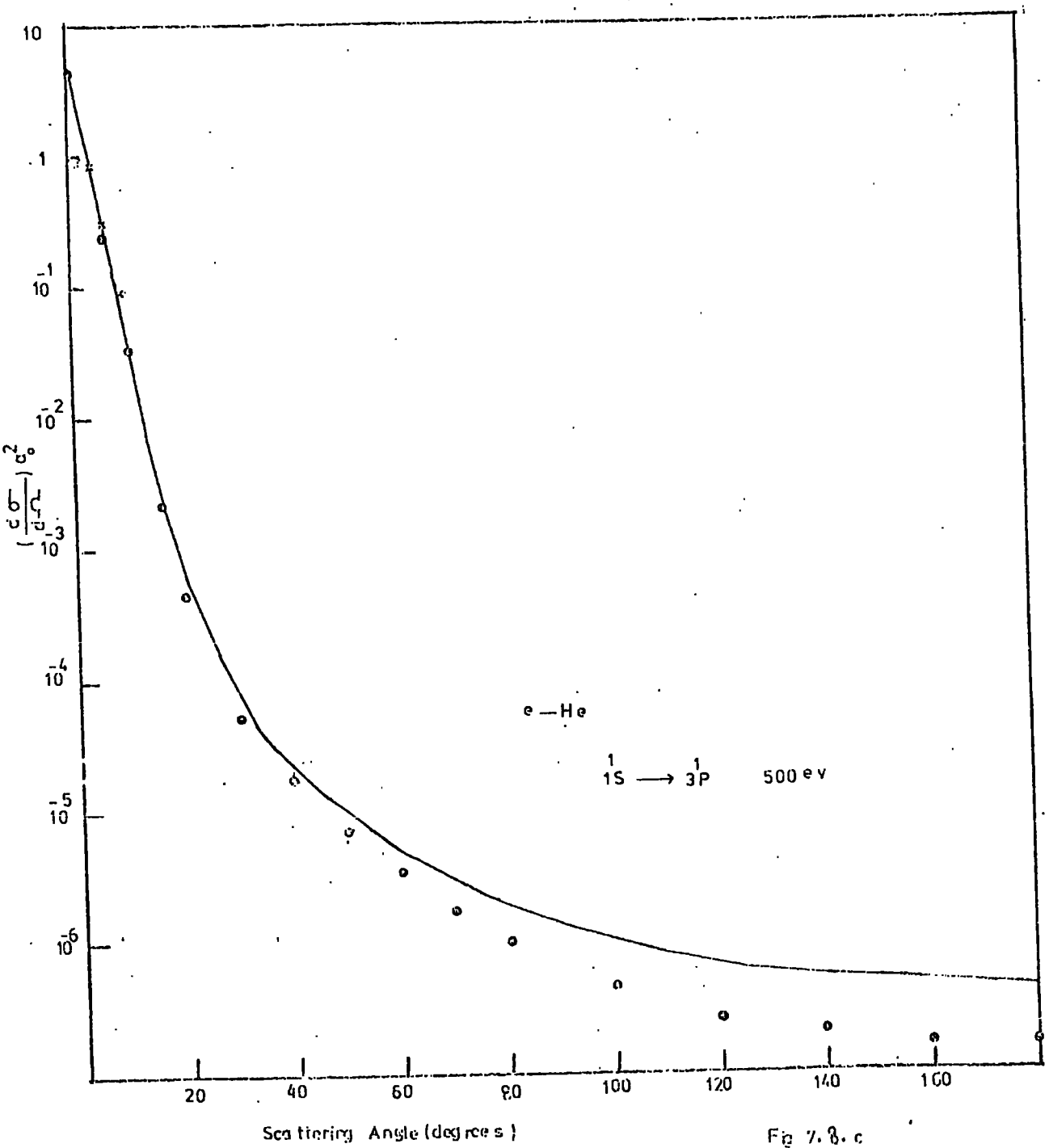
10
1
10^{-1}
10^{-2}
10^{-3}
10^{-4}
10^{-5}
10^{-6}
$\left(\frac{d\sigma}{d\Omega}\right) a_0^2$
e — He
$^1S \longrightarrow {}^1P$
500 ev
20
40
60
80
100
120
140
160
Scattering Angle (degrees)

Fig 7.8.c

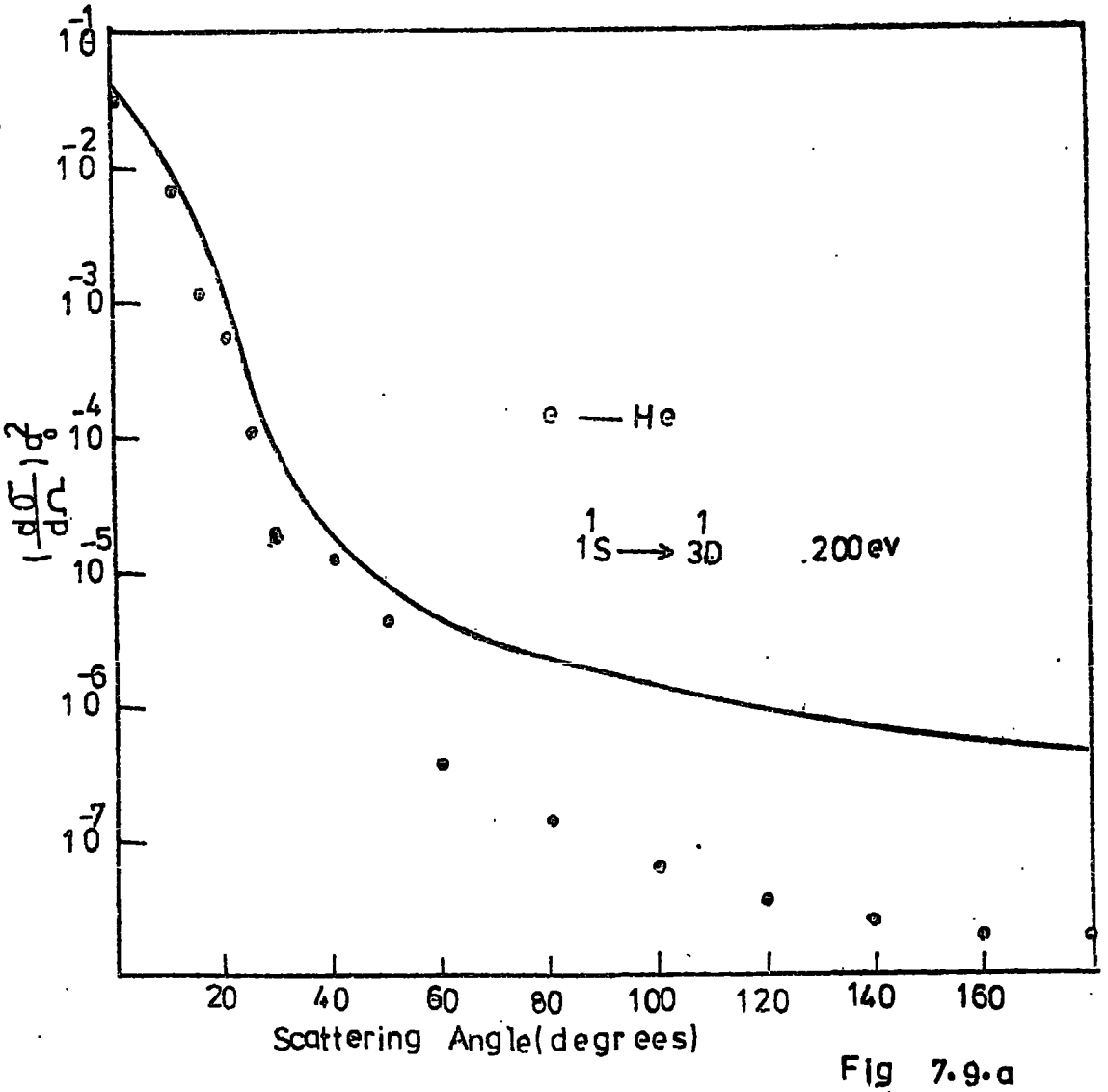
10^{-1}
10^{-2}
10^{-3}
10^{-4}
10^{-5}
10^{-6}
10^{-7}
$(\frac{d\sigma}{d\Omega})a_0^2$
e — He
$^1_1S \longrightarrow ^1_3D$ .200ev
20
40
60
80
100
120
140
160
Scattering Angle(degrees)

Fig 7.9.a

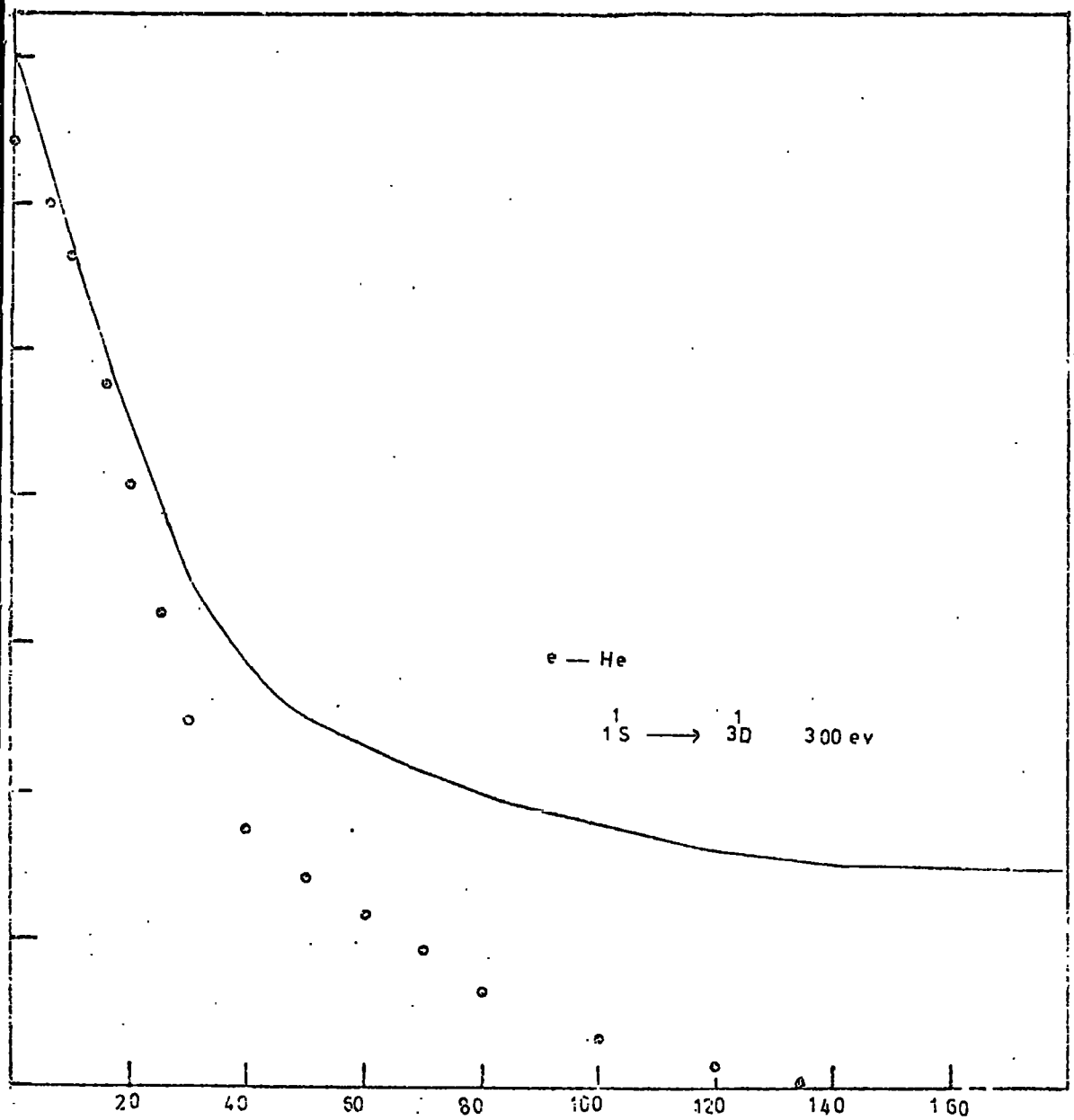
e — He
$^1S \longrightarrow {}^1D$ 300 ev
20
40
60
80
100
120
140
160
Scattering Angle (degrees)

Fig 7.9.b

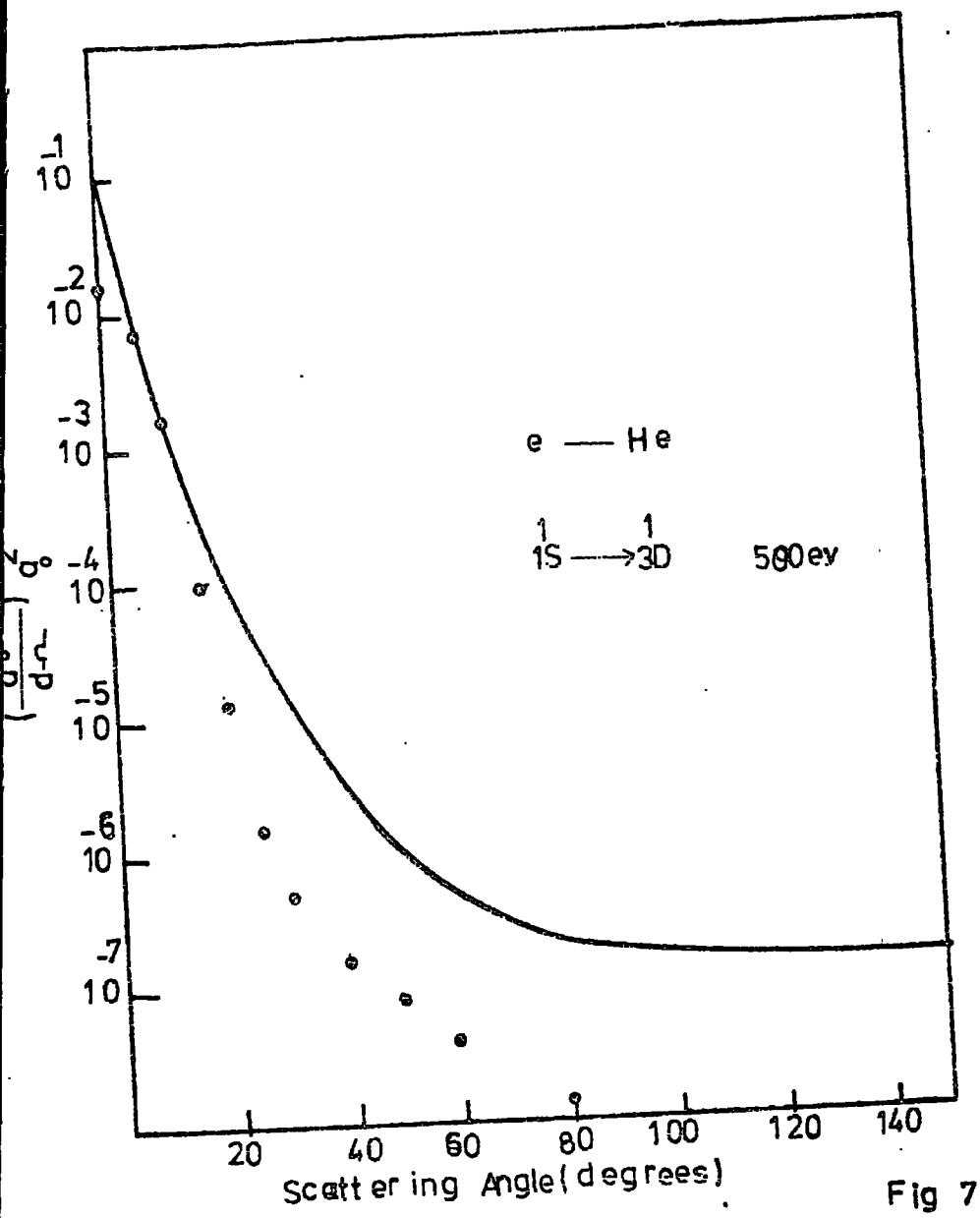
e — He
1 1
1S ⟶ 3D
500ev
10^-1
10^-2
10^-3
10^-4
10^-5
10^-6
10^-7
20
40
60
80
100
120
140
Scatt er ing Angle(degrees)

Fig 7. 9.C

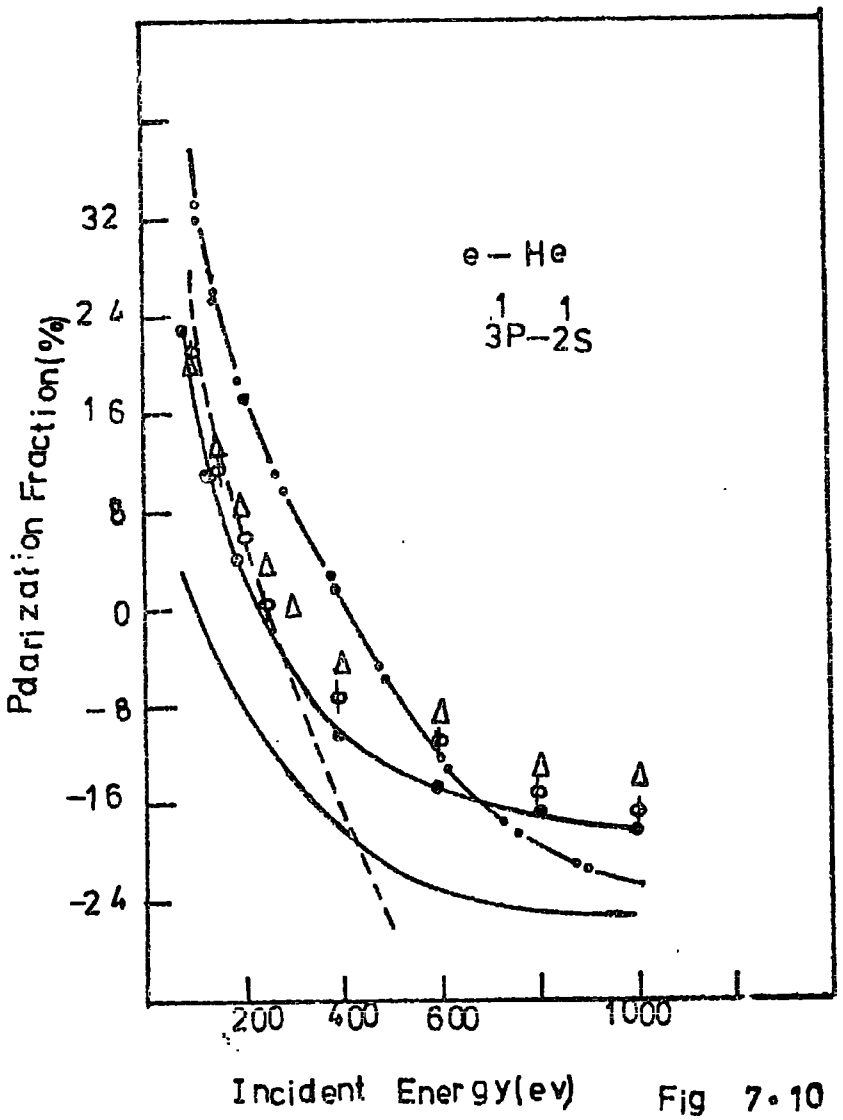
e – He
1 1
3P–2S
32
24
16
8
0
-8
-16
-24
200
400
600
1000
Pdarization Fraction(%)
Incident Energy(ev)

Fig 7.10

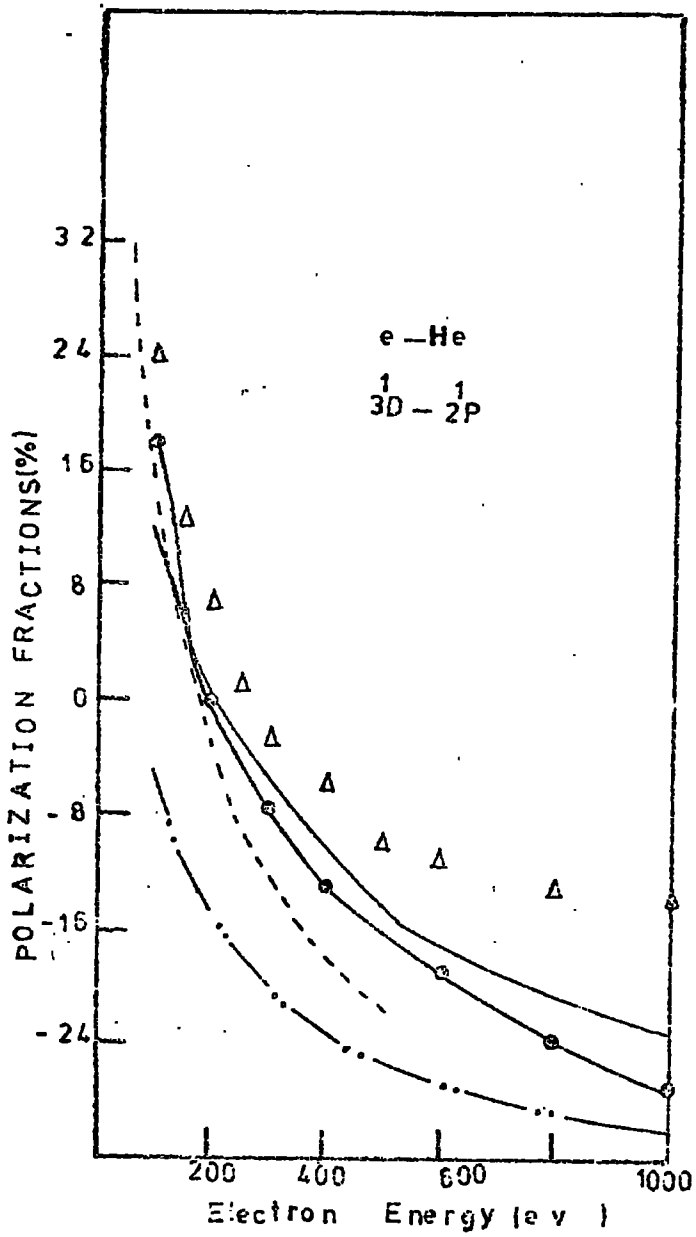

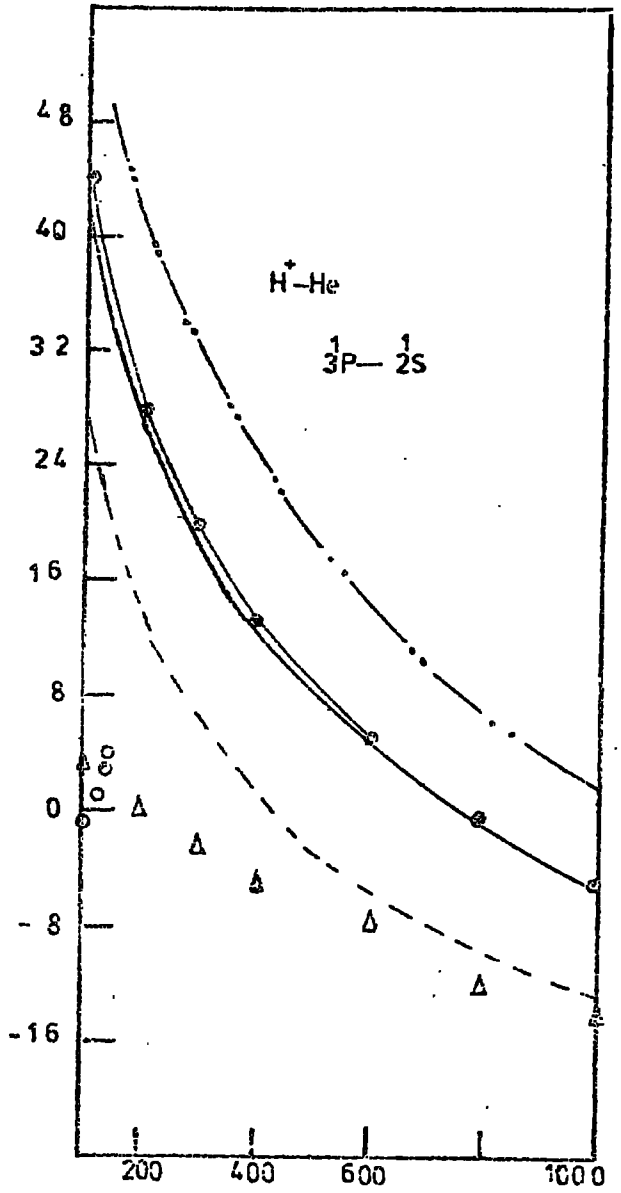

Fig 7.12